EXPERIMENTAL INVESTIGATION INTO SWATH SHIP MOTIONS AND LOADINGS

by

EKO BUDI DJATMIKO

This thesis is submitted for
the Degree of Master of Science

Department of Naval Architecture and Ocean Engineering
University of Glasgow
November, 1987

TABLE OF CONTENTS

LIST OF FIGURES

Chapter 4.

Chapter 5.

Chapter 6.

Chapter 7.

LIST OF TABLES

ACKNOWLEDGEMENTS

The author is deeply indebted to Professor D. Faulkner, Head of Department, for allowing him to carry out this research.

The author is particularly grateful to his supervisor and the superintendent of the Hydrodynamics Laboratory, Dr. A.M. Ferguson, and to his joint supervisor, Dr. R.C. McGregor, for their unflagging enthusiasm, encouragement and advice during the study.

Gratitude is also addressed to all the technicians, the computer manager and staff at the laboratory for their help during the author conducting the experiments and data analysis. Special thanks are conveyed to Dr. M. Atlar, who has given much information and guidance in the early stages of this work, to Dr. A. Incecik and Mr. J.R. MacGregor, who have spared their time for discussing the manuscript, and other fellow researchers at the laboratory who have one way or another been very cooperative.

The author would like to express his sincere thanks for encouragements given by his colleagues, especially to Ir. Soegiono, the Dean of Faculty, at the Faculty of Marine Technology, Institute of Technology, Surabaya.

The author gratefully acknowledges the financial support for the British Council.

Finally the author is mostly grateful to his mother and family at home in Indonesia for their support and encouragement throughout his study in Scotland.

DECLARATION

The material presented in this thesis, except where the reference is made to the work of others, is original work of the author.

SUMMARY

The main objectives of this thesis are firstly to present experimental data of SWATH (Small Waterplane Area Twin-Hull) ship motions and dynamic loadings, and secondly to compare the experimental data with the existing numerical modellings for validation purposes.

The experiments were conducted by employing a model of tandem strut per hull configuration (SWATH1). The basic idea of using this configuration is as the SWATH ship is a relatively new concept of advanced marine vehicle, and as there can be a wide range of configurations, experimental data on any particular configuration, such as the SWATH1 model, is very limited.

The first and second chapters of this thesis will overview the basic concept of SWATH ships development and the theoretical background of SWATH ship motions.

SWATH1 model motions in three different sea heading, namely beam, quartering and head seas are investigated. The experimental results are then presented together with the theoretical predictions based on two-dimensional strip theory and three-dimensional sink-source technique. The agreement amongst the three sources is then discussed. The usefulness of the experimental data from the previous work in improving SWATHL computer program is briefly described.

Further experiments are set up to investigate the dynamic loads on the SWATH1 model in regular beam and quartering seas. The investigations are focused on the bending moment on the cross structure and vertical forces on the struts. The data generated is important for a study of SWATH structures.

From a practical point of view, the motion and

structural loading characteristics of a SWATH ship in regular seas are meaningful if the data generated can be used for predicting the motions and loadings in random seas. The only reliable method to accomplish this task is the application of spectral analysis. This is outlined in chapter seven, including evaluation by making use of SWATH seakeeping criteria.

Recommendations for future experiments on SWATH model motions and loadings are outlined in the conclusions.

NOMENCLATURE.

A	hydrodynamic added mass (or mass moment of inertia)
AF'	non-dimensional axial force
AF	axial force
A_{jk}	added mass matrix containing added mass and added mass moment of inertiaper unit acceleration, which are frequency dependent
A_w	waterplane area
AVM_z	heave added virtual mass
B	breadth characteristic
B	hydrodynamic damping per unit velocity
B_{jk}	damping matrix containing damping force and moment of inertia per unit velocity
BM'	non-dimensional bending moment
BM	bending moment
C	restoring force coefficient
C_{jk}	restoring matrix containing restoring force and moment per unit acceleration
C_p	hull prismatic coefficient
D	hull diameter (or depth)
f	wave frequency
f_z	natural frequency for heaving
f_ϕ	natural frequency for rolling
f_θ	natural frequency for pitching
F_A	hydrodynamic inertial force
F_B	hydrodynamic velocity force
F_C	hydrostatic force
F_D	diffracted wave force
F_I	incident wave force

F_j	complex wave exciting force and moment vector per unit wave amplitude
F_W	wave induced force
g	acceleration due to gravity
$H_{1/3}$ or $\zeta_{1/3}$	significant wave height
I_ϕ	mass moment of inertia for rolling
I_θ	mass moment of inertia for pitching
$I_{A\phi}$	added mass moment of inertia for rolling
$I_{A\theta}$	added mass moment of inertia for pitching
j	mode of excitation and takes the values similar to k for the corresponding modes
k	mode of motion takes 1,2,3,4,5, and 6 for the surge, sway, heave, roll, pitch and yaw, respectively
k_o	wave number
l	strut length
L	hull length
m_A	amplitude of any mode of motion
m_o	moment area under the spectrum curve
m_n	n^{th} moment area under the spectrum curve
M	total body mass (or mass moment of inertia)
M_{jk}	mass matrix containing the mass, mass moment of inertia and products of inertia of the body
$M_3^{(0)}$	vertical bending moment
p	hydrodynamic pressure
Q_j	Green's function at any segment j
s	motion displacement
$\dot{s}$	motion velocity
$\ddot{s}$	motion acceleration
S	hull submergence

s_k	complex motion displacement vector per unit wave amplitude
$S(\omega)$	wave spectral density
$S_m(\omega)$	Spectral density of ship response for any mode of motion
t	strut thickness
T	draught
T_z	natural period for heaving
T_ϕ	natural period for rolling
T_θ	natural period for pitching
T_o, T_m	modal period
T_1 or $T_{1/3}$	average mean period
T_{-1}	energy average period
T_2 or T_z	average zero crossing period
T_4 or T_c	crest to crest period
$T_5^{(0)}$	torsional moment
V	ship (or model) speed
$V_2^{(0)}$	horisontal shear force
$V_3^{(0)}$	vertical shear force
x	surge motion displacement
x_A	surge amplitude
y	sway motion displacement
y_A	sway amplitude
$Y'_{x\zeta}$	non-dimensional surge response
$Y'_{y\zeta}$	non-dimensional sway response
$Y'_{z\zeta}$	non-dimensional heave response
$Y'_{\phi\zeta}$	non-dimensional roll response

$Y'_{\theta\zeta}$	non-dimensional pich response
$Y'_{\psi\zeta}$	non-dimensional yaw response
z	heave motion displacement
z_A	heave amplitude
α_k	phase shift of the maximum of the motion displacement from the incident wave at the origin of the wave coordinate system
β	flatness of a spectrum curve
Δ	displacement
∇	displacement volume
ε	bradness of a spectrum curve
ε_j	phase shift of the maximum of the wave exciting force from the incident wave at the origin of the wave coordinate system
ϕ	roll motion displacement
ϕ_A	roll amplitude
$\bar{\phi}$	velocity potential
ϕ_D	diffracted wave velocity potential
ϕ_I	incident wave velocity potential
$\Gamma(x)$	gamma function in the spectrum
λ	wave length
μ	wave heading angle
μ	scale factor
τ	skewness of a spectrum curve
θ	pitch motion displacement

θ_A	pitch amplitude
ρ	water density
ω (or ω_o)	wave (circular) frequency at zero speed
ω_o	(circular) frequency of the spectrum peak
ω'	non-dimensional wave frequency
ω_e	encounter wave (circular) frequency
ω_e'	non-dimensional encounter wave (circular) frequency
ω_m	modal wave (circular) frequency
ω_z	natural (circular) frequency for heaving
ω_ϕ	natural (circular) frequency for rolling
ω_θ	natural (circular) frequency for pitching
ψ	yaw motion displacement
ψ_A	yaw amplitude
ζ_A	wave amplitude
GM_L	longitudinal metacentric height
GM_T	transverse metacentric height
KG	centre of gravity above keel
KM_L	longitudinal metacentre above keel
KM_T	transverse metacentre above keel
LCB	longitudinal centre of buoyancy
LCF	longitudinal centre of floatation
LCG	longitudinal centre of gravity
MTI	Moment to change trim one inch
TPI	tons per inch immersion
VCB	vertical centre of buoyancy

CHAPTER 1

INTRODUCTION

Chapter 1
I N T R O D U C T I O N

The acronym SWATH, which was chosen by the U.S. Navy in the early 1970's [1], refers to Small-Waterplane-Area Twin/Three-Hull Ships. This is but one of a number of high-performance advanced marine vehicles, substantially different from conventional monohull ships, such as planing crafts, hydrofoil boats, air cushion vehicles, and surface effect ships [2].

Other names, for instance SSS (Semi-Submerged Ship), MODCAT (Modified Catamaran), LWP (Low Waterplane) Area Catamaran and TRISEC (Trisected) Ship have been employed during the projects conducted on this new "species" at the Naval Ocean System Center, at the DTNSRDC, at the Naval Ship Engineering Center and at Litton Industries respectively. SWATH is also well recognised by other names, ie SSP (Semi-Submerged Platform) in the USA, and SSC (Semi-Submerged Catamaran) which is most commonly used in Japan [3].

1.1. History and Development of SWATH Ships.

The development of advanced marine vehicles today places more emphasis on better seakeeping to perform specific tasks rather than improving merchant freight storage, the area in which the present monohull/conventional ship seems to be most efficient. However, in some circumstances a novel concept might possibly lead to a better capability in handling a certain kind of cargo.

The concept behind the development of SWATH ship is similar to that mentioned above. The idea of the SWATH concept is to design a vessel which can sail in waves with as low degradation in its speed as possible, without slamming and without shipping green water. The conceptual

approach is that of an aerofoil slender body at the sea-air surface intersection and the majority of the buoyant volume concentrated away from wave action in a submerged torpedo-like lower hull. By the attachment of an upper hull well above the sea surface slamming and the shipping of green seas may be minimised. This single hull small waterplane area design, which is not dissimilar as the concept proposed in [4], has insufficient transverse restoring moment. The solution to this problem lies in constructing another structure and coupling the two together with an extension of the upper hull, as is done for catamaran ships. The appearance of a SWATH ship, therefore, can be characterised by submerged hulls away from the surface and streamlined surface-piercing struts, attached to the hulls, which support a deck structure well above the waterline. The combination of these three sections is usually referred to as the hull girder, see fig. 1.1. [1].

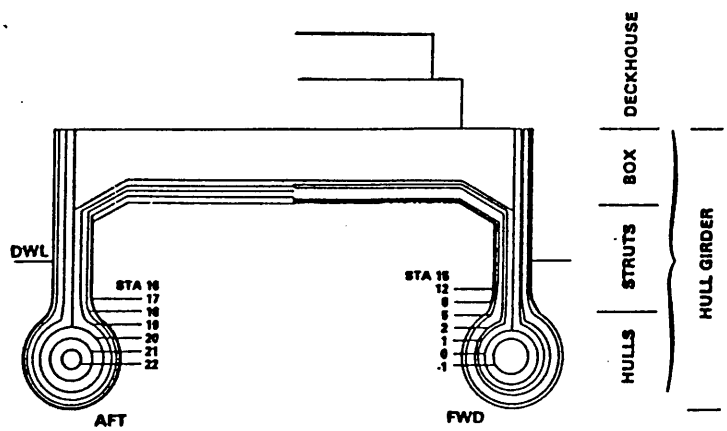

Figure 1.1. SWATH Ship Geometry [1]

In considering the SWATH concept, one may trace the history of SWATH development from two sources, ie multi-hulls and submerged hulls. The first multi-hulls introduced into Europe by Sir Willam Petty were followed by the construction of early catamarans in the 1660's [5,6].

However, it is unwise not to mention the Polynesians, who some centuries ago had sailed on multi-hull craft [7]. Submerged hulls were first introduced by Lundborg in 1880 [8,9,10]. The first SWATH can probably be credited to the design proposed by Nelson in 1905 [11]. The original design of this vessel, however, was not aimed at improved seakeeping performance, but more concerned with the storage of certain freights related to the changing of the weather [12]. Another early design leading to modern SWATHs was by Faust in 1932 [13]. Creed and Lewis first proposed their 'Mobile Seadrome', as a steady mobile landing field for aircraft operations, to the British Admiralty in 1942 and the U.S. Navy. Although an interesting idea, due to other wartime priorities this was not considered a serious contender for an aircraft carrier. Therefore, neither the British Admiralty nor the U.S. Navy attempted to develop the concept further [3,14]. Nonetheless, Creed applied for and was awarded patent for the design [15]. Two decades later Leopold of Litton Indsustries introduced a design labelled as TRISEC, which apparently resembled Creed's with considerable development [16,17]. At about the same time, a moderate waterplane area twin-hull vessel 'Duplus' was built in the Netherlands. The vessel had a maximum speed of 8 knots with control surfaces mounted on the hulls. In 1971 Lang claimed his patent on SWATH, covering stabilising and canard fins in conjunction with control systems [18]. Fig. 1.2. [33] shows SWATH patents claimed by these inventors, and for the sake of simplicity to understand the SWATH history, a diagram is given in fig 1.3 [11].

The first SWATH ship built was a work boat for the Hawaiian Laboratory of the Naval Ocean System Center (NOSC), the 190-ton SSP 'Kaimalino'. This vessel was a creation of a team led by Lang in the U.S. Naval Undersea Center (NUC), based in San Diego. The design of this SWATH was begun in the late 1960's, followed by the construction in the U.S. Coast Guard Shipyard in Curtis Bay in 1972. By 1973 the ship was completed [19-22].

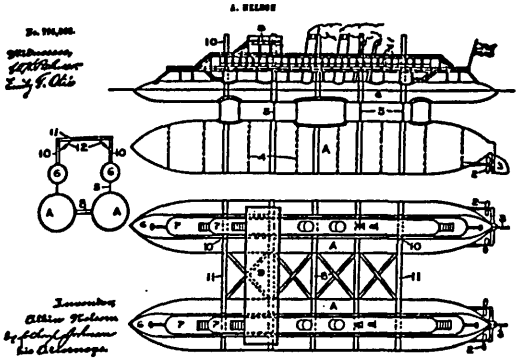

NELSON - 1905

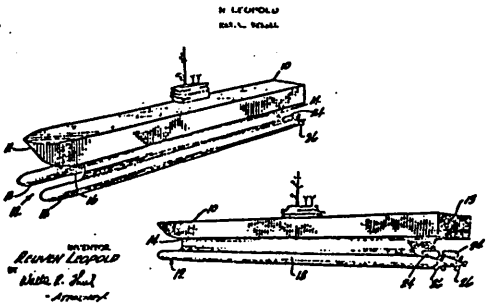

LEOPOLD - 1967

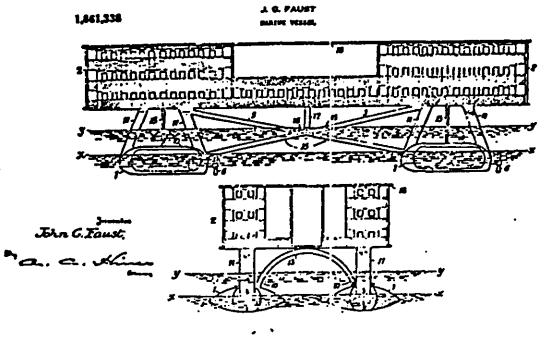

FAUST - 1932

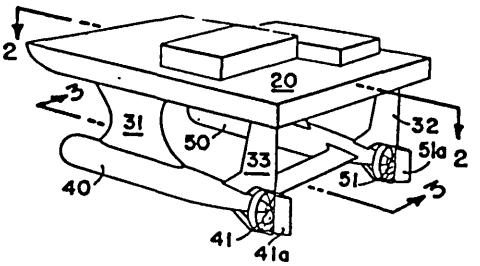

LANG - 1971

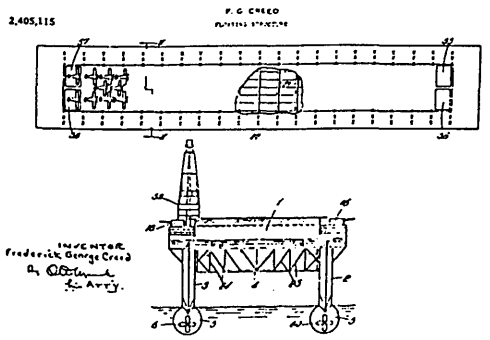

CREED - 1946

Figure 1.2. SWATH Patents [33]

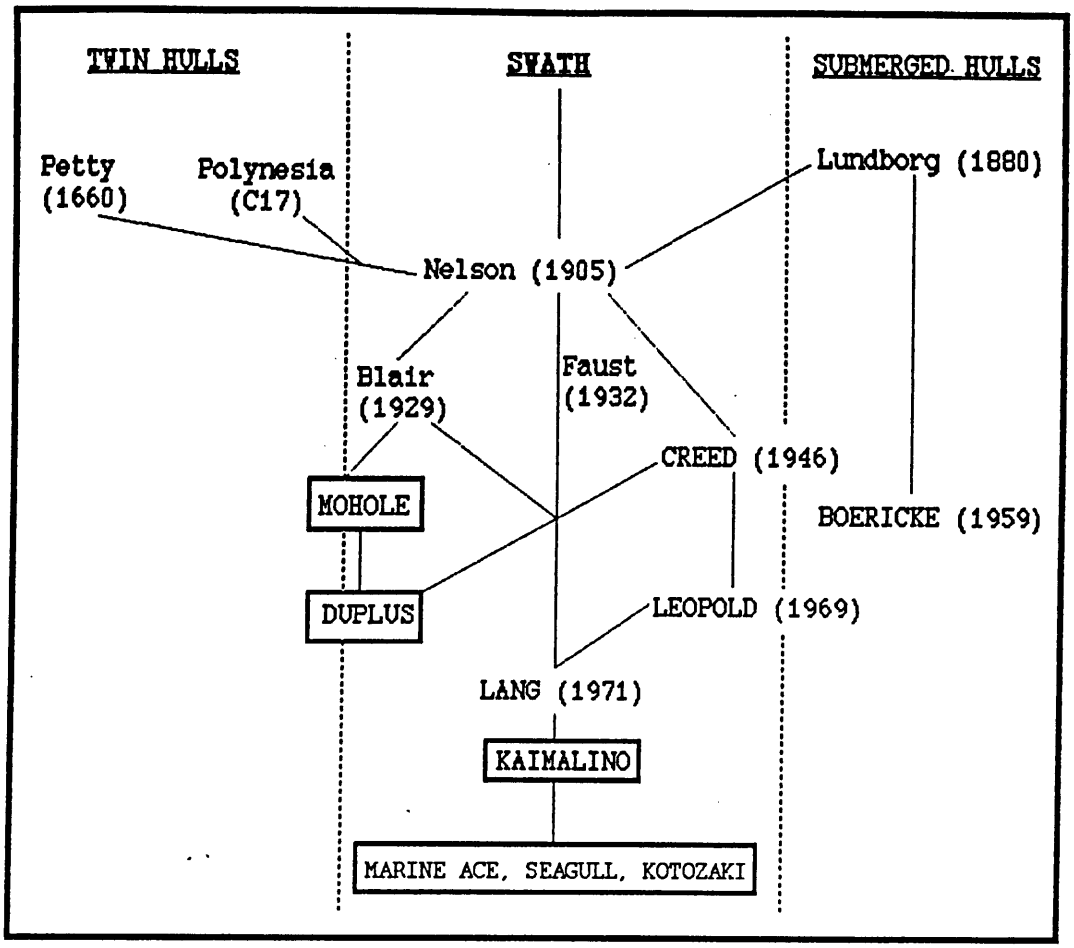

Figure 1.3. A Schematic History of SWATH [11]

Since the 'Kaimalino', SWATH efforts in the U.S., and widespread SWATH research internationally, has resulted in a number of designs as well as the construction of a demonstrator vessel, the 'Suave Lino'. Concurrently, SWATH development commenced in Japan with the Mitsui Engineering & Ship Building Co., Ltd. Five vessels have been built by this company since 1977. These are the test vehicle 'Marine Ace', followed by the construction of a 343-ton ferry the 'Seagull', which was formerly named 'Mesa 80', then a 236-ton hydrographic survey vessel 'Kotozaki', the 2849-ton diver support vessel 'Kaiyo' and the latest a 19-ton leisure

cruiser 'Marine Wave'. Another SWATH hydrographic survey ship, the 'Ohtori', was built by Mitsubishi Heavy Industry, Ltd., which together with Mitsui had been encouraaged by the Japanese Government to foster the exploitation of the SWATH concept. Both hydrographic vessels built in Japan are of similar size to the SSP 'Kaimalino' [14,22].

For a period there was an absence of SWATH ship building in the U.S.A. Then RMI, Inc.,commenced the construction of a 58-ton SWATH in the early 1980's. The SD-60-SWATH, since named 'Halycon' was designed as a commercial or government service boat. The exact application of this ship has not been decided yet. However, the design was projected for operations, such as oceanographic research vessel, diving support vessel, patrol boat, sports fishing vessel etc. The construction was completed and available for demonstration on March 1985 [23]. Existing SWATH ships are listed in table 1.1 and some are illustrated in figs 1.4 up to 1.10, including the 1200-ton medium waterplane area twin hull drilling ship 'Duplus'.

1.2. SWATH Ship Geometry and Characteristics.

As has been briefly outlined in the previous study, a SWATH ship is a displacement vessel in which most of the buoyancy is provided by the twin-hulls positioned well below the water surface clear of the buffeting of winds and ocean waves. A twin-hull form would supply beam adequate for the necessary hydrostatic restoring moments. The slender hydrofoil struts afford increased operational capability through greatly improved seakeeping performances in seaways, including minimising speed degradation in rough water. The arrangement of the hulls and struts in such a way presents a much smaller waterplane area to dynamic wave action than conventional monohull ships or catamarans. This concept has been advantageously applied to the semi-submersible platform employed in the offshore oil industry. The rectangular box

Table 1. Existing SWATH Ships

SHIP NAME	KAIMALINO	MARINE ACE	SEAGULL	OHTORI	KOTOZAKI	SUAVE LINO	KAIYO	HALYCON
KIND OF SHIP	WORK & DEMONSTRATION	EXPERIMENTAL CRAFT	PASSENGER FERRY	HYDROGRAPHIC SURVEY	HYDROGRAPHIC SURVEY	FISHING DEMONSTRATION	SUPPORT SHIP	DEMONSTRATION
COMPLETION	1973	Oct. 1977	Sep. 1979	Dec. 1980	Dec. 1980	1981	Oct. 1984	Mar. 1985
LENGTH O.A. (m)	26.80	12.35	35.90	27.00	27.00	19.20	60.00	18.30
LENGTH P.P. (m)	23.50	11.00	31.50	24.00	25.00	16.80	53.00	---
BREADTH O.A. (m)	13.70	6.50	17.10	12.50	12.50	9.10	28.00	9.15
DEPTH (m)	---	2.70	5.85	5.10	4.60	---	10.60	---
DRAUGHT (m)	4.66	1.55	3.15	3.40	3.20	2.13	6.30	2.13
DISPLACEMENT (MT)	193/244	18.4/22.3	343.00	239.00	236.00	53.00	~ 3500.00	57.00
PAYLOAD (COMPLEMENT)	---	(20 Personnel)	402-446 Pass	(20 Persennel)	~ 36.00 tons	~ 14.00 tons	~ 860.00 tons	5.25~1tons (20 Passenger
STRUT TYPE	TWIN	TWIN/SINGLE	SINGLE	SINGLE	SINGLE	SINGLE	SINGLE	SINGLE
HULL MATERIAL	HYBRID	ALL AL	ALL AL	STEEL (Hull) AL (Deck House)	HYBRID	ALL AL	ALL STEEL	ALL A
PROPULSION SYSTEM	GAS TURBINE & CHAIN DRIVE 2 x 2250 PS	GASOLINE BEVEL GEAR 2 x 200 PS	DIESEL BEVEL GEAR 2 x 4050 PS	DIESEL BEVEL GEAR 2 x 1900 PS	DIESEL BEVEL GEAR 2 x 1900 PS	DIESEL BEVEL GEAR 2 x 425 PS	DIESEL/ELECTRIC D/G 4 x 1250KW MOTOR 4x860 KW	DIESEL
PROPELLER	C.P.P	F.P.P.	F.P.P.	C.P.P.	C.P.P.	F.P.P.	C.P.P.	C.R.P.P.
FIN CONTROL	AUTOMATIC	AUTOMATIC	AUTOMATIC	MANUAL	MANUAL	AUTOMATIC	MANUAL	AUTOMATIC

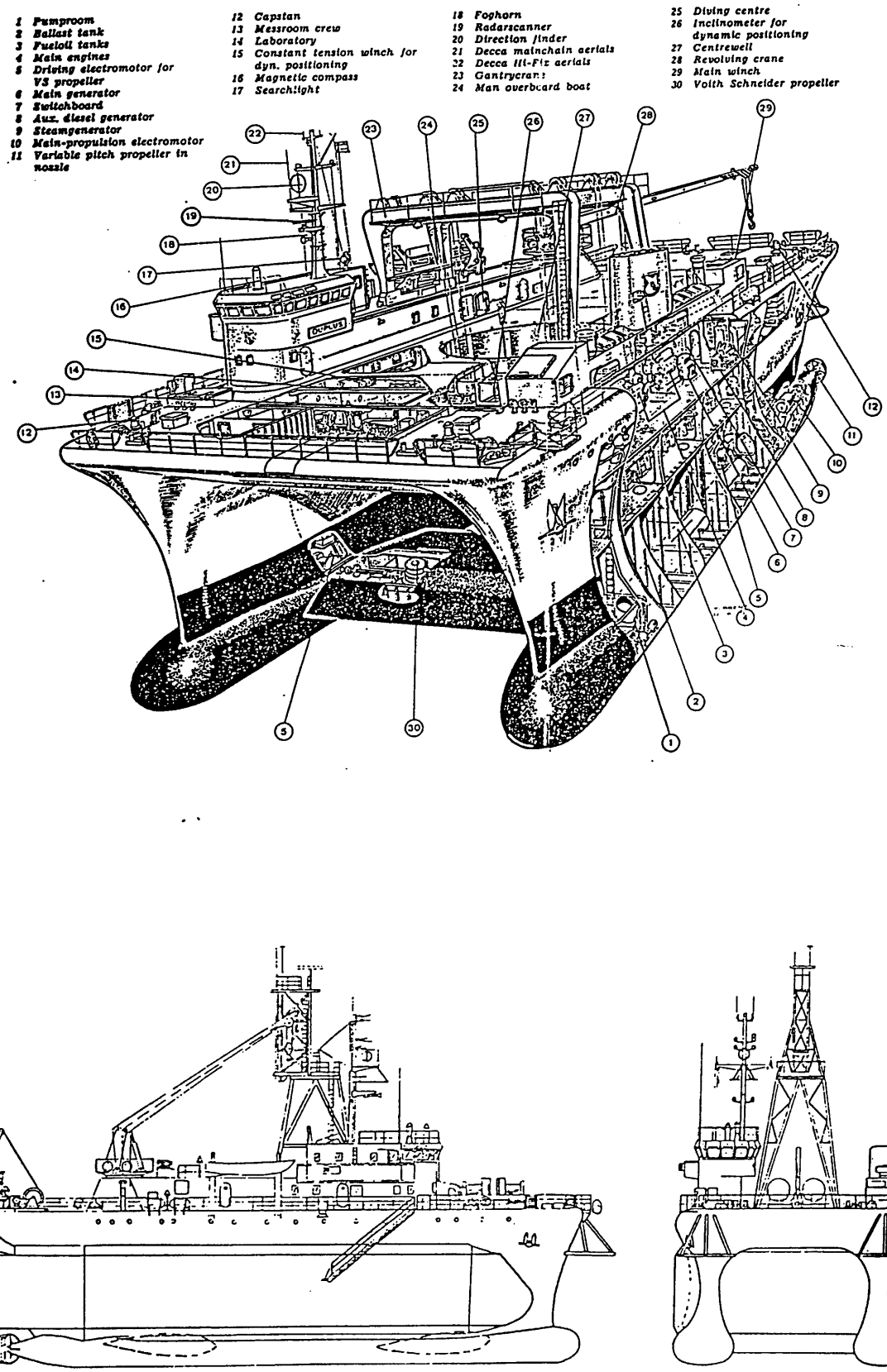

Figure 1.4. The 'Duplus'

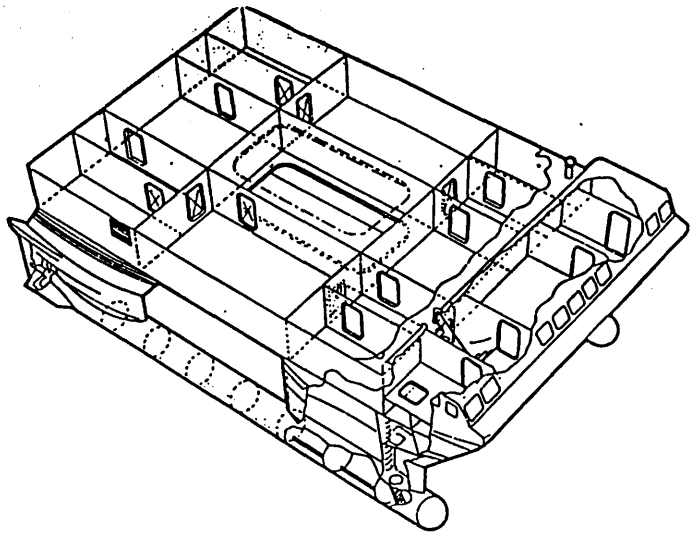

Cutaway showing basic hull configuration of SSP *Kaimalino*

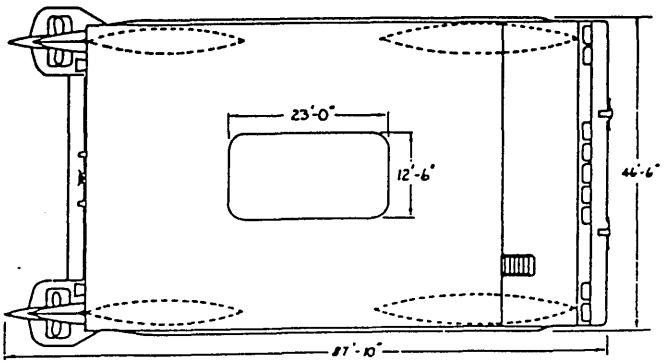

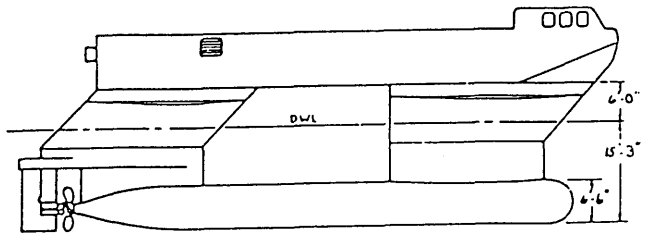

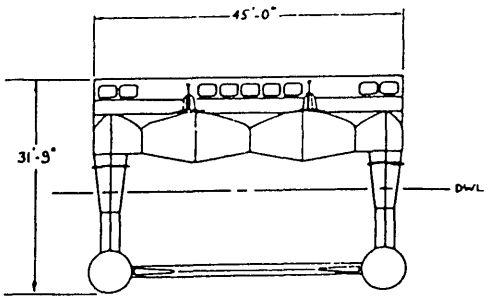

General arrangement of SSP *Kaimalino*

Figure 1.5. General Arrangement Plan for the SSP 'Kaimalino'

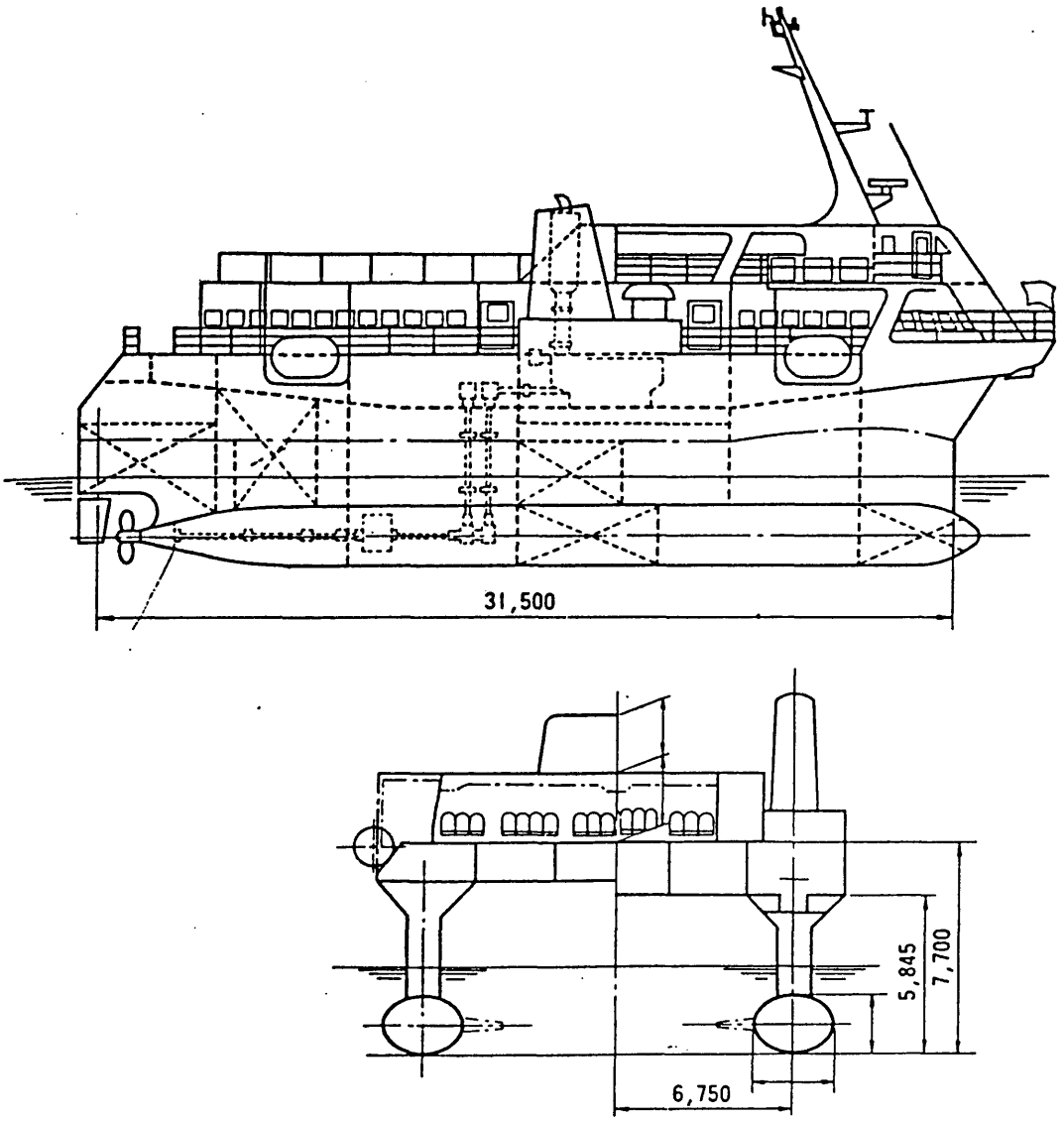

Figure 1.6. Profile and Section Drawing of Mitsui's Passenger Vessel SSC 'Seagull'

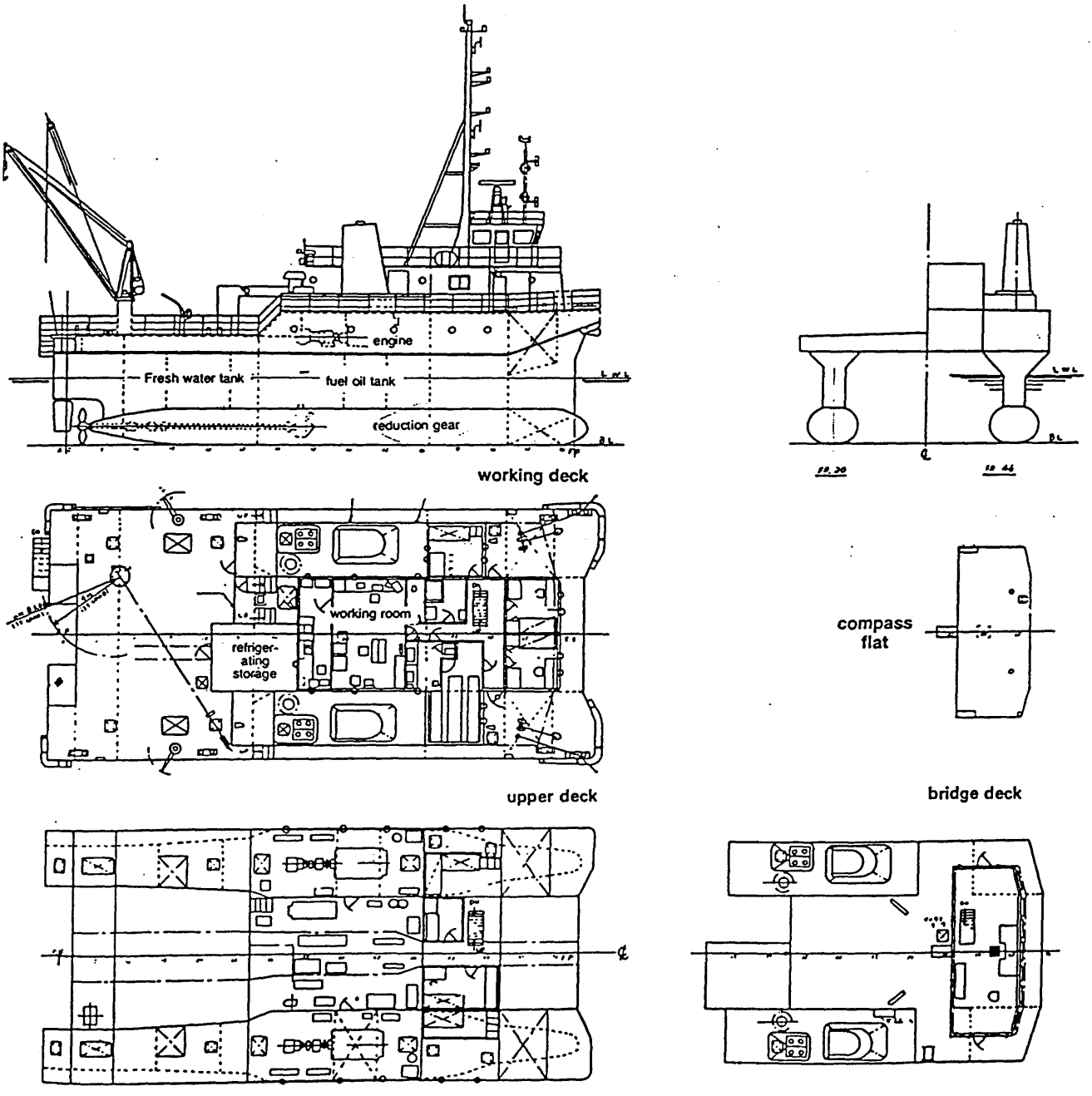

Figure 1.7. General Arrangement of 'Kotozaki'

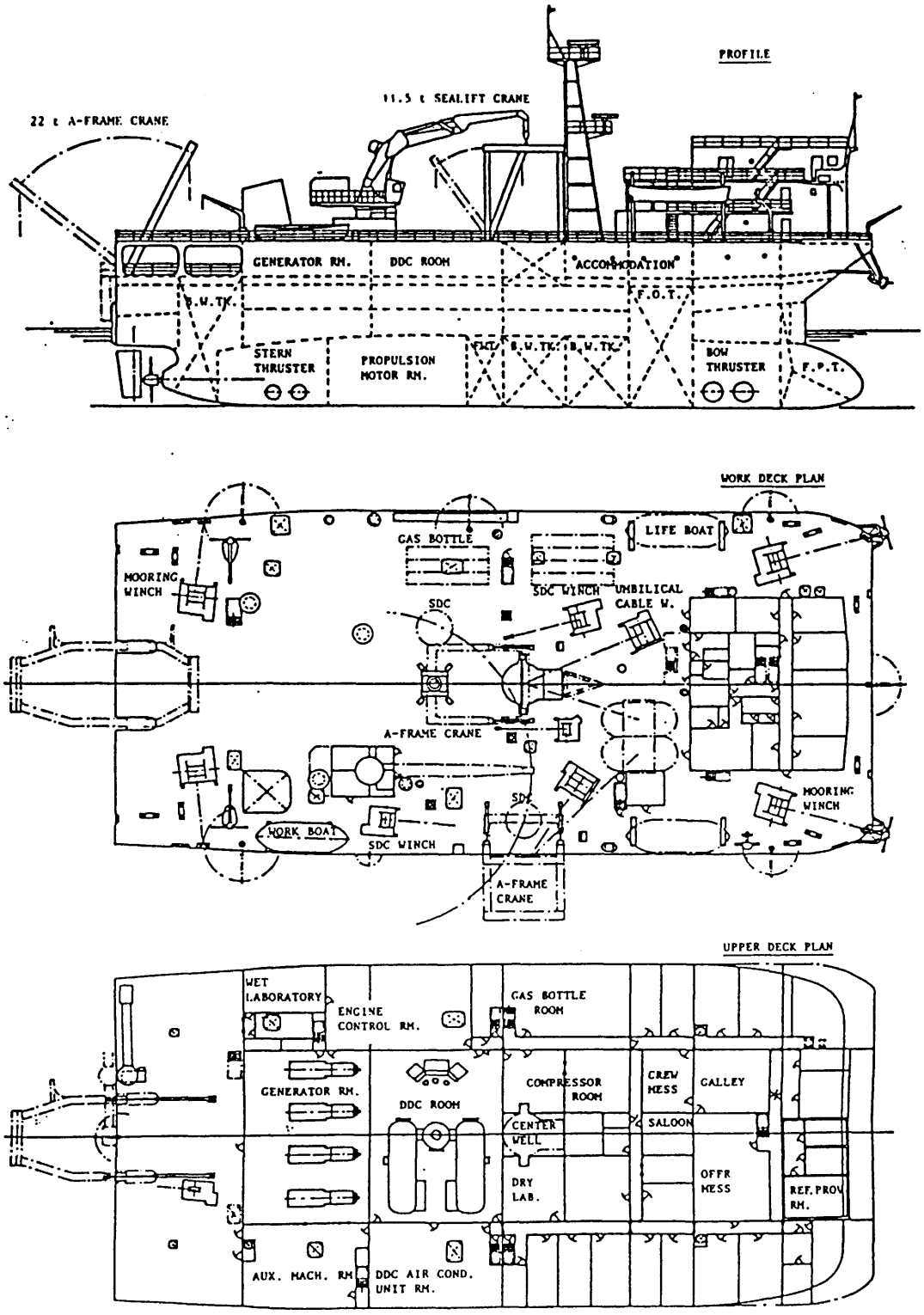

Figure 1.8. General Arrangement Plan for the 'Kaiyo'

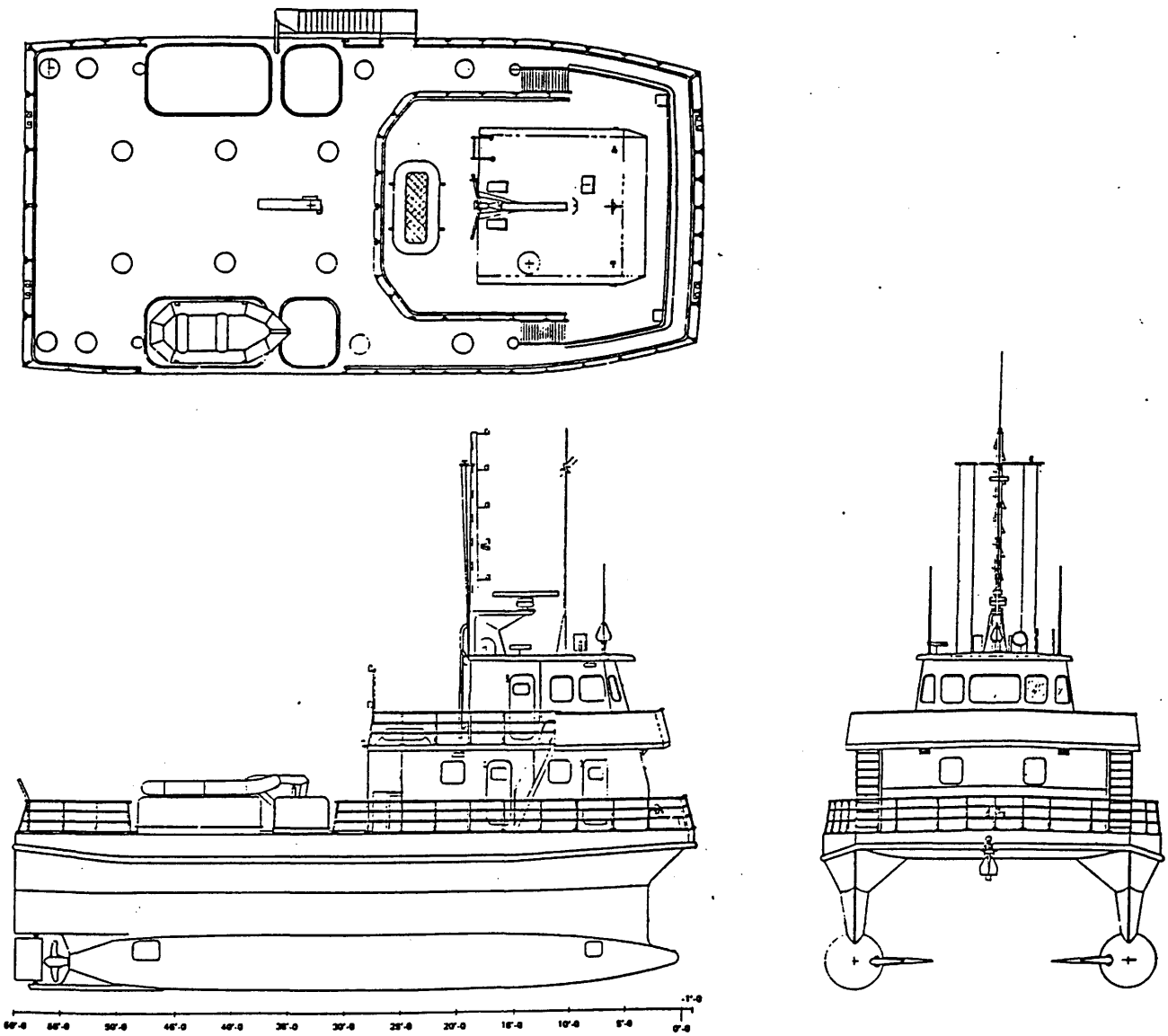

Figure 1.9. RMI's SWATH Demonstrator
the 'Halycon'

cross structure supported by struts a considerable distance above the water make adverse wave effects, like deck bottom slamming or deck wetness, avoidable.

1.2.1. The SWATH Hulls.

A SWATH ship incurs a penalty in greater frictional resistance due to the greater wetted surface area compared to a comparable monohull. Nevertheless, substantial achievement can be made in overall resistance by shaping the lower hulls and selecting the best length diameter ratio. The aspect of hull shaping on a submerged hull had been explored by Boericke [4] and more recently by Chapman [24]. The cross sectional area shape of the submerged hulls can be circular, elliptical or rectangular. Other alternatives include circles with flattened tops and bottoms and vertical oval sections. The circular shape of the cross sectional area gives the minimum wetted surface area per unit cross-section, so it may lead to low frictional resistance. Moreover, this shape is more efficient to withstand the design pressure. As an example, circular hulls are applied for the SSP 'Kaimalino', fig. 1.5.

The elliptical cross-section shape, such as that constructed for the 'Seagull', fig. 1.6, provides less hydrodynamic side loads but it may increase damping effects and added virtual mass. Furthermore, elliptical hulls can allow lower draught. The disadvantages of the use of elliptical shapes are increases in weight and consequently higher manufacturing costs. Although the rectangular cross-section hull is the cheapest to construct, it may not be suitable for high speed SWATH ships since this shape tends to be heavier, gives greater drag and also provides smaller headroom. However, this shape remains suitable for stationary marine vehicles such as semi-submersible offshore drilling rigs.

Hull shaping not only applies to the cross-section but also the longitudinal plane section. In this aspect efforts are primarily directed to improve the capability of arranging the machinery space in the lower hulls as well as improving resistance and seakeeping characteristics. Simple hull designs with constant cross-section along the hull length and contoured nose and tail offer ease of construction but for a small ship may not allow machinery installation. Another option is that the hull cross-section can remain constant with a local bulge to accommodate machinery. Alternatively, a simply contoured hulll may be chosen, constructed with a maximum cross-section at the mid length. The addition of bulges at the nose and tail may reduce resistance at high speeds and allow even greater control over the buoyancy distribution. More details of this review can be found in [25].

Hull dimension is mainly characterised by the length diameter ratio, L/D, which radically influences the ship features. L/D lies between 10 and 15 for the hull length below 60 metres. For the bigger ship, where the increase in the hull diameter with respect to the requirement of machinery installation is no longer critical, increasing the ratio to between 15 and 20, reductions of resistance and form drag becomes possible. Nevertheless, the skin friction will increase as a result of the larger wetted surface area. Meanwhile, a higher ratio changes the water flow velocities into the propeller which in turn alters the quasi propulsive coefficient. From another viewpoint, a smaller diameter improves the ability to withstand external pressures. Deeply submerged hulls give a better sonar performance and permit easier diver and submersible operations.

1.2.2. The SWATH Struts.

There are three shapes of cross-section generally constructed as the column of a floating structure, namely circular, rectangular and aerofoil or streamline shaped.

Only the first two shapes are commonly utilised for offshore drilling rig vertical columns since the resistance is not the most prominent consideration on a stationary marine vehicle. Therefore, for a SWATH ship either aerofoil shaped or streamlined struts are the best option, as these shapes give the less drag. In SWATH design, determining the number of struts per hull is one fundamental decision that must be made by the designer. The number of struts per hull affects the magnitude of side loads as well as the resistance experienced by the ship.

The tandem strut configuration should offer lower side loads, which also means lower bending moment imposed on the cross structure. With regard to maneouvring, a tandem strut SWATH theoretically gives a turning circle of approximately five times the ship length, compared to ten times for a single strut SWATH. Another attribute, is that four independent struts provide a high degree of control towards LCB and LCF adjustment so that desired motion performances may be achieved, in addition a tandem strut design, leads to the least wetted surface area and the least structural weight.

A single strut design certainly offer some advantages compared to a tandem strut configuration. This offers more freedom in the machinery arrangement as well as easier access to the lower hull. Although control over LCB and LCF is slightly restrained, however, as a result of higher GM_T the roll stiffness can obviously be adequate to ensure that quasi static heel angles are avoidable.

The most extensive comparison between single and tandem strut per hull has been carried out experimentally on SSC 'Marine Ace' by Mitsui under the sponsorship of Japan Marine Machinery Development Association (JAMDA) [26]. During the test it was found that the resistance of the single strut type is lower than the tandem strut, indicating

a greater miscellaneous resistance due to spray drag, induced drag on fins etc contributes the total resistance significantly.

The strut height dictates the deck bottom clearance and draught. A relatively deeper draught allows a flexibility in choosing the propeller diameter. This also ensures that the propeller submergence can be maintained in any sea state. However, deeper draught in turn influences the ship resistance and, moreover, a limitation in usable dock and harbour facilities, should also be considered by a designer.

Strut dimensions are generally described by strut thickness to chord ratio, t/l, strut thickness to hull diameter ratio, t/D, or in term of strut thickness to ship displacement$^{1/3}$ ratio, $t/\Delta^{1/3}$. A low t/l ratio offers lower wave making resistance at the expense of limitation on the machinery access into the lower hulls. Most designs have t/D ratio lying between 0.5 to 0.25. In order to improve TPI, GM_T and ease access, the U.S. Navy recommends a $t/\Delta^{1/3}$ ratio of about 0.17, whereas most of the existing SWATH ships have a ratio of between 0.2 and 0.1 [25].

1.2.3. The SWATH Cross Deck Structures.

The cross deck geometry of a SWATH ship is rectangular in section with an option for port and/or starboard sponsons. The bottom of the deck is the wet deck, and the distance from this deck to the waterline is defined as box clearance. When apportioning volume between struts and box, the line of demarcation is at the wet deck. Control of strut and box longitudinal separation is gained through the use of box set back. The box clearance is remain an unknown parameter until an adequate clearance to avoid adverse wave effects is thoroughly investigated. Based on the SSP 'Kaimalino' model investigation, Lang reported that

bottom slamming can be reduced by mounting well faired double bows on a 20^0 flat section [21]. Another observation shows that a three hulled SWATH provides more benefit because of its smaller deck area forward, so slamming loads will be much lower [27].

The box depth should be designed by considering the bending moment and shear force imposed by the wave loads on the deck structure through the struts. A ship length below 30 metres should be able to have one full deck in the cross structure, whereas the larger ships could be designed with multiple decks.

1.2.4. Some Basic Design Parameters.

Basic ship parameters are always the most important data required in the design process, and this is also true of SWATH ship design. The terms used here are, therefore, not different from those used for monohull ships with, of course, many more additional parameters as a consequence of the more complex SWATH geometry. In early days of SWATH ship development researchers suffered from the lack of historical design data, so that early SWATH ships owed nothing to conventional ship design data.

The SWATH ship overall length is related to the submerged hull length and the strut length. Early SWATH ships had an overall length the same as the hull length. The hull length is mainly dictated by the displacement required, resistance characteristics, machinery, ballast, fuel arrangement and strut length arrangement.

The relationship of beam to length or displacement, ie L/B or $B/\Delta^{1/3}$, of a SWATH ship is different from monohull experience, this results in new challenges and even opportunities in the top side arrangement. Beam is the parameter that influences the transverse stability most, thus beam should be considered carefully. A greater value of

L/B means shortening the righting arm but an excessive beam also means greater bending moment to be resisted by the cross structure.

A consequence of locating most of the SWATH ship buoyant volume well below the water surface is a much deeper draught compared to an equivalent size of a monohull ship. For large ships this deeper draught leads to some limitations due to dry docking facilities and harbour water depth. However an increase in draught allows better support on underwater work. In addition propeller cavitation and ventilation which are significantly affected by the shallow submergence of the propeller can be substantially reduced [1].

The summation of deeper draught, considerably high box clearance and box depth is relatively greater depth to the main deck, which also means greater freeboard. The drier deck of a SWATH ship is one of the particular benefits of greater depth and freeboard.

The SWATH basic design parameter relationships are summarised and listed in tables 1.2 [1,3] and 1.3 [25]. The comparison between a SWATH ship with an equivalent size of monohull in term of basic design parameters is given in table 1.4 [3].

1.3. Advantages, Disadvantages and Some Potential Applications of SWATH Ships.

Having studied the concept, some characteristics and basic design parameters of the SWATH ship, one can try to clarify advantages and disadvantages of a SWATH ship compared to a monohull, as well as some potential applications of a SWATH ship.

Table 1.2. SWATH Ship Basic Design Parameters [1,3]

Volume of displacement :	
∇	: 65 ~ 90% contained in the hulls (average 80%)
	: 15 ~ 20% contained in the struts
Hull :	
L/D	: 14 ~ 22 (average 15 ~ 17) (>L/D for the design ≥ 15,000 tons)
Hull Prismatic Coefficient :	:
C_p	: 0.45 ~ 0.93 (average 0.7 ~ 0.9)
Strut thickness :	
t/D	: 30 ~ 60%
l/t	: 5 ~ 15 for tandem strut per hull
	: 20 ~ 40 for single strut per hull (for $\Delta \geq$ 15,000 tons average l/t 30 ~ 40)
Strut Waterplane Area Coefficient	: 0.7 ~ 0.8
Deck :	
L/B	: 2.0 ~ 5.0 (>L/B for ships ≥ 15,000 tons)
Vol. of Deck Houses	: 1/3 of total vol. of hull girder (average 20 ~ 25%)
Vol. of struts and hulls	: 30 ~ 50% of total internal vol. (average 35 ~ 40%)
SWATH ship density	: 15 ~ 20 lbs/cuft

Table 1.3. Basic Design Parameter Relationships [25]

$V_{hull}/\nabla = 0.8$	
Length overall :	$L = 5.4\Delta^{1/3}$
	$L = 6.2\Delta^{1/3}(\frac{v}{\sqrt{v+2}})^2$
Breadth overall :	$B = 2.39\Delta^{1/3}$
	$B = 0.46L$
Design draught :	$T = 0.57\Delta^{1/3}$
Depth :	$D_{Wet\ Deck} = 1.56T$
$D_{Main\ Deck} = 2.08T$	
Hull dimensions :	$L/D = 10 \sim 15$ $(L < 60m)$
(circular hulls)	$L/D = 15 \sim 20$ $(L > 60m)$
	$D = 0.336\Delta^{1/3}$
	$D = 0.6T$
Hull submergence :	$S = 0.32\nabla^{1/3}$
	$S/D = 1.00$ $(D < 4)$
	$S/D = 1.25$ $(D > 4)$
	$S/T = 0.70$
Strut thickness :	$t/\Delta^{1/3} = 0.1 \sim 0.2$
	$t/D = 0.25 \sim 0.5$
Structural Weight/Δ = 0.43	
Payload/Δ = 0.13	
Endurance :	
$Log_{10}(endurance) = 2.092 - 2.9\ log_{10}(\frac{v}{\sqrt{g\Delta^{1/3}}})$	

Table 1.4. Comparison Between SWATH and Monohull Ship

Total internal volume :	SWATH 20 ~ 30% > monohull
Length :	SWATH 30 ~ 40% < monohull
Beam :	SWATH 60 ~ 70% > monohull
Draught :	SWATH 60 ~ 70% > monohull
Wetted surface area :	SWATH ± 60% > monohull
Depth to main deck :	SWATH ± 75% > monohull
	SWATH ± 50% > monohull
	(for larger ships)
Freeboard :	SWATH ± 25% > monohull

The primary advantage of a SWATH ship is its relatively lower magnitude of deck motions, ie heave, roll and pitch, in a seaway while at rest or underway, which also means lower magnitude of acceleration of the related modes. This remarkable feature directly influences the improvement of shipboard activities and safety, such as crew performance, deck equipment operability and passenger comfort. From this view point a SWATH ship is suitable to be employed as an air-capable ship and as a passenger ferry.

The combination of steadiness with its station-keeping ability makes a SWATH ship capable to carry out over-the-side work. This capability was demonstrated when the SSP 'Kaimalino' successfully recovered floating equipment in a seaway after a 1000-ton monohull failed in several attempts [28]. In addition, as a result of the high degree of directional stability such work can be conducted by a SWATH ship at any heading angle without difficulties while a monohull is restricted to head seas. The SWATH seakeeping could possibly be enhanced as much as 50 percent by fitting active control surfaces, that is canards forward and stabilisers aft [3]. Considering this performance a SWATH ship offers a great potential to be employed as a support vessel.

In terms of regular transportation, reliability in maintaining the maximum speed in foul weather in accordance with the required schedule often can not be fulfilled by a moderate, or even large, monohull ship. A relatively small SWATH ship, however, could possibly satisfy such requirement, as its combination of slender streamlined wave-piercing struts and deeply submerged hulls with a reasonable installed power makes it amenable for operation in heavy seas. Thus a SWATH ship can be considered as the merging of the speed qualities of vehicles such as hovercraft, planing boats or hydrofoil with the good seakeeping qualities of semi-submersibles [29]. Comparative studies of SWATH and monohulls were made by the U.S. Navy in 1979. One of these was in speed performance in higher sea states, where the SWATH ship shows its superiority over the monohull, as shown in the curves of fig. 1.10 [30].

A SWATH ship is well known for having a spacious unobstructed stable deck. This certainly is of great importance for naval activities, such as V/STOL (Vertically/Short Take Off and Landing) aircraft carrier or as a missile launching base, as well as for some commercial and research operations. Due to this characteristic accommodation spaces above the main deck level can be arranged more conveniently. Odd volumes in the hull girder, especially in the struts and hulls should be compensated by correct arrangement of deck houses. Existing designs have provided as much as one third of the total usable volume in deck houses.

A SWATH ship offers a high degree of survivability when damaged. This is mainly provided by the cross box which provides a huge reserve of buoyancy in case of underwater damage. The impact of a large missile on the side can possibly sink a small monohull frigate, but this would not be the case for a SWATH frigate. As the first strut that is hit resists the missile blast, the other strut may survive

and the propeller of this side can still maintain its function. The situation would be more beneficial when a tandem strut per hull configuration is utilised. Nonetheless, a versatile counter flooding ballast system should still be installed due to vulnerability towards asymmetric flooding and static heeling after damage.

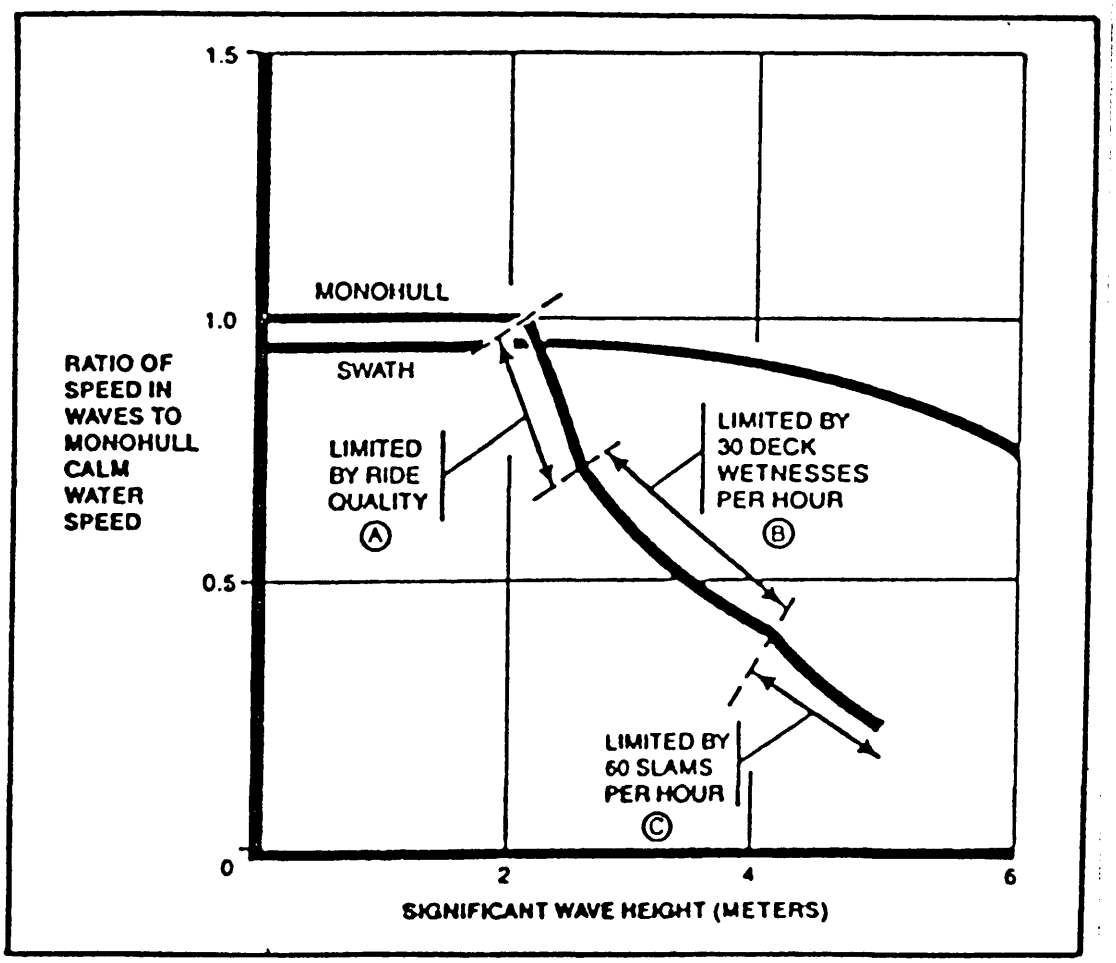

Figure 1.10. SWATH and Monohull Speeds in Rough Seas [30]

For an underwater work support vessel the deeply submerged hull is a particular advantage [31]. Sonar systems and other equipment installed in the lower hulls should work with higher accuracy, particularly when using electric power

as the prime mover giving reduction in noise and vibration. The capability of underwater observation could be improved by mounting a plexiglass dome at the fore part of the hull to allow 180 degrees underwater viewing, as was done on the SSP Kaimalino [32]. In naval activities these features could obviously satisty the mission carried out by a mine sweeper ship.

Although the concept of SWATH ship is new but, the required technology, unlike other advanced marine vehicles which require high technology considerations, is not much different from the technology of monohull ships. This means that SWATH construction can be implemented using standard shipbuilding technology with, of course, some extensions to match the unusual SWATH geometry [32]. Nevertheless, some believe that SWATH ship owes more to the technology experiences of semi-submersibles rather than to the conventional ship [33].

The advantages of SWATH ships mentioned previously are not achieved without drawbacks. The first significant drawback as a result of low waterplane area of a SWATH ship is a lower tons per inch immersion (TPI). TPI indicates the sensitivity of a ship's draught to changes in weight during design or operation. As a consequence of reduced TPI in SWATH designs, a much greater draught change would occur on aSWATH than on an equal displacement monohull for a given change in weight. This is then followed by considerable change of box clearance so that in certain cases deck bottom slamming becomes more adverse.

Secondly, a low waterplane area with short strut length brings about a reduction of mement to change trim one inch (MTI), which is a direct measure of the trim sensitivity of a ship. A ship with very low MTI, which also means low hydrostatic restoring moment, would be vurnerable towards pitch instabilities in following seas. An extra careful consideration of weight distribution including the

accuracy of LCB and LCG estimation is therefore required in SWATH ship design. In addition, this would also require a sophisticated counter ballast system. Because of these deficiencies a SWATH ship certainly would not satisfy the mission of general cargo ships which require large variable payload capability.

Another problem which has arisen in association with the weight sensitivity, is exploration of new alternatives for lighter structural material than steel for SWATH construction in order to increase DWT/Δ ratio and further increase in payload. So far only alumunium is technically and economically considered as an appropriate material substitute for steel. Existing SWATH ships to date, apart from SSC 'Kaiyo' which is all steel constructed, were either constructed using all alumunium or hybrid, usually alumunium upper hull and steel struts and lower hulls. No serious problems have been reported concerning the use of all alumunium or hybrid structure except on 'Suave Lino' which experienced reccurent cracking on the welding joints [34]. The use of Dupont's explosion bonded alumunium plate Dataclad to the primary joint between alumunium and steel has been successfully adopted in the construction of SSP 'Kaimalino' [35].

Two hulls geometry of SWATH ships result in larger wetted surface area than monohulls, see fig. 1.11 [36]. This creates higher total resistance in calm water operations as it is only a very high speed that the reduced wavemaking resistance of SWATH will give low total resistance than an equivalent monohull. Theoretically, with the same amount of power installed, a SWATH ship will have a maximum speed approximately two knots less than an equivalent displacement monohull ship [3]. Another consequence of increasing resistance is higher fuel consumption. Moreover, such a geometry entails more skin plating and stiffening.

Small SWATH ships suffer from limitations in

machinery arrangement. Small struts make machinery installation and access for maintenance very difficult. Placing the prime mover in the box brings about problems in designing the transmission system, in addition to the reduction in shaft transmission efficiency. Some transmission systems, namely chain-drive, Z-drive, hydraulic and electrical, have been proposed to overcome the problem. The use of chain system tends to be more complex and more costly. SSP 'Kaimalino' experienced a broken shaft in one of the chain-drive system early in her life [37]. The Z-drive system is generally considered to be the most suitable as this gives higher efficiency, low cost and lighter weight [31].

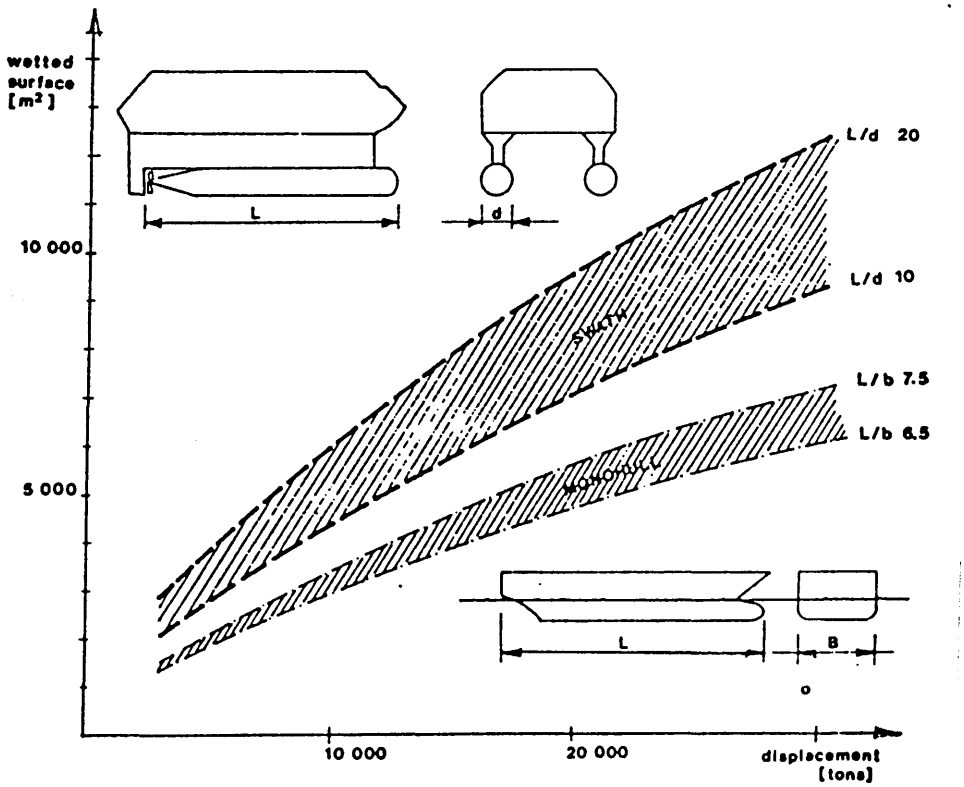

Figure 1.11. SWATH and Monohull Wetted Surface Area [36]

The SWATH ship's wider beam and deeper draught restrict the harbours, drydocks and channels to which it will have access. Higher freeboard makes passenger and cargo transfer onto the quayside (or smaller craft when working alongside) more difficult.

The bending moment on the cross deck structure and the motion characteristics of SWATHs with a large single strut per hull are likely to be troublesome while at rest in beam seas. Strenghtening should be provided at the strut-box intersection to resist any fatigue loads as SWATHs are inbraced structures.

Some advantages in motion performance gained by the inherently high degree of directional stability are obtained in expense of large turning circle diameters and difficulty in turning at high speeds [38].

The most severe hindrance to the development of the concept is concern over cost and lack of design data which have discouraged progress in development and construction of SWATH vessels.

1.4. Experimental Studies on SWATH Ship Motions and Structural Loadings.

Research conducted to investigate SWATH ship motion and structural loadings experimentally constitutes a part of the overall SWATH design programme at the University of Glasgow. Active research on SWATHs at the university began in 1978 and evolved from a history of research into semi-sumersible vessels of the type used in the oil industry [11]. The earliest project was concentrated on the design of a small research vessel using a three-hulled SWATH configuration [27, 39-43]. This was designed for restricted waters and identified the merits of various configurations and the operational superiority of SWATH over the conventional monohull for certain roles. The project since then has broadened into the design of larger, faster vessels intended for several applications, namely large open sea research vessels, higher speed small warships/offshore patrol vessels, oil industry emergency support and rescue

vessels and as oil industry service support vessels [38].

The main effort in the early stages of the programme was the development of computer programs to produce the stability, resistance, seakeeping, dynamic structural loads and basic design parameter simulation data and thus enable the designer to compare SWATH configurations with other platform alternatives. Gradual improvement in the computer programs was made by revising and modifying the initial work and the application of more sophisticated methods. The improved computer programs with their high degree of versatility are now able to satisfy naval and commercial demands and those of research establishments.

The objective of the research reported in this thesis is to generate experimental data on SWATH ship motions and dynamic structural loads. Such data is aimed at providing a comparison reference and validating the analytical models developed. Ultimately the data is expected to be useful for considerations in the design of high performance SWATH ships.

The experiments were all conducted in the 76m x 4.6m x 2.5m towing tank at the Hydrodynamics Laboratory of Glasgow University. The model employed was the SWATH1 model which has circular hulls each with two struts. The existing facilities and instrumentation at the laboratory, supported by experienced technicians are important factors in obtaining reliable data from experiments. During the experiments, data acquisitions was carried out using a multi-channel chart recorder and/or applying a computer program run in the VAX 11/730 computer system available at the Hydrodynamics Laboratory.

In order to maximise the experiment data acquisition some other investigations on hydrodynamic performance, such as upwelling, sinkage and trim, were also carried out simultaneously. Data obtained from regular seas was then

analysed with respect to random seas by using some computer programs written for this purpose.

Another SWATH model, ie SWATH2 model with hulls of rectangular cross-section, had been built for resistance experiments. Investigation on its motion in regular head seas with forward speed has been conducted and the results compared with those from the SWATH1 model. Observations on its motion in other sea hedings have not yet been carried out due to limited time.

The SWATH1 model has recently been converted into a single strut per hull configuration by connecting the outer sides of its original struts with flat PVC plates. This model was then renamed SWATH3. Only a few investigations on resistance features of this modified model have been conducted at the present time. It is essential to observe the motion and other hydrodynamic performance of this design so that a comparison with the tandem strut prototype can be presented.

CHAPTER 2

THEORETICAL BACKGROUND OF SWATH SHIP MOTIONS

Chapter 2.

THEORETICAL BACKGROUND OF SWATH SHIP MOTIONS

2.1. The Nature of SWATH Ship Motions.

SWATH ship has been proved to have much lower motion than monohull ship in any mode of oscillation. This lower motion is obtained from the combination of deeply submerged hulls and the small waterplane area of the struts. The deeply submerged hulls, which provide the buoyancy, will experience low wave exciting forces, whereas a small waterplane area of a SWATH ensures the natural frequency will be much lower compared to an equivalent conventional vessel. The relationship between the natural frequency and the waterplane area can be seen in heave mode of motion as follows :

$$\omega_z = \sqrt{\frac{\rho g A_w}{M + AVM_z}} \qquad (2.1)$$

This expression shows that a decrease in A_w (waterplane area) brings about lower natural frequency ω_z. The other expressions of natural frequency, for roll and pitch modes of motion are

$$\omega_\phi = \sqrt{\frac{\rho g \nabla GM_T}{I_\phi + I_{A\phi}}} \qquad (2.2)$$

$$\omega_\theta = \sqrt{\frac{\rho g \nabla GM_L}{I_\theta + I_{A\theta}}} \qquad (2.3)$$

Again, compared to monohull ships the roll and pitch natural frequencies of SWATH ships will be much lower. The lower natural frequencies in heave, pitch and roll motions also means that longer natural periods are gained. Long natural periods prevent the resonance with the most sea waves, thus degradation of SWATH operability will be avoided. The most striking comparison of ship motions

resulted from the joint U.S. Navy and Coast Guard trial sea trials conducted off Hawaii in 1978 [44,45]. The ship used during the comparative trials are a 3100-ton high endurance Coast Guard cutter, USCGC 'Mellon', a 220-ton U.S. Navy SWATH, SSP "Kaimalino' and a 110-ton USCG patrol boat 'Cape Corwin'. The SWATH experienced slightly less pitch and heave, and much less roll. The curves in fig. 2.1 show the superior seakeeping of small SWATH ship as compared to a monohull ship which is 15 times larger. It should also be noted the 200-ton SWATH has half the roll motion of the 3100-ton monohull.

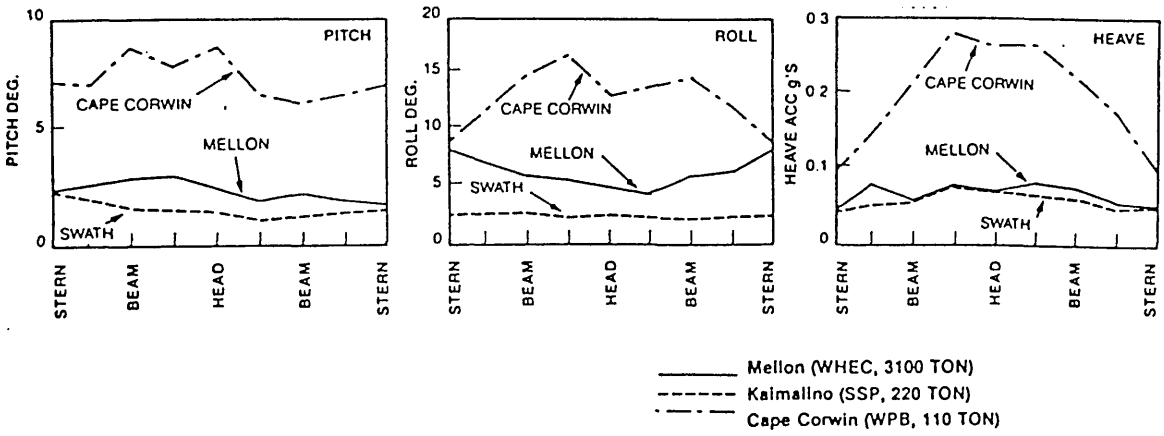

Figure 2.1. US Navy/Coast Guard Seakeeping Trials Motions Comparisons [44,45]

2.2. Concept of Fluid Forces on a Cylinder in Waves.

The basic understanding of ship motion can easily be studied by considering the case of a freely floating cylinder in a train of regular harmonic (sinusoidal) waves which are long with respect to the cylinder [46].

When surface waves pass through a floating body the ambient fluid will exert hydrodynamic forces and moments on

the body. These forces and moments consist of two components, ie the unsteady exciting components, which are known as the first order forces, lead to the body oscillations and these components are linearly proportional to the wave height. On the other hand, second order forces are attributable to the non-linear effects and these components are generally small and proportional to the square of the wave height.

Fig. 2.2 [47] shows the diagram of the division of the fluid forces and moments exerted by the surrounding fluid on the floating body which subjected to the surface waves. The following clarification is concerned with the division of forces (or moments).

The first order oscillatory forces can be divided into two main components, namely the viscous force and the pressure force. The viscous force, F_V is brought about the fluid viscosity and it deals with the fluid flow velocities relative to the body. The flow velocities are generated by the body motion and by waves. The former, ie flow velocities generated by the body motion, create damping force on the body, which is known as damping force due to viscosity. The later In certain cases, such as rolling cylinders in fluid where the pressure force is very small, the fluid force will be dominated by viscosity force.

The pressure force consists of the hydrostatic restoring force and the hydrodynamic force. The hydrostatic force, F_C, is the force caused by the fluid displaced when the floating body changes its submerged volume. This force usually corresponds linearly to the motion displacement and acts in opposition to it. Therefore, F_C can be written as

$$F_C = -Cs \qquad (2.4)$$

where C = restoring force coefficient, and

s = motion displacement.

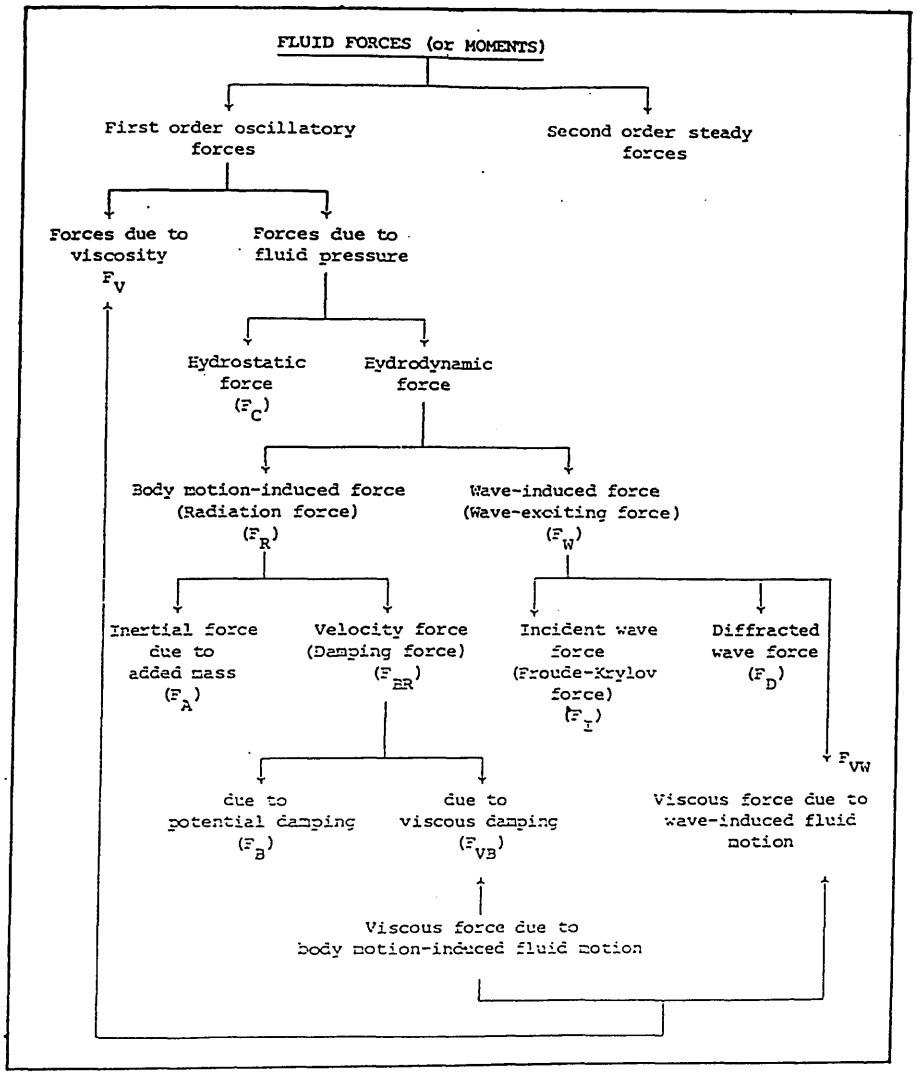

Figure 2.2. Fluid Forces and Moments Diagram [47]

The hydrodynamic inertial force, F_A, which is created by the hydrodynamic added mass A corresponds with the acceleration, s, and opposes the motion and is written as

$$F_A = -A\ddot{s} \qquad (2.5)$$

where A = hydrodynamic added mass (or mass moment of inertia).

The hydrodynamic velocity force, F_B, is proportional to the velocity, s and acts in opposition to it. This force is as a result of energy losses of the body due to radiate

surface waves

$$F_B = -B\dot{s} \qquad (2.6)$$

where B = hydrodynamic damping per unit velocity.

The wave induced force, F_W, is the summing of the incident wave force, F_I and the diffracted wave force, F_D. This force is also known as the wave exciting force and since, its magnitude varies with time, it is included as follows :

$$F_W = (F_I + F_D)e^{-i\omega t} \qquad (2.7)$$

where $i = \sqrt{-1}$

ω = radian frequency of the incident waves,

and t = time

According to Newton's second law, the sum of the above fluid forces will be balanced by the inertial forces (or moments). F_M is equal to the body mass (or mass of moment inertia) multiplied by the acceleration of the body motion

$$F_M = M\ddot{s} = F_W - F_A - F_B - F_C \qquad (2.8)$$

where M = total body mass (or mass moment inertia)

By substituting equations (2.4) to (2.6) into equation (2.8), the force (or moment) equation becomes

$$M\ddot{s} = F_W - A\ddot{s} - B\dot{s} - Cs \text{ or}$$

$$(M + A)\ddot{s} + B\dot{s} + Cs = F_W \qquad (2.9)$$

2.3. Motion Equation of a SWATH Ship.

The theoretical background to solve the problem of the six-degree of freedom coupled motions of a SWATH ship in regular quartering seas studied in this section is extracted from [48-50].

2.3.1. Definition of Coordinate System.

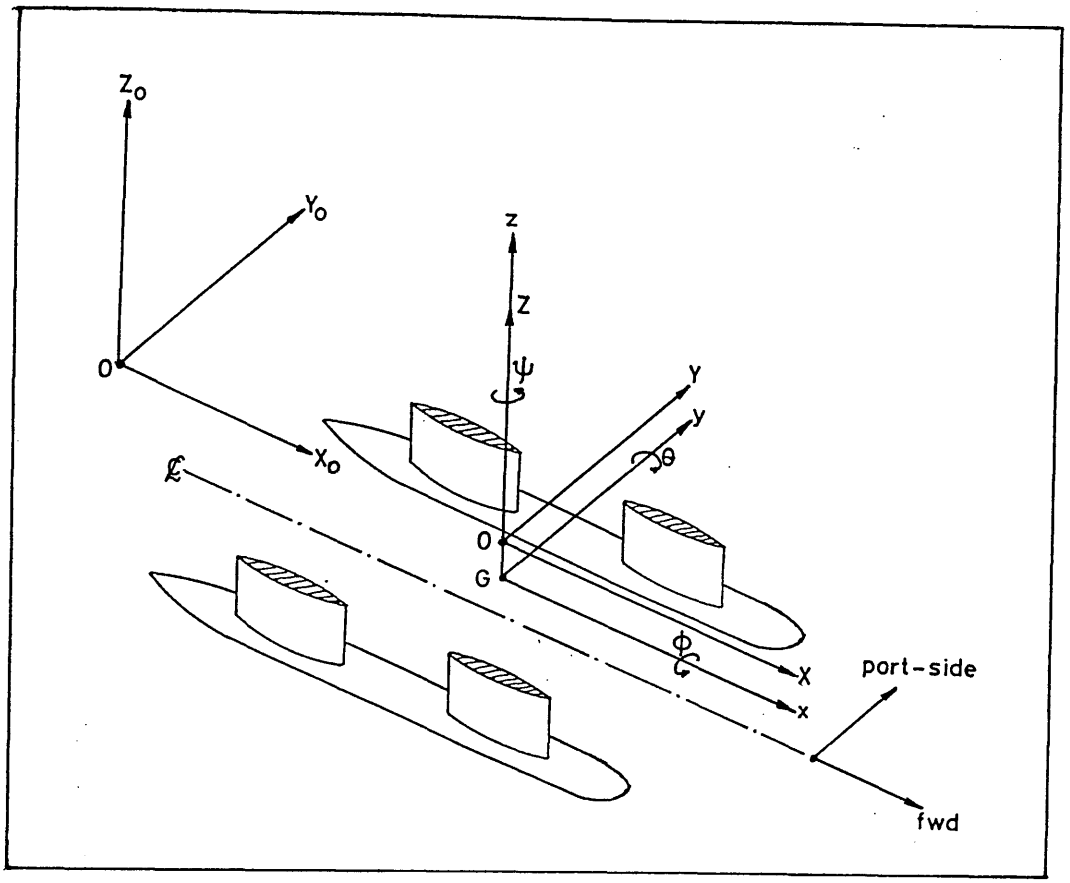

Figure 2.3. Coordinate System

The coordinate system applied in the analysis is a right handed rectangular coordinate system, as shown in fig. 2.3 This coordinate system can be described as follows.

a. Earth fixed axis ($O\text{-}X_0Y_0Z_0$) are fixed with respect to earth. Their origin is located arbitrarily but usually at the calm-water surface.
b. Body fixed axis (G-xyz) have their origin at the centre of gravity of the body and are coincident with the intersections of the principal planes of inertia.
c. Space-fixed or mean body axis (O-XYZ) originate at

the main position of the body centre of gravity and are used to discribe the body oscillations. The system is parallel to the earth-fixed ($O-X_0Y_0Z_0$) system but translates with the ship speed U.

2.3.2. Formulation of Equation of Motions.

There are some assumptions that should be stated in this analysis so that the solution performed could be justified. These assumptions are

a. the exciting forces and moments are assumed to be solely contributed by free surface waves,
b. the wave amplitudes or the wave slopes are assumed to be small,
c. the vessel is operated in an infinitely deep ocean, therefore, no appreciable currents or winds would cancel the linear response assumption, and
d. the submerged parts of the vessel are assumed to be reasonably slender.

Considering these assumptions the six-degree of freedom linear coupled equation of motion for a floating body subject to sinusoidal wave excitation of frequency ω may be expressed in the following form

$$\sum_{k=1}^{6} (M_{jk}+A_{jk})\ddot{s}_k + B_{jk}\dot{s}_k + C_{jk}s_k = F_j \qquad (2.10)$$

where k = mode of motion takes 1,2,3,4,5 and 6 for the surge, sway, heave, roll, pitch and yaw respectively,

j = mode of excitation and takes the values similar to k for the corresponding modes,

M_{jk} = mass matrix containing the mass, mass moment of inertia and products of inertia of the body,

A_{jk} = added mass matrix cintaining added mass and added moment of inertia per unit acceleration, which are frequency dependent,

B_{jk} = damping matrix containing damping force and moment of inertia per unit velocity,

C_{jk} = restoring matrix containing restoring force and moment matrix per unit displacement,

s_k = complex motion displacement vector per unit wave amplitude, and

F_j = complex wave exciting force and moment vector per unit wave amplitude.

In some references M_{jk} and s_k that are presented by the index notation as given in equation (2.10), can also be identified according to the initial definition and the correspond axes defined in fig. 2.3, as follows.

$M_{11}=M_{22}=M_{33}=M$; ie. the mass of the ship.

$M_{44}, M_{55}, M_{66}=I_4, I_5, I_6$; ie. mass moment of inertia in the roll, pitch, and yaw mode respectively,

$s_1, s_2, s_3, s_4, s_5, s_6=x, y, z, \phi, \theta, \psi$; ie. motion displacement in the surge, sway, heave, roll, pitch, and yaw respectively.

As the wave exciting force and moment vector in the right hand side of equation (2.10) is a complex function, so it can be expressed as

$$F_j = \mathrm{Re}\{\bar{F}_j e^{-i\omega t}\} \qquad (2.11)$$

where $\bar{F}_j$ is the complex force amplitude which can be written in terms of the real (R) and imaginary (I) part as

$$\bar{F}_j = F_{jR} + iF_{jI} \qquad (2.12)$$

By substituting eqn. (2.11) into eqn. (2.12), it can be found that

$$F_j = \{(F_{jR} + iF_{jI})e^{-i\omega t}\} \quad \text{or}$$

$$F_j = F_{jR}\cos\omega t + F_{jI}\sin\omega t \qquad (2.13)$$

and eqn. (2.13) can be written as

$$F_j = |F_j|\cos(\varepsilon_j - \omega t) \qquad (2.14)$$

where

$$|F_j| = \sqrt{(F_{jR}^2 + F_{jI}^2)} \qquad (2.15)$$

= maximum of the wave exciting force, and

$$\varepsilon_j = \arctan(F_{jI}/F_{jR}) \qquad (2.16)$$

= the phase shift of the maximum of the wave exciting force from the incident wave at the origin of the wave coordinate system. (see p. 4 of [48]).

To be compatible with the complex expression of F_j, the motion displacement s_k is also assumed to be complex function given by

$$s_k = \mathrm{Re}\{\bar{s}_k e^{-i\omega t}\} \qquad (2.17)$$

Furthermore, the velocity and the acceleration components can be expressed as

$$\dot{s}_k = -i\omega\bar{s}_k e^{-i\omega t} \qquad (2.18)$$

$$\ddot{s}_k = -\omega^2\bar{s}_k e^{-i\omega t} \qquad (2.19)$$

Following similar sequence from eqn. (2.11) upto (2.16) the motion displacement can be written also as follows.

$$\bar{s}_k = s_{kR} + is_{kI} \qquad (2.20)$$

$$s_k = s_{kR}\cos\omega t + s_{kI}\sin\omega t \qquad (2.21)$$

$$|s_k| = \sqrt{(s_{kR}^2 + s_{kI}^2)} \qquad (2.22)$$

$$\alpha_k = \arctan(s_{kI}/s_{kR}) \qquad (2.23)$$

$$s_k = |s_k|\cos(\alpha_k - \omega t) \qquad (2.24)$$

where $|s_k|$= the maximum of the motion displacement,
and α_k = the phase shift of the maximum of the motion displacement from the maximum of the incident wave at the origin of the wave coordinate system.

2.3.3. Solution of the Motion Equation.

The surge mode is assumed to be decoupled from other modes. Moreover, the added mass, damping and diffracted wave force in the x-direction are assumed to be small and negligible. The equation of surge motion, therefore, can be expressed by

$$M_{11}\ddot{s}_1 = F_1 \qquad (2.25)$$

or by using the coordinate system as a reference, eqn.(2.25) becomes,

$$M\ddot{x} = F_1 \qquad (2.26)$$

The symmetry of the hull with respect to the longitudinal centreplane leads to the decoupling of the vertical plane (heave and pitch) from the horizontal plane (sway, roll and yaw) modes. Consequently the equation of motion can be divided into two groups.

By expanding eqn. (2.10) for heave and pitch modes, ie. j,k = 3 and 5, this can be written as

$$(M_{33} + A_{33})\ddot{s}_3 + B_{33}\dot{s}_3 + C_{33}s_3 + A_{35}\ddot{s}_5 + B_{35}\dot{s}_5 + C_{35}s_5 = F_3$$

$$(M_{55} + A_{55})\ddot{s}_5 + B_{55}\dot{s}_5 + C_{55}s_5 + A_{53}\ddot{s}_3 + B_{53}\dot{s}_3 + C_{53}s_3 = F_5 \qquad (2.27)$$

or by using the corresponding coordinate system, eqns.(2.27), becomes

$$(M_{33} + A_{33})\ddot{z} + B_{33}\dot{z} + C_{33}z + A_{35}\ddot{\theta} + B_{35}\dot{\theta} + C_{35}\theta = F_3$$

$$(I_5 + A_{55})\ddot{\theta} + B_{55}\dot{\theta} + C_{55}\theta + A_{53}\ddot{z} + B_{53}\dot{z} + C_{53}z = F_5 \qquad (2.28)$$

Substituting eqns. (2.18) and (2.19) into eqn.

(2.27) for j,k = 3 and 5 the following equations are derived

$$[(M_{33}+A_{33})(-\omega^2)+B_{33}(-i\omega)+C_{33}]\bar{s}_3+[A_{35}(-\omega^2)+B_{35}(-i\omega)+C_{35}]\bar{s}_5 = \bar{F}_3$$

$$[(M_{55}+A_{55})(-\omega^2)+B_{55}(-i\omega)+C_{55}]\bar{s}_5+[A_{53}(-\omega^2)+B_{53}(-i\omega)+C_{53}]\bar{s}_3 = \bar{F}_5 \qquad (2.29)$$

By substituting eqns. (2.12) and (2.20) into eqn. (2.29) for k,j = 3 and 5 and arranging the right and left hand-side of the above equation in terms of the real and imaginary part, the following matrix form of the resulting equation is obtained :

$$\begin{bmatrix} -\omega^2(M_{33}+A_{33})+C_{33} & -\omega^2A_{35}+C_{35} & \omega B_{33} & \omega B_{35} \\ -\omega^2A_{35}+C_{35} & -\omega^2(M_{55}+A_{55})+C_{55} & \omega B_{53} & \omega B_{55} \\ -\omega B_{33} & -\omega B_{35} & -\omega^2(M_{33}+A_{33})+C_{33} & -\omega^2A_{35}+C_{35} \\ -\omega B_{53} & -\omega B_{55} & -\omega^2A_{53}+C_{53} & -\omega^2(M_{55}+A_{55})+C_{55} \end{bmatrix} * \begin{bmatrix} s_{3R} \\ s_{5R} \\ s_{3I} \\ s_{5I} \end{bmatrix} = \begin{bmatrix} F_{3R} \\ F_{5R} \\ F_{3I} \\ F_{5I} \end{bmatrix} \qquad (2.30)$$

or by using the index notation corresponded to the coordinate system eqn. (2.30) can be written as

$$\begin{bmatrix} -\omega^2(M_{33}+A_{33})+C_{33} & -\omega^2A_{35}+C_{35} & \omega B_{33} & \omega B_{35} \\ -\omega^2A_{35}+C_{35} & -\omega^2(I_5+A_{55})+C_{55} & \omega B_{53} & \omega B_{55} \\ -\omega B_{33} & -\omega B_{35} & -\omega^2(M_{33}+A_{33})+C_{33} & -\omega^2A_{35}+C_{35} \\ -\omega B_{53} & -\omega B_{55} & -\omega^2A_{53}+C_{53} & -\omega^2(I_5+A_{55})+C_{55} \end{bmatrix} * \begin{bmatrix} z_R \\ \theta_R \\ z_I \\ \theta_I \end{bmatrix} = \begin{bmatrix} F_{3R} \\ F_{5R} \\ F_{3I} \\ F_{5I} \end{bmatrix} \qquad (2.31)$$

By expanding eqn. (2.10) for sway, roll and yaw modes, ie. j,k = 2,4 and 6, this can be written as

$$(M_{22}+A_{22})\ddot{s}_2 + B_{22}\dot{s}_2 + A_{24}\ddot{s}_4 + B_{24}\dot{s}_4 + A_{26}\ddot{s}_6 + B_{26}\dot{s}_6 = F_2$$

$$(M_{44}+A_{44})\ddot{s}_4 + B_{44}\dot{s}_4 + C_{44}s_4 + A_{42}\ddot{s}_2 + B_{42}\dot{s}_2 + A_{46}\ddot{s}_6 + B_{46}\dot{s}_6 = F_4$$

$$(M_{66}+A_{66})\ddot{s}_6 + B_{66}\dot{s}_6 + A_{62}\ddot{s}_2 + B_{62}\dot{s}_2 + A_{64}\ddot{s}_4 + B_{64}\dot{s}_4 = F_6 \qquad (2.32)$$

Applying the corresponding coordinate system, motion equation (2.29) becomes

$$(M + A_{22})\ddot{y} + B_{22}\dot{y} + A_{24}\ddot{\phi} + B_{24}\dot{\phi} + A_{26}\ddot{\psi} + B_{26}\dot{\psi} = F_2$$

$$(I_4 + A_{44})\ddot{\phi} + B_{44}\dot{\phi} + C_{44}\phi + A_{42}\ddot{y} + B_{42}\dot{y} + A_{46}\ddot{\psi} + B_{46}\dot{\psi} = F_4$$

$$(I_6 + A_{66})\ddot{\psi} + B_{66}\dot{\psi} + A_{62}\ddot{y} + B_{62}\dot{y} + A_{64}\ddot{\phi} + B_{64}\dot{\phi} = F_6 \qquad (2.33)$$

A similar procedure as in the coupled heave and pitch is implemented for the sway, roll and yaw, ie. k,j = 2,4 and 6, which yields the following matrix form of eqn. (2.32)

$$\begin{bmatrix} -\omega^2(M_{22}+A_{22}) & -\omega^2 A_{24} & -\omega^2 A_{26} & \omega B_{22} & \omega B_{24} & \omega B_{26} \\ -\omega^2 A_{24} & -\omega^2(M_{44}+A_{44})+C_{44} & -\omega^2 A_{46} & \omega B_{24} & \omega B_{44} & \omega B_{46} \\ -\omega^2 A_{62} & -\omega^2 A_{44} & -\omega^2(M_{66}+A_{66}) & \omega B_{62} & \omega B_{64} & \omega B_{66} \\ -\omega B_{22} & -\omega B_{24} & -\omega B_{26} & -\omega^2(M_{22}+A_{22}) & -\omega^2 A_{24} & -\omega^2 A_{26} \\ -\omega B_{24} & -\omega B_{44} & -\omega B_{46} & -\omega^2 A_{24} & -\omega^2(M_{44}+A_{44})+C_{44} & -\omega^2 A_{46} \\ -\omega B_{62} & -\omega B_{64} & -\omega B_{66} & -\omega^2 A_{62} & -\omega^2 A_{44} & -\omega^2(M_{66}+A_{66}) \end{bmatrix} \cdot \begin{bmatrix} s_{2R} \\ s_{4R} \\ s_{6R} \\ s_{2I} \\ s_{4I} \\ s_{6I} \end{bmatrix} - \begin{bmatrix} F_{2R} \\ F_{4R} \\ F_{6R} \\ F_{2I} \\ F_{4I} \\ F_{6I} \end{bmatrix} \qquad (2.34)$$

or by using the index notation in conjunction with the coordinate system equation above can be written as

$$\begin{bmatrix} -\omega^2(M_{22}+A_{22}) & -\omega^2 A_{24} & -\omega^2 A_{26} & \omega B_{22} & \omega B_{24} & \omega B_{26} \\ -\omega^2 A_{24} & -\omega^2(I_4+A_{44})+C_{44} & -\omega^2 A_{46} & \omega B_{24} & \omega B_{44} & \omega B_{46} \\ -\omega^2 A_{62} & -\omega^2 A_{44} & -\omega^2(I_6+A_{66}) & \omega B_{62} & \omega B_{64} & \omega B_{66} \\ -\omega B_{22} & -\omega B_{24} & -\omega B_{26} & -\omega^2(M_{22}+A_{22}) & -\omega^2 A_{24} & -\omega^2 A_{26} \\ -\omega B_{24} & -\omega B_{44} & -\omega B_{46} & -\omega^2 A_{24} & -\omega^2(I_4+A_{44})+C_{44} & -\omega^2 A_{46} \\ -\omega B_{62} & -\omega B_{64} & -\omega B_{66} & -\omega^2 A_{62} & -\omega^2 A_{44} & -\omega^2(I_6+A_{66}) \end{bmatrix} \cdot \begin{bmatrix} y_R \\ \phi_R \\ \psi_R \\ y_I \\ \phi_I \\ \psi_I \end{bmatrix} - \begin{bmatrix} F_{2R} \\ F_{4R} \\ F_{6R} \\ F_{2I} \\ F_{4I} \\ F_{6I} \end{bmatrix} \qquad (2.35)$$

2.3.4. The Hydrodynamic Forces.

The first order, external oscillatory fluid forces acting on a ship can be divided into two linearly

superimposable components, ie wave-induced (or excitation) forces and motion-induced (or reaction) forces [51]. The first force consists of the incident wave force, calculated on the assumption that the presence of the body does not distort the wave which can be derived from Froude-Krylov theory, and the diffracted wave force, which accounts for the scattering of the incident wave by the presence of the body.

The reaction force, as has been described in the foregoing section, is considered a property of the structure and consists of three components that directly related to the three components of hydrodynamic excitation. The three components are a quasi-static (or buoyancy) restoration in heave, roll and pitch modes and a body-generated hydrodynamic force which is subdivided into an inertial (added mass) force and damping force as a result of the circumfusion of energy from the body in radiating surface wave, which are linearly proportional to the body acceleration and velocity respectively. This force is calculated under the assumption that the body undergoes the same motion in calm water as in waves. The problem is termed a radiation problem.

It should be borne in mind that the excitation and reaction forces possess viscous component caused by the wave-induced viscous fluid damping and the body-induced viscous fluid motion, respectively. Both components are combined into a single viscous force resulting from the relative velocity of body and fluid.

2.3.4.1. Problem Formulation at Forward Speed.

The body fixed axis (G-xyz) which coincides with the space-fixed co-ordinate system (O-XYZ) at time t=0, moves along the X-axis with a steady forward speed U. The relationship between the fixed and translating co-ordinate system [51] can be written as follows.

$$X = x + Ut;\ Y = y;\ Z = z \qquad (2.36)$$

whereas the relationship between the wave frequency and the frequency of encounter, ω_e, is given by

$$\omega_e = \omega_o - Uk_o\cos\mu \qquad (2.37)$$

where ω_0 = the incident wave frequency at zero speed,

μ = the wave heading angle, which is defined so that $\mu = 0$ indicates following or overtaking seas directly from astern,

k_o = the wave number = ω_0^2/g, and

g = the acceleration due to gravity.

In a reference frame (G-xyz) moving with steady forward motion the incident wave potential which generates the wave is expressed as

$$\phi_I(x,y,z;k_0,\mu,t) = \phi_I(y,z;k_0,\mu)e^{i(k_0\cos\mu - \omega t)} \qquad (2.38)$$

with

$$\phi_I(y,z;k_0,\mu) = -\frac{ig\zeta_A}{\omega_0} e^{(k_0 z)} e^{(ik_0 y\sin\mu)} \qquad (2.39)$$

where ζ_A = wave amplitude.

If the influence of the phase shift due to the longitudinal location of the strip section relative to the crest of the incident wave through the body axis is omitted until the final calculation for the force on the body, then the expression of the incident wave velocity potential given in eqn. (2.39) can be written in its odd (o) and even (e) parts as follows.

$$\phi_I^{(o)}(y,z,k_0,\mu) = \mathrm{Re}\,[\phi_I(y,z,k_0,\mu)] = \frac{g\zeta_A}{\omega_0} e^{k_0 z} \sin(k_0 y\sin\mu)$$

$$\phi_I^{(e)}(y,z,k_0,\mu) = \mathrm{Im}\,[\phi_I(y,x,k_0,\mu)] = \frac{g\zeta_A}{\omega_0} e^{k_0 z} \cos(k_0 y\sin\mu) \qquad (2.40)$$

2.3.4.2. The Froude-Krylov Component.

When the body fixed axis, G-xyz, moving with steady forward motion, the incident wave potential is identical to that at zero-speed except for the change in frequency of encounter.

In matrix notation [52], the Froude-Krylov sectional forces per unit wave amplitude, $f^{K}_{(m)}$, in the in-plane modes of motion are (ommiting the time factor)

$$\begin{bmatrix} f^{K}_{(2)}(x) \\ f^{K}_{(3)}(x) \\ f^{K}_{(4)}(x) \end{bmatrix} = \rho g \int_{S(x)} e^{k_0 z} \begin{bmatrix} \sin \\ \cos \\ \sin \end{bmatrix} (k_0 y \sin\mu) \begin{bmatrix} -dz \\ dy \\ ydy + (z-z_0)\,dz \end{bmatrix} \qquad (2.41)$$

where $\int_{S(x)}$ = the contourwise integral at station x
ρ = density, and
subscript (m) = denotes the dependence on the mode of motion

Integrating the foregoing sectional forces along the ship length, taking into account the phase angle, yields the resultant Froude-Krylov forces and moments per unit wave amplitude, $F^{K}_{(m)}$,

$$\begin{bmatrix} F^{K}_{(2)} \\ F^{K}_{(3)} \\ F^{K}_{(4)} \\ F^{K}_{(5)} \\ F^{K}_{(6)} \end{bmatrix} = \int_{L} e^{ik_0 x\cos\mu} \begin{bmatrix} if^{K}_{(2)}(x) \\ f^{K}_{(3)}(x) \\ if^{K}_{(4)}(x) \\ f^{K}_{(3)}(x) \\ if^{K}_{(2)}(x) \end{bmatrix} \begin{bmatrix} dx \\ dx \\ dx \\ -xdx \\ xdx \end{bmatrix} \qquad (2.42)$$

where $\int_{L}$ = the length wise integral for the component

Whenever a product with the imaginary unit i is involved,

only the real part of the product will be recognised.

2.3.4.3. The Diffraction Component.

The sectional sway, heave and roll-exciting forces and moments due to diffraction, $f^{D}_{(m)}$, are given by,

$$\begin{bmatrix} f^{D}_{(2)}(x) \\ f^{D}_{(3)}(x) \\ f^{D}_{(4)}(x) \end{bmatrix} = i\rho\omega \int_{S(x)} \begin{bmatrix} \phi_D^{(o)}(y,z,k,\mu) \\ \phi_D^{(e)}(y,z,k,\mu) \\ \phi_D^{(o)}(y,z,k,\mu) \end{bmatrix} \begin{bmatrix} -dz \\ dy \\ ydy+(z-z_0)dz \end{bmatrix} \qquad (2.43)$$

where $\phi_D^{(o)}$ = the odd complex diffraction velocity potential which corresponds to $\phi_I^{(o)}$,

and $\phi_D^{(e)}$ = the even complex diffraction velocity potential which corresponds to $\phi_I^{(e)}$

The diffraction velocity potential ϕ_D can be expressed as a function of Green's theorem and the complex source strength. By taking the normal derivative of the function as

$$\frac{\partial}{\partial n}\phi_D^{(m)} = \left[\sum_{j=1}^{N} Q_j^{(m)} I_{ij}^{(m)} + \sum_{j=1}^{N} Q_{N+j}^{(m)} J_{ij}^{(m)}\right] + i\left[\sum_{j=1}^{N} Q_j^{(m)} J_{ij}^{(m)} - \sum_{j=1}^{N} Q_{N+j}^{(m)} I_{ij}^{(m)}\right] \qquad (2.44)$$

where Q_j = the Green's function at any segment j

I_{ij}, J_{ij} = termed as the 'influence coefficients' [51]

By separating the right hand side of eqn. (2.44) into its real and imaginary part, the odd function can be written as,

$$\sum_{j=1}^{N} Q_j^{(m)} I_{ij}^{(m)} + \sum_{j=1}^{N} Q_{N+j}^{(m)} J_{ij}^{(m)}$$

and the even function as,

$$\sum_{j=1}^{N} Q_j^{(m)} J_{ij}^{(m)} + \sum_{j=1}^{N} Q_{N+j}^{(m)} I_{ij}^{(m)}$$

The even functions for both the incident and the diffraction produce wave exciting forces in heave, while the odd functions produce sway and roll forces.

Taking into account the phase angle, the resultant diffraction forces and moments per unit wave amplitude are, $F^D_{(m)}$,

$$\begin{bmatrix} F^D_{(2)} \\ F^D_{(3)} \\ F^D_{(4)} \\ F^D_{(5)} \\ F^D_{(6)} \end{bmatrix} = \begin{bmatrix} F^D_{(2)}(k) \\ F^D_{(3)}(k) \\ F^D_{(4)}(k) \\ F^D_{(5)}(k) \\ F^D_{(6)}(k) \end{bmatrix} + \begin{bmatrix} 0 \\ 0 \\ 0 \\ \frac{U}{i\omega} F^D_{(3)}(k) \\ -\frac{U}{i\omega} F^D_{(2)}(k) \end{bmatrix} + \Gamma \begin{bmatrix} f^D_{(2)}(x) \\ f^D_{(3)}(x) \\ f^D_{(4)}(x) \\ -xf^D_{(3)}(x) \\ xf^D_{(2)}(x) \end{bmatrix}_L \qquad (2.45)$$

with

$$\Gamma = \frac{U}{i\omega} e^{ik_0 x \cos\mu}$$

The elements of the first matrix in the right hand side of eqn. (2.45), $F^D_{(m)}(k)$, are independent of speed but dependent of encounter frequency. The elements of the second matrix are the so-called speed dependent terms which influence only the pitch and yaw modes. The terms in the third matrix are the end terms. x refers to the longitudinal distance from the origin of the co-ordinate system and

$$\Big|_L \text{ indicates } \Big|_{l_a}^{-l_f}$$

with l_f, l_a, respectively, the distance of the forwardmost and aftermost sections from the origin of the co-ordinate system used in the calculation.

The resultant wave exciting force per unit wave amplitude excerting on the SWATH-type ship proceeding in regular oblique seas is obtained by adding the Froude-Krylov

force, eqn. (2.42), and the diffraction force, eqn. (2.45).

The phase relationship is introduced by taking a cosine and a sine component (in phase with the acceleration and velocity, respectively) of all the quantities involved in the calculation [50].

2.3.5. The Hydrodynamic Coefficients.

Table 2.1. Motion Induced Coefficients (potential)

$$A_{22} = \int_L a_{22}dx + \frac{U}{\omega^2}b_{22}(x)\Big|_L$$

$$B_{22} = \int_L b_{22}dx - Ua_{22}(x)\Big|_L$$

$$A_{24} = \int_L a_{24}dx + \frac{U}{\omega^2}b_{24}(x)\Big|_L$$

$$B_{24} = \int_L b_{24}dx - Ua_{24}(x)\Big|_L$$

$$A_{26} = \int_L a_{22}xdx - \frac{U}{\omega^2}B_{22}^0 + \frac{U}{\omega^2}xb_{22}(x)\Big|_L$$

$$B_{26} = \int_L b_{22}xdx + UA_{22}^0 - Uxa_{22}(x)\Big|_L$$

$$A_{33} = \int_L a_{33}dx + \frac{U}{\omega^2}b_{33}(x)\Big|_L$$

$$B_{33} = \int_L b_{33}dx - Ua_{33}(x)\Big|_L$$

$$A_{35} = -\int_L a_{33}xdx + \frac{U}{\omega^2}B_{33}^0 - \frac{U}{\omega^2}xb_{22}(x)\Big|_L$$

$$B_{35} = -\int_L b_{33}xdx - UA_{33}^0 + Uxa_{33}(x)\Big|_L$$

$$A_{55} = \int_L a_{33}x^2dx + \frac{U^2}{\omega^2}A_{33}^0 - \frac{U^2}{\omega^2}xa_{33}(x)\Big|_L + \frac{U}{\omega^2}x^2b_{33}(x)\Big|_L$$

$$B_{55} = \int_L b_{33}x^2dx + \frac{U^2}{\omega^2}B_{33}^0 - Ux^2a_{33}(x)\Big|_L - \frac{U^2}{\omega^2}xb_{33}(x)\Big|_L$$

$$A_{53} = A_{35}^0 - \frac{U}{\omega^2}B_{33}^0 + \frac{U^2}{\omega^2}a_{33}(x)\Big|_L - \frac{U}{\omega^2}xb_{33}(x)\Big|_L$$

$$B_{53} = B_{53}^0 + UA_{33}^0 + Uxa_{33}(x)\Big|_L + \frac{U^2}{\omega^2}b_{33}(x)\Big|_L$$

$$A_{44} = \int_L a_{44}dx - \frac{U}{\omega^2}b_{44}(x)\Big|_L$$

$$B_{44} = \int_L b_{44}dx - Ua_{44}(x)\Big|_L$$

$$A_{42} = A_{24}$$

$$B_{42} = B_{24}$$

$$A_{46} = \int_L a_{24}xdx - \frac{U}{\omega^2}B_{42}^0 + \frac{U}{\omega^2}xb_{24}\Big|_L$$

$$B_{46} = \int_L b_{24}xdx + UA_{42}^0 - Uxa_{24}(x)\Big|_L$$

$$A_{66} = \int_L a_{22}x^2dx + \frac{U^2}{\omega^2}A_{22}^0 - \frac{U^2}{\omega^2}xa_{22}(x)\Big|_L + \frac{U}{\omega^2}x^2b_{22}(x)\Big|_L$$

$$B_{66} = \int_L b_{22}x^2dx + \frac{U^2}{\omega^2}B_{22}^0 - Ux^2a_{22}(x)\Big|_L - \frac{U^2}{\omega^2}xb_{22}(x)\Big|_L$$

$$A_{62} = A_{26}^0 + \frac{U}{\omega^2}B_{22}^0 + \frac{U}{\omega^2}xb_{22}(x)\Big|_L - \frac{U^2}{\omega^2}a_{22}(x)\Big|_L$$

$$B_{62} = B_{26}^0 - UA_{22}^0 - Uxa_{22}(x)\Big|_L - \frac{U^2}{\omega^2}b_{22}(x)\Big|_L$$

$$A_{64} = A_{46}^0 + \frac{U}{\omega^2}B_{42}^0 - \frac{U^2}{\omega^2}a_{24}(x)\Big|_L + \frac{U}{\omega^2}xb_{24}(x)\Big|_L$$

$$B_{64} = B_{46}^0 - UA_{42}^0 - Uxa_{24}(x)\Big|_L - \frac{U^2}{\omega^2}a_{24}(x)\Big|_L$$

The three-dimensional added mass/inertia and wave damping coefficients, A_{ij} and B_{ij} respectively ,as given in

table 2.1 [51], are expressed in terms of the corresponding sectional coefficients which are assumed frequency dependent, a_{ij}, b_{ij}, with $\int_L$ the lengthwise integral for the component.

When the areas of the end-sections are zero, the end terms vanish. The remaining terms, if any, in aa certain mode mode of motion are the speed dependent terms which are characterised by U. The subscripts of the coefficients denote a coefficient in i^{th} force or moment equation due to motion in j^{th} mode. The superscript '0' denotes terms evaluated at zero speed. The expressions in table 2.1 are only the potential part of the motion coefficients of an unappended SWATH ship. In order to obtain a reasonable predictions of SWATH ship motions alternative formulations which include both the hull viscous effects and the hydrodynamic effects due to the fins contribution. Such a formulation can be found in [50].

2.3.6. Hydrostatic Restoring Forces.

Based on the hydrostatic considerations the restoring forces in the equation of motions are given in table 2.2. Where GM_T and GM_L are the transverse and longitudinal metacentric height, respectively, M_{AW} is the moment of the waterplane area about the y-axis, and ∇ is the volume of displacement.

Table 2.2. Hydrostatic Restoring Forces.

$$C_{33} = \rho g A_w$$

$$C_{35} = C_{53} = -\rho g M_{AW}$$

$$C_{44} = \rho g \nabla (GM_T)$$

$$C_{55} = \rho g \nabla (GM_L)$$

2.4. Some Methods of SWATH Ship Motion Assessment.

As for conventional monohull ship, there are three main methods can be applied to estimate the wave induced loads and motions on a SWATH ship. These methods are well known as

a. Morison's Formula
b. Strip Theory, and
c. Three-dimensional Sink-source Technoque.

The application of Morison's formula is justified when three assumptions on the submerged body can be satisfied. Firstly, the diameter of the SWATH hulls should be small compared to the wave length. When the hulls are subdivided into several small cylinders, the ratio of the hull diameter to the wave length should be less than 0.2. Furthermore, Morison's formula requires the potential damping attributed by waves to be ignored. Secondly, the hulls are assumed to be deeply submerged and, thus, unbounded ambient fluid can be used for added mass and damping. The third assumption is the hulls are not closely spaced. This implies that the hull spacing should be large with respect to the cross-sectional element dimensions so the hydrodynamic interference between the elements may be neglected. These assumptions lead to restrictions in the application of Morison's formula particularly for SWATH ships. Therefore, this method is considered to be inappropriate.

By using the strip theory, the solutions are found basically in the same way as for Morison's formula, that is the submerged hulls are sliced into several elements. Each element is considered individually, thus, the hydrodynamic interference between the elements can be neglected and the forces on each element are calculated utilising the two-dimensional Frank Close-fit technique [53]. There is an

assumption in the application of strip theory, ie the submerged hulls should satisfy the longitudinal slenderness. In this theory the SWATH vertical struts are considered as surface-piercing extensions of the hulls and included in the two-dimensional beamwise strip sections. The hydrodynamic interference between the hulls and the struts is treated separately. This theoretical approach has been successfully applied for SWATH ship designs by some researchers [48,54-56].

For some types of large twin-hull semi-submersibles such as pipelying barges, with relatively short columns and cross-sectional dimensions which are similar to the hull separation, Morison's formula and the strip theory approach are no longer suitable. Therefore, the calculation of wave loads should be determined by the three-dimensional sink-source technique. This approach is considered as an accurate method since the scattering of the incident waves by the columns is taken into account [57,58]. However, there is a disadvantage of this method which takes a large amount of computer time and computational efforts, consequently much more costly.

Comparisons [59,60] of the above methods have been made and it was concluded that in operational draughts there is a good agreement between strip theory and Morison's formula. Furthermore, it was also found that the strip theory had good agreement in transit draughts with the three-dimensional sink-source technique. Nevertheless, considerations of cost and time required by the three -dimensional sink-source technique and the restrictions of Morison's formula in application make the strip theory the most attractive method to be developed and employed in predicting wave loads and motions of the SWATH ship.

2.5. Existing Computer Programs for SWATH Ship Motions and Dynamic Structural Loadings Assessment.

Two different computer programs to assess the SWATH ship motions and dynamic structural loadings have been written in the department. The first program is based on the strip theory method and the second is based on the three-dimensional sink-source technique.

2.5.1. The Computer Program Based on the Strip Theory.

This program, SWATHL, was written for and run on the VAX 11/730 computer system and was evolved by some researchers at the Hydrodynamics Laboratory [52,61-66]. The program was originally written to predict the motions and loadings of twin-hulled semi-submersibles. Nevertheless, the versatility and the sophistication of the technique utilised have led to a wider range of its application. This program, therefore, is also applicable for other configurations of twin-hulled semi-submersible vehicles such as SWATH ships and even for monohull conventional vessels. The computer program since has been enhanced to meet the demand of control surfaces for SWATH. The earliest study on aft fins for the computer program has been compared with the experimental data can be found in [29,67-69] and the more comprehensive improvement in [66,70]. Recently the routine of SWATHL to assess the SWATH structural responses has been extensively improved [71]. In this section review is mainly concerned with the running of the program SWATHL which the results will be compared with the experimental data.

There are some input data required to run the program and these can be classified into processed input data and pure input data [66,72]. The processed input data is the geometry data from SW11.DAT and the mass data from SW11MAS.DAT, where SW stands for SWATH, 11 stands for SWATH1 model with geometry configuration 1, see the next chapter.

By running the program SWATHL and inputing the SW11.DAT the hydrostatic data of the model can be obtained whereas inputing SW11MAS.DAT results in the mass distribution data of the model.

The pure input data required is wave frequency, model characteristic length and draught, model speed, the water density and the model heading angle towards the wave trains. Additional input data, ie the mass of the deck and the deck beam are required in order to obtain the dynamic structural loads.The number of wave frequencies in radians/second input into the running program varies from one to thirty and this input influences the running time. The variation of the model position with respect to the wave propagations is between 0^{o} and 180^{o}.

The output data obtained from the running of the main program is motion induced coefficients, wave exciting force/moment and phases, motion amplitudes and phases and bending moments and shear forces at the midpoint of crossdeck and phases.

2.5.2. The Computer Program Based on the Three-dimensional Sink-Source Technique.

The computer program to assess the motions and dynamic loadings of SWATH ships based on the three-dimensional sink-source technique is entitled GM-1, was written to run on the ICL computer system at the University. This computer program has been developed from a basic understanding of ship hydrodynamics [57,73-74] and then gradually improved to solve the problem of six-degree of freedom of ship motion and dynamic loads.

The GM-1 computer program comprises three routines, namely GPART1, GPART2 and HFORCE. The GPART1 routine calculates the hydrodynamic forces imposed on a floating body without the effect of free surface. Whereas the GPART2

routine takes into account the free surface effect or viscosity which are frequency dependent, and consequently to run this computer program more time is consumed than for running GPART1. The HFORCE computes the hydrodynamic forces, motions and wave loads, and to create graphs of motion and structural responses.

Two types of input data, ie geometry data and variable data, are required to run the GM-1 computer program. The geometry data is a large data set which specially generated and permanently stored. To create a geometry data of a ship, half of the hull geometry is needed and the whole ship geometry data is obtained by applying a symmetrical hull body principle. Such a data set has been created for the SWATH model reported in this thesis and is labelled SWATHD.

The variable data comprises of five parts. These are

a. frequency of wave : the number of frequencies and the values offrequencies,
b. forward speed : the number of speeds and their values,
c. wave heading angle : the number of headings and the values of the heading angles in degrees,
d. Inertia and restoring coefficients : ship main dimensions and hydrostatic data (ie L, B, D, A_W, GM_T, and GM_L) and the mass and mass moment of inertia data (ie m, I_{44}, I_{55}, I_{66}, and I_{26}), and
e. control data : the program asks wether or not output data is required. 1 or 0 corresponding to yes or no should be entered in response.

There are four kinds of output data can be generated by the program, that is pressure distributions (this is a large data and hardly required), motion responses with or without viscous effect, structural responses (ie vertical

and horisontal shear forces, bending moment and torsional moment), and graphs of motion and structural responses etc.

The computer program capable of assessing the motion and structural responses of monohull and SWATH ships. The versatility of the program has also been successfully examined to predict the motion and loading behaviour of a semi-submersible type crane barge [76]. This barge having four large circular columns on each hulls and the two hulls relatively very close to each other. Such a structure is very difficult to analyse using two-dimensional theory since that approach assumes that the column that the column should be a slender body and the interference effects between the two hulls are negligible.

CHAPTER 3

SWATH1 MODEL MOTIONS IN REGULAR BEAM SEAS

Chapter 3.

SWATH1 MODEL MOTIONS IN REGULAR BEAM SEAS

3.1. SWATH1 Model Descriptions.

The SWATH1 model employed in the motion and dynamic structural loading investigations has a simple geometry. The model has twin-circular cross section hulls with paraboloid and tapered ends and two biogival struts mounted on each hull, see fig. 3.1a-c. The model was designed in a way to provide a flexibility for alteration of its main dimensions and geometrical configuration. The hull spacing and draught can be varied over a wide range. There is also possibility of replacing the twin struts by a single strut and changing the strut spacing by stretching the model. A removable control fin is also fitted and may be preset at a particular angle of attack for a range tests [11]. The model data is listed in table 3.1.

Table 3.1. Hydrostatic Data of SWATH1 Model

Weight	21.8 kg
Hull Length (L)	1.5000 m
Strut Length	0.4000 m
Hull Diameter (D)	0.0892 m
Draught (2xD)	0.1784 m
Hull Spacing Between Centres of the Hull	0.7200 m
Water Plane Area (A_{wp})	0.0540 m^2
Longitudinal Distance from Nose of the Hull to Forward Strut End	0.1550 m
Longitudinal Distance from Tail of the Hull to Rear Strut End	0.2000 m
Longitudinal Metacentre Above Keel (KM_L)	0.4290 m
Transverse Metacentre Above Keel (KM_T)	0.5120 m
Centre of Gravity Above Keel (KG)	0.1763 m
Vertical Centre of Buoyancy (VCB)	0.0640 m
Long. Centre of Gravity (LCG)	0.7275 m
Long. Metacentre Above Centre of Gravity (GM_L)	0.2528 m
Transverse Metacentre Above Centre of Gravity (GM_T)	0.3278 m

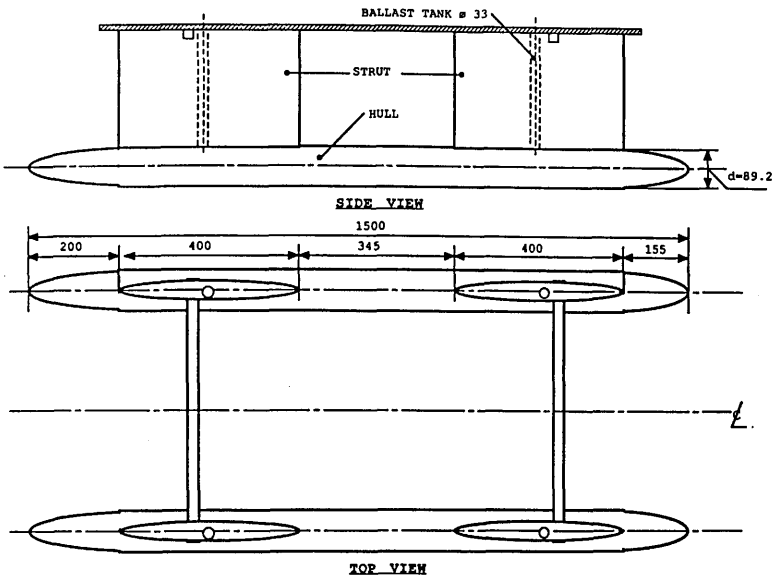

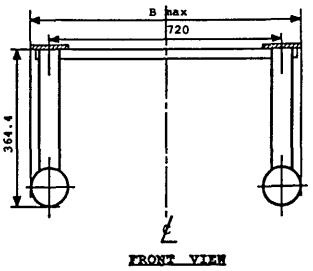

All dimension are in m

SAWTH1 Model at :
Lmax = 1.5 m
Draft = 2.0 d
d = hull diameter

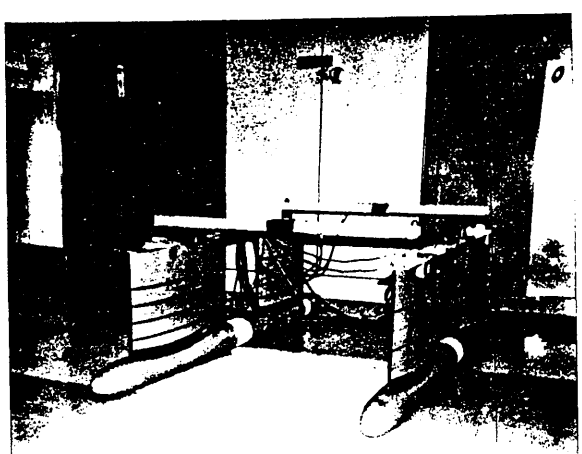

Figure 3.1. SWATH1 Model

3.2. Experiment and Analysis.

3.2.1. Instrumentations and Running the Tests.

The SWATH1 model was positioned beam on to the wave trains in the towing tank. It was moored to the tank sidewalls to ensure that the model stays close its original calm water position. Lead shot ballast was put in the centre of each strut in order to keep the model draught at double the hull diameter.

In order to investigate heave, sway and roll mode of oscillation of the model there were three linear variable displacement transformers (LVDTs) utilised in the model test arrangement, see fig. 3.2. Fixed on the carriage over the model, the two LVDTs deal with the heave and roll whereas the third LVDT at the side deals with the sway motion. All these LVDTs were connected to the multiple-channel pen recorder which records the motion amplitude via an amplifier. In the amplifier the electric signal voltages sent by the LVDTs were first processed in the sum and difference unit, thereafter, the output recorded on the chart will give directly the summation of the signal voltages of LVDT1(x) and LVDT2(y) divided by two ((x+y)/2), which gives the heave right away. The difference of the signal voltages of LVDT1 and LVDT2 (x-y) gives the pitch of the model. Fig. 3.3 shows a simple diagram of the circuit for this task.

The waves generated by the parabolic wavemaker move along the tank and were measured by four wave probes which were also connected to the pen recorder via an amplifier. Three wave probes were placed on a bridge approximately 4.2 metres from the centreline of the model with the distance B/2, B/3 and B/4, where B is the tank width, from the tank sidewall, these are WP9, WP10 and WP11 in fig. 3.2 respectively. The spreading of the wave probes is mainly to

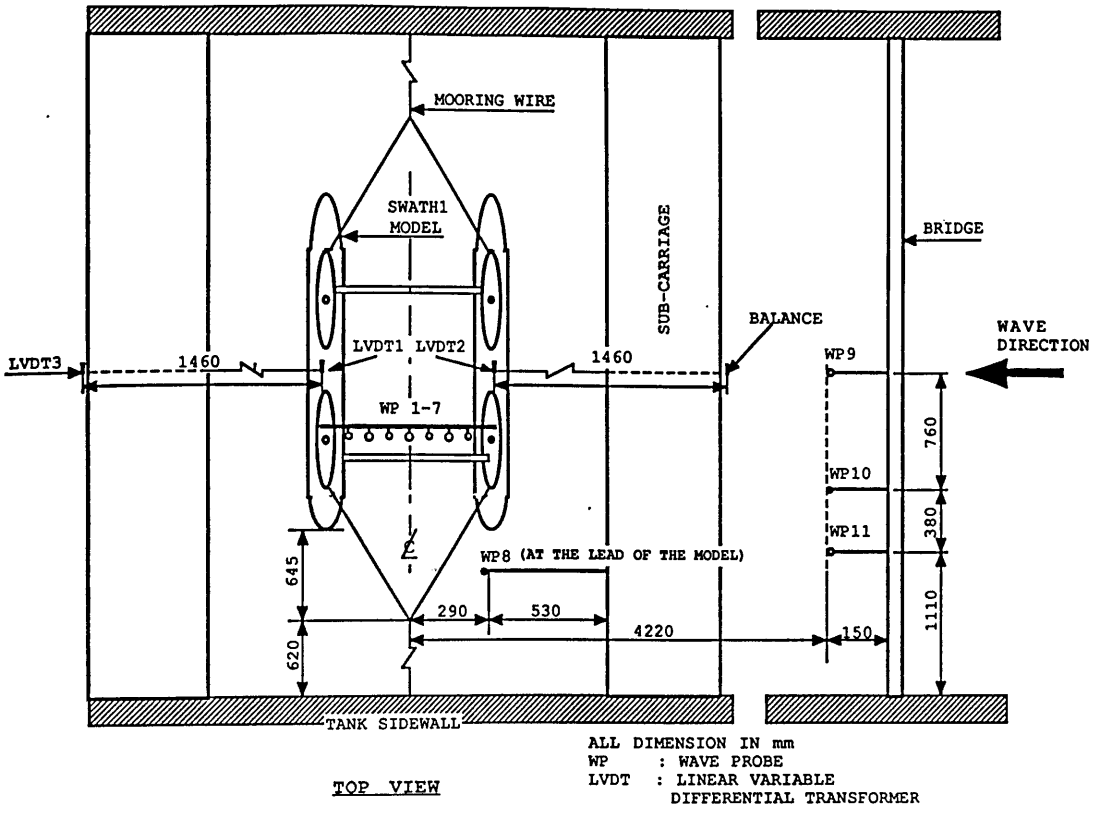

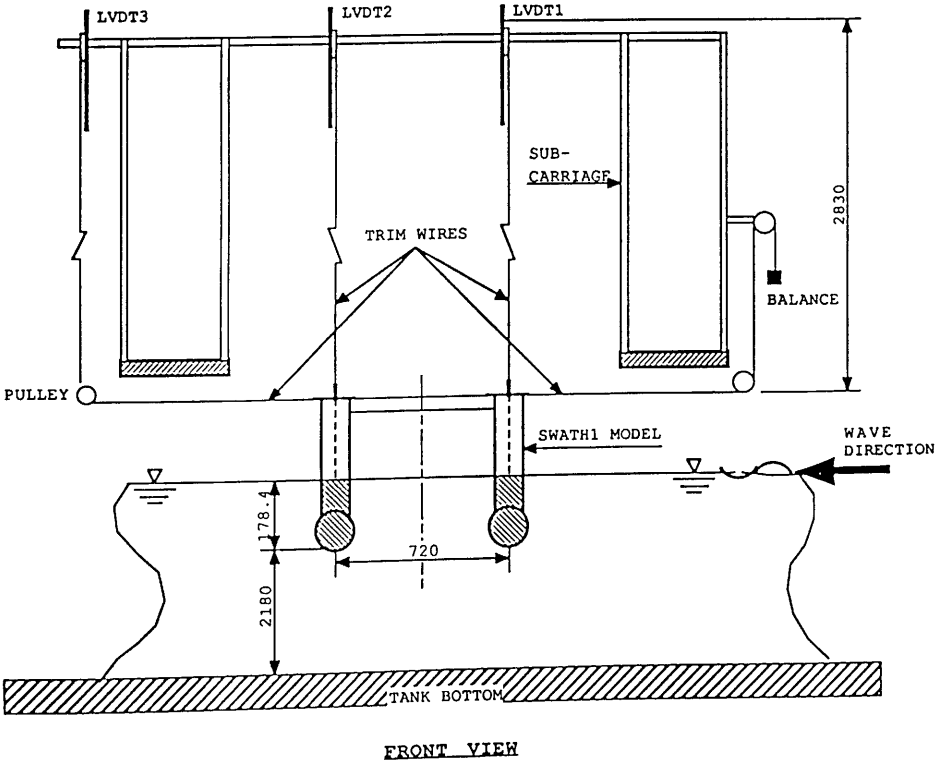

Figure 3.2. Model Test Arrangement

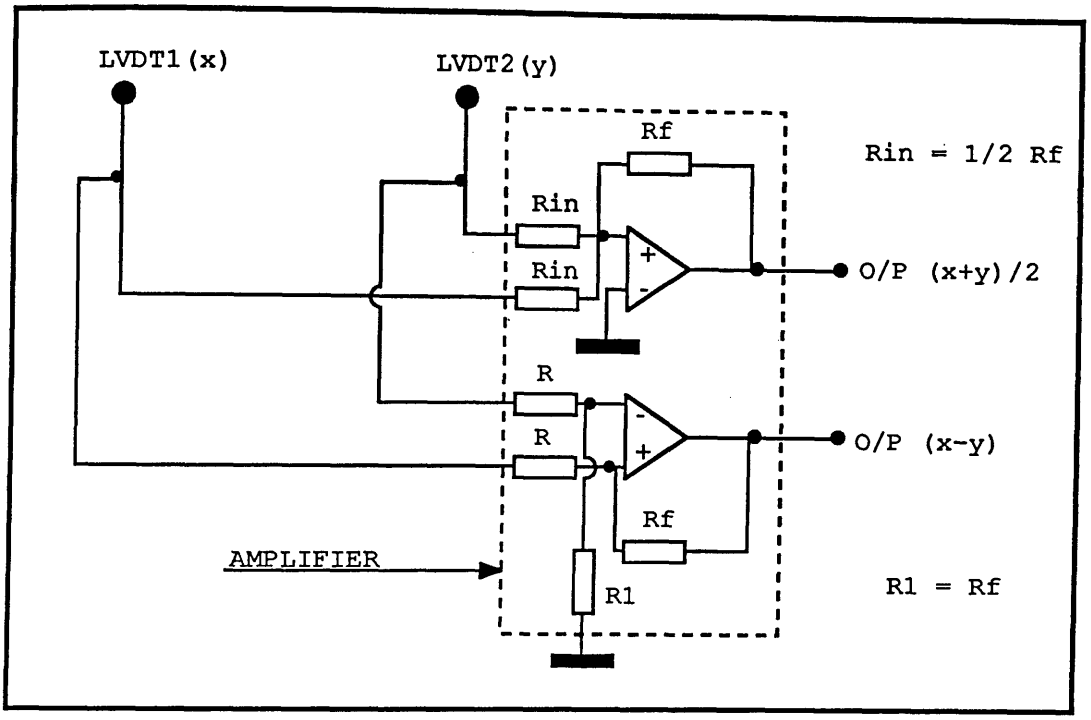

Figure 3.3. Sum and Difference Unit in the Amplifier

allow for possible changing of the wave patterns caused by the tank walls. Another wave probe was situated at the lead of the model (WP8 in fig. 3.2), so that when there was any effect of the model motion on the wave profile in the model's vicinity it could be studied easily. During the experiment it was found that the wave height recorded by this wave probe was generally lower than that recorded by other wave probes.

In the model test arrangement, it is also shown seven wave probes fixed at the fore part of the model in between the two struts. These wave probes were used to generate the data on upwelling. The data analysis for the SWATH1 model upwelling was treated separately from the motion analysis and can be found in [76].

The experiment was conducted by generating the wave frequency in a range from 0.3 Hz up to 1.2 Hz with the

interval of 0.05 Hz. The wave maker was also set in two different voltages, ie 4 volts and 12 volts, in order to produce wave heights of approximately 5cms and 10cms, respectively. This allowed information regarding non-linearities effect of waves on the motions to be found. The heave and sway second resonant frequency regions were investigated by running the wave frequencies between 1.3Hz and 1.5Hz and 1.07Hz. In addition, the heave and roll natural frequencies have also been observed.

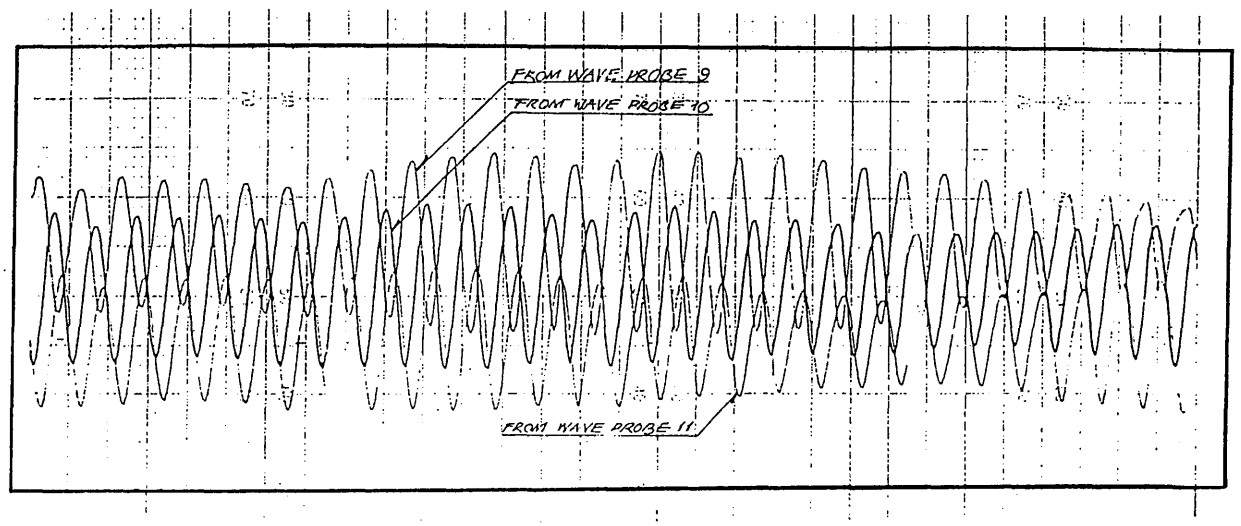

Figure 3.4. Typical Wave Records
(from multi-channels pen-recorder)

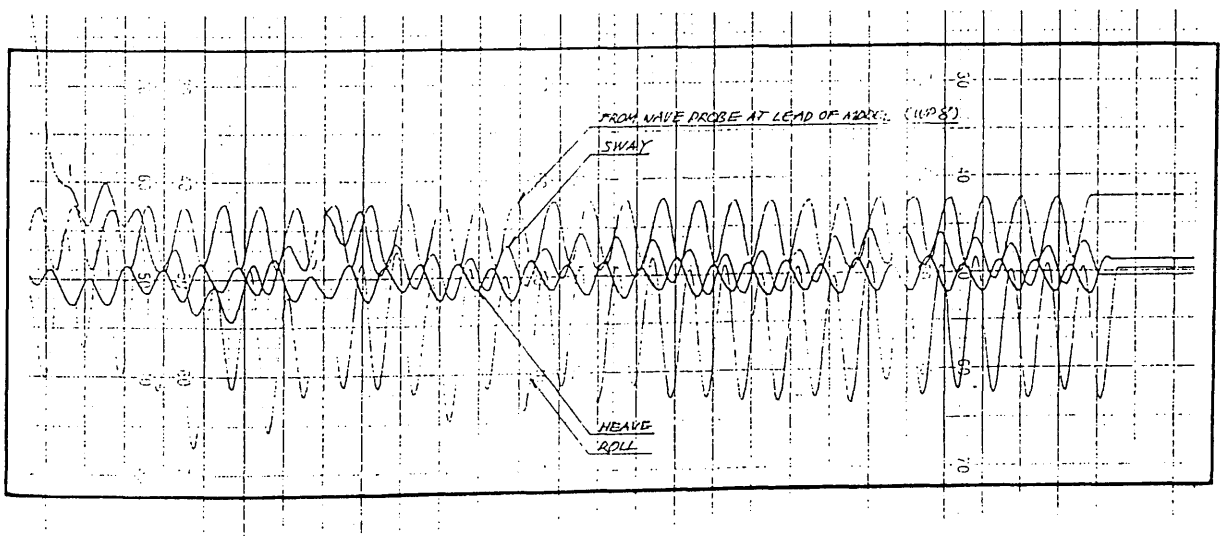

Figure 3.5. Typical Motion Records
(from multi-channels pen-recorder)

The results of data acquisitions in the experiment can be seen in figs. 3.4 and 3.5, which show a typical pen recording of the wave amplitudes and motion amplitudes, respectively. The actual motion and wave amplitudes can be obtained directly by measurement taking into account the appropriate calibration constants.

3.2.2. Test Data Analysis.

The analysis of the experimental data is started by reading the pen-records for waves and SWATH1 model motion responses.

The readings of the three recordings from the wave probes situated on the bridge are then analysed to give the average of the wave amplitudes. Thus, there are two amplitudes used in the calculation of motion responses below, ie those are drawn from the wave probe at the lead of the model and the average from the wave probes on the bridge. Since the roll amplitudes obtained from the pen-recordings were in centimetres, it must be converted into radians by taking the breadth characteristic into account, as follows :

$$\phi_A = \arctan\left(\frac{\phi'_A}{B}\right) \qquad (3.1)$$

where ϕ_A = roll amplitude (rad)

ϕ'_A = roll amplitude obtained from the pen-recorder (cms), and

B = breadth characteristics of the model (= 72cms).

Non-dimensional transational motion responses can simply be determined as motion amplitude divided by the wave amplitude :

$$Y'_{y\zeta} = \frac{y_A}{\zeta_A} \qquad (3.2)$$

$$Y'_{z\zeta} = \frac{z_A}{\zeta_A} \qquad (3.3)$$

where $Y'_{y\zeta}$ = non-dimensional sway response
$Y'_{z\zeta}$ = non-dimensional heave response
y_A = sway amplitude (cm or m)
z_A = heave amplitude (cm or m), and
ζ_A = wave amplitude (cm or m).

In order to non-dimensionalise the roll amplitude operator the wave frequency should be applied in the calculation together with the acceleration due to gravity :

$$Y'_{\phi\zeta} = \frac{\phi_A}{\zeta_A \, \omega^2/g} \qquad (3.4)$$

where ω = wave frequency in $rads^{-1}$, and
g = acceleration due to gravity
(= 9.81 ms^{-2}).

It was mentioned in the previous section that each wave frequency the experiment was run at two different voltage settings of the wavemaker to generate two different wave heights. Therefore, four variations of each motion response at each wave frequency can be acquired since there are two values of wave amplitude to be taken into account. This variation to permit investigation of the effect of model-induced profile and tank sidewall induced waves on the motion responses.

In addition, the calculation to non-dimensionalise the wave frequency has also been carried out in order to generalise the plotting of motion responses as the function of non-dimensional frequency. The non-dimensionalisation was taken as

$$\omega' = \frac{\omega}{\sqrt{g/L}} \qquad (3.5)$$

where ω' = non-dimensional wave frequency, and
L = characteristic length of the model (= 1.5m).

3.3. Comparison with Computer Program Results.

The motion responses resulting from the computer program based on strip theory and 3-D theory, have been plotted, together with the experimental results, in one graph. Thus, it is more convenient to analyse them. The computer program results presented herein constitute the revision from those reported in [77,78]. The revision of 2-D theory mainly dealt with the improvement in the SWATHL computer program [79], whereas from the 3-D theory there has been a correction in the value of GM_T [57].

In the heave response, fig. 3.6, generally the agreement between the experiment and the theories is seen to be good, although there is a little difference especially in the resonant frequency region and in the maximum value of the non-dimensional heave response. Here, the resonant frequency performed by the strip theory is slightly lower than both the 3-D theory and the experiment, which are seen to have almost exactly the same value of the resonant frequency.

If this discrepancy is caused by a slight difference in the calculation of added virtual mass for heaving in the strip theory, then this can be improved by increasing the number of segments on the beamwise sections and/or increasing the number of stations. As can be seen in ref. [79], although the segmentation of the hull sections has been attempted to be reliable, it is still rather inadequate when approaching a circular shape. Nonetheless, the difference is considered as acceptable since the improvement

can easily be done by increasing the number of segments.

Increasing the numbers of stations will also give a more accurate calculation of added mass. This, however, simultaneously raises the computational time, and is thought as inefficient with respect to the accuracy that can be achieved.

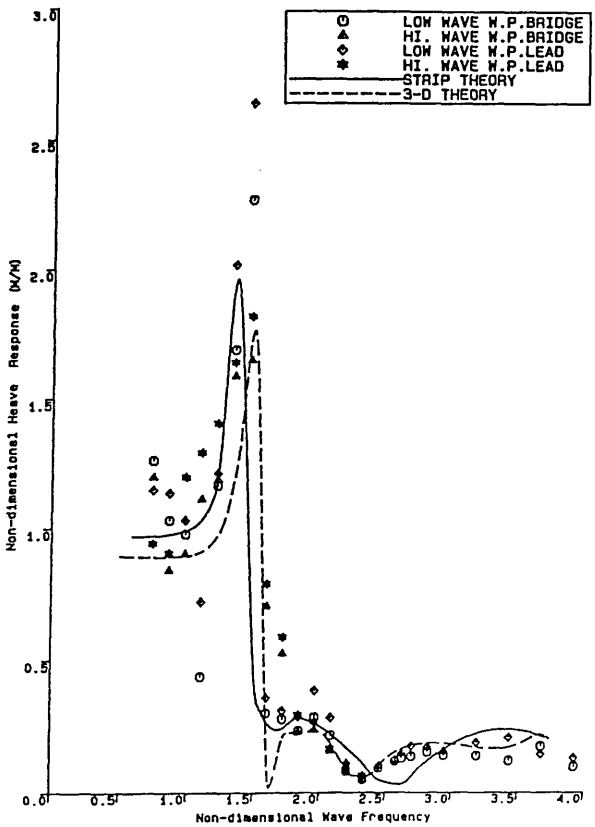

Figure 3.6
HEAVE RESPONSES
SWATH1 MODEL IN REGULAR BEAM SEAS

The maximum value of non-dimensional heave response from the experiment is around 2.6. The maximum from the 3-D theory seen to be the lowest, ie. around 1.65, this might be explained in that this theory the damping effect due to viscosity was taken slightly high. As is also shown , this maximum value matches the value from the experiment measured at the high wave, where in this circumstance, the water viscosity affects the increasing of damping magnitude. For the strip theory, where the viscosity is not applied in the computation, the maximum response is approximately 2.0.

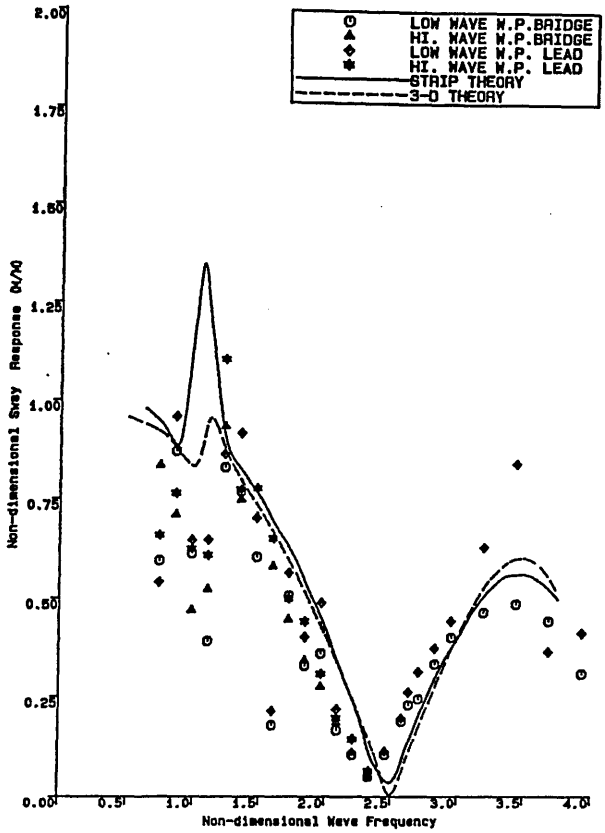

Figure 3.7
SWAY RESPONSES
SWATH1 MODEL IN REGULAR BEAM SEAS

The major improvement in the computer program SWATHL has been achieved when the implementation of the hydrodynamic interference effect between the twin hull is taken into account [47,60,79,80]. Compared to the old results of the strip theory for sway, fig. 3.7, the latest one is far more satisfactory. The peak difference could be the result of the absence of a viscous effect in the strip theory. In the low frequency region the experimental value is lower than the results of the two theories. The major effect which made this difference might be the use of mooring lines. As has been stated, the model was tied up to the tank sidewall and it is obvious that the stiffness considerably influenced the sway motion, especially at low frequencies. Considering the rest of the frequencies, the confirmation from the three sources can be judged as very satisfactory.

For the roll responses, fig. 3.8, it can be seen that in general the experimental result agrees very well with both theories for most frequencies. The discrepancy in the maximum value from the strip theory will be influenced by the viscous effect which was not applied in the computation.

Earlier results from the 3-D theory with an approximate GM_T showed how sensitive the peak is to this value. It is important that GM_T should be accurately known.

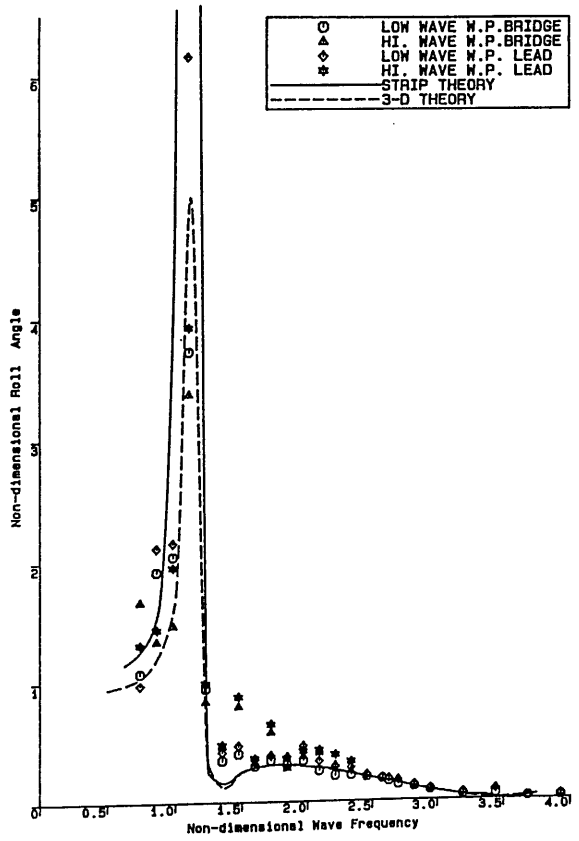

Figure 3.8
ROLL RESPONSES
SWATH1 MODEL IN REGULAR BEAM SEAS

3.4. Conclusions.

Based on the comparison between the theoretical analysis and the experiment, the conclusions from this study are set out below.

1. The agreement of the experiment and the two theories is excellent. The trends of heave, sway and roll responses, as shown in figs. 3.6-3.8 respectively, may be accepted as the standard pattern of motion responses for SWATH ships having generally similar characteristics as the SWATH1 model when exposed regular beam seas.

2. A small discrepancy in the low frquency region of sway response, fig. 3.7, may be removed by improvement in both the experimental arrangement and the computer program. Stiffness effect of mooring system on sway should be minimised as much as possible. The replacement of LVDT by the camera recorder in this case seems to be desirable to reduce the damping effect of balancing system for LVDT.

3. As far as the experimental arrangement is concerned, the roll response obtained in fig. 3.8 is satisfactory. The difference of the strip theory and the other can only be refined by developments in computer program SWATHL. For instance the viscous effect should be taken into account.

4. In general the experimental result is satisfactory and the pen recordings obtained from the experiment can be used for further investigations of SWATH ship motions in time domain. Moreover, further experiments should be carried out for the different wave heights,thus more accurate

investigation on the non-linear effect of wave height on motion responses may well be required.

CHAPTER 4

SWATH1 MODEL MOTIONS IN REGULAR QUARTERING SEAS

Chapter 4.
SWATH1 MODEL MOTIONS IN REGULAR QUARTERING SEAS

Experimental data of SWATH ship motions, and even for conventional monohull ship, in oblique seas is very limited. The majority of experimental investigation on ship motions are objected to generate data in head sea case, which is considered as the most important. The consideration is based mainly on the thought that a ship in her lifetime will be operated mostly in head seas, and other sea headings, which could be hazardous to the ship operationss, should be avoided as possible. The consideration is no longer acceptable when a certain mission which entails a high capability of a ship to expose any sea heading should be accomplished.

An experiment in regular quartering seas allows the observation on aSWATH ship motions in the six-degree of freedom, which do not occur in beam or head seas, to be made. The reliable data collected certainly is worthy to examine the numerical modellings that have been written to be able to assess the SWATH ship motions at any sea heading.

4.1. Experiment and Analysis.

The SWATH1 model was positioned in the 77x4.6x2.4 (metres) towing tank, 135° towards the regular waves propagation as shown in fig. 4.1. The draught of the model was set at double of the hull diameter by placing lead shot ballast in the centre of each strut. The model was lightly moored in some directions to minimise the drifting from its original position while the wave is exerted on the model, therefore, the assumption that the model tested in pure stationary condition can be justified.

At first the model was moored only on its centreline direction to the tank side wall. In this condition the model was still enable to maintain its

original direction (135°) in long waves, ie. waves with the frequency ranges from 0.30Hz upto 0.80Hz in this case. However, this was no longer the case when short waves were experienced, since the frequency of oscillation became higher and hence the motions were more likely to be out of line with its initial direction. Two additional mooring lines were, therefore, installed perpendicular onto the first two mooring lines in order to overcome this problem.

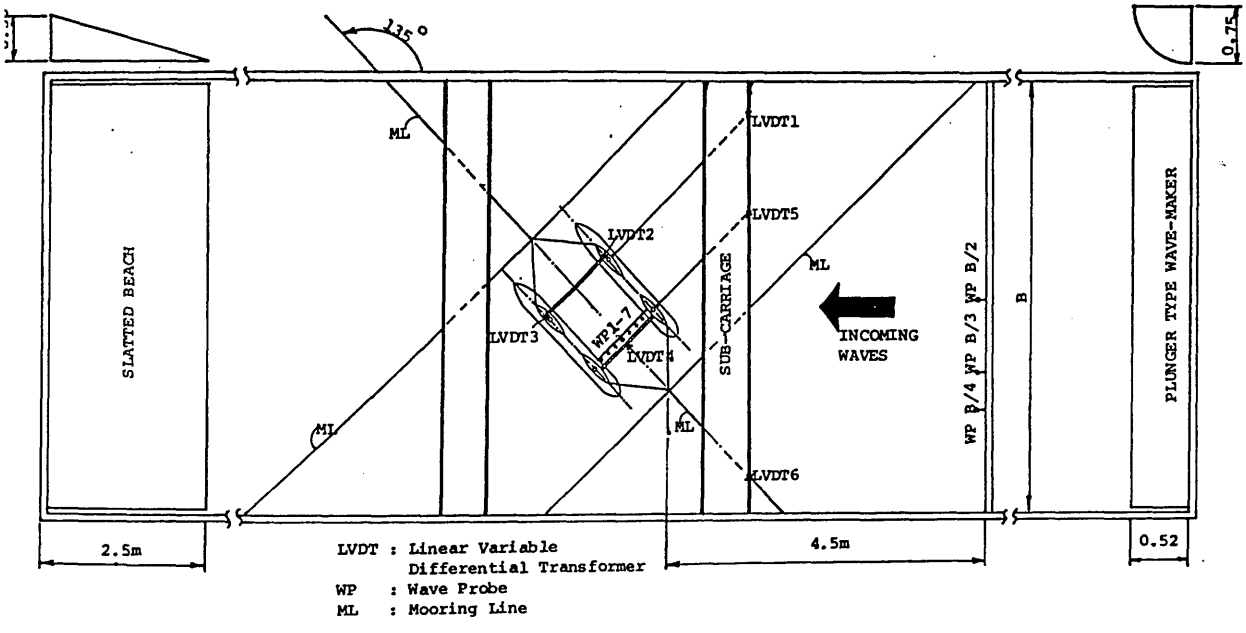

Figure 4.1. Model Test Arrangement

4.1.1. Instrumentation.

As is stated in chapter two the SWATH ship experiences six-degrees of freedom in motion when it is excited by quartering seas. During this experiment, the six mode of motions, namely surge, sway, heave, pitch, roll and yaw were measured by means of six Linear Variable Differential Transformers (LVDTs). As can be seen in fig. 4.1 of the test arrangement, one LVDT (LVDT6) was positioned on the carriage at the front of the model connected by a piano wire parallel the centreline onto the centre part of the front transverse beam. This LVDT dealt with the surge mode of motion. Two LVDTs (LVDT1 and LVDT5) which were

related to the sway and yaw were placed on the left side of the model connected by wires, that were parallel about the two transverse beams at the front and stern part of the model. The other three LVDTs (LVDT2, LVDT3 and LVDT4) were employed to measure the heave, pitch and roll, and set up above the model. All of these LVDTs were positioned vertically and their weights were balanced so that any accelerations being induced on transformers during the model motions could be eliminated.

The regular wave profiles created by a parabolic plunger type wave-maker were measured by capacitance wave probes. Three wave probes were placed on a bridge across the tank width, 4.5 metres in distance from the model bow, so that there were no model motion effects on waves. The placing of wave probes was arranged in such way, ie. B/2, B/3 and B/4 from the tank side wall where B is the tank width, so that any changing in the wave patterns across the tank can easily be identified. Eventhough, it has been found that the changing of wave patterns generally was not significant.

From the point of view of efficiently employing the tank facilities as much data as possible should be collected in an experiment. This principle was adopted in this experiment. As can be seen in fig. 4.1 seven wave probes aimed to collect the data of standing wave in between the struts were attached on an alumunium bar at the fore part of the model. The analysis of data on upwelling of the SWATH ship can be found in [81].

Since more than 16 electronic channels must be provided to record the electrical signals from those instruments, complete data collection was not possible using the pen recorder since this only provides eight channels. The data was recorded directly on the VAX 11/830 at the Hydrodynamics Laboratory using a computer program entitled PROGB.FOR had been applied to the place of the pen recorder.

(Some channels of the pen recorder were still utilised for checking). The relative channels to the electronic instruments is listed in table 4.1.

Table 4.1. The Relative Channels to the Electronic Instruments

Channel No.1	related to	Start-stop signal
Channel No.2	related to	LVDT1
Channel No.3	related to	LVDT2
Channel No.4	related to	LVDT3
Channel No.5	related to	LVDT4
Channel No.6	related to	LVDT5
Channel No.7	related to	U/S as O/C
Channel No.8	related to	LVDT6
Channel No.9	related to	Wave Probe B/4
Channel No.10	related to	Wave Probe B/3
Channel No.11	related to	Wave Probe B/2
Channel No.12	related to	Wave Probe 1
Channel No.13	related to	Wave Probe 2
Channel No.14	related to	Wave Probe 3
Channel No.15	related to	Wave Probe 4
Channel No.16	related to	Wave Probe 5
Channel No.17	related to	Wave Probe 6
Channel No.18	related to	Wave Probe 7
Channel No.19	related to	Signal sent to wave-maker

4.1.2. Calibration Procedures.

Before the first test run of the day was commenced, calibrations were carried out to eliminate any changes in signal levels caused mainly by atmospheric state surrounding the devices, ie. temperature, humidity etc.

There were nine stages to be carried out for the calibration. The first calibration took place in calm water (original zero position) with the model and measurement devices in their original position without any disturbances.

The reading of the digital recorder was then taken. The record was labelled acording to the sequence of the test run, for instance ZR512S0, where ZR stands for the initial for zero, 512 for the number of the first test of that day and S0 for original position. The S0 initial is essential to distinguish from other test zero positions which were always taken before each run. The next calibration was then done on the wave probes which were fixed to the model. Firstly the model was clamped on to two steel bars positioned at the fore and aft parts. These two bars were then lifted up to the same level and rested on wooden blocks with a known thickness of 4.3 cms, such that the model was still on an even keel. In this position the calibration for wave probes, which were raised together with the model, was recorded. A specific note, such as CL512S1, was given on the record, where CL stands for calibration and S1 is the initial of the calibration carried out on the wave probes attached on the model.

A similar procedure was then adopted to calibrate the three wave probes positioned on the bridge. Here, both ends of the bridge were lifted and then supported by two 5cm thick wooden blocks. The name given to this calibration is, such as CL512S2, where S2 is the notation of the calibration for wave probes on the bridge.

The rest of the calibration will then be done on the six LVDTs in which each LVDT will be treated independently from the others. LVDT1 was the first LVDT that was calibrated. The LVDT was displaced five centimetres using a vertical vernier attached to the piano wire which connects the LVDT to the model. The record of the calibration on LVDT1 is specified by S3 in CL512S3. In the same way of calibrations were then conducted for LVDT2 upto LVDT6, with the record initials, such as CL512S4, CL512S5, CL512S6, CL512S7 and CL512S8, respectively.

4.1.3. Running of the Test.

In this investigation of the SWATH1 model motions in regular quartering seas, the waves were generated in the frequency ranges from 0.3Hz upto 1.2Hz. To enable the observation on the effect of wave height on the model motions the voltage of the wave-maker was set as low as 4 volts and as high as 16 volts, to create two different wave heights of approximately five and ten centimetres, respectively.

The recording of motions and wave patterns in each test using the computer program was taken after the established wave train had passed the model and when the model had drifted from its original position to a new mean position about which it was oscillating steadily. A test record is specified by TS followed by the run number followed by S to separate the run number with the channel number (will be described later), for example TS512S.

4.1.4. Test Data Analysis.

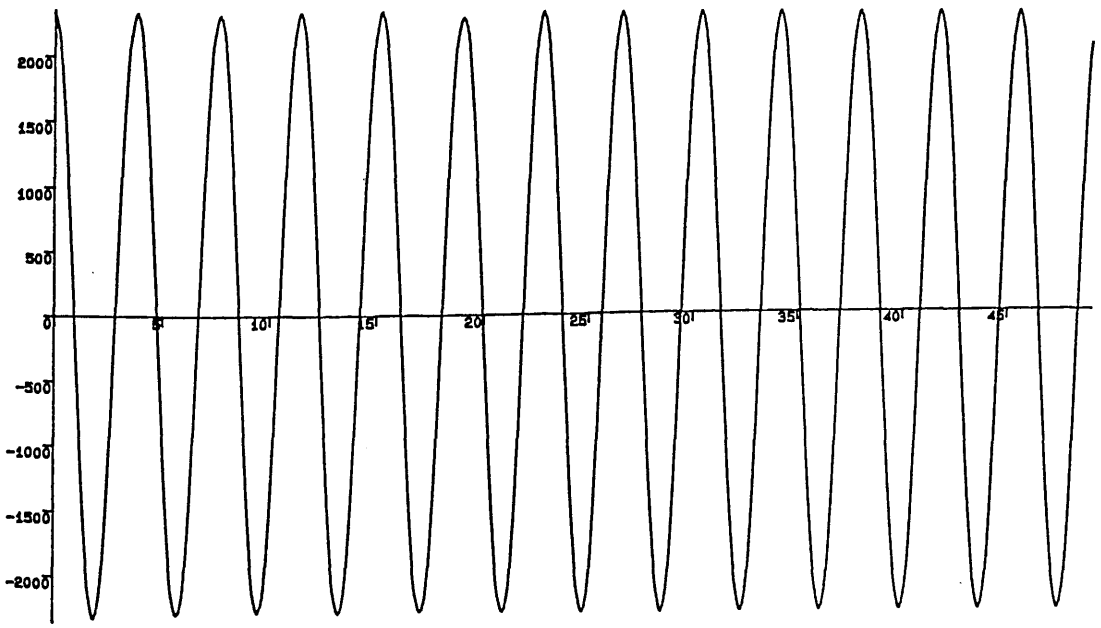

Figure 4.2. Typical Output of PROGBGRPH.FOR

The analysis of the experimental results was begun by obtaining the calibration factors of all measurement instruments. Amplitudes recorded by the digital recorder wer not stored in centimetres, but in a certain unit governed by the related computer program. Figure 4.2, which was plotted by running the computer program PROGBGRPH.FOR, shows a typical chart created by the digital recorder employed in this experiment.

As an example, how to find the calibration factor for LVDT2 is described below.

First find the average value of the zero position and the calibrated position of LVDT2. The zero position and the calibrated position are identified by ZR512S03 and CL512S43 respectively, where the initial 3 represents the channel number of LVDT2. Running a computer program, PROGBAVE.FOR, the average values obtained are found to be

Average value of ZR512S03 = 1843
Average value of CL512S43 = 3164

Since the relationship between the displacement of the LVDT and the displacement in the record is linear, the calibration factor can be calculated as

$$CF = \frac{\text{Ave. val. of CL512S43 - Ave. val. of ZR512S03}}{\text{Displacement of LVDT2}}$$

$$CF = \frac{3164 - 1843}{5 \text{ cms}} = \frac{1321}{5 \text{ cms}} = 264.2 \text{ cm}^{-1}$$

The other calibration factors can be obtained using the same procedure.

All of these calibration factors were then set as an input data for computer program CONVERSION.FOR which was written to change the original unit into centimetre. In this computer program, computations due to obtain the records of

waves and motions in the six modes of motions were carried out. The calculation of motions elevations were accomplished by the combination of the LVDTs elevations as follows :

a. the surge elevations,
   SU. el(evations) = LVDT6 el(evations),

b. the sway elevations,
   SW. els. = (LVDT1 els. + LVDT5 els.)/2,

c. the heave elevations,

$$\text{HV els.} = \frac{(\text{LVDT2 els.} + \text{LVDT3 els.})/2 + \text{LVDT4 els.}}{2},$$

d. the pitch elevations,
PT. els. = (LVDT2 els. + LVDT3 els.)/2 - LVDT4 els.,

e. the roll elevations,
   RL. els. = LVDT2 els. - LVDT3 els., and

f. the yaw elevations,
   YW. els. = LVDT1 els. - LVDT5 els.

Figs. 4.a-g are typical of waves and motions elevations produced by CONVERSION.FOR and then plotted by running the computer program OBLIGRPH.FOR. Utilising OBLIGRPH.FOR wave and motion elevations can also be read between any succesive crests and troughs in the elevations. After some readings had been done in every single wave or motion elevation chart the average value of wave and motion amplitudes can be calculated for a specific frequency. Wave and motion amplitudes of all wave frequencies used in the experiment were then compiled as the input data of computer program GRAPH.FOR.

The main purpose of GRAPH.FOR is to plot the graph of non-dimensional motion responses versus non-dimensional frequency, see figs. 4.4-4.9. Non dimensional motion

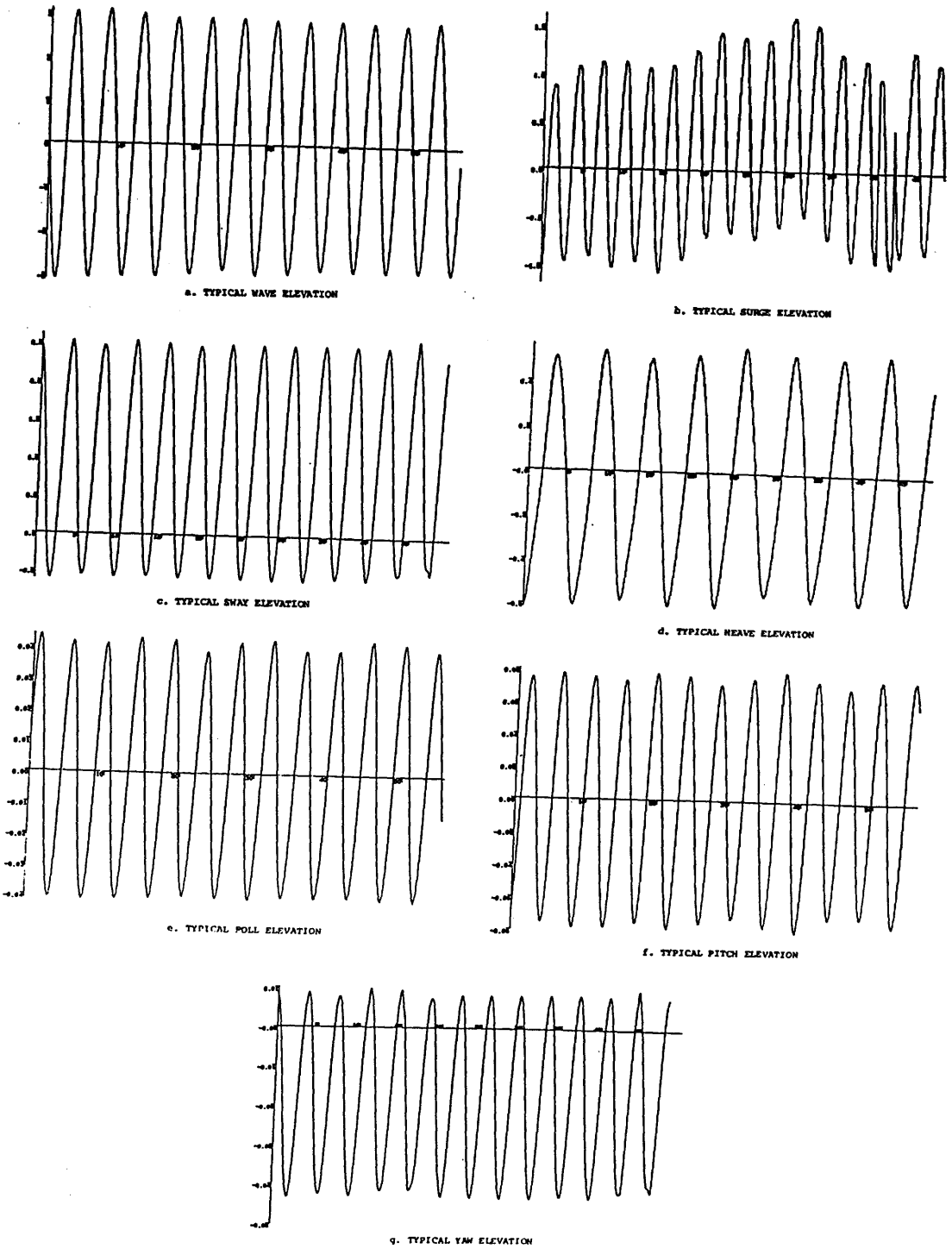

Figure 4.3. Typical Wave and Motion Elevations
Output of CONVERSION.FOR

responses of translational motions can be simply determined as follows

$$Y'_{x\zeta} = \frac{x_A}{\zeta_A} \qquad (4.1)$$

$$Y'_{y\zeta} = \frac{y_A}{\zeta_A} \qquad (4.2)$$

$$Y'_{z\zeta} = \frac{z_A}{\zeta_A} \qquad (4.3)$$

where $Y'_{x\zeta}$ = Non-dimensional surge response,
$Y'_{y\zeta}$ = Non-dimensional sway response,
$Y'_{z\zeta}$ = Non-dimensional heave response,
x_A = surge amplitude (m),
y_A = sway amplitude (m),
z_A = heave amplitude (m), and
ζ_A = wave amplitude (m).

In order to non-dimensionalise the rotational motion resposes wave number, which takes into account wave frequency and the acceleration due to gravity, should be included in the calculation, as set out below

$$Y'_{\phi\zeta} = \frac{\phi_A}{\zeta_A \omega^2/g} \qquad (4.4)$$

$$Y'_{\theta\zeta} = \frac{\theta_A}{\zeta_A \omega^2/g} \qquad (4.5)$$

$$Y'_{\psi\zeta} = \frac{\psi_A}{\zeta_A \omega^2/g} \qquad (4.6)$$

where $Y'_{\phi\zeta}$ = non-dimensional roll angle,
$Y'_{\theta\zeta}$ = non-dimensional pitch angle,
$Y'_{\psi\zeta}$ = non-dimensional yaw angle,
ϕ_A = pitch amplitude (rad),

θ_A = roll amplitude (rad),
ψ_A = yaw amplitude (rad),
ω = wave frequency ($rads^{-1}$), and
g = acceleration due to gravity
(= 9.81 ms^{-2}).

The non-dimensionalisation of the wave frequency was taken as,

$$\omega' = \frac{\omega}{\sqrt{g/L}} \qquad (4.7)$$

where L = characteristic length of the model
(= 1.5m)

The use of two different wave heights was to allow non-linear effects to be identified. However no consistent trends are seen in figs. 4.4-4.9, except at lower frequencies where the lower waves generally induced the higher response.

4.2. Comparison with Theoretical Results.

The results from the two-dimensional strip theory [72] and the three-dimensional theory [57] are also plotted in figs. 4.4-4.9 allowing comparison to be made.

For the surge response (fig. 4.4) only the results from the experiment and the 3-D theory are shown since the strip theory program does not calculate this mode [48,49,72]. The agreement of the observation and the theory is good. The difference in the resonant frequency region, ie. around 1.0 in non-dimensional wave frequency, if it were addressed to the 3-D theory than it may be caused by a slightly high value of hydrodynamic damping coefficient and damping due to viscosity taken in the computation.

For the sway mode of motion, fig. 4.5, the trend in the experiment matches the two theories quite well.

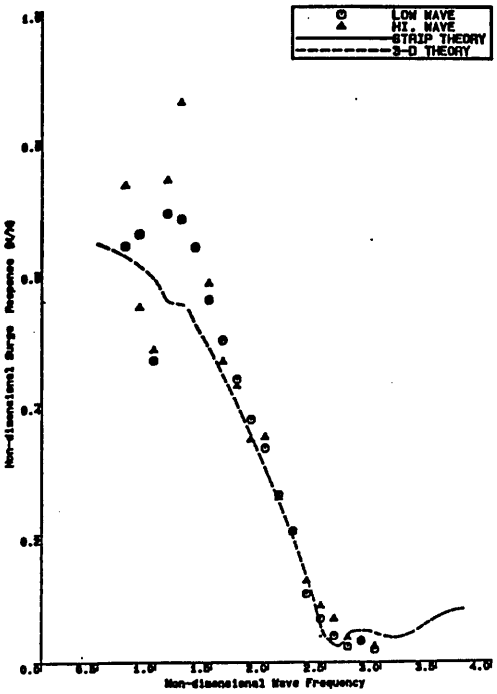

Figure 4.4.
SURGE RESPONSE
SWATH1 MODEL IN REGULAR QUARTERING SEAS

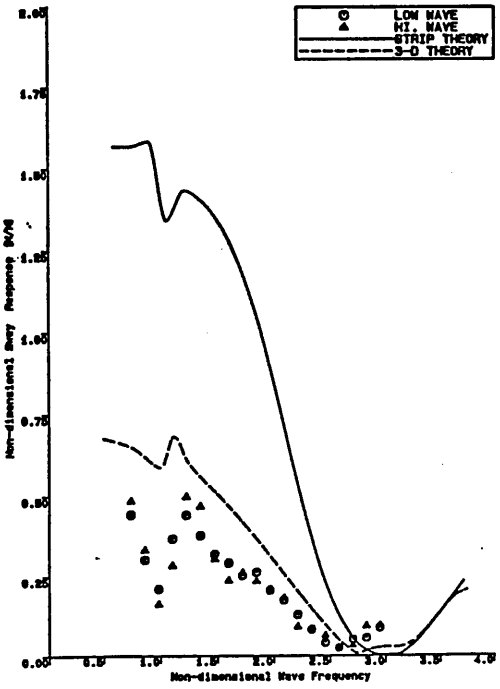

Figure 4.5.
SWAY RESPONSES
SWATH1 MODEL IN REGULAR QUARTERING SEAS

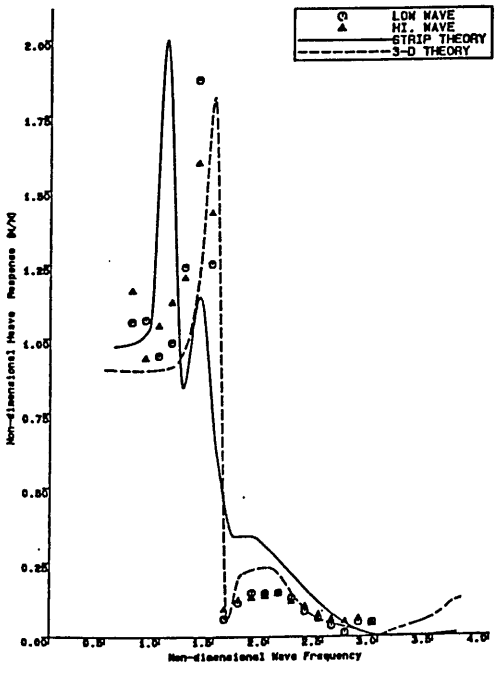

Figure 4.6.
HEAVE RESPONSES
SWATH1 MODEL IN REGULAR QUARTERING SEAS

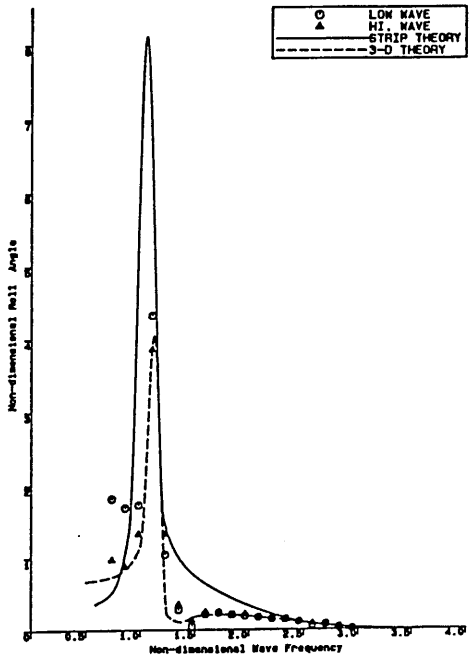

Figure 4.7.
ROLL RESPONSES
SWATH1 MODEL IN REGULAR QUARTERING SEAS

Referring back to the comparison of this motion in beam seas, ie. fig. 3.7 and in [77,78], the curve obtained from the 3-D theory is considered reliable, whereas from the experiment seem to be slightly low and from the strip theory seem to be very high. The most probable cause of low responses in the experiment is the influence of the mooring lines stiffness on the model motions, see fig. 4.1.

It was expected that the values of the sway motion responses in quartering seas would not exceed the values in beam seas. In this case, however, the strip theory performs the other way around. This circumstance possibly be brought about an overestimation in the computation of the interference effect between the twin-hull, particularly in the prediction of wave diffraction induced hydrodynamic coefficient. In the strip theory it was only the diffraction of the standing waves in between the two tandem-struts that was considered and the diffraction of the incoming waves is not taken into account [68,82]. Nonetheless, this is a limitation of the theory and such complex phenomenon of wave diffraction are better treated by three-dimensional approach. Other factors such as the absence of the viscous damping coefficient and other hydrodynamic coefficient computations may be important.

The 3-D theory is in satisfactory accord with the experiment in the heave response. It is interesting to observe that the curve drawn from the strip theory shows two peaks in the resonant frequency region. Comparing with fig. 3.6 the maximum value of the heave response should be in the range between 1.35-1.4 of the non-dimensional wave frequency. In fig. 4.6, however, the maximum value is found in the non-dimensional frequency of about 1.0. From fig. 4.8 this may be seen to be the pitch natural frequency of the SWATH1 model. At present this occurrence may be explained by the fact that the heave and pitch coupled added mass, damping and hydrostatic restoring force coefficients effect the heave motion. So far the three sources having the

maximum value of the non-dimensional heave response in the range 1.75 upto 2.0.

The roll response curve from the 3-D theory illustrated in fig. 4.7 is the revision of that presented in [78]. The revision mainly dealt with the correction of GM_T value in the computation. Matching the GM_T in the computation to the model's gives a better confirmation of the curve peak, which is the roll natural frequency.

From strip theory, the roll response curve obtained produces a reliable trend for the low frequencies, but the absence of viscous damping coefficient leads to a relatively high maximum response in the natural frequency. Above the natural frequency, when it is compared to the roll response in beam seas, it seems to be too high since in the frequency of about 1.3 - 1.4 the curve should steeply turn down approaching zero and then slightly raise at higher frequencies. As far as the theoretical approach is concerned this could possibly be caused by an over estimation in computing the hydrodynamic coefficient and the interference effects. It should also be borne in mind that roll motion through the coupled added mass and damping coefficient contributes the magnitude of sway motion and vice versa. Therefore high roll response would lead to high sway responses over almost entire frequency range, (cf. fig. 4.5).

In the pitch mode of motion, as shown in fig. 4.8, the three sources give consistent results for most frequency range. Relatively high pitch response of the strip theory curve and relatively low from the 3-D theory curve in the natural frequency possibly be caused by the absence and an over prediction of viscous induced damping coefficient respectively. As has been mentioned earlier that from the coupled motion point of view the pitch motion influences the surge motion. This relation can be observed in figs. 4.4 and 4.8 for the 3-D theory. As in the resonant frequency the

pitch response obtained is quite low consequently in the surge response is also low. By correcting the viscous damping coefficient the discrepancy in the surge response will be reduced.

As in the sway responses, the curves of yaw responses from the 3-D theory, the strip theory and the experiment, shown in fig. 4.9, exhibit the similar patterns. Higher and lower responses given by the two theories than the measurement could not possibly be influenced by the viscosity since in this mode of motion its effect is not significant. This, however, might be related to the presence of roll hydrodynamic coefficient induced yaw rotational motion. An almost similar unexplained case relating to semi-submersible can be found in [83]. From the experiment arrangement standpoint the mooring lines arrangement could adversely effect in this matter.

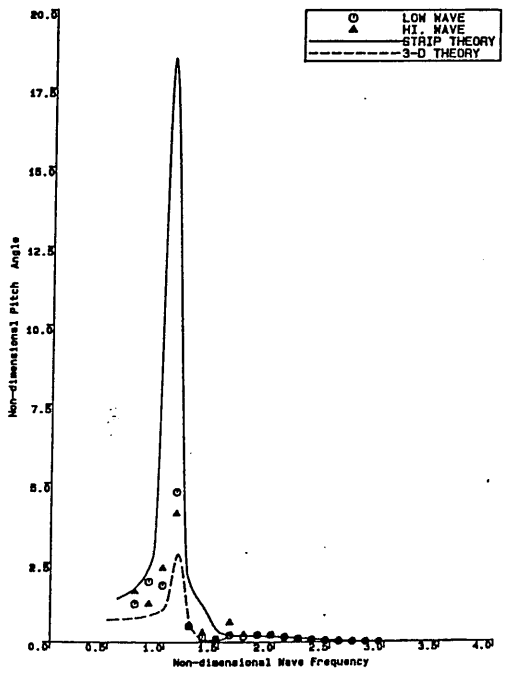

Figure 4.8.
PITCH RESPONSE
SWATH1 MODEL IN REGULAR QUARTERING SEAS

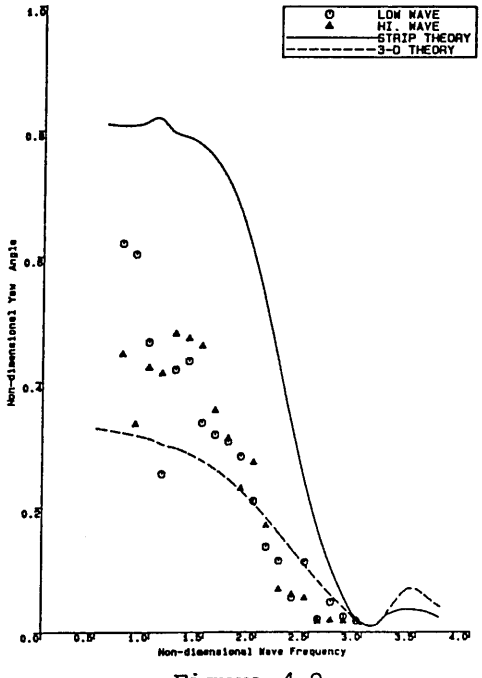

Figure 4.9.
YAW RESPONSES
SWATH1 MODEL IN REGULAR QUARTERING SEAS

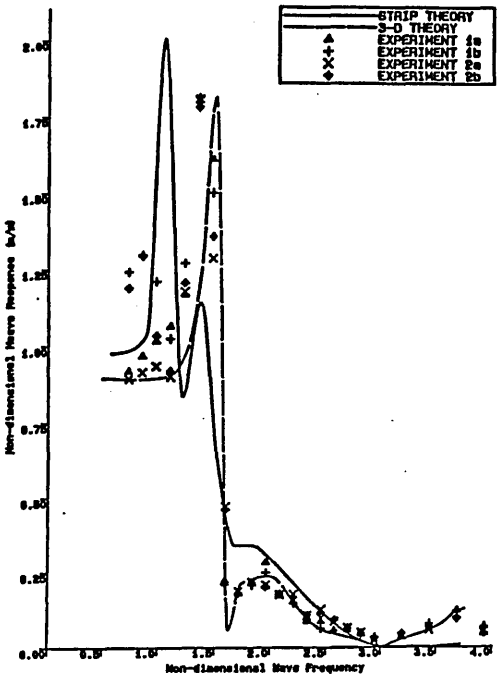

Figure 4.10.
HEAVE RESPONSES
SWATH1 MODEL IN REGULAR QUARTERING SEAS

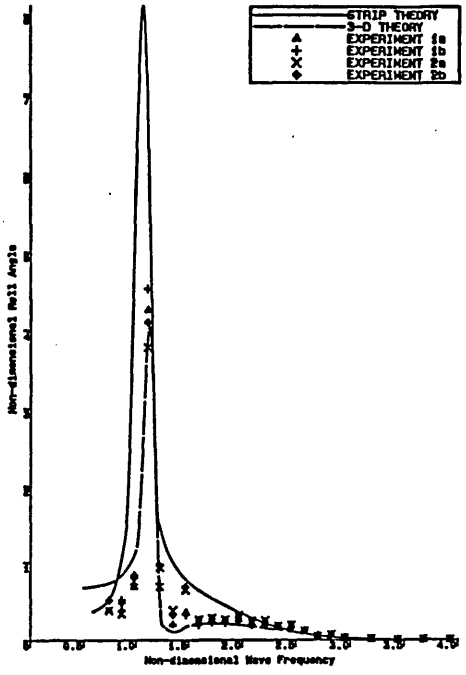

Figure 4.11.
ROLL RESPONSES
SWATH1 MODEL IN REGULAR QUARTERING SEAS

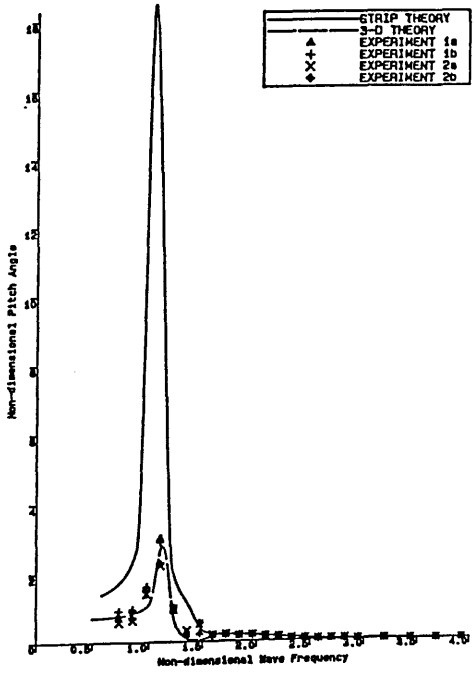

Figure 4.12.
PITCH RESPONSES
SWATH1 MODEL IN REGULAR QUARTERING SEAS

Addition experimental data, which was generated as a by product of the observation on SWATH1 structural loadings in quartering seas (see chapter six), is presented for the three vertical plane motions (ie heave, roll and pitch) shown in figs. 4.10-4.12, respectively. Although the results are not much different from the preceeding investigation but some distinct features are worthy of comment. Experiment 1 and 2 in the graphs denote the experiments were carried out in low and high waves, respectively, whereas initial a and b are to distinct between those correlated to the wave amplitudes measured at the lead of the model and at the bridge,respectively.

It is quite noticeable in the heave response that the experiment results which are related to high wave amplitudes, although these are not as high as performed by the strip theory, also show a second peak in the low frequencies. In the moderate frequencies the experiment matches the two theories even better. The absence of counter balance systems on the LVDTs to measure surge, sway and yaw in the second experiment may account for this improvement.

There was not much changes in both the roll and pitch responses, except for those experiment results in pitch which were closer to the 3-D theory and lower roll responses in the lower frequencies. These might be caused by a slight difference in the experimental arrangement. It should also be borne in mind that in the later experiment the model's transverse bars have been modified.

4.3. Conclusions.

The conclusions of this chapter are set out below.

1. The experiment results of SWATH1 model motions in quartering seas confirm the two numerical approaches very well in most mode of motions.

2. Viscous damping effect quite significantly influences the motion responses near resonant frequency region, but not so at higher frequencies.

3. The experimental arrangement to observe seakeeping performance in oblique presents many difficulties to be overcome. Any discrepancy in the experimental data may, therefore, be partially caused by these limitations. It is not very easy, however, to alter the mooring system in order to minimise its effects on the model motions. The use of LVDTs to measure the horisontal plane motions apparently could be altered by employing the selspot system which would eliminate the need for balancing weights in some modes.

4. The second experiment data drawn together with the observation of loadings in quartering seas confirms the validity of experimental results presented, particularly for the vertical plane motions of SWATH1 model.

CHAPTER 5

SWATH1 MODEL MOTIONS IN REGULAR HEAD SEAS WITH AND WITHOUT FORWARD SPEEDS

Chapter 5.

SWATH1 MODEL MOTIONS IN REGULAR HEAD SEAS WITH AND WITHOUT FORWARD SPEEDS

Motions of a ship in head seas are always of particular intersest to be exploited and discussed. This is understandable because a ship will mostly be operated in this sea heading. Experimental data on a SWATH ship model in head seas is a valuable contribution that should be generated to complement the theoretical predictions. Two series of experiment on SWATH1 model motions in regular head seas, namely in stationary and with forward speed, have been carried out.

Data acquisition for the experiment with the model at forward speed is not a problem in that the model length is relatively small compared to the effective length of the tank. This means that enough data can be collected in each test run.

In this experiment other aspects such as sinkage, trim and resistance can also be observed.

5.1. SWATH1 Model Motions with Zero Speed.

The experiment conducted to investigate the SWATH1 model motion in head seas at zero speed was quite similar to that in beam seas of chapter 3. In this experiment the model was positioned in between the two sub-carriage's bridges heading into the regular wave trains, as shown in fig. 5.1. Two mooring lines were attached on each strut and tied to the tank side walls, thus the model would not drift further from the original position when waves were run.

Pitch and heave motions of the model were measured by means of two LVDTs mounted on the sub-carriage's gantry over the fore and aft transverse beams. A camera detector

(selspot) was applied to measure the surge motion. The use of a selspot proves more reliable than an LVDT in this case, as the balancing effect imposed on the model surge can be completely be eliminated. Any effect of the tank side walls on the wave elevations were observed by three different wave probe positions relative to the tank side walls. The wave probes were fixed on a bridge 4.5 m from the midship of the model in calm water. All of these electronic devices were connected to a pen recorder through an amplifier. The electric signal voltages sent by the LVDTs were first processed in a sum and difference unit, thereafter, the output recorded on the chart gave directly the summation of the signal voltages of LVDT1(x) and LVDT2(y) divided by two (x+y/2), which produces the heave elevation, and the difference of the signal voltages of LVDT1 and LVDT2 (x-y), relates to the pitch elevation of the model, see fig. 3.3.

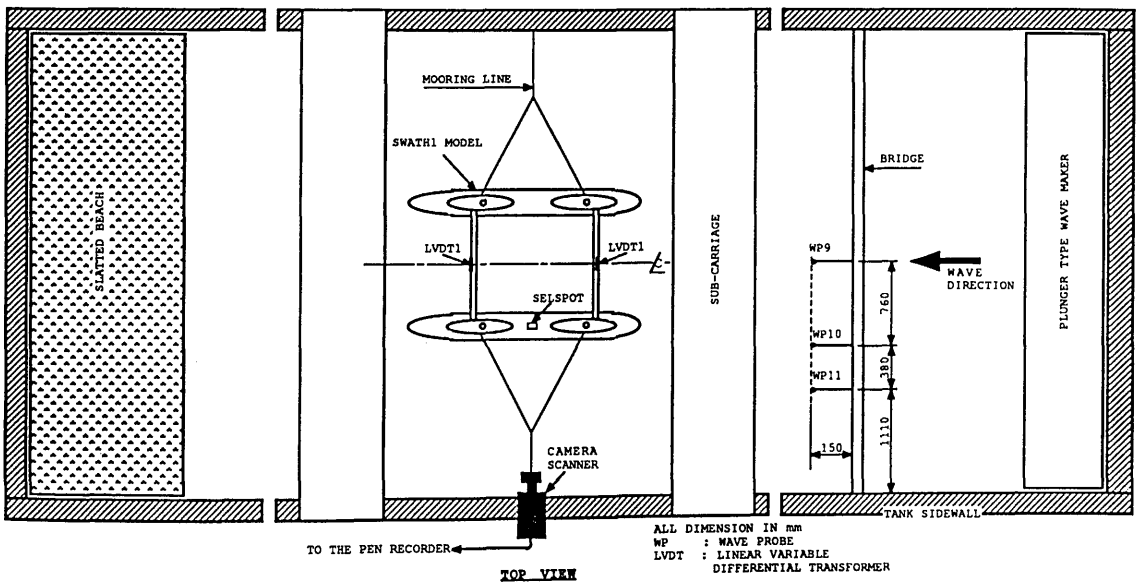

Figure 5.1. Experimental Arrangement of SWATH1 Model in Head Seas (stationary)

5.1.1. Calibration Procedures.

Four calibrations were carried out, namely calibration of the wave probe, calibration for surge, and

calibrations related to heave and pitch.

5.1.2. Running the Test.

The frequency range of the waves generated during the test was from 0.3Hz upto 1.6Hz with interval of 0.05Hz for wave frequencies upto 1.2Hz and interval of 0.1Hz for the remaining frequencies. The non-linear effect of the wave height on the model motion was observed by running the test in two different wave height for each frequency. These two different wave height were created by adjusting the wave maker in two different voltages such that the waves created were approximately five and ten centimetres. The recording of the model motions was made after the model had obtained a regular oscillation.

In addition to the main experiment the heave and pitch natural frequency were also measured. This is very important as the data obtained can be used to determine how many wave frequencies need to be carried out in the experiment, particularly in the natural frequency proximity, see figs. 5.2 and 5.3.

5.1.3. Test Data Analysis.

The readings of the wave and model motion responses were taken for every wave frequency. The results of the double amplitudes of the elevations were then processed to give their average values. The actual model and wave average double amplitudes in centimetres (metres) can be found by multiplying these values with the corresponding calibration factors. As the pitch amplitudes obtained in this stage is in the metre unit, ie. the difference of LVDT1 and LVDT2 amplitudes, it was necessary that they be converted into rotational unit (radian or degree) by taking into account the distance of the two LVDTs. The next steps of the analysis such as to obtain the motion responses etc. were calculated in the same way as that given in the foregoing

chapters. The results are presented as the motion responses of SWATH1 model in frequency domain, see figs. 5.10-5.12.

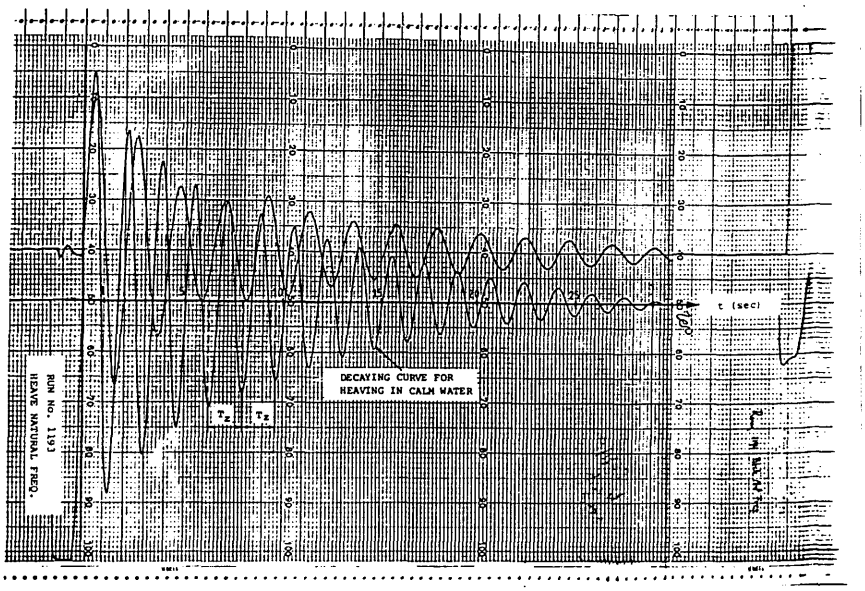

Figure 5.2. Decaying Curve for Heaving in Calm Water

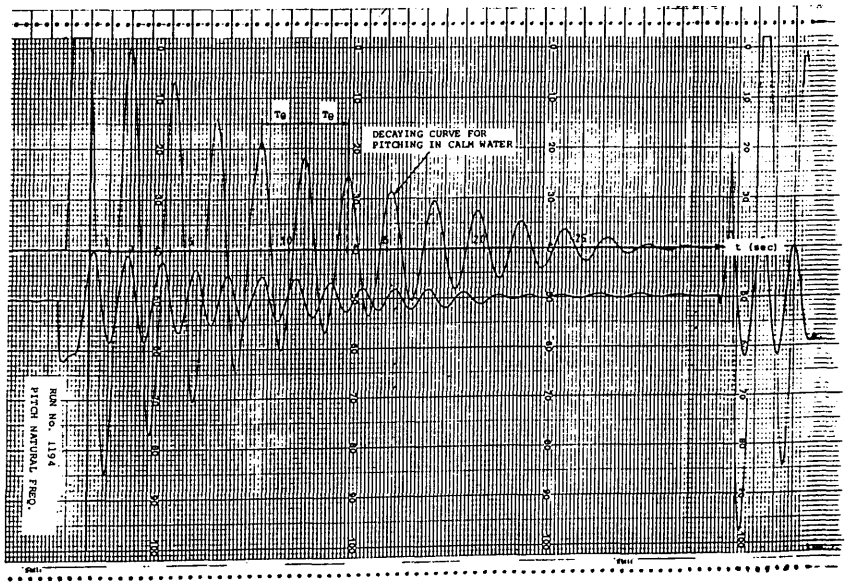

Figure 5.3. Decaying Curve for Pitching in Calm Water

The heave and pitch natural frequencies were measured from figs. 5.2 and 5.3. This was accomplished by measuring the

length of the oscillation periods in centimetres. As the record paper was set to move with the speed of 1cm/sec during the recording, the natural periods in seconds, therefore, can be obtained directly with exactly same values as measured from peak to peak, and the results are as follow :

Natural period for heaving, T_z = 1.7 secs.
Natural period for pitching, T_θ = 2.2 secs.
Natural frequency for heaving, f_z = 0.588 Hz.
Natural frequency for pitching, f_θ = 0.454 Hz.

5.2. SWATH1 Model Motions with Forward Speeds.

In this experiment the model was mounted under the mobile main-carriage, as shown in fig. 5.4. Two LVDTs to measure heave and pitch modes of motion as well as measure sinkage and static bow-trim were mounted on the gantry. The only connecting line used had two functions, first to drag the model along the tank and second to connect the model with a dynamometer where the surge motion and the resistance of the model were recorded. Four guide rods, two in each side of the model, were utilised to maintain the model in the right course, such that there was no yaw, roll or sway.

The model was tested at four speeds, ie 0.5m/s, 1.0m/s, 1.5m/s and 2.0m/s which correspond to the Froude number of 0.13, 0.26, 0.39 and 0.52, respectively. These characteristic speeds conducted in the experiment are associated with a medium speed SWATH. The model was run in a given speed which was controlled by an operator from the control desk. The recording was taken both on the multi-channel pen-recorder and on the dynamometer recorder when steady speed had been achieved. Another series of experiments has been carried out on the SWATH2 model, fig. 5.5, with the same Froude number as that of the SWATH1 model, so that a comparative study of the different hull cross-section effects on the SWATH ship motions can be accomplished.

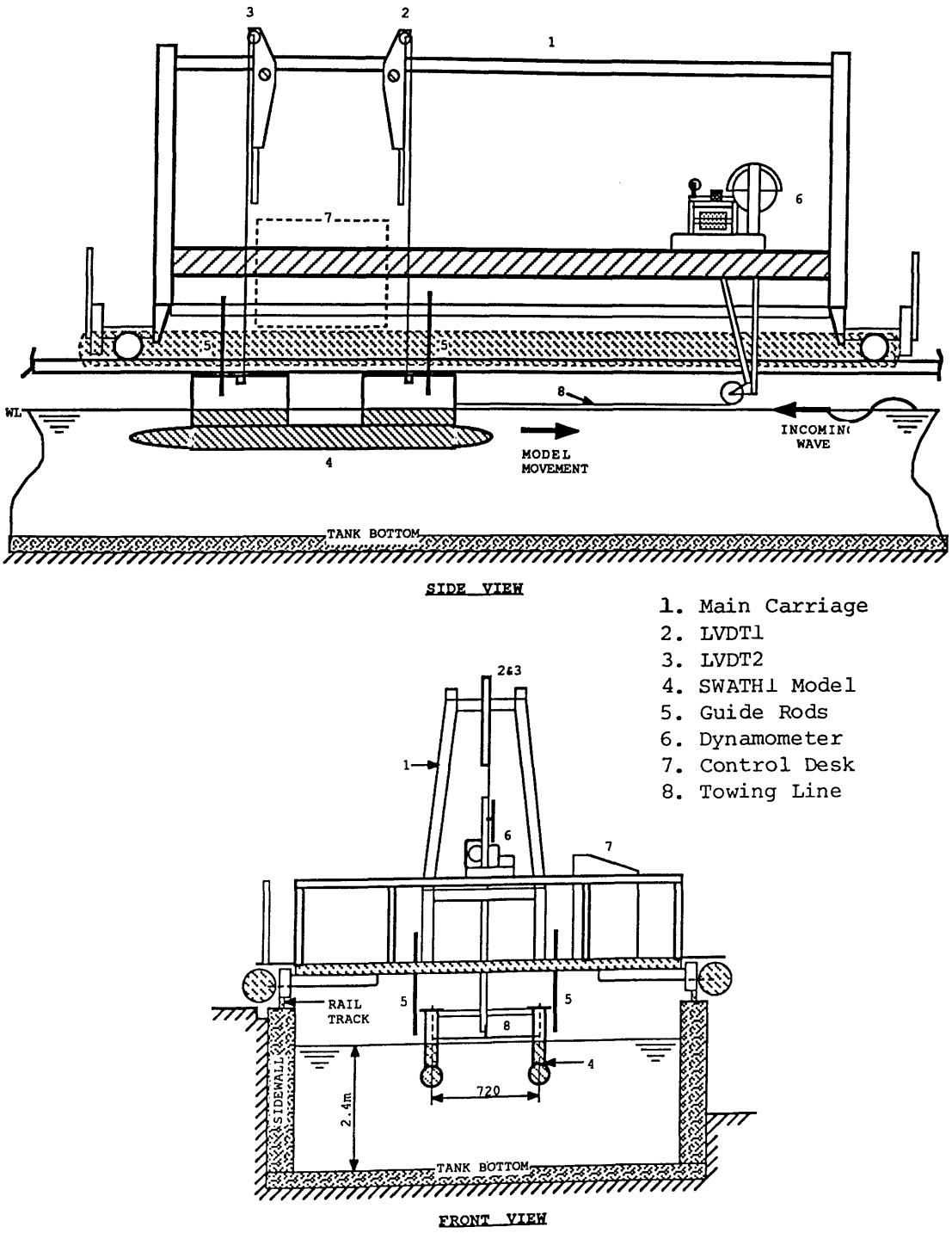

Figure 5.4. SWATH1 Model at the Towing Carriage

Calibration was conducted for the LVDTs and three wave probes which were placed on a bridge at the wavemaker end of the tank. The calibration of the dynamometer for resistance is given by graph in fig. 5.6 which illustrate the drag at the model as a function of the model movement.

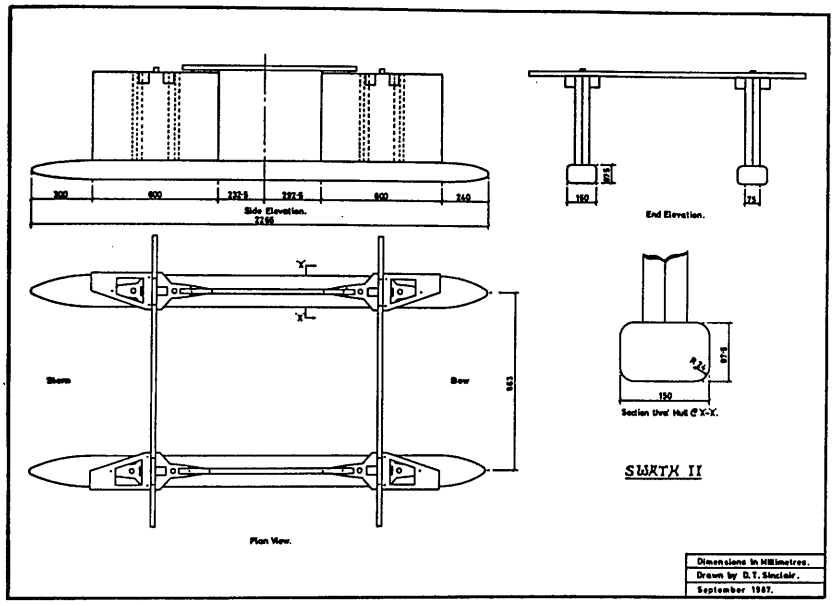

Figure 5.5. SWATH2 Model

5.2.1. Test Data Analysis.

The procedure to obtain the heave and pitch responses of the model from the record data can be found in the previous sections.

The magnitude of the model surges are read from the records taken from the dynamometer, see fig. 5.7. Fig. 5.8 illustrates the wheel system in the dynamometer. The record of surge is generated by a pen which is connected to the wheel with D=1. Since the model is connected to the pendulum wheel with D=3, whose diameter ratio is 3 to 1 to the wheel of the pen, the actual surge amplitude of the model is,

therefore, three times of that measured from the record within the appropriate unit.

The total resistance imposed on the model is obtained from the same record of surge as indicated in figs. 5.7 and 5.8. A more detail explanation in SWATH1 model resistance observations and results is presented in [84].

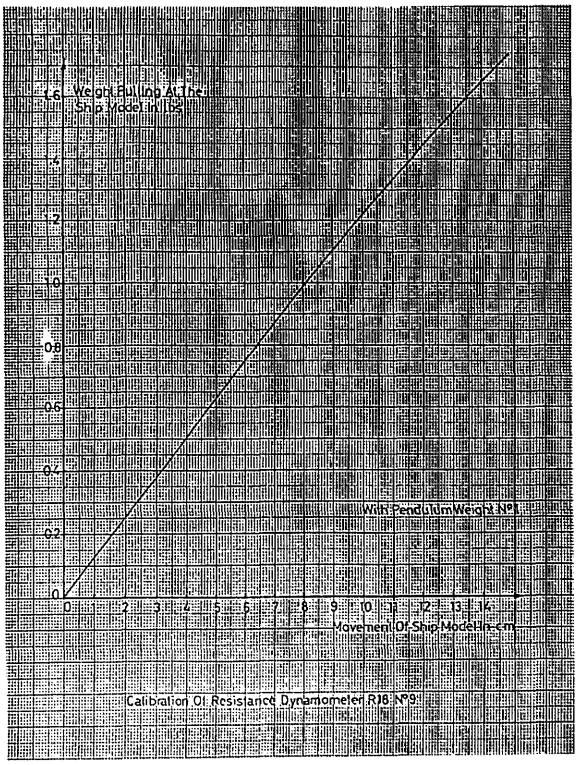

Figure 5.6. Calibration Graph for Resistance Measurement

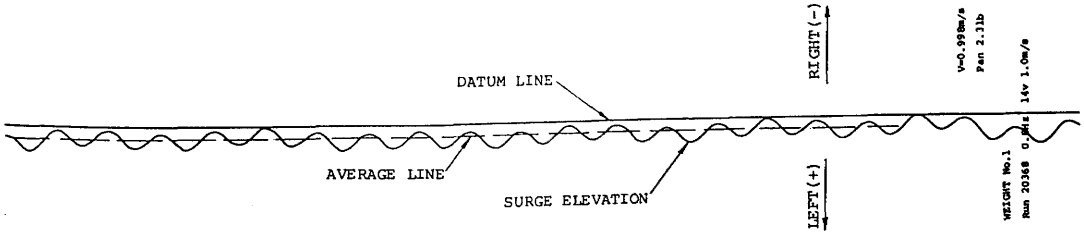

Figure 5.7. Typical Chart Record for Surge and Resistance

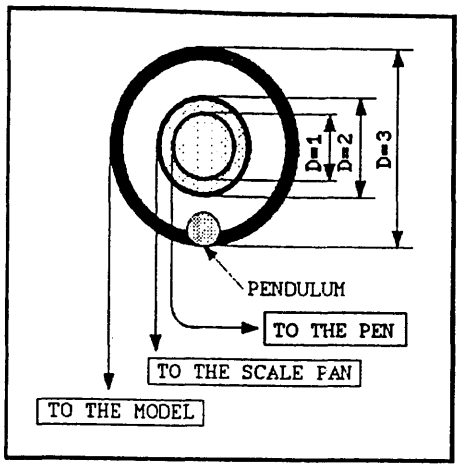

Figure 5.8. Wheel System in the Dynamometer

To observe the sinkage and trim, pen records of heave and pitch are needed, see fig. 5.9. Sinkage is related to the heave motion of the model and static bow-trim, which develops with forward speed due to the Munk moment that is proportional to heave added mass times the square of the model speed [69]. The magnitude of sinkage is taken as the offset of the average line of heave elevation from the zero (or datum) line times the heave calibration factor. Similarly, the static bow-trim is taken as the displacement of the average line of pitch elevation times the pitch calibration factor.

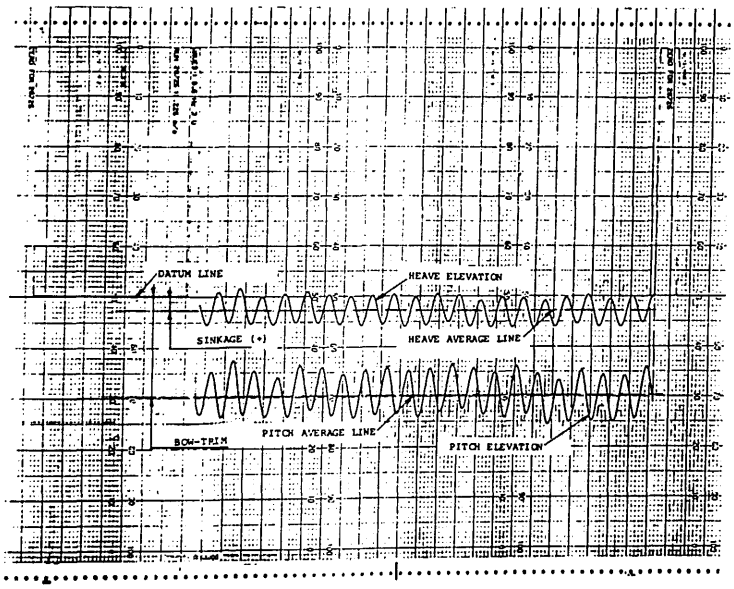

Figure 5.9 Heave and Pitch Record to Measure Sinkage and Trim

To plot the surge, heave and pitch responses in frequency domain, the wave encounter frequency should then be introduced as

$$\omega_e = \omega(1 - \frac{\omega V}{g} \cos\mu) \qquad (5.1)$$

where ω_e = encounter wave frequency in $rads^{-1}$,
ω = wave frequency in $rads^{-1}$,
V = ship(or model) speed in ms^{-1},
g = acceleration due to gravity (=9.81 ms^{-2}), and
μ = ship(or model) heading angle.

Consequently the non-dimensional encounter wave frequency, which is derived by taking into account the acceleration due to gravity and the model's characteristic length, is

$$\omega_e' = \frac{\omega_e}{\sqrt{g/L}} \qquad (5.2)$$

5.3. Comparison with Theoretical Results.

5.3.1. SWATH1 Model with Zero Speed.

In fig. 5.10 of SWATH1 model surge response, the agreement between the 3-D theory and the experiment seem satisfactory. The discrepancy in the resonant frequency vicinity could not be described further but a similar result has been clarified in chapter four for the corresponding mode of motion.

For the heave mode of motion the two theories can be said as to confirm the experiment as shown in fig. 5.11. The peak responses given by the experiment is consistent with those observed in beam and quartering seas (see chapter three and four and [77,78]).

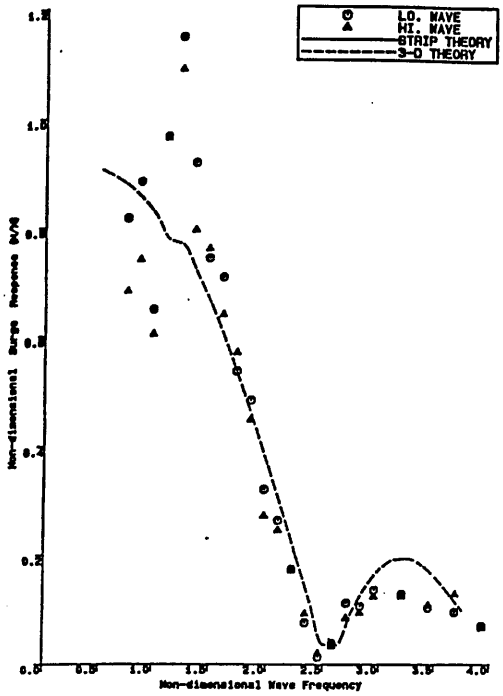

Figure 5.10.
SURGE RESPONSES
SWATH1 MODEL IN REGULAR HEAD SEAS

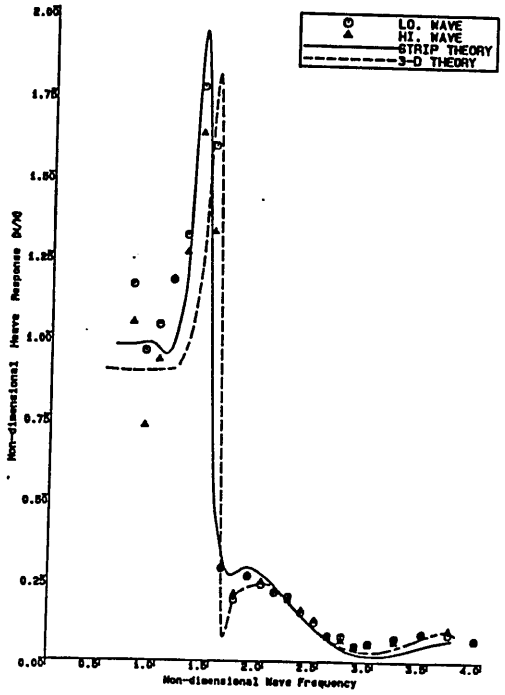

Figure 5.11
HEAVE RESPONSES
SWATH1 MODEL IN REGULAR HEAD SEAS

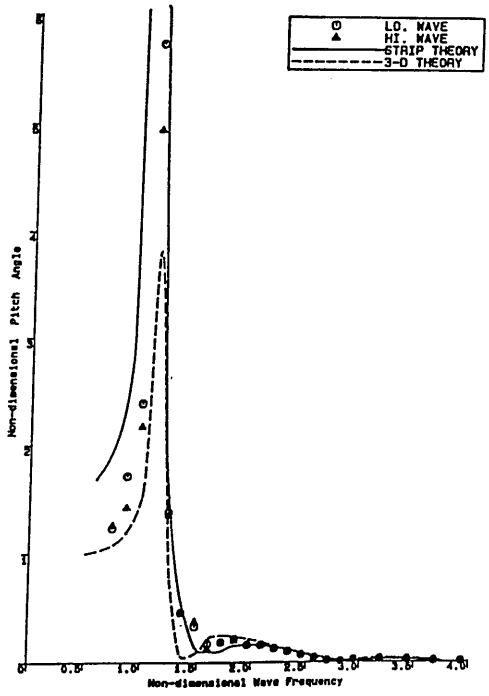

Figure 5.12.
PITCH RESPONSES
SWATH1 MODEL IN REGULAR HEAD SEAS

The prediction of SWATH1 model pitch motion in head seas using strip theory, as can be seen in fig. 5.12, seems to be slightly over estimated in the sub-critical frequency zone. This might possibly be caused by the absence of a viscous damping coefficient in the computer program SWATHL. Nonetheless, as far as the pattern is concern, the three sources give quite good agreement.

5.3.2. SWATH1 Model with Forward Speeds.

In order to ease the observation of the speed influences on the motions of SWATH1 model the graphs are grouped according to the mode of motion. Experiment 1 and 2 denote that the investigations were conducted in low and high regular wave amplitudes, respectively.

Fig. 5.13. of surge responses show that the agreement between the results from the experiment and the 3-D theory to be quite satisfactory, particularly for Fn of 0.13 and 0.52. In the Fn of 0.26 and 0.39 the discrepancy occurs only within the low frequencies (±1.5 of non-dimensional encounter wave frequency and below). The high surge responses performed by the experimental data in this region might be caused by the absence of a restoring force, which in vertical plane motions is the dominant factor that determines the motion magnitude in such a region. In higher frequencies, however, the two sources match each other very well. Furthermore, in the first frequency of harmonic the experimental data gives approximately the same maximum value of surge response (approximately 0.1) in the four Fns.

In the heave mode, fig. 5.14, the experimental results confirm the two theories very well primarily in higher frequencies. An absence of damping due to viscosity in the strip theory leads to a slightly higher heave response in the critical zone for Fn of 0.26 up to 0.52.

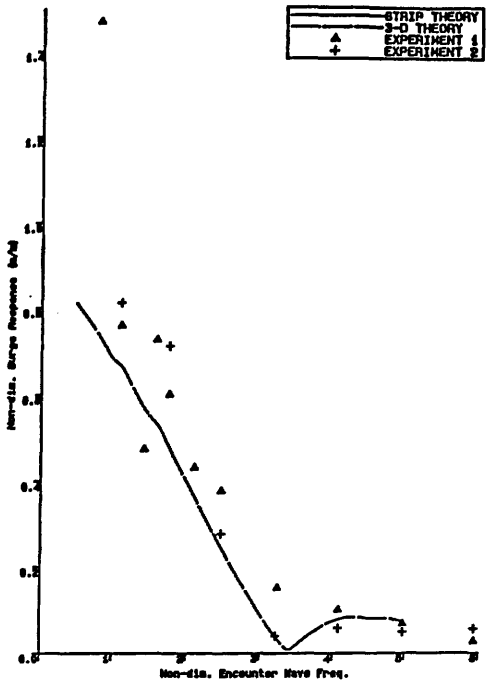

SWATH1 MODEL SURGE RESPONSES
IN REGULAR HEAD SEAS (Fn=0.13)

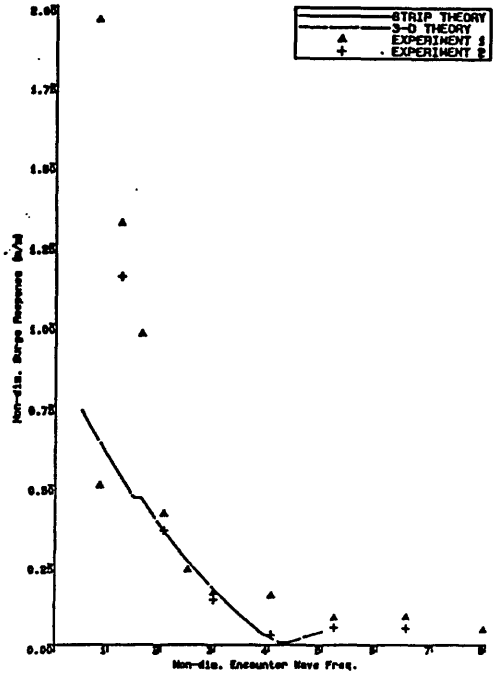

SWATH1 MODEL SURGE RESPONSES
IN REGULAR HEAD SEAS (Fn=0.26)

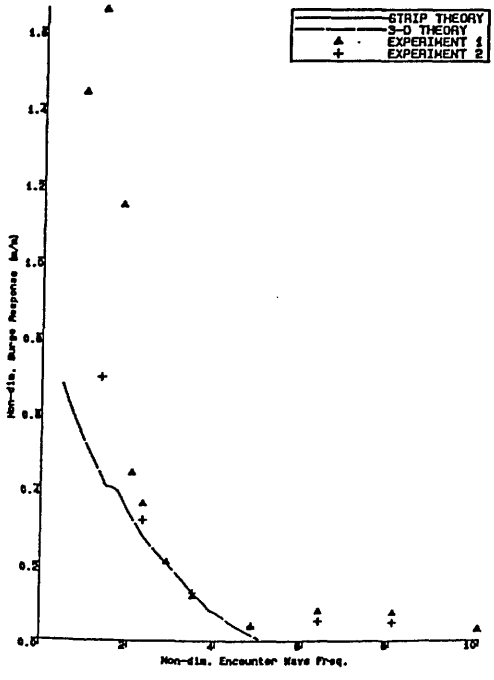

SWATH1 MODEL SURGE RESPONSES
IN REGULAR HEAD SEAS (Fn=0.39)

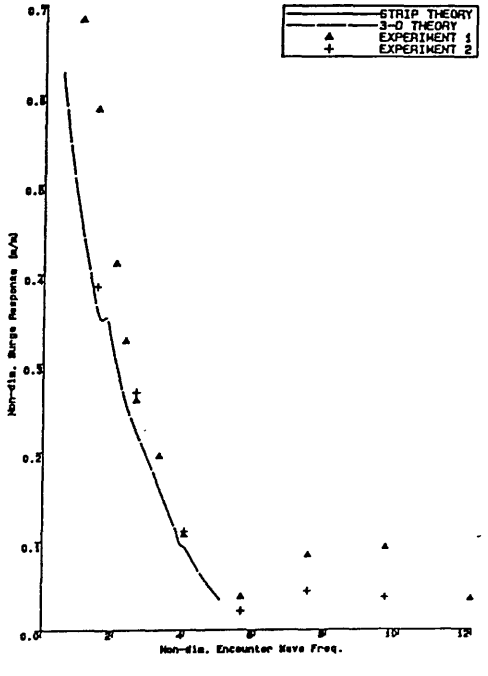

SWATH1 MODEL SURGE RESPONSES
IN REGULAR HEAD SEAS (Fn=0.52)

Figure 5.13. SWATH1 Model Surge Responses in Regular Head Seas with Forward Speeds

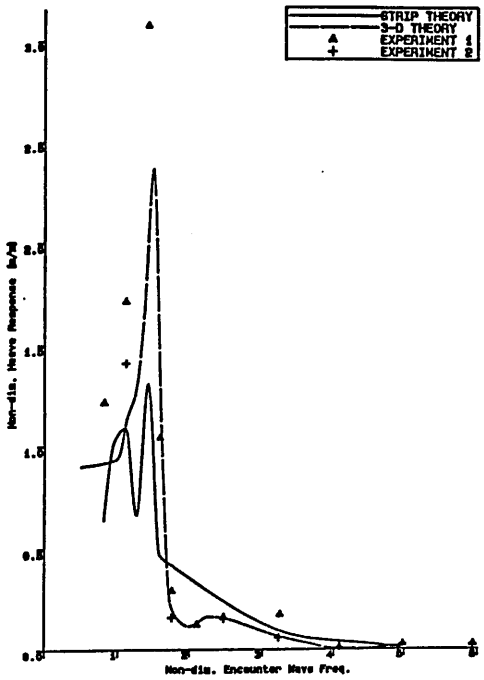

SWATH1 MODEL HEAVE RESPONSES
IN REGULAR HEAD SEAS (Fn=0.13)

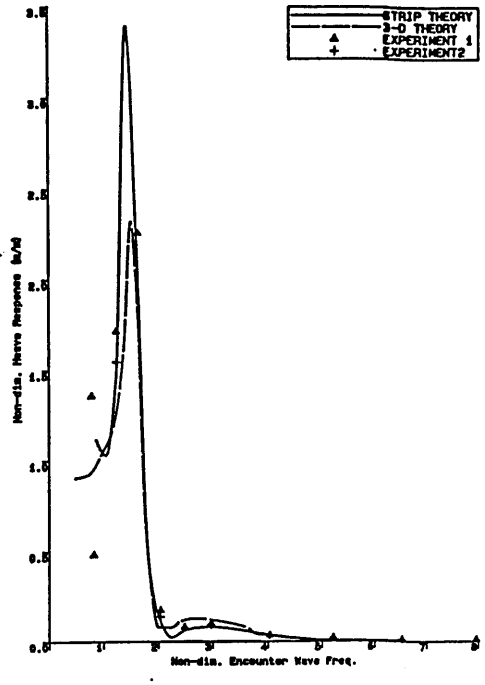

SWATH1 MODEL HEAVE RESPONSES
IN REGULAR HEAD SEAS (Fn=0.26)

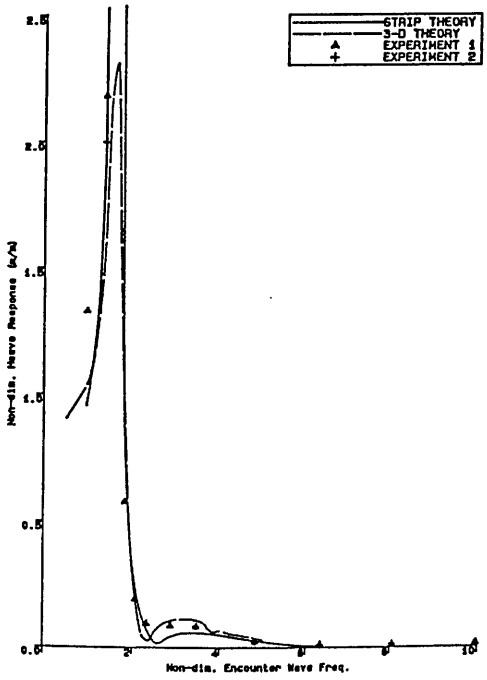

SWATH1 MODEL HEAVE RESPONSES
IN REGULAR HEAD SEAS (Fn=0.39)

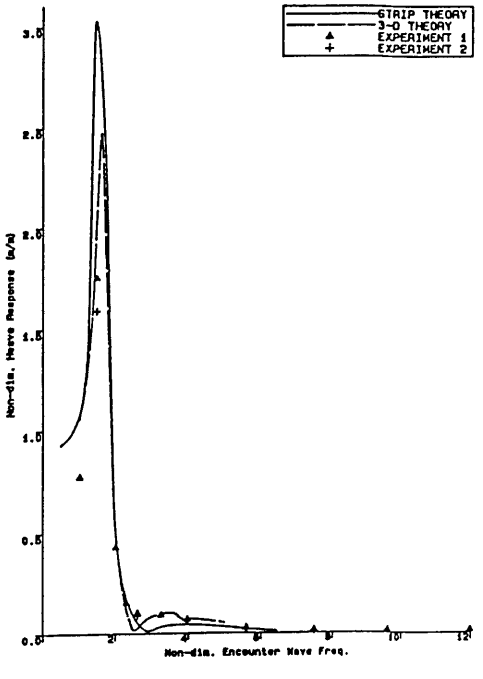

SWATH1 MODEL HEAVE RESPONSES
IN REGULAR HEAD SEAS (Fn=0.52)

Figure 5.14. SWATH1 Model Heave Responses in Regular Head Seas with Forward Speeds

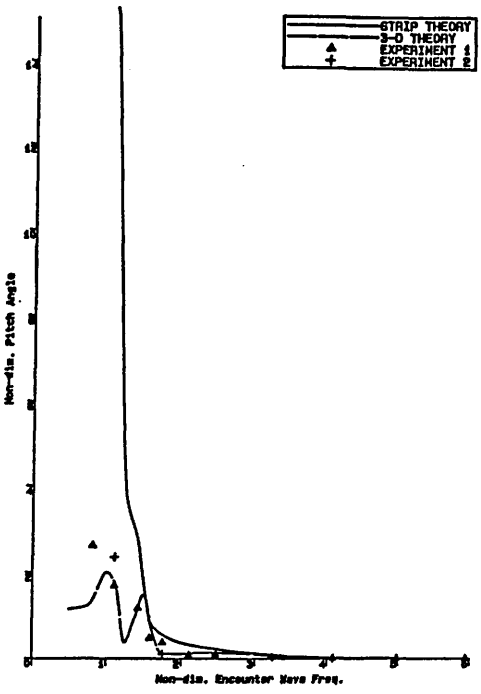

SWATH1 MODEL PITCH RESPONSES
IN REGULAR HEAD SEAS (Fn=0.13)

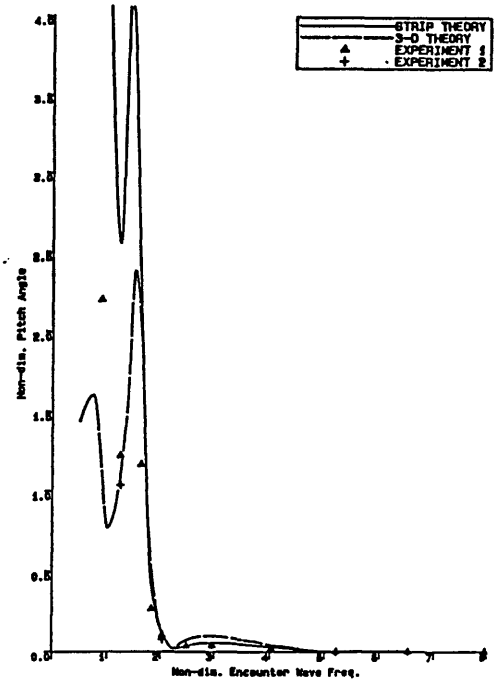

SWATH1 MODEL PITCH RESPONSES
IN REGULAR HEAD SEAS (Fn=0.26)

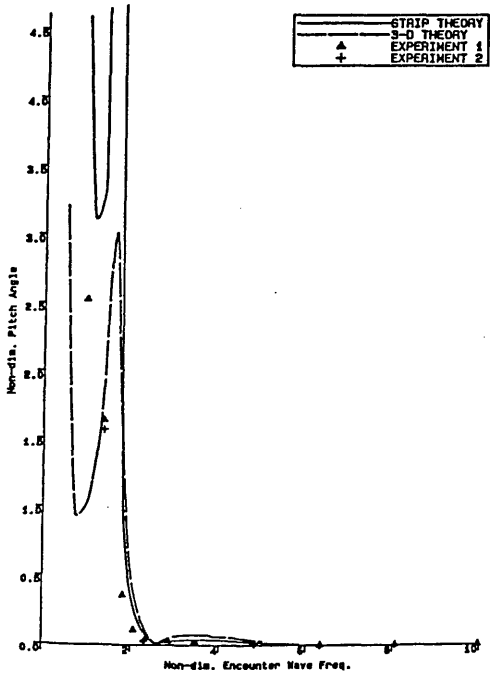

SWATH1 MODEL PITCH RESPONSES
IN REGULAR HEAD SEAS (Fn=0.39)

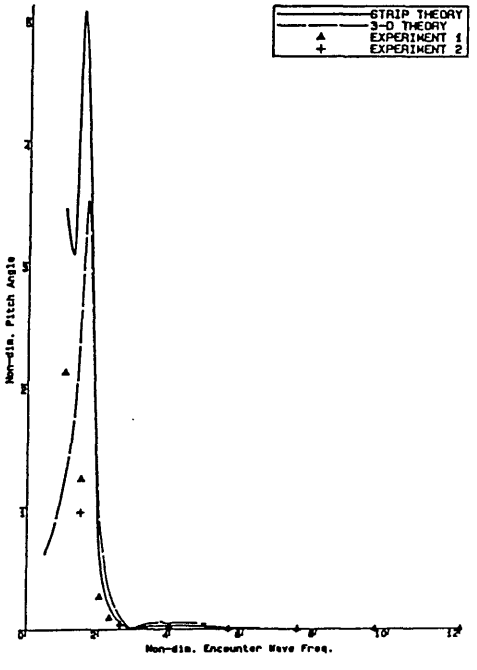

SWATH1 MODEL PITCH RESPONSES
IN REGULAR HEAD SEAS (Fn=0.52)

Figure 5.15. SWATH1 Model Pitch Responses in Regular Head Seas with Forward Speeds

An almost similar case as found in quartering seas performed by the strip theory in Fn of 0.13. As is seen, the curve has two peaks although not as high as in quartering seas, see fig. 4.4.

Similarly, in the pitch mode (fig. 5.15) the experiment accords the two theories in supercritical zone in which a SWATH ship, as expected, will mostly be operated. Referring to fig. 5.12. the experimental data in forward speeds gives consistent pitch resonant frequency, ie 1.0 in non-dimensional frequency. In the 3-D theory the coupling effect of heave on pitch motion in the resonant frequency region seem to be significant, particularly for Fns 0.26 up to 0.52. This effect can be identified in that the peaks of pitch responses in these three forward speed occur at the non-dimensional encounter frequency of about 1.5, which apparently is the heave natural frequency. The curves from strip theory also show almost similar trends as in the 3-D theory for the corresponding Fns.

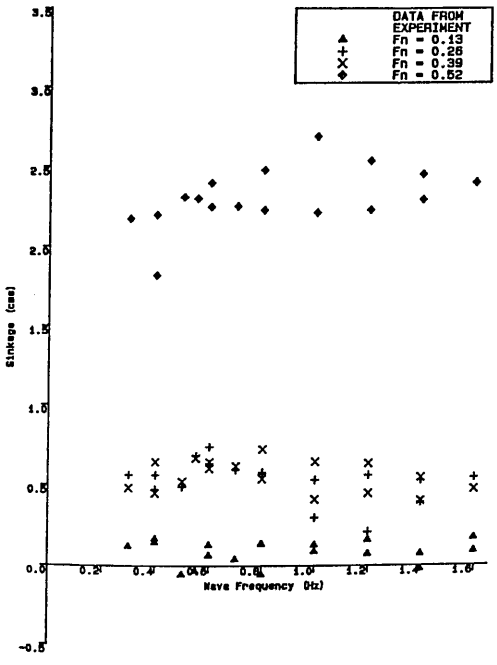

Figure 5.16.
SWATH1 MODEL SINKAGE
IN REGULAR HEAD SEAS

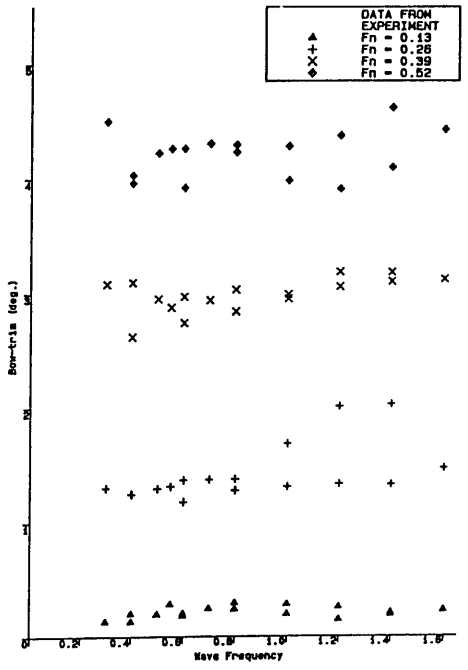

Figure 5.17.
SWATH1 MODEL BOW-TRIM
IN REGULAR HEAD SEAS

The sinkage and trim experienced by SWATH1 model when tested in regular head seas with forward speeds, are presented in frequency domain as shown in figs. 5.16 and 5.17, respectively. These scatter diagrams show that sinkage and trim increase with the increasing of model speed. In the Fn of 0.13, in some frequencies the values of sinkage are found to be negative, which means the model slightly emerged from the water. Eventhough this is only a rare case. In conjunction with the resistance of a SWATH sihp increasing of sinkage brings about higher frictional resistance which might be significant in low speed and low wave amplitudes. A relatively high bow-trim when a SWATH is operated in high speed may cause deck wetness and emergence of the propeller. Fig. 5.18 shows a picture when SWATH1 model moving with a speed of 2.0m/s, which relates to Fn=0.52, in an approximately 5cms wave height of 0.6Hz. Water spray at the bow of the model is quite visible in this picture.

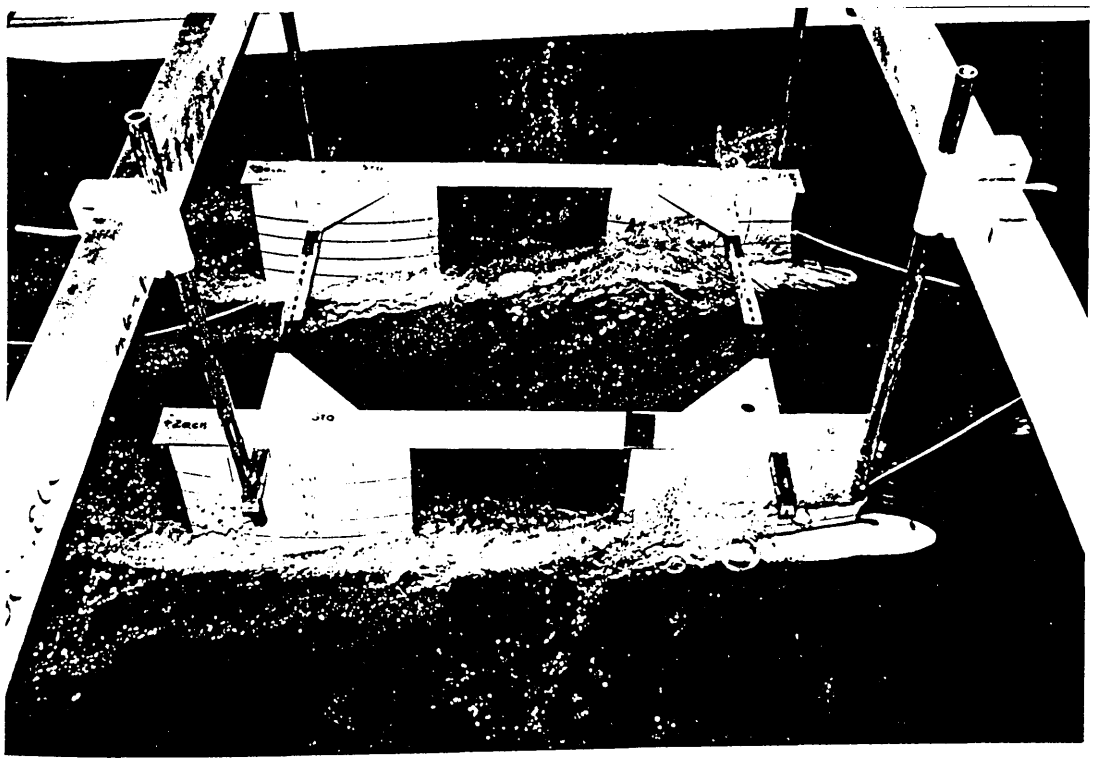

Figure 5.18. SWATH1 Model Underway

5.3.3. SWATH2 Model Motions in Regular Head Seas with Forward Speed.

The experimental data of SWATH2 model is compared with the prediction using strip theory in the heave and pitch mode of motions. Although SWATH2 and SWATH1 models having basically similar geometry, because of the difference in draught characteristics of the two models when they were tested a direct comparison could not be made.

In fig. 5.19 as far as the trend is concerned SWATH2 gives a reliable surge response. In heave and pitch modes, shown in figs. 5.20 and 5.21 respectively, the experimental data of SWATH2 model is in satisfactory agreement with the results presented by the strip theory. High heave and pitch responses given by the theory in the critical zone are caused by the absence of viscous damping. In these two modes the pattern of SWATH2 motion responses confirms well with SWATH1.

In general it can be justified that the hydrodynamic damping of rectangular hulls is higher than circular hulls. In the resonant frequency region where damping effect is dominant SWATH2 model gives lower motion responses than SWATH1 model.

SWATH2 model presents a rather distinctive feature of sinkage when referred to SWATH1 model. Fig. 5.22 shows that sinkage is not increasing together with the increase in speed up to Fn of 0.39. Even at this speed SWATH2 sinkage is mainly a negative value. The bow-trim of SWATH2 (fig. 5.23) having similar pattern as in SWATH1 model, that is trim increases as speed increases.

In addition, the resistance analysis of SWATH2 model which has been observed simultaneously with its motions reported herein can be found in [85].

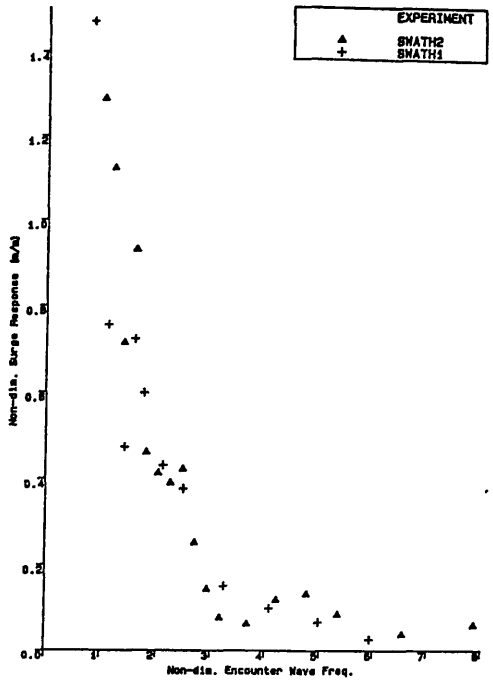

SWATH1 & 2 MODELS SURGE RESPONSES
IN REGULAR HEAD SEAS (Fn=0.13)

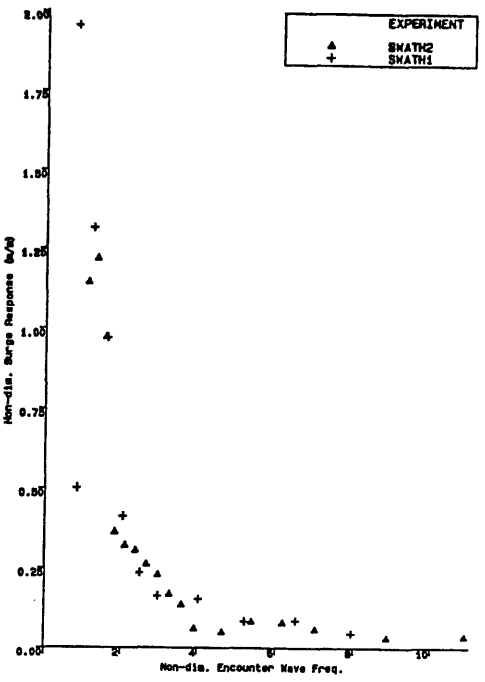

SWATH1 & 2 MODELS SURGE RESPONSES
IN REGULAR HEAD SEAS (Fn=0.26)

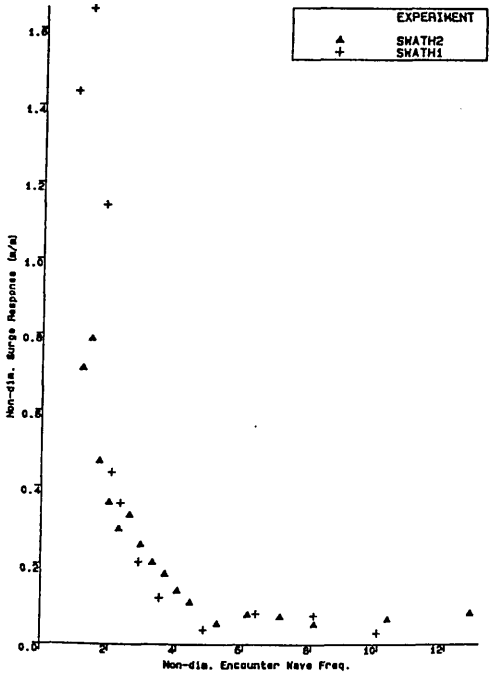

SWATH1 & 2 MODELS SURGE RESPONSES
IN REGULAR HEAD SEAS (Fn=0.39)

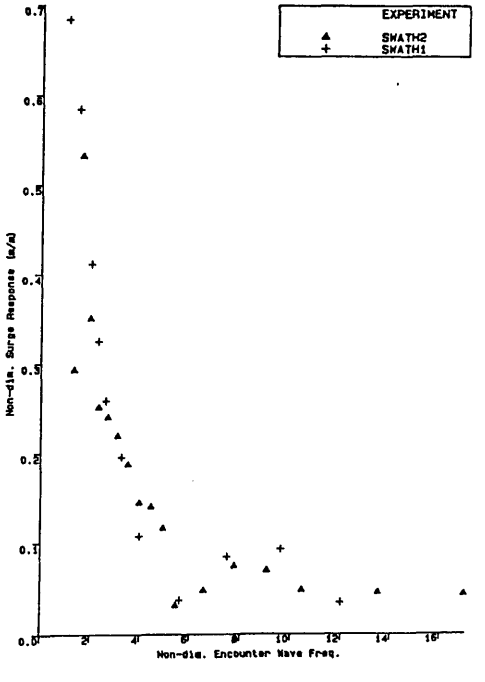

SWATH1 & 2 MODELS SURGE RESPONSES
IN REGULAR HEAD SEAS (Fn=0.52)

Figure 5.19. SWATH2 Model Surge Responses in Regular Head Seas with Forward Speeds

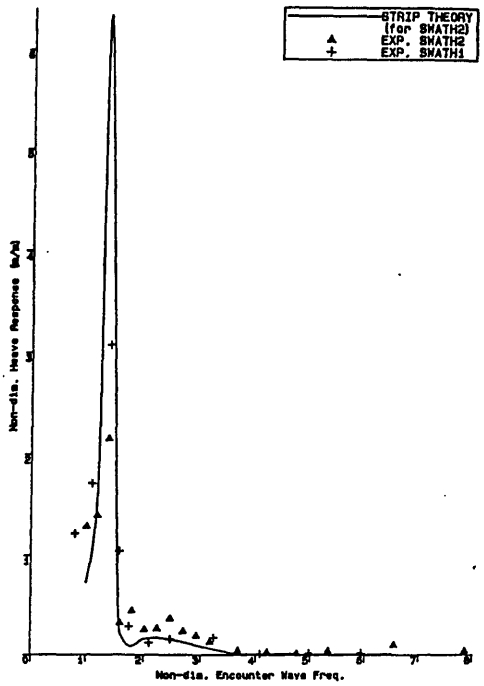

SWATH1 & 2 MODELS HEAVE RESPONSES
IN REGULAR HEAD SEAS (Fn=0.13)

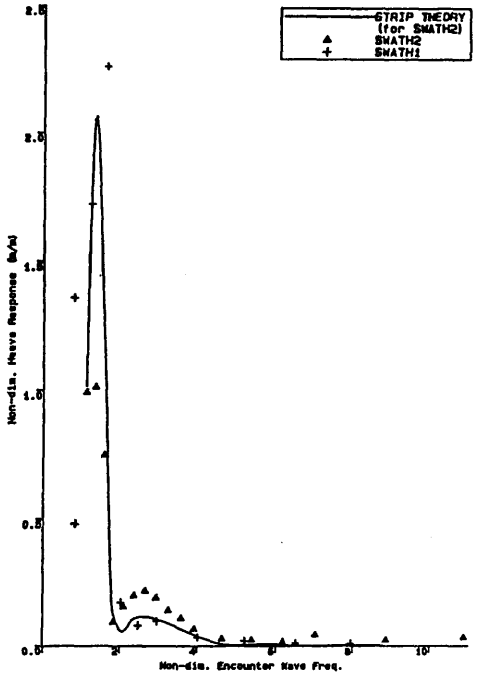

SWATH1 & 2 MODELS HEAVE RESPONSES
IN REGULAR HEAD SEAS (Fn=0.26)

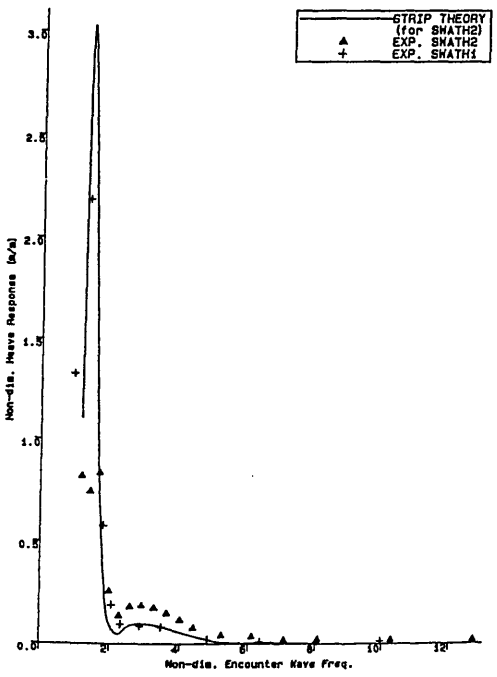

SWATH1 & 2 MODELS HEAVE RESPONSES
IN REGULAR HEAD SEAS (Fn=0.39)

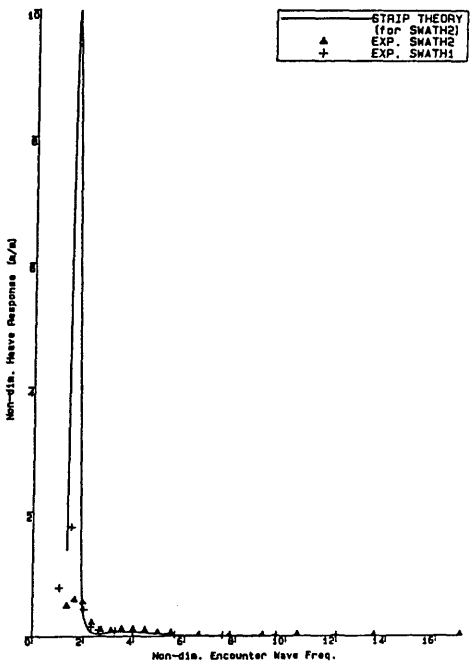

SWATH1 & 2 MODELS HEAVE RESPONSES
IN REGULAR HEAD SEAS (Fn=0.52)

Figure 5.20. SWATH2 Model Heave Responses in Regular Head Seas with Forward Speeds

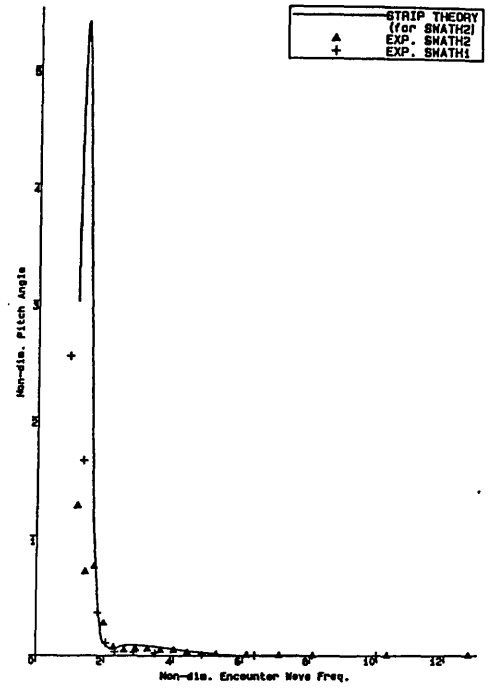

SWATH1 & 2 MODELS PITCH RESPONSES
IN REGULAR HEAD SEAS (Fn=0.39)

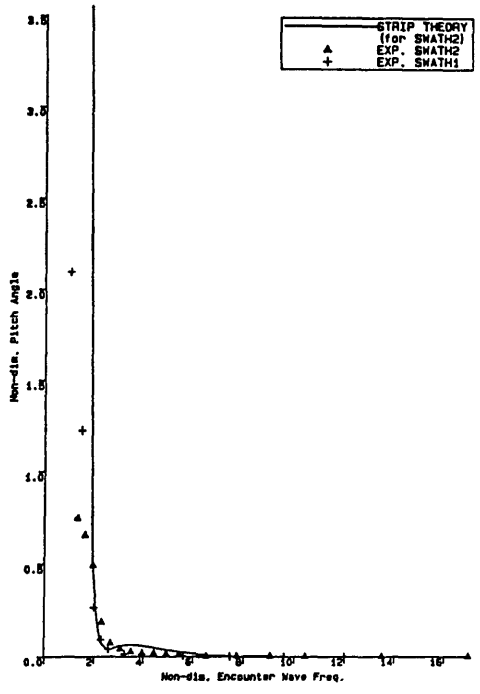

SWATH1 & 2 MODELS PITCH RESPONSES
IN REGULAR HEAD SEAS (Fn=0.52)

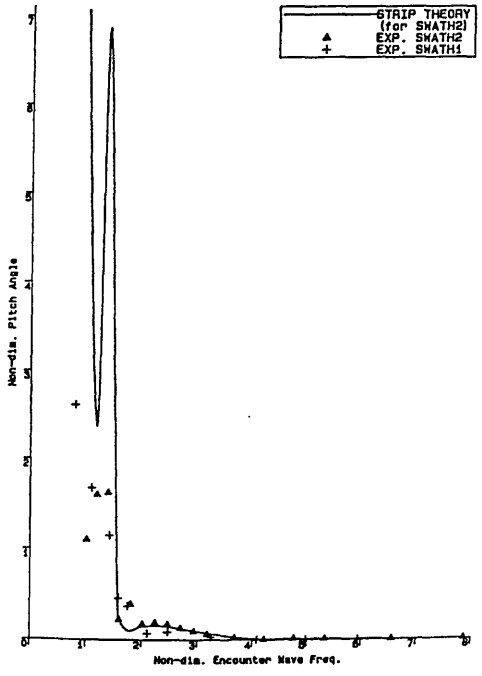

SWATH1 & 2 MODELS PITCH RESPONSES
IN REGULAR HEAD SEAS (Fn=0.13)

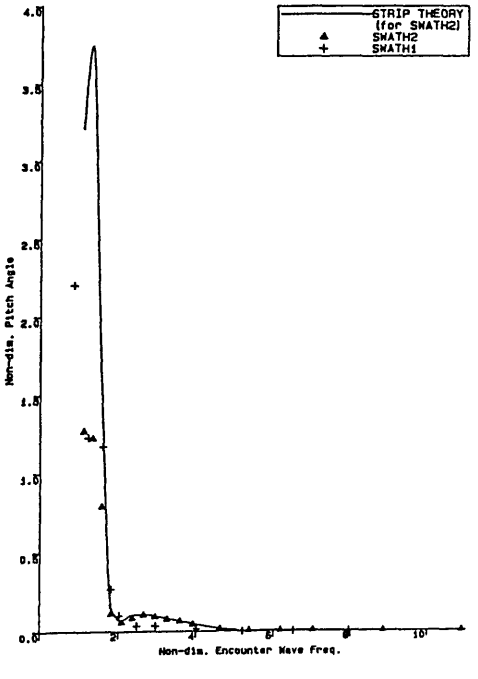

SWATH1 & 2 MODELS PITCH RESPONSES
IN REGULAR HEAD SEAS (Fn=0.26)

Figure 5.21. SWATH2 Model Pitch Responses in Regular Head Seas with Forward Speeds

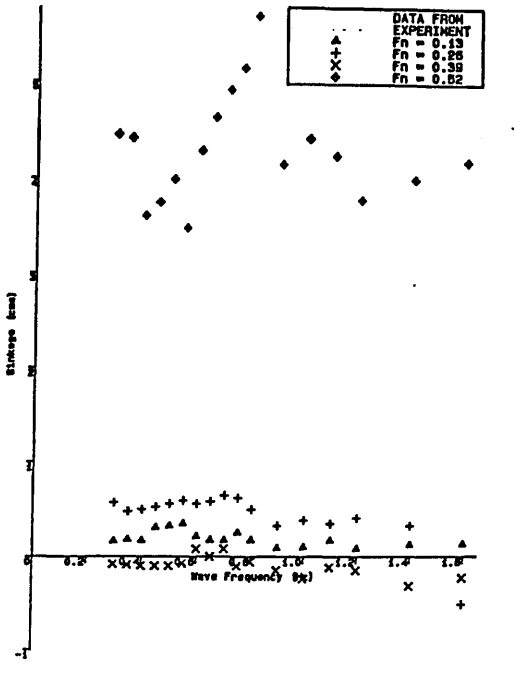

Figure 5.22.
SWATH2 MODEL SINKAGE
IN REGULAR HEAD SEAS

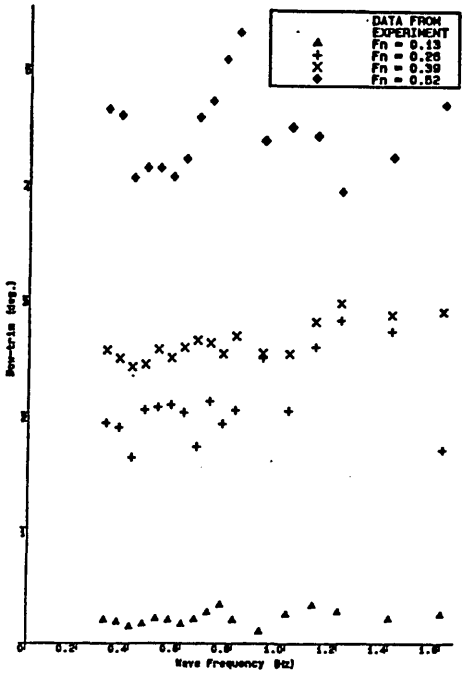

Figure 5.23.
SWATH2 MODEL BOW-TRIM
IN REGULAR HEAD SEAS

5.4. Conclusions.

The main conclusions in the study of SWATH1 model motions in head seas are set out below.

1. The experimental results are in good agreement with the two theoretical predictions. Additional experimental data might be necessary for the subcritical and critical zones to confirm the existing data.

2. In the head sea case, unlike a conventional ship, a SWATH when operated in high speed will be clear of the critical zone, that is the zone where the encountering frequency coincides with the natural

frequency, thus the frequency of resonance can be safely avoided. In other words a SWATH can without difficulty operate in the supercritical zone, in which relatively low motion responses occur.

3. The use of control fins proves to be a very efficient method of minimising (and even to eliminate) a large bow trim and improving the vertical plane motions characteristics of a SWATH ship when operated in head seas. However, these appendages are not so efficient in minimising sinkage [29,68,69]. In addition, sinkage and trim and resistance of a SWATH ship is of a particular interest to be thoruoghly investigated. A method that has been developed for monohull ships in this matter as presented in [86] can be enhanced for SWATH ships.

CHAPTER 6

DYNAMIC STRUCTURAL LOADINGS ON SWATH1 MODEL IN REGULAR BEAM AND QUARTERING SEAS

Chapter 6.

DYNAMIC STRUCTURAL LOADINGS ON SWATH1 MODEL IN REGULAR BEAM AND QUARTERING SEAS

In designing the structural members of a SWATH ship the estimation of loads acting on the cross deck and struts represents an important part of the design process. Accurate estimation of loads will be essential for safe and economic design of a SWATH ship. For instance, one of the disadvantages of a SWATH ship is her inability to carry greater payload compared to an equivalent size of monohull. The accurate estimation of loads, that will be imposed on the structure, particularly on the cross deck, may lead to a reduction in the structural weight which also means an increase in payload. The experiments carried out in this study were aimed at generating sea load information on a SWATH ship geometry and validating the theoretical predictions.

There are six components of the loads acting on the cross deck structure of a SWATH ship, as follows :

a. vertical bending moment, ie. the moment which tends to roll the hulls relative to each other,
b. vertical shear force, ie. the force which tends to heave the two hulls opposes each other,
c. horizontal shear force, ie. the force which tends to differentially translate the hulls athwartships,
d. torsion moment, ie. the moment which tends pitch the hulls with respect to each other,
e. yawing moment, ie. the moment which tends to create differential yawing on the hulls, and
f. longitudinal force, ie. the force which tends to surge the hulls differentially.

Model experiments on a catamaran, which from some points of view have a geometry similar to a SWATH ship, show that the most critical wave loads were experienced when experiencing beam seas without forward speed [87]. This condition might possibly be even worse if experienced on a SWATH ship. This is because the greater deck clearance, needed to avoid wave slamming on the bottom of the deck, will also increase the vertical bending moment on the cross deck. This increase is induced by the increase in vertical moment arm for the horizontal hydrodynamic forces acting on the struts and the demihulls [50,88].

6.1. Theoretical Background.

In order to simplify the problem, so that two-dimensional strip theory can be applied, some assumptions have been proposed [89], and are briefly described as follows :

a. the hulls are assumed to be symmetrical about the vertical centre plane and possess longitudinal symmetry, therefore, only the sway, heave and roll modes of motions are excited by the incident beam waves,
b. without pitching or yawing motion, the three-dimensional loading problem has been simplified into loadings on an equivalent two-dimensional body,
c. the ship is approximated by uniform twin cylinders having cross sectional shape equal to a representative section (usually midship section) of the ship analysed, and
d. the prediction is limited to the loads exerted in the transverse cross section plane. Thus, only the vertical bending moments, horizontal shear forces and vertical shear forces are considered.

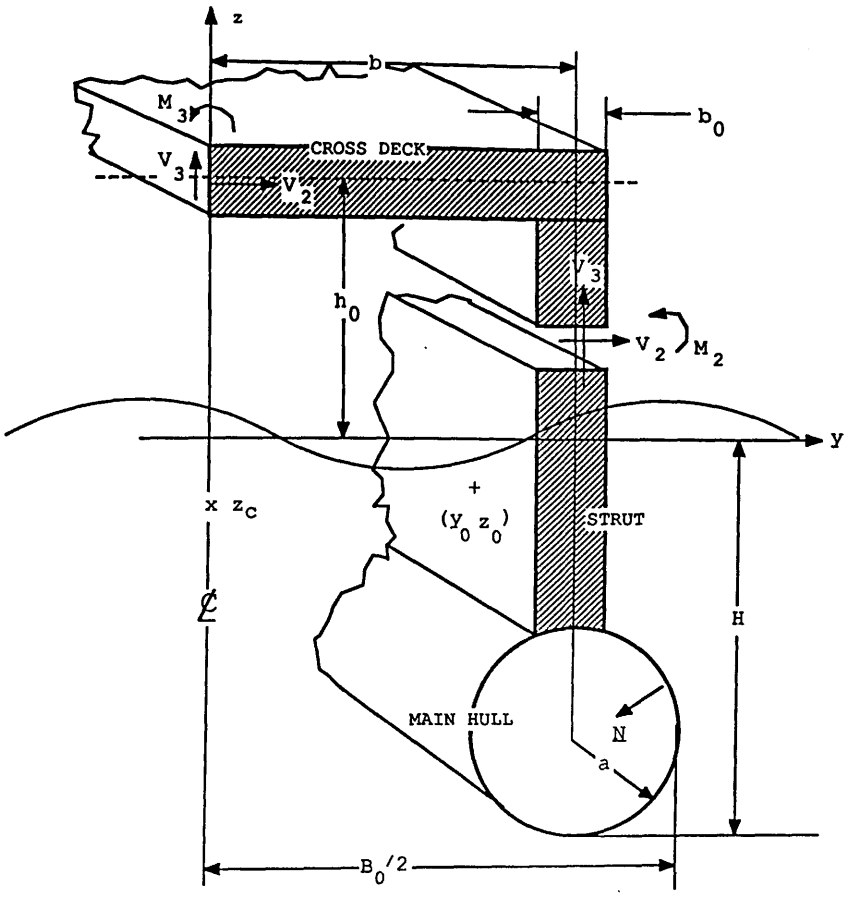

Figure 6.1. Definition Sketch of SWATH Cross-section [2]

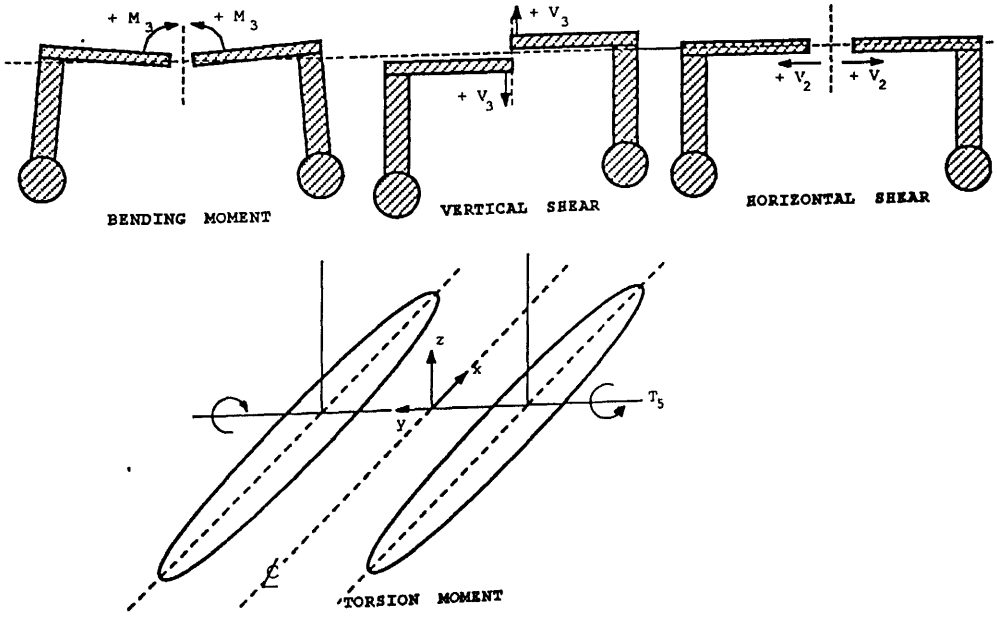

Figure 6.2. Load Convention on a SWATH [2]

Referring to the assumptions above and figs. 6.1 and 6.2 [50] various loadings per unit length on a cross section of a SWATH ship requires the motion of the body and pressure distribution of the hull [50,90,91] which can be expressed as

-. horizontal shear force,

$$V_2^{(0)} = -1/2\int_{R+L} pN_2(\pm y)\,dl \qquad (6.1)$$

-. vertical shear force,

$$V_3^{(0)} = 1/2my_0\ddot{s}_4 - 1/2\int_{R+L} pN_3(\pm y)\,dl \qquad (6.2)$$

-. vertical bending moment,

$$M_3^{(0)} = 1/2my_0\ddot{s}_3 - 1/2\int_{R+L} p\{N_3|y|+N_2(h_0-z)(\pm y)\}dl \qquad (6.3)$$

From the standpoint of torsional loads twin-hull ship configuration experienced the worst condition in quartering seas. In most cases the prediction of torsional loads can not bo solved using 2-D theories, which usually takes into account the equivalent two dimensional hull form assumption, so the pitch and yaw motions effect is neglected. Such a problem, however, can be approached by applying a three-dimensional theory [57].

-. Torsional Moment,

$$T_5^{(0)} = -1/2\int_{R+L} pN_5(\pm y)\,dl \qquad (6.4)$$

where $\int_{R+L} dl$ = integral over the submerged contour of the cross section on the right and left demihulls at the mean position,

p = the hydrodynamic pressure,

m = mass of the cross section (per unit length),

N = (N_2, N_3, N_5) the unit normal vector

pointing into the body,

y_0 = the y-coordinate of the centre of gravity of the right half portion of the hull cross section,

$+y$ = the y variable on the right half side,

$-y$ = the y variable on the left half side,

$\ddot{s}_4$ = roll angular acceleration, and

$\ddot{s}_3$ = heave acceleration.

The hydrodynamic pressure on any segment on the hull section may be determined by applying Bernoulli's equation for the time-varying velocity potential plus additional terms representing the change in the static pressure head as the hull experiences heave and roll motion,

$$p(x,y,z,t) = \frac{\partial}{\partial t}\bar{\phi}(x,y,z,t) - \rho g(s_3 + ys_4 - xs_5) \qquad (6.5)$$

and the velocity potential is expressed as,

$$\bar{\phi}(x,y,z,t) = \phi(x,y,z)e^{-i\omega_0 t} = (\phi_I + \phi_D + \sum_{j=1}^{6}\phi_j s_{j0})e^{-i\omega_0 t} \qquad (6.6)$$

where s_{j0} = complex amplitude of s_j,

s_3 = heave displacement,

s_4 = roll angular displacement,

s_5 = pitch angular displacement,

ϕ_I = complex velocity potential which represents incoming wave,

ϕ_D = wave diffraction potential and represents scattering of incident wave by body, and

ϕ_j = fluid disturbance caused by oscillatory body motion in j^{th} mode.

6.2. The Experiment.

An experiment on the SWATH1 model was conducted to determine the dynamic structural loadings in regular beam and quartering seas. This was compared to an experiment on a semi-submersible model [92] as a reference. For the beam sea case, the test arrangement is similar to that shown in fig. 3.2, the model was positioned 90^0 to the wave trains. Harnesses were used to tie the model on to the tank side walls so that the model would be stopped from drifting along the tank. To measure the bending moments experienced by the transverse beams, two pairs of strain-gauges were attached on the top and bottom surfaces of the beams, whereas the vertical forces on the struts were measured by strain gauges mounted on the vertical alumunium bars, as shown in figs. 6.3.

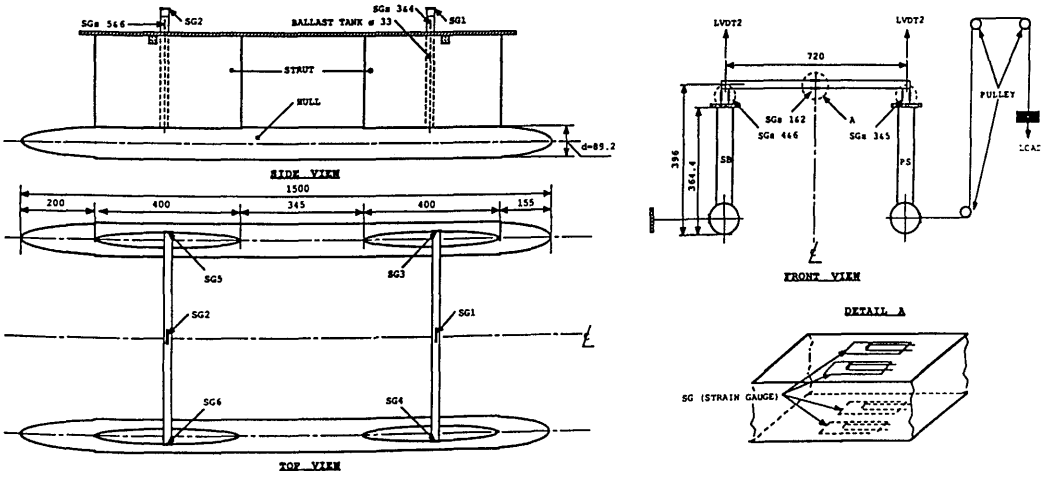

Figure 6.3. Strain Gauges Arrangement and Calibration for Bending Moment

The strain gauges on the transverse beams were set up in a way, such that if the beams are excited by bending moments and axial forces, then only signals due to the bending moments would be sent to the recorder. A similar adjustment was done on the strain gauges to measure the vertical forces. Details of this type of strain-gauge can be found in [93].

Three wave probes were mounted on a bridge well away from the model, to measure the wave amplitudes, which were in the range of 0.3Hz upto 1.6Hz. Another wave probe, was set up at the bow of the model on its centreline. This wave probe is mainly intended to observe the phase shifts, beside measuring the wave patterns in the model vicinity. The measurement of phase shifts can be done simply from the record as the pen recorder utilised has a capability to plot all components measured at the same starting point. Therefore the phase shifts obtained in the records are the same as the actual phase shifts.

Two LVDTs were also used in the experiment to measure the heave and roll motions of the model in conjunction with the observation of phase shifts which had not been carried out in the previous experiments. In addition to the pen recorder a computer program run in the VAX 11/730 computer system was employed for data acquisition.

The calibration of the strain gauges to measure the bending moment was carried out by imposing sideloads on the portside hull, where the starboard hull was fixed, through a wire rope connected to a scale pan in which weights were. The weight increased from 1kg upto 5kgs with increment of 1kg, see fig. 6.3. Each load was then recorded and the calibration factor, which is the relation between the displacement of the recording in cms with the appropriate load in kgs, was then plotted in a graph as presented in fig. 6.4. The calibration of the strain gauges to measure

the vertical axial forces was conducted separately before the vertical bars were mounted on the model. The calibration procedures for other instruments used in the experiment can be found in the previous chapters.

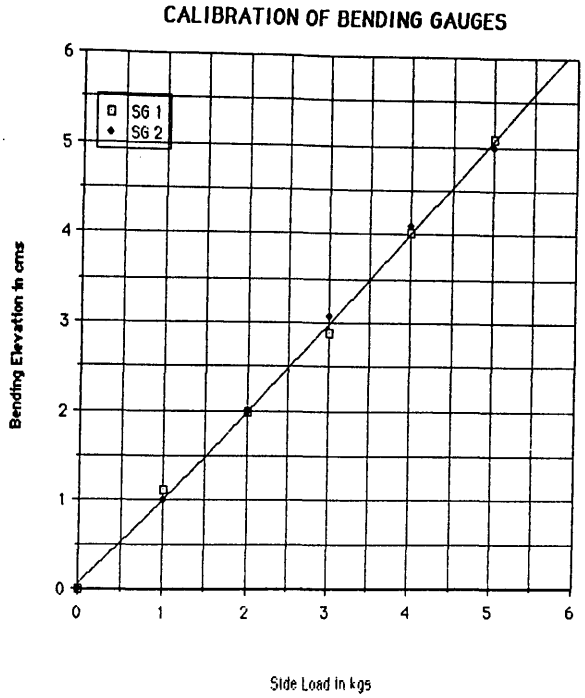

Figure 6.4. Calibration of Bending Gauges

The measurements in quartering seas were basically similar to that in beam seas. All the instruments used were unchanged from the former experiment, the only addition being two LVDTs, thus four LVDTs were utilised to observe the three vertical plane motions of the SWATH1 model, namely heave, pitch and roll.

6.3. Experiment Results Analysis.

The analysis reported below are only concerned with the derivation of loadings data generated from the tests to obtain dynamic structural loads on the cross deck structure of SWATH1 model. Other than this, ie the wave and motion analysis, will not be given since the preceeding chapters have explained those at some length.

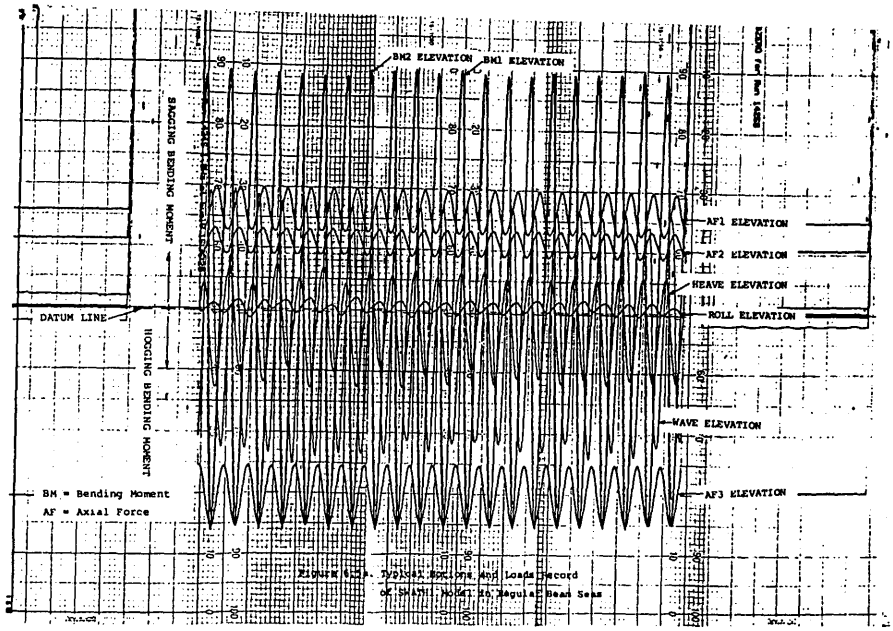

Figure 6.5a. Typical Motions and Loads Record of SWATH1 Model in Regular Beam Seas

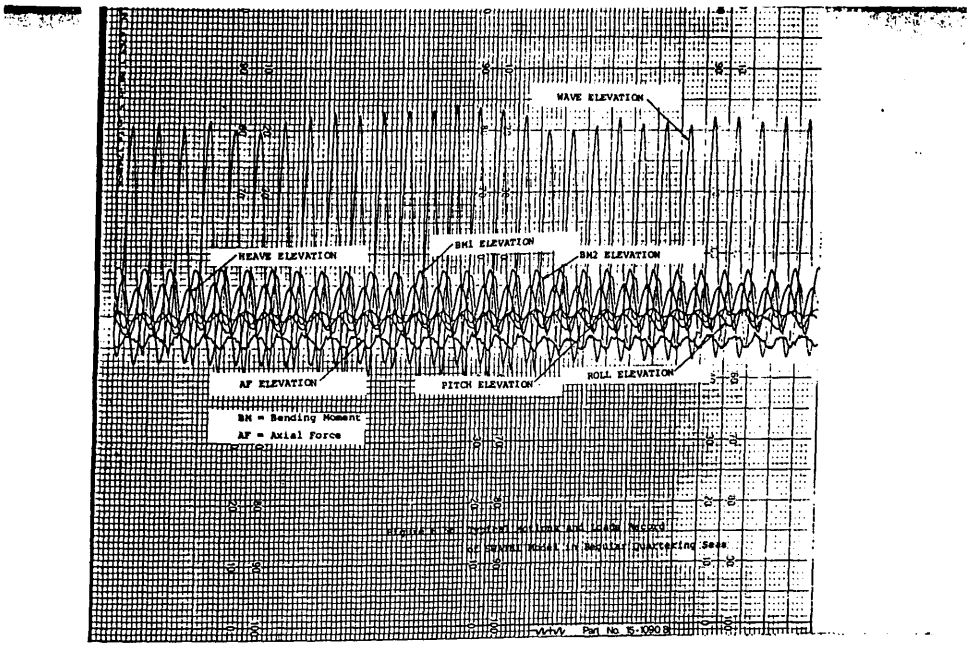

Figure 6.5b. Typical Motions and Loads Record of SWATH1 Model in Regular Quartering Seas

The readings on the loading records, see figs. 6.5a and b which show beam and quartering sea cases, respectively, are taken in the usual manner as for motion analysis. From this measurement, which is in cms, the loads measured by the corresponding strain-gauge in kgs can then be obtained using an appropriate calibration graph. The force unit in Newtons imposed on each strain-gauge is calculated by taking into account the acceleration due to gravity. Bending moments at the mid-point of the transverse alumunium bars, measured through strain-gauges 1 and 2 stuck on these positions, are obtained as the forces times the height of the centre bars from the centre of gravity of the hulls. These are associated with the procedure of calibrations for the two strain-gauges, where the side loads were excerted at the portside hull's centre of gravity perpendicularly sideward.

In addition the difference between maximum bending moments in sagging and hogging conditions is also observed. This is done by considering the difference of displacements of the troughs and peaks of the bending moment records from the corresponding datum lines.

The presentations of structural loadings on such a twin hull ship configuration are in the form of non-dimensional loads (ie axial forces or bending moments) against wave-length/characteristic beam ratio, λ/B. The non-dimensionalitation of the axial forces is taken as

$$AF' = \frac{AF.L}{g.\Delta.\zeta_A} \qquad (6.7)$$

and non-dimensional bending moment as

$$BM' = \frac{BM}{g.\Delta.\zeta_A} \qquad (6.8)$$

where AF = axial force (N),
L = characteristic length of the model (=1.5m),

g = acceleration due to gravity ($=9.81 ms^{-2}$),

Δ = displacement of the model (kgs),

ζ_A = wave amplitude (cms), and

BM = bending moment (Ncms).

From the frequency generated in the experiment, the wave-length in metres can be calculated as follows :

$$\lambda = \frac{g}{2\pi f^2} \qquad (6.9)$$

where f = wave frequency in Hz

6.4. Comparison with Theoretical Predictions.

In regular beam seas (see fig. 6.6), the experimental data for low amplitude waves confirms the 3-D theory very well. The curve from the strip theory performs similar trend as the other with a slightly higher magnitude. One factor which could lead to this discrepancy is that the strip theory does not take into account the damping due to viscosity [71]. The viscosity affects the magnitude of phase difference between the wave exciting force and the motions, which further influences the wave loads due to motions. The maximum bending moment, as is expected, occurs at the first standing wave, which in this term is when the wave length is twice of the hull separation (ie. related to $\omega=6.283$ $rads^{-1}$). Another maximum bending moment, which is about one half of the magnitude of the former one, occurs approximately in the second standing wave, ie when the wave length is equal to the hull separation (ie. $\omega=10.052$ $rads^{-1}$).

In fig. 6.7 for the regular quartering seas, in the first standing wave the experiment data is slightly higher than the 3-D theory, but matches the strip theory quite well. At the second standing wave, where the maximum bending

moment occurs in the quartering sea case, the experiments agree with the 3-D theory better.

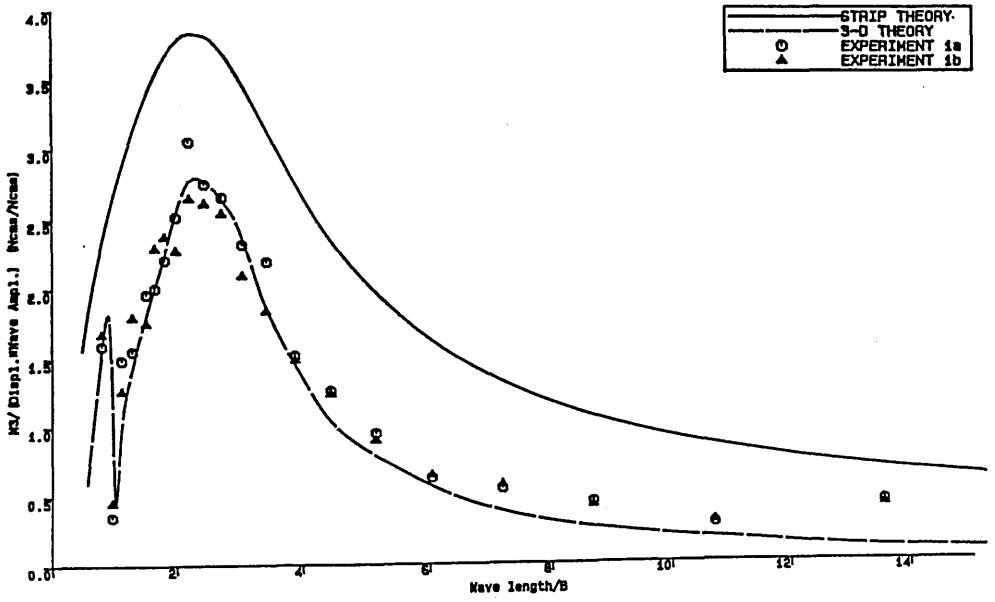

Figure 6.6.
BENDING MOMENT AT MID-POINT OF CROSS-STRUCTURE
SWATH1 MODEL IN REGULAR BEAM SEAS

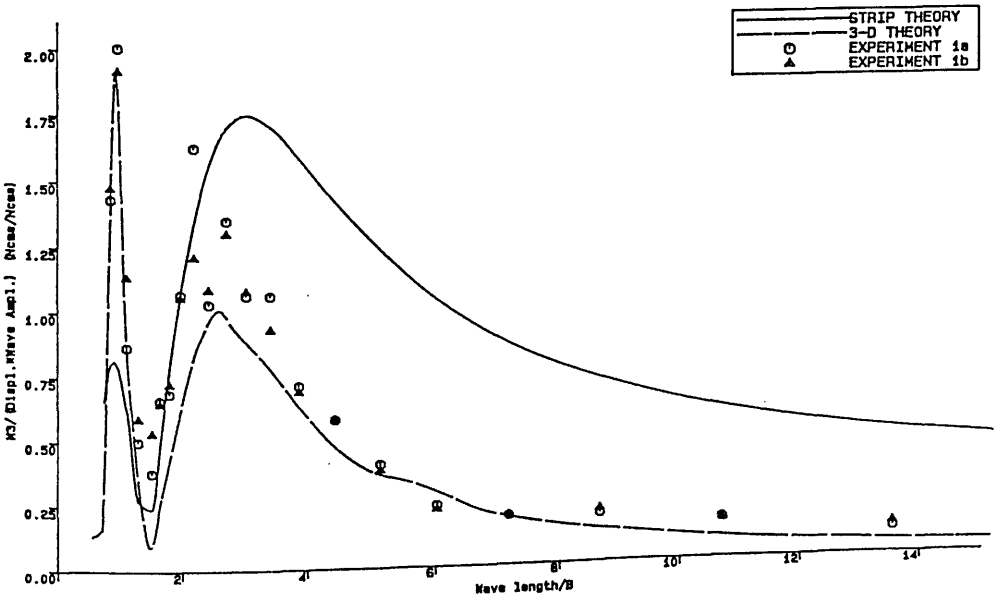

Figure 6.7.
BENDING MOMENT AT MID-POINT OF CROSS-STRUCTURE
SWATH1 MODEL IN REGULAR QUARTERING SEAS

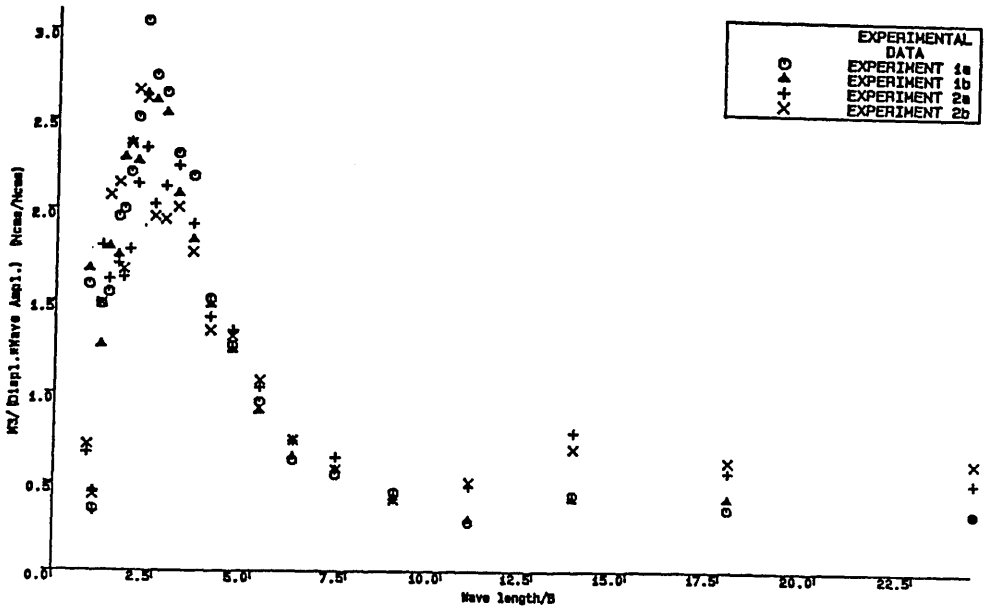

Figure 6.8a.

BENDING MOMENT AT MID-POINT OF CROSS-STRUCTURE
SWATH1 MODEL IN REGULAR BEAM SEAS
(NON-LINEARITIES DUE TO DIFFERENT WAVE HEIGHT)

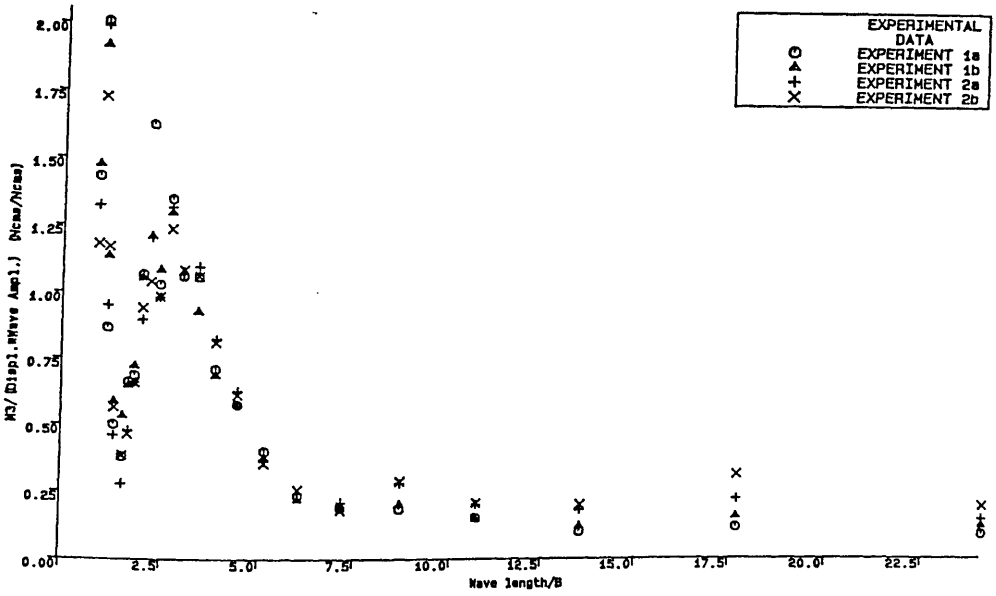

Figure 6.8b.

BENDING MOMENT AT MID-POINT OF CROSS-STRUCTURE
SWATH1 MODEL IN REGULAR QUARTERING SEAS
(NON-LINEARITIES DUE TO DIFFERENT WAVE HEIGHT)

The effect of non-linearities due to differences in wave amplitudes on the bending moment can be observed in figs. 6.8a and b, where initial 1 and 2 denote the experiment carried out in the low and high amplitude waves, respectively. Unlike in the SWATH1 model motion cases, the non-linearities caused by wave height on bending moment are consistent. Generally at high λ/B values higher wave amplitudes create higher bending moment and conversely in low λ/B values. The experimental data generated from high waves would not be expected to match the theories perfectly as these are developed by assuming that the model is operated in low wave amplitudes.

Hogging and sagging phenomenon on monohull ships advancing in head waves has been fully reviewed in [94] and other references. There is no single reference, however, which has discussed this matter for SWATH ships. In the present experimental investigation, effort has been made to identify the difference of sagging and hogging bending moments on the SWATH1 model, and figs. 6.9a and b are examples of the observation results. These figures show that in most wave lengths the sagging bending moment is the higher. Such a non-linearity is not considered in the two theories. In the two theories, the integration to compute the wave exciting force is taken up to the still water level, and do not take into account the wave elevation which contributes to the changing of displaced volume of the column. Consequently these linear theories predict the same magnitude of wave bending moment for both hogging and sagging.

The measurement of the vertical shear forces on the struts were not as successful as on the bending moment. As can be seen in fig. 6.10a, the trend of experimental data is different from the trends of vertical forces performed by both the strip and 3-D theories (fig. 6.10b). It is worthwhile to note, however, that the experimental data is

similar to the transverse shear forces from the two theories as shown in fig. 6.10c.

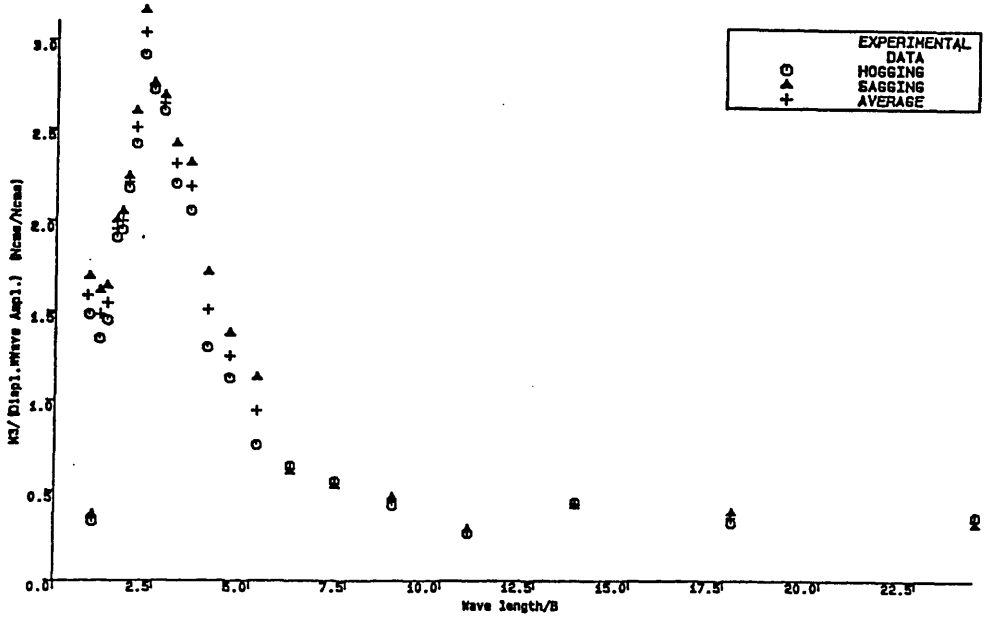

Figure 6.9a.

BENDING MOMENT AT MID-POINT OF CROSS-STRUCTURE
SWATH1 MODEL IN REGULAR BEAM SEAS
(NON-LINEARITIES DUE TO HOGGING AND SAGGING)

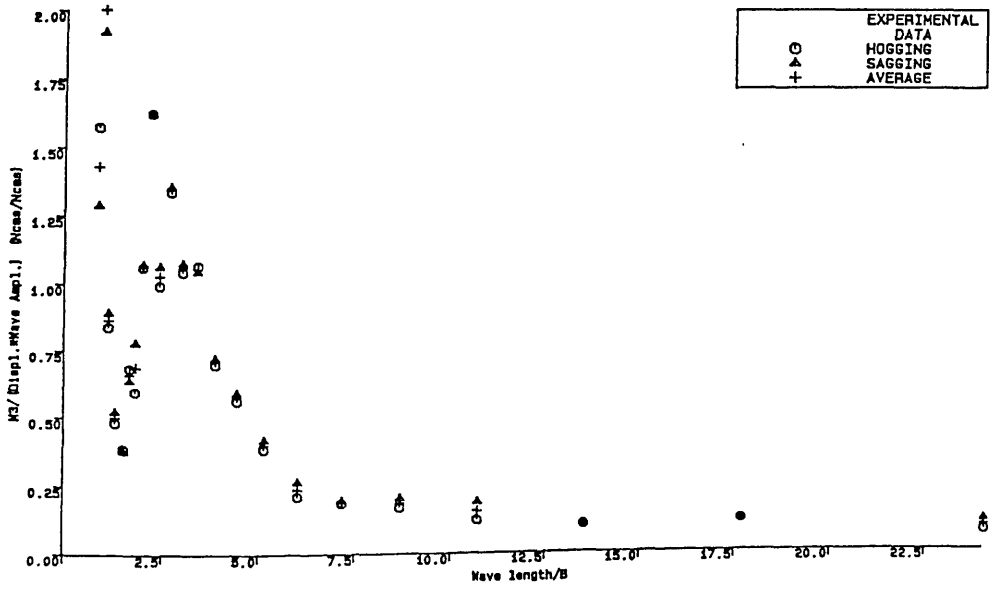

Figure 6.9b.

BENDING MOMENT AT MID-POINT OF CROSS-STRUCTURE
SWATH1 MODEL IN REGULAR QUARTERING SEAS
(NON-LINEARITIES DUE TO HOGGING AND SAGGING)

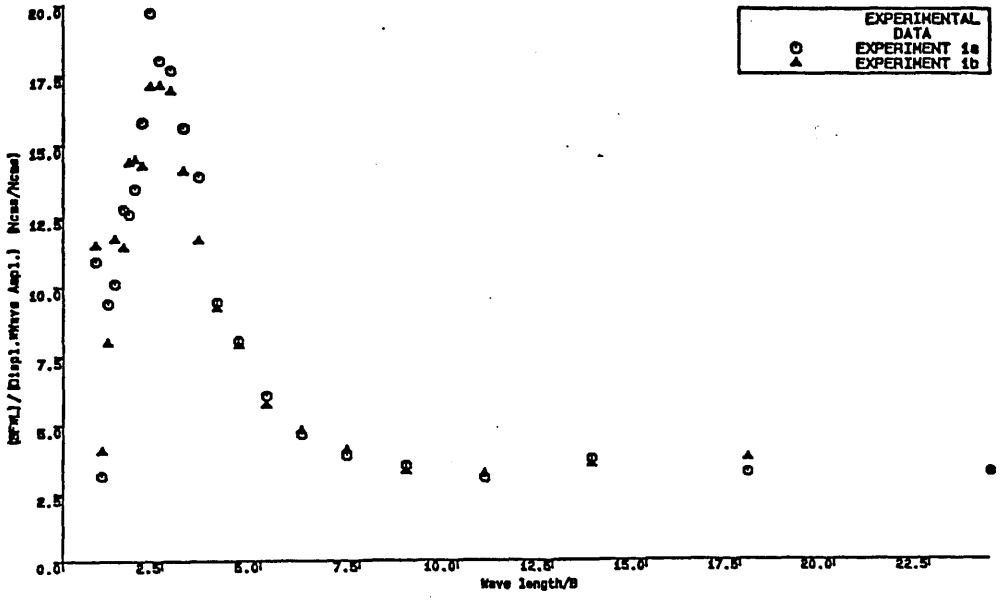

Figure 6.10a.
SHEAR FORCES
SWATH1 MODEL IN REGULAR BEAM SEAS

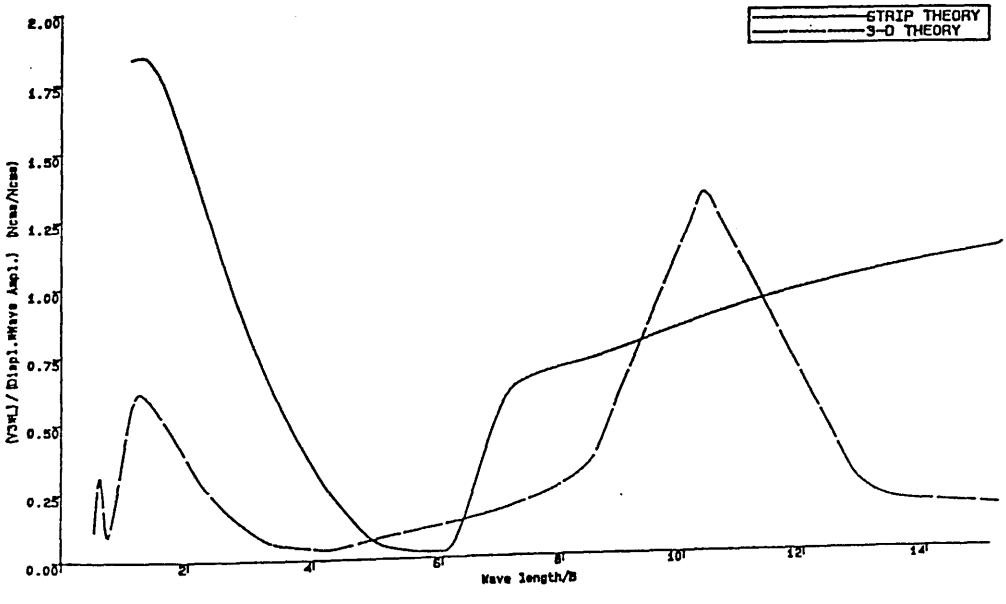

Figure 6.10b.
VERTICAL SHEAR FORCES
SWATH1 MODEL IN REGULAR BEAM SEAS

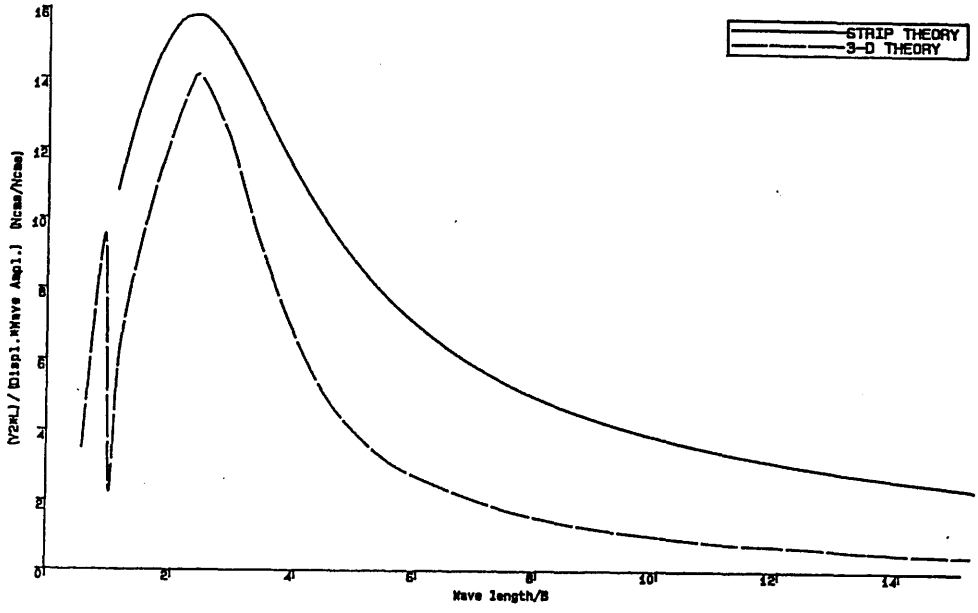

Figure 6.10c.
HORISONTAL SHEAR FORCES
SWATH1 MODEL IN REGULAR BEAM SEAS

Although the strain gauges for this had been set up in a way so that only the signals due to axial forces should have been recorded, the sensitivity of such instruments to any changing in the atmospheric level, for instance temperature, humidity etc., may have caused this effect. Some recalibrations hhave indicated that when the model has side loadsapplied to it those strain gauges produced signals. Because of limited time it has not been possible to investigate other possibilities which may have created this situation.

6.5. Conclusions.

The conclusions of the study in this chapter are set out below.

1. For bending moments in regular beam and quartering seas the experimental data confirms the 3-D theory well. This data can be very useful to improve the computer program SWATHL in predicting the wave load.

2. In general sagging bending moments are higher than hogging. In high amplitude waves sagging could be higher than hogging, in certain λ/B value, by as much as 30% (see experimental data in appendix 1f). The two theories could be enhanced to include the non-linear effects due to sagging and hogging on bending moments by applying a method such as that developed in [95].

3. The observation on the vertical force could not be explained except by suspecting that the transverse force has a substantial effect on the signal produced by the strain gauges on the vertical bars. The use of a load cell to measure the vertical axial force on such a structure could possibly solve the problems that have arisen when using strain gauges.

CHAPTER 7

SPECTRAL ANALYSIS OF SWATH1 MOTIONS AND DYNAMIC STRUCTURAL LOADINGS

Chapter 7

SPECTRAL ANALYSIS OF SWATH1 MODEL MOTIONS AND DYNAMIC STRUCTURAL LOADINGS

When a ship is subjected to random excitation from waves elevation and force changes, as a result it moves both translationally and rotationally. In other words the ship is in a state of six-degree of freedom random motion. However the rate and amount of the movement of the ship are not only dependent on the severity of wave excitation, but also on the mass, stiffness and inherent damping in the ship system. The subject of random process is concerned with finding out how the statistical characteristics of the motion of a randomly excited system, depend on the statistics of the excitation [96].

Fig. 7.1. shows part of a possible time history of heave record in random seas. The displacement z from an arbitrary datum is plotted against the time t. Since the motion is random, the accurate value of z at any given time $t = t_o$ cannot be precisely estimated. The best way to proceed is to determine the probability, that z at t_o will lie within certain limits. The subject of probability is therefore the basis of random process theory, and the study can be begun by considering some of fundamental ideas of probability theory. The matter is briefly summarised [97].

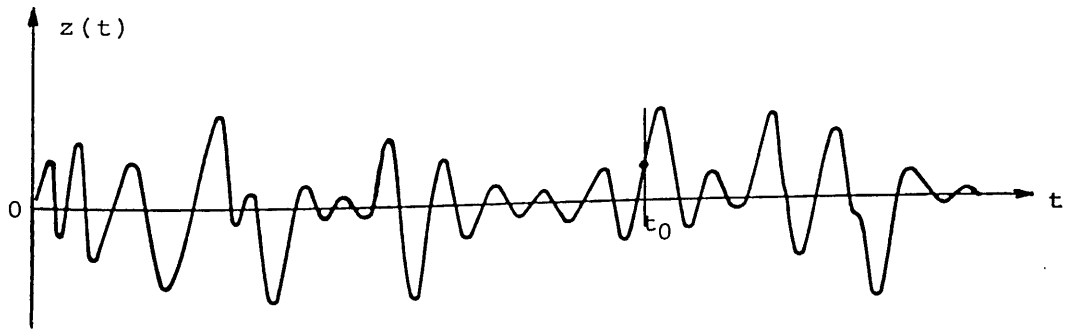

Figure 7.1. Heave Record of a Ship in a Random Sea

The mathematical approach predicting ship motions in irregular seas was put forward by Weinblum and St.Denis [98]. Based on the work associated with random analysis in other fields and the study of actual ocean waves [99], the spectral analysis of seas waves and ship motions was then extensively advanced by St.Denis and Pierson [100].

7.1. Spectral Formulations Applied in Analysing of SWATH1 Motions and Structural Loadings in Irregular Seas.

There are a number of different wave energy spectrum formulations that can be derived from wave data. The wave spectra in most common usage include two deep water (fully arisen and fetch unlimited) spectra and one fetch-limited spectra. Formulae relating to a family of spectral forms is given in appendix 2 [97].

Two different computer programs based on fully aroused seas and fetch limited spectral formulations have been written. For a fully aroused sea one of the most commonly used energy spectrum formula is the Pierson-Moskowitz wave spectra (1964) [101], which belongs to the deep water spectra. The P-M spectra is also well recognised as the wind speed spectra since wind speed is included directly in the spectral density function [102].

The P-M wave spectra is formulated as [103],

$$S(\omega) = \frac{\alpha g^2}{\omega^5} \exp\left[-\beta \left(\frac{g}{U_{19.5}\omega} \right)^4 \right] \qquad (7.1)$$

where $S(\omega)$ = spectral density (m^2s),

ω = wave frequency ($rads^{-1}$),

α = 8.10×10^{-3},

β = 0.74,

g = acceleration due to gravity (= 9.81ms^{-2}), and

$U_{19.5}$ = wind velocity at 19.5m above the calm-water surface (ms^{-1}).

Two other wave spectrum formulations for fully developed seas, ie Bretschneider and ITTC/ISSC'75 formulations, have also been studied to allow a comparison to be made. The Bretschneider spectrum takes form [104],

$$S(\omega) = \frac{1.25}{4} \frac{\omega_m^4}{\omega^5} \zeta_{1/3}^2 \exp\left[-1.25\left(\frac{\omega_m}{\omega}\right)^4\right] \qquad (7.2)$$

where ω_m = modal wave frequency (rads^{-1})

$\zeta_{1/3}$ = significant wave height (m)

The spectral formulation recommended by the International Towing Tank Conference (ITTC) and the International Ship Structures Congress (ISSC) was derived by Mirokhin and Kholodilin, having the form [105],

$$S(\omega) = \frac{A}{\omega^5} \exp\left(-B/\omega^4\right) \qquad (7.3)$$

where $A = (8.10 \times 10^{-3})g^2$, and

$B = (3.11 \times 10^4)/\zeta_{1/3}^2$ for $\zeta_{1/3}$ in m

The only fetch limited spectral formulation applied in this analysis is that recommended by ITTC in 1984, which replaces the former spectral form. This form is derived from the one proposed by JONSWAP. The formulation of this spectrum is

$$S(\omega) = 155 \frac{\zeta_{1/3}^2}{T_1^4 \omega^5} \exp\left\{\frac{-944}{T_1^4 \omega^4}\right\} (3.3)^Y \qquad (7.4)$$

where

$$Y = \exp -\left[\frac{0.191\omega T_1 - 1}{\sqrt{2\sigma}}\right]^2$$

and $\sigma = 0.07$ for $\omega \leq 5.24/T_1$

$\sigma = 0.09$ for $\omega > 5.24/T_1$

Other characteristic periods below can be used in this formulation,

$T_1 = 0.924\ T_{-1} = 0.834\ T_0 = 1.073\ T_2$

where T_{-1} = the energy average period, $2\pi m_{-1}/m_0$

T_0 = the modal period, $2\pi/\omega_0$ where ω_0 is the frequency of the spectrum peak

T_1 = the average period $2\pi m_0/m_1$

T_2 = the average zero crossing period, $2\pi\sqrt{m_0/m_2}$.

7.2. SWATH1 Motions and Loads in Irregular Seas.

As the spectral formulation given above have been derived for real seas they are applicable only for full scale ships. In this respect SWATH1 model is geometrically scaled up to be a real SWATH ship. The SWATH1 ship is assumed to be fifty times larger than the model (the ship displacement is approximately 2701 metric tons) and is operated in zones 1 and 2, ie North Atlantic, as defined in the chart of wave observation [106]. To analyse the experimental data of SWATH1 model in irregular seas the sea wave frequency is obtained as

$$\omega_s = \frac{\omega}{\sqrt{\mu}} \qquad (7.5)$$

where ω = wave frequency in the experiment

$(rads^{-1})$

μ = scale factor (=50)

The response spectrum is calculated by taking into account the response amplitude operator

$$S_m(\omega) = \left[\frac{m_A}{\zeta_A}\right]^2 S(\omega) \qquad (7.6)$$

where $S_m(\omega)$ = spectral density of ship response for any mode of motion (m^2s for surge, sway and heave or deg^2s for roll, pitch and yaw),

m_A = motion amplitude (m or deg), and

ζ_A = wave amplitude (m).

From a known spectrum one can then obtain wave and motion characteristic amplitudes by using simple formulations given in table 7.1 [2].

Table 7.1. Wave and Motion Amplitudes

Average amplitudes	$= 1.25\sqrt{m_0}$
Significant amplitudes	$= 2.00\sqrt{m_0}$
Average of 1/10 highest amplitudes	$= 2.55\sqrt{m_0}$
Average of 1/100 highest amplitudes	$= 3.34\sqrt{m_0}$

where m_0 = moment area under the spectrum (see appendix 2)

Since the formulations in table 7.1 are derived for narrow frequency spectrum (ie. Rayleigh distribution of the wave height histogram), then a correction factor has been

introduced for response spectrum [2] as

$$CF = \sqrt{(1 - \varepsilon^2)} \qquad (7.7)$$

where ε = the broadness parameter which is found from the even moments of the spectrum (see appendix 2)

For bending moment, the amplitude operator of the SWATH1 ship is counted as follows :

$$\left(\frac{BM}{\zeta_A}\right) = g\Delta_s \times BM' \times 10^{-3} \quad (MN) \qquad (7.8)$$

where g = acceleration due to gravity (=9.81 ms^{-2}),

Δ_s = ship displacement (= 2701 tonnes), and

BM' = non-dimensional bending moment, see eqn.(6.8)

The axial force amplitude operator is taken as

$$\left(\frac{AF}{\zeta_A}\right) = \frac{g\Delta_s}{L_s} \times AF' \times 10^{-3} \quad (MNm^{-1}) \qquad (7.9)$$

where L_s = characteristic length of the ship (=75.0m)

AF' = non-dimensional axial force, see eqn. (6.7)

7.3. Computation and SWATH Seakeeping Criteria.

The computer program for SWATH1 motions and loads spectral analysis was written for the VAX 11/730 computer system. Input data required to run this program are wave frequency and response amplitude operator from the experimental data. The integration to calculate the area under the spectrum curve has been fixed to use Simpsons three point integration rule. For this purpose the input data should be formatted to match that integration rule. The

output data generated by the computer program are various probability values of motion, velocity and acceleration for any mode of motion and loading. If required the program output will also include the spectrum curves as shown in figs. 7.2 and 7.3. The computational results which relate to the experimental data from the previous chapters are presented in appendix 3.

From the data in appendix 3, graphical relationships between the significant double motion amplitude of SWATH1 proceeds irregular beam waves and the significant wave height are plotted, as shown in figs. 7.4a-c. These graphs show the results given by the four spectral formulations described in the former section. The three graphs indicate that the spectral formulations for fully aroused seas, ie P-M, Bretschneider and ITTC/ISSC'75 wave spectra, give similar patterns. This is understandable because the determining factors in the computation of response spectra using the three forms are conditioned for the same sea characteristics. Whereas the fetch limited wave spectra (ITTC'84) gives rather distinctive trends, particularly for sway and heave modes, see figs. 7.4a and b. The more detail explanation of the comparison of how spectral formulations effects on the motion response prediction can be found in [107].

The seakeeping criteria to evaluate the SWATH1 ship performance in irregular seas (table 7.2) are adopted from [108]. Some of SWATH criteria constitute modification of monohull ship criteria. Additional criteria concerning the workability of people on deck due to heave acceleration is given as in point (4) of the general criteria.

Not all of these criteria, however, will be evaluated on SWATH1 because of the limitation of the investigation. Some of the criteria from table 7.2 that will be used herein is relisted in table 7.3.

Table 7.3. Selected Seakeeping Criteria and Categories for SWATH1

General Criteria

Monohulls and SWATH

(1) 12^{o} single amplitude average roll.
(2) 3^{o} single amplitude average pitch.
(3) Motion sickness indicator (20% of laboratory subjects experience emesis within two hours).
(4) Significant heave acceleration $\leq$ 0.4g (no people working on deck).
(5) Significant heave acceleration $\leq$ 0.2g (people working on deck).

Monohulls only

(6) Bottom plate damage.
(7) Three slams in 100 motion cycles.
(8) One deck wetness every two minutes.

SWATH only

(9) 5.5m average of highest $1/10^{th}$ relative bow motion.
(10) 3.9m significant relative motion at the propeller.

Helicopter Operating Criteria for Monohulls and SWATH

(11) 12.8^{o} double amplitude significant roll.
(12) 2.55m double amplitude significant vertical displacement at the flight deck due to pitch.
(13) $2.13ms^{-1}$ significant vertical velocity at the flight deck.

Hull Mounted Sonar Criterion for Monohulls Only

(14) Sonar dome emergence criterion (three-out-of-five detection opportunities).

Table 7.3. Selected Seakeeping Criteria and Categories for SWATH1

General Criteria

(1) 12^{o} single amplitude average roll.
(2) 3^{o} single amplitude average pitch.
(3) Significant heave acceleration $\leq$ 0.4g (no people working on deck).
(4) Significant heave acceleration $\leq$ 0.2g (people working on deck).

Helicopter Operating Criteria

(5) 12.8^{o} double amplitude significant roll.
(6) 2.55m double amplitude significant vertical displacement at the flight deck due to pitch.
(7) $2.13ms^{-1}$ significant vertical velocity at the flight deck.

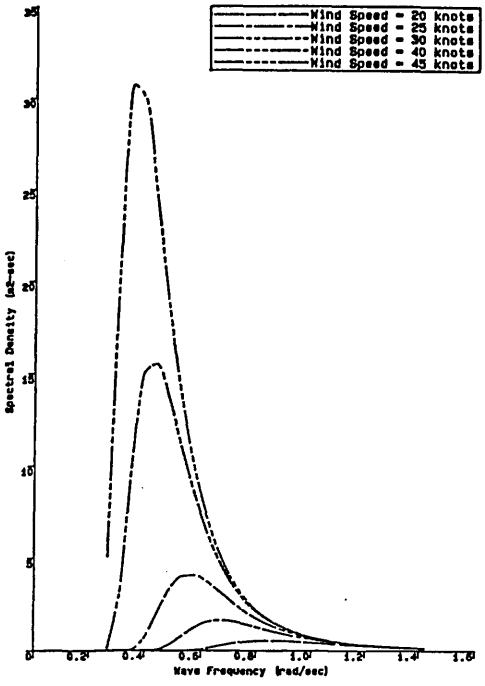

PIERSON-MOSKOWITZ WAVE SPECTRUM

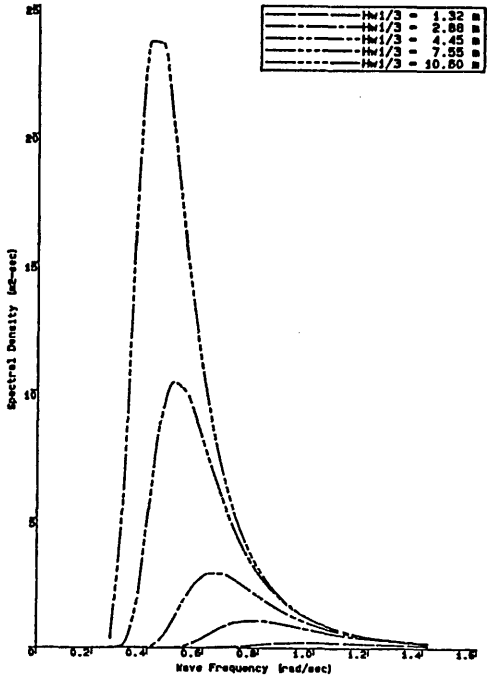

BRETSCHNEIDER WAVE SPECTRUM

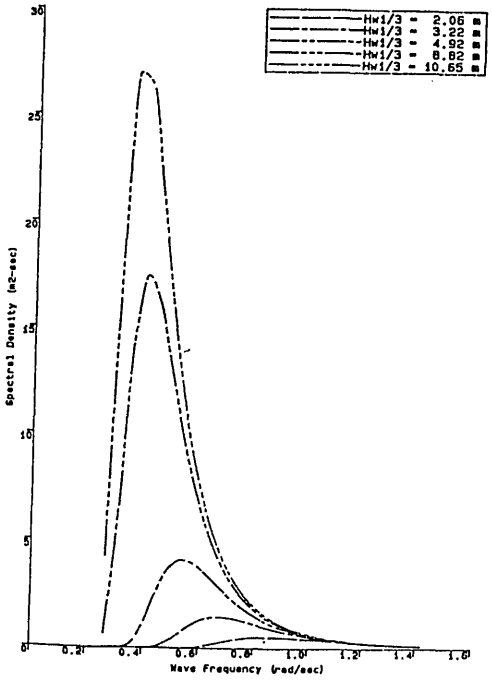

ITTC/ISSC 75 WAVE SPECTRUM

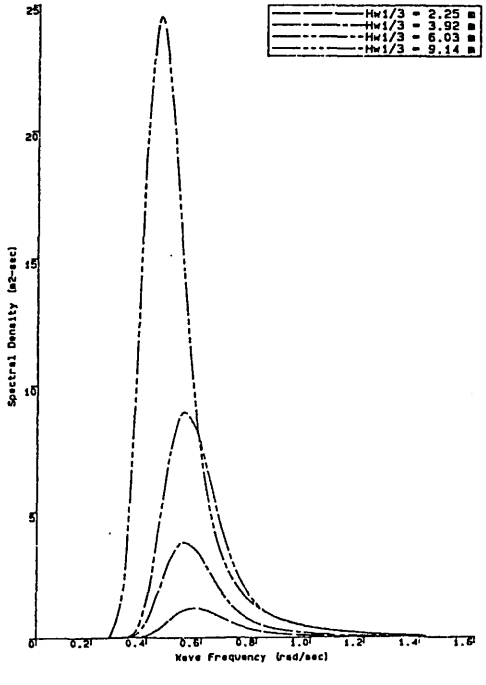

ITTC 84 WAVE SPECTRUM

Figure 7.2. Various Plots of Wave Spectrum

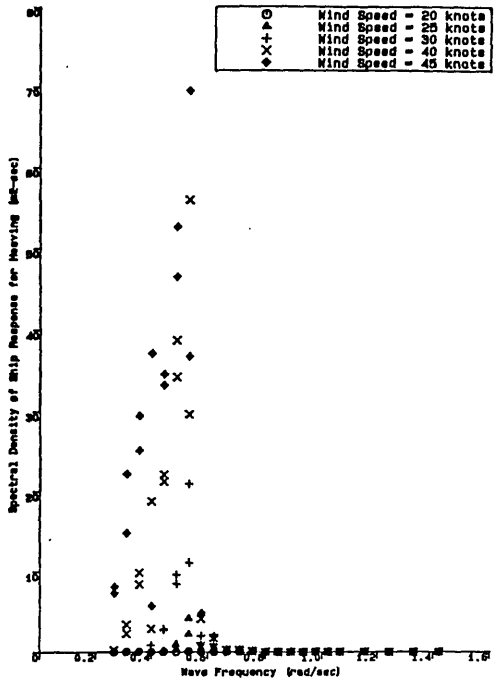

RESPONSE SPECTRUM FOR HEAVING MOTION
OF SWATH1 SHIP IN IRREGULAR BEAM SEAS

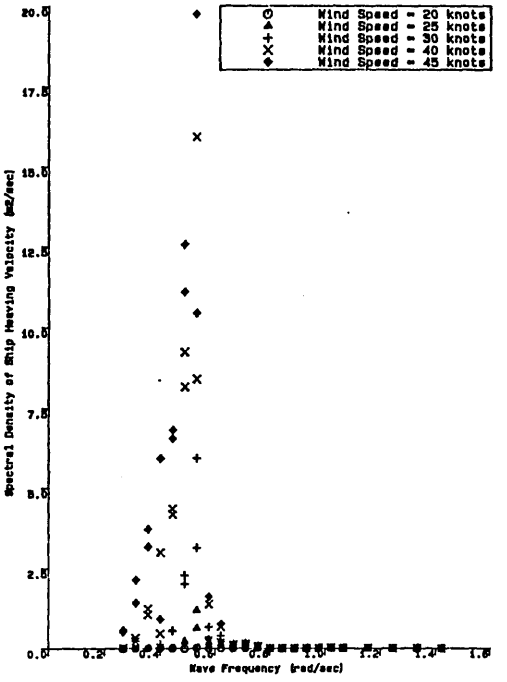

HEAVE VELOCITY SPECTRUM
OF SWATH1 SHIP IN IRREGULAR BEAM SEAS

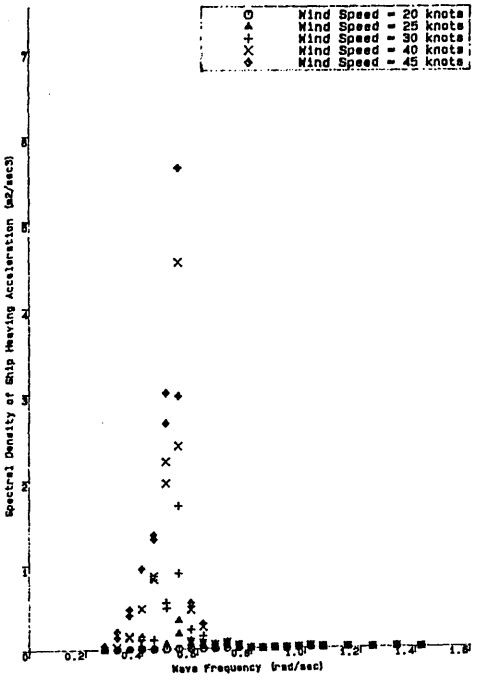

HEAVE ACCELERATION SPECTRUM
OF SWATH1 SHIP IN IRREGULAR BEAM SEAS

Figure 7.3. Response, Velocity and Acceleration Spectrum

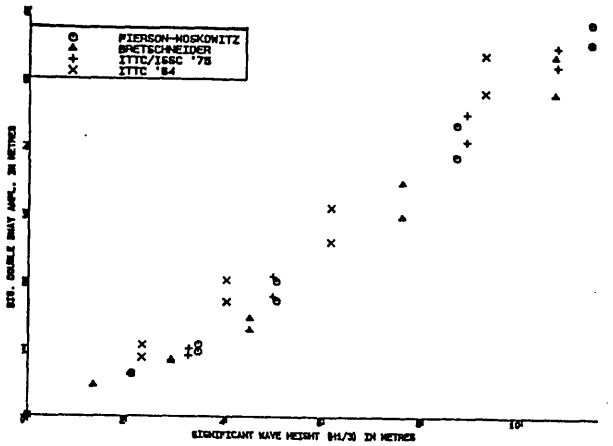

(a)

PROBABLE SIGNIFICANT DOUBLE SWAY AMPLITUDE
SWATH1 SHIP IN IRREGULAR BEAM SEAS

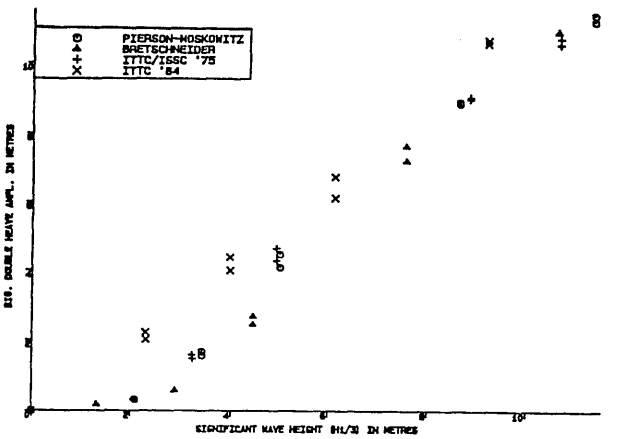

(b)

PROBABLE SIGNIFICANT DOUBLE HEAVE AMPLITUDE
SWATH1 SHIP IN IRREGULAR BEAM SEAS

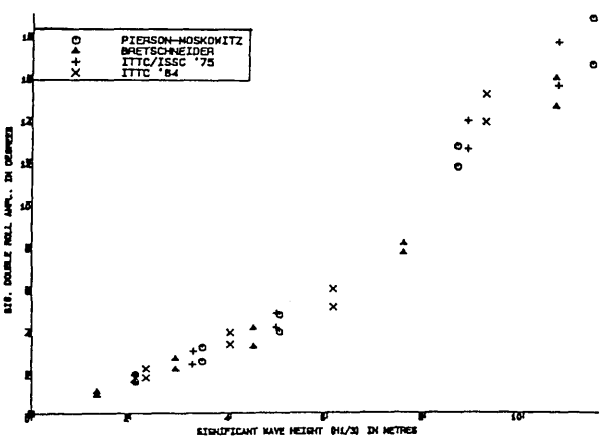

(c)

PROBABLE SIGNIFICANT DOUBLE ROLL AMPLITUDE
SWATH1 SHIP IN IRREGULAR BEAM SEAS

Figure 7.4. Probable Significant Double Motion Amplitudes of SWATH1 in Irregular Beam Seas

The probability values obtained from the computer program which have been derived from the experimental data are then observed by using two matrices as shown in table 7.4 to determine the seakeeping qualities of SWATH1. The first matrix contains codes according to the above criteria (0 means no treshold violated for waves with significant wave height up to 9.75m) as a function of ship speed and heading of the seas. The second indicates the significant wave height (in metres) at which the specified criterion in the first matrix is being exceeded.

Table 7.4a. SWATH1 General Criteria (1-4)

Ship Speed (knots)	Beam Sea 90^{o}	Quartering Sea 135^{o}	Head Sea 180^{o}
0.00	0	2	2
3.50	-	-	2
7.05	-	-	2
10.50	-	-	2
14.10	-	-	2

Acceptable Significant Wave Height (m)

Ship Speed (knots)	Beam Sea 90^{o}	Quartering Sea 135^{o}	Head Sea 180^{o}
0.00	9.75	7.91	7.77
3.50	-	-	7.79
7.05	-	-	6.82
10.50	-	-	6.32
14.10	-	-	6.27

Table 7.4b. SWATH1 Helicopter Criteria (5-7)

Ship Speed (knots)	Beam Sea 90°	Quartering Sea 135°	Head Sea 180°
0.00	7	6	6
3.50	-	-	6
7.05	-	-	6
10.50	-	-	6
14.10	-	-	6
Acceptable Significant Wave Height (m)			
Ship Speed (knots)	Beam Sea 90°	Quartering Sea 135°	Head Sea 180°
0.00	8.37	5.03	4.94
3.50	-	-	4.70
7.05	-	-	3.76
10.50	-	-	3.77
14.10	-	-	3.50

The seakeeping qualities of a ship can also be described in term of box scores. The box scores is composed making use of information from the seakeeping criteria and the wave height distributions of a certain area where the ship will be operated. In case of SWATH1, information is obtained from table 7.4 and table 7.5 [108], which is the wave distributions data of the North Atlantic. Information that can be drawn from the box scores is the percent of time a ship could be expected to operate in her environment without violating the specified criteria.The box scores of SWATH1 as shown in table 7.6 is calculated by assuming that the probability of encountering a sea at a specific heading

angle relative to the ship is equally likely for the three headings.

Table 7.5. Wave Height Distributions in the North Atlantic

Summer (June,July) Significant Wave Height (Z metres)	Wave Period (T_z second) T≤7	8≤T≤9	10≤T≤11	12≤T
≤Z≤0.75	0.12	0.00	0.00	0.00
0.75≤Z≤1.75	0.37	0.06	0.01	0.01
1.75≤Z≤2.75	0.15	0.09	0.03	0.01
2.75≤Z≤3.75	0.04	0.03	0.02	0.01
3.75≤Z≤5.75	0.01	0.02	0.01	0.01
5.75≤Z≤7.75	0.00	0.00	0.00	0.00
7.75≤Z≤9.75	0.00	0.00	0.00	0.00
Winter (December,January) Significant Wave Height (Z metres)	**Wave Period (T_z second) T≤7**	**8≤T≤9**	**10≤T≤11**	**12≤T**
≤Z≤0.75	0.03	0.00	0.00	0.00
0.75≤Z≤1.75	0.15	0.03	0.00	0.01
1.75≤Z≤2.75	0.13	0.10	0.04	0.02
2.75≤Z≤3.75	0.06	0.07	0.05	0.03
3.75≤Z≤5.75	0.02	0.05	0.06	0.04
5.75≤Z≤7.75	0.01	0.02	0.02	0.02
7.75≤Z≤9.75	0.00	0.01	0.00	0.02

Table 7.6. Seakeeping Box Scores for SWATH1 Operating in North Atlantic

	Summer	Winter
General Criteria (1-4)	1.00	0.84
Helicopter Criteria (5-7)	0.92	0.67
General and Helicopter Criteria (1-7)	0.92	0.67

The numbers presented in table 7.6 reflect the proportion of time that the SWATH1 effectively could be operated in the North Sea. On the other hand the values of one minus the numbers in the box scores are the proportion of time that the operation of SWATH1 is degraded due to motion in a certain season. A similar procedure can be applied to assess the duration of effective operation and down time of a ship in a whole year when the information of one year wave distributions in a specific area is available. Such a presentation is given in [109].

7.4. Conclusions.

The conclusions of the study in this chapter are set out below.

1. A brief evaluation of the SWATH1 seakeeping qualities through the seakeeping criteria and the box scores reveals the high capability of such a ship to overcome the motion problem in a harsh

environment. If it can be assumed that the wave distribution given in table 7.5 represents the extreme minimum and maximum waves of a whole year in the North Atlantic, box scores of all year can then be added in table 7.6 as follows :

Table 7.6a. Seakeeping Box Scores for SWATH1 Operating in North Atlantic (all year added)

	Summer	Winter	All Year
General Criteria (1-4)	1.00	0.84	0.92
Helicopter Criteria (5-7)	0.92	0.67	0.80
General and Helicopter Criteria (1-7)	0.92	0.67	0.80

From table 7.6a one can conclude that the seakeeping performance of a relatively small SWATH ship (2701 tonnes), is excellent. It should be borne in mind SWATH1 is a bare hull ship, the downtime of 20% (if helicopter criteria is required) may reduce by half or more if control fins are fitted. A more reliable assessment on the SWATH1 ship can be gained if more data concerning the sea headings and ship speeds are available.

2. Spectral analysis is the most suitable method in the design process to predict the behaviour of a ship, ie. motion, loadings etc, in irregular seas. The accuracy of the predictions is dependent on the quality of information regarding the sea

properties where the ship will be operated and the criteria used.

CHAPTER 8

GENERAL CONCLUSIONS AND RECOMMENDATIONS

Chapter 8

GENERAL CONCLUSIONS AND RECOMMENDATIONS

Generally the experimental results presented in this thesis are in satisfactory agreement with the results from the two theories. The discrepancies with regard to the theories are mainly caused by their limitations. For example, the numerical models are established upon an assumption that the SWATH model is a rigid body. The three-dimensional hydroelastic theory has been proposed to solve such a problem [110]. Nonetheless, concern over cost and computational effort have discouraged the development of such a theory.

8.1. SWATH1 Model Motions.

The experimental data indicates that in all heading angles observed, SWATH ships could, without any difficulty, attain low motion responses in the supercritical zone. This would not be the case for monohull ships. From the seakeeping stand point this means that a SWATH ship could be safely operated in most moderate seas. This is confirmed by a brief evaluation on SWATH1 making use of seakeeping criteria (as explained in chapter 7).

To investigate SWATH ship motions experimentally care should be taken in arranging the tethering system so as its effect on the model motions can be minimised as much as possible. The use of Selspot is preferable to measure lateral motions rather than LVDTs.

Other aspects of seakeeping, such as sinkage, trim and upwelling can be observed together with the motion observation if the experiment is appropriately planned and arranged. Further, the record of SWATH1 model motions could be useful to investigate SWATH1 model's relative bow motion and/or free racing of the engine due to propeller emergence.

For future work, investigation on SWATH ship motions can be conducted on SWATH2 and SWATH3 models which are now available in the laboratory. One of the objectives of these investigations could be to compare the motion characteristics of different SWATH ship configurations. To do this comparative study, however, a code or criteria for comparison should be outlined first.

8.2. SWATH1 Model Dynamic Loadings.

Maximum bending moment at the mid-point of cross-structure, ie the most critical position of such a SWATH structure, occurs with the SWATH at rest in beam seas, particularly at wave length twice of the hull separation. The maximum bending moment will be experienced by a SWATH ship when the wave length is approximately equal to the hull separation in quartering waves. Serious attention should be paid by the SWATH designers to this particular part of the SWATH ship structure.

From observation of the structural response, non-linearity due to different wave elevations is clear. Waves will cause higher bending moments in sag than in hog. In relatively high waves the maximum sagging bending moment could be up to 30% higher than the hogging bending moment. It is concluded that it is neccessary to develop a numerical model that can deal with this phenomenon.

The strain gauges gave satisfactory results in measuring the bending moment on the cross-structure of the SWATH1 model. However, the reliability of the strain gauges to measure vertical forces on the vertical bars attached on the struts is questionable. It is suggested that compression/tension load cells are desirable to replace the strain gauges to measure the vertical forces on such a structure.

8.3. Closure.

The generated experimental data can be useful for further research on SWATH ships at the Department. Finally, it is hoped that this thesis will be a valuable contribution in the development of SWATH ship technology.

REFERENCES.

1. KENNELL, C. "SWATH Ship Design Trends", Int. Conf. on SWATH Ships and Advanced Multi-Hulled Vessels, London, Apr. 1985.

2. BHATTACHARYYA, R. "Dynamics of Marine Vehicles", John Wiley & Sons, Inc., 1980.

3. GORE, J.L. (Editor) "SWATH Ships", Naval Engineers Journal, Vol. 97, No. 2, pp. 83-112, Feb. 1985.

4. BOERICKE, H. Jr. "Unusual Displacement Hull Forms for Higher Speeds", Int. Shipbuilding Progress Magazine, Vol. 6, No. 58, pp 249-264, Jun. 1959.

5. PETTY, W., Manuscripts concerning "Ye Double Bodyed Shippe", National Maritime Museum SPB/16.

6. "The Double Bottom or Twin Hull Ship of Sir William Petty", Oxford University Press.

7. "Many Hulls Make Light Work", Seascape, Int. Maritime Magazine No. 2, p 21, Jun. 1987.

8. LUNDBORG, C.G. "Construction of Ships", U.S. Patent, No. 234,794, 1880.

9. LANG, T.G. "S^3 - New Type of High Performance Semi-Submerged Ship", ASME, Journal Engineering for Industry, 1972.

10. LEOPOLD, R., JOHNSON, R.S., HADLER, J.B. and GENALIS, R. "The Low Water Plane Multi-Hull Ship Principles, Status and Plans for Naval Development", AIAA, Paaper No. 72-603, 1972.

11. McGREGOR, R.C. "An Illustration of Some SWATH Vessel Characteristics", High-Speed Surface Craft Conf., London, May 1983.

12. NELSON, A. "Vessel", U.S. Patent, No.795,002, Jul. 1905.

13. FAUST, J.G. "Marine Vessel", U.S. Patent, No. 1,861,338, 1932.

14. PIEROTH, C.G. and LAMB, G.R. "The SWATH Option as a V/STOL Aircraft Carrier", The SNAME, Hampton Road Sect., Mar. 1985.

15. CREED, F.G. "Floating Structure", U.S. Patent, No. 2,405,115, 1946.

16. LEOPOLD, R. "Marine Vessel", U.S. Patent, No. 3,447,502, 1969.

17. LEOPOLD, R. "A New Hull Form for High Speed Volume Limited Displacement Type Ships", SNAME, Spring Meeting, Paper No. 8, Beverly Hills, May 1969.

18. LANG, T.G. "High-Speed Ship with Submerged Hulls", U.S. Patent, No.3,623,444, Nov. 1971.

19. LANG, T.G. et al "Naval Feasibility of the NUC Semi-Submerged Ship Concept", Naval Under Sea Research and Development Center, TP 235, 1971.

20. LANG, T.G. et al "Design and Development of the 190-ton Stable Semisubmersible Platform (SSP)", ASME, Winter Annual Meeting, Paper No. 73-WA/Oct.-2, Nov. 1973.

21. LANG, T.G. and HIGDON, D.T. "Hydrodynamics of the 190-ton Stable Semisubmerged Platform (SSP)", AIAA/SNAME, Advanced Marine Vehicles Conf., Paper No. 79-328, Feb. 1974.

22. GUPTA, S.K. and SCHMIDT, T.W. "Developments in SWATH Technology", Naval Engineers Journal, May 1986.

23. LUEDEKE, G. Jr. and MONTAGUE, J. "RMI's Small Waterplane-Area-Twin-Hull (SWATH) Boat Project", SNAME, San Diego Section, Nov. 1984.

24. CHAPMAN, R.B. "Wave Resistance and Kelvin Wake of Generalised Semi-Submersible", SAI, Report No. 77-980-LJ, Lajolla, 1977.

25. MacGREGOR, J.R. "An Analysis of SWATH Design and Performance Data", Dept. of NAOE, University of Glasgow, Report No. NAOE-86-30, Nov. 1986.

26. OSHIMA, M., NARITA, H. and KUNITAKE, Y. "Experience With 12-meter Long Semi-Submerged Catamaran 'Marine Ace' and Building of SSC Ferry for 445 Passengers", AIAA/SNAME, Int. Conf. on Advanced Marine Vehicles, Paper No. 79-2019, Baltimore, Maryland, 1979.

27. SMITH, S.N. "Discussion of Some Design Considerations for Small Semi-Submersible (SWATH) Ships", Dept. of NAOE, University of Glasgow, Paper No. NAOE-HL-78-23, Jun. 1979.

28. HIGHTOWER, J.D. and SEIPLE, R.L. "Operational Experiences with the SWATH Ship SSP Kaimalino", AIAA/SNAME Advanced Marine Vehicles Conf., Paper 78-741, San Diego, Apr. 1978.

29. WU, J.Y. "SWATH Vertical Motions with Emphasis on Fixed Fins Control", PhD Thesis, Dept. of NAOE, University of Glasgow, Dec. 1985.

30. MANTLE, P.J. "A Technical Summary of Air Cushion Craft Development", DTNSRDC, Report No. 80/012 (4727 revised), Jan. 1980.

31. MABUCHI, T., KUNITAKE, Y. and NAKAMURA, H. "A Status Report on Design and Operational Experiences with the Semi-Submerged Catamaran (SSC) Vessels", Int. Conf. on SWATH Ships and Advanced Multi-Hulled Vessels, Paper No. 5, London, Apr. 1985.

32. HIGHTOWER, J.D., PARNELL, L.A., STRICKLAND, A.T. and WARNSHUIS, P.L. "SWATH Technology Development mat the Naval Ocean System Center", Int. Conf. on SWATH Ships and Advanced Multi-Hulled Vessels, Paper No. 14, London, Apr. 1985.

33. McGREGOR, R.C., written discussion on "A Concept Exploration Model for SWATH Ships" by NETHERCOTE, W.C.E. and SCHMITKE, R.T., Trans. RINA, Vol. 124, pp. 113-130, 1982.

34. "RMI's Prototype SWATH on Sea Trials at San Diego", Combat Craft, May/Jun. 1985.

35. "The Viability of Naval SWATH Ships", Combat Craft, Sep./Oct. 1985.

36. ROUTA, T. "Application of the SWATH Principle to Passenger `Vessels", Int. Conf. on SWATH Ships and Advanced Multi-Hulled Vessels, Paper no. 3, RINA, London, Apr. 1985.

37. STENSON, R.J. "Full Scale Powering Trials of the Stable Semi-Submerged Platform, SSP Kaimalino", DTNSRDC Report SPD-650-01, Apr. 1976.

38. SEREN, D.B. "SWATH - the Shape of Ships to Come", High-Speed Surface Craft, Dec. 1983.

39. SMITH, S.N. "An Investigation into the Hydrodynamics of Small SWATH Ships", 3rd High-Speed Surface Craft Conf., Brighton, 1980.

40. SMITH, S.N. "Design and Hydrodynamic Assessment of a Small Semi-Submersible (SWATH)", PhD Thesis, University of Glasgow, Dept. of NAOE, 1982.

41. SMITH, S.N. "Design and Hydrodynamic Performance of a Small Semi-Submersible (SWATH)", RINA Spring Meeting, 1982.

42. SMITH, S.N. and ATLAR, M. "On the Large Amplitude Extreme Motions of Floating Vessels", BOSS 82, Norway, 1982.

43. SMITH, S.N. "Parasitic Motion and Capsize Safety of a SWATH-Type Ship", OTC Report no. 4619, 1983.

44. WOOLAVER, D.A. and PETERS, J.B. "Comparative Ship Performance Sea Trials for the U.S. Coast Guard Cutters 'Mellon' and 'Cape Corwin' and the U.S. Navy Small Waterplane Area Twin Hull Ship 'Kaimalino'", DTNSRDC, Report 80/037, Bethesda, Maryland, Mar. 1980.

45. HOLCOMB, RICHARD, S. and ALLEN, R.G. "Investigation of the Characteristics of Small SWATH Ship Configured for United States Coast Guard Missions", DTNSRDC/SSD-83-3, Jun. 1983.

46. COMSTOCK, J.P. "Principles of Naval Architecture", The SNAME, 1977.

47. ATLAR, M., LAI, P.S.K. and McGREGOR, R.C. "On Hydrodynamic Aspects of a Two-Dimensional Prediction of Loads and Motions of a Twin-Hull Semi-Submersible", IMAEM 4th Int. Congress, Paper No. 25, Varna-Bulgaria, May 1987.

48. SEREN, D.B. and ATLAR, M. "An Overview of the Concepts Employed to Predict the Hydrodynamic Forces Imposed on An Unappended SWATH Ship Proceeding in a Seaway", University of Glasgow, Dept. of NAOE, Report no. NAOE-84-63, Dec. 1984.

49. ATLAR. M. "Method of Solution for 5 Degrees of Freedom Coupled Equations of Motions of a SWATH Ship", University of Glasgow,Dept. of NAOE, Report no. NAOE-86-36,Nov. 1986.

50. LEE, C.M. and CURPHEY, R.M. "Prediction of Motion, Stability, and Wave Load of Small-Waterplane-Area, Twin-Hull Ships", Trans. SNAME, vol. 85, pp. 94-130, 1977.

51. SEREN, D.B., MILLER, N.S., FERGUSON, A.M. and McGREGOR, R.C. "Some Motion and Resistance Aspects of SWATH-Ship Design", Int. Conf. on SWATH Ships and Advanced Multi-Hulled Vessels, RINA, London, Apr. 1985.

52. SEREN, D.B. and ATLAR, M."The SWATH Wave-Load Program, Progress Report No 6; An Overview of the Concepts Employed to Predict the Hydrodynamic Forces Imposed on an Unappended SWATH-ship Proceeding in a Seaway ", University of Glasgow,Dept. of NAOE, Report No. NAOE-84-63, 1984.

53. FRANK, W. "On the Oscillations of Cylinders In or Below the Free Surface of Deep Fluids", DTNSRDC, Report No. 2375, Oct. 1976.

54. KIM, C.H. and CHOU, F. "Motions of a Semi-Submersible Drilling Platform in Head Seas", Marine Technology, pp 112-123, Apr. 1973.

55. NORDENSTROM, N., FALTINSEN, O. and PEDERSON, B. "Prediction of Wave-Induced Motions and Loads for Catamarans", OTC, Paper No. 1418, Houston, 1971.

56. LEE, C.M. "Theoretical Predictions of Motion of Small-Waterplane Area, Twin Hull (SWATH) Ships in Waves", DTNSRDC, Report No. 76-0046, Dec. 1976.

57. ZHENG, X. "Three Dimensional Seakeeping Analysis", PhD Thesis, University of Glasgow, Dept. of NAOE, (in preparation).

58. PAULLING, J.R. and HONG, Y.S. "Analysis of Semi-Submersible Catamaran Type Platforms", OTC, Paper No. 2977, Houston, 1977.

59. MATHISEN, J. and CARLSEN, C.A. "A Comparison of Calculation Methods for Wave Loads on Twin Pontoon Semi-Submersibles", Int. Sympo. on Ocean Engineering and Ship Handling, Gothenburg, 1980.

60. ATLAR, M., SEREN, D.B. and VALIDAKIS, J. "The Effect of Tilt and Interference on the Hydrodynamic Coefficients of SWATH-Type Sections", Int. Conf. on SWATH Ships and Advanced Multi-Hulled Vessels, RINA, London, Apr. 1985.

61. SEREN, D.B. and LEITCH, E. "The SWATH Wave-Load Program, Progress Report No 1; The Wave Input", University of Glasgow, Dept. of NAOE, Report No. NAOE-82-30, 1982.

62. SEREN, D.B. and MILLER, N.S. "The SWATH Wave-Load Program, Progress Report No 2; The Tentative Outline of the Treatment of the Geometry", University of Glasgow, Dept. of NAOE, Report No. NAOE-82-31, 1982.

63. SEREN, D.B., LEITCH, E. and MILLER, N.S. "The SWATH Wave-Load Program, Progress Report No 3; Manual for Structure Geometry Description", University of Glasgow, Dept. of NAOE, Report No. NAOE-83-38, 1983.

64. SEREN, D.B., LEITCH, E. and MILLER, N.S. "The SWATH Wave-Load Program, Progress Report No 4; Program for Offshore Structures Hydrostatics (POSH)", University of Glasgow, Dept. of NAOE, Report No. NAOE-83-35, 1983.

65. SEREN, D.B., LEITCH, E. and MILLER, N.S. "The SWATH Wave-Load Program, Progress Report No 5; A Package to Compute and Control the Weight Distribution, Dynamic Properties and Static Loads of Floating Offshore Configurations (MAD)", University of Glasgow, Dept. of NAOE, Report No. NAOE-84-32, 1984.

66. DRYSDALE, L.H. "Solution of Linear Motion Equation for Coupled Heave and Pitch for a SWATH Ship (including programming manual)", University of Glasgow, Dept of NAOE, Report No. NAOE-86-53, Dec. 1986.

67. WU, J.Y. "A Study of Effects of Fin Size on the Pitching and Heaving of a SWATH Ship", University of Glasgow, Dept. of NAOE, Report No. NAOE-84-55, Jun. 1984.

68. WU, J.Y. "Experimental Investigation of Vertical-Plane Response of a SWATH Ship with and without Aft Fins in Head Seas", University of Glasgow, Dept. of NAOE, Report No. NAOE-85-31, Jan. 1985.

69. WU, J.Y. and McGREGOR, R.C. "SWATH Seakeeping in the Presence of Control Fins", 5th Int. High-speed Surface Craft Conf., Southampton, May 1986.

70. DRYSDALE, L.H. "Effect of Active Control Fins on the Vertical Plane Response of SWATH Ships", University of Glasgow, Dept. of NAOE, Report No. NAOE-86-61, Dec. 1986.

71. DRYSDALE, L.H. "Structural Loads Acting on a SWATH Ship", University of Glasgow, Dept. of NAOE, Report No. NAOE-HL-45, 1987.

72. LEITCH, E. "User Manual for SWATHL - Seakeeping in Frequency Domain", University of Glasgow, Dept. of NAOE, (Report in preparation).

73. ZHENG, X. "Calculation of Potential Flow about Arbitrary Three-Dimensional Bodies, Part I - Flow about Submerged Bodies", University of Glasgow, Dept. of NAOE, Report No. NAOE-86-52, Nov. 1986.

74. ZHENG, X. "Calculation of Potential Flow about Arbitrary Three-Dimensional Bodies, Part II - Free Surface Flow", University of Glasgow, Dept. of NAOE, Report No. NAOE-85-54, 1985.

75. ZHENG, X. and McGREGOR, R.C. "Prediction of Force and Motion Response in Crane Vessels", Marintec China 87, Shanghai, Dec. 1987.

76. McGREGOR, R.C. "Experimental Study of Upwelling on the SWATH1 Model in Beam Seas: Compliant Systems Cohesive Programme", University of Glasgow, Dept. of NAOE, Report No. NAOE-87-00, 1987.

77. DJATMIKO, E.B. "Experimental Studies on SWATH Ship Motions in Regular Beam Seas", University of Glasgow, Dept. of NAOE, Final Year Project, NAOE-86-11, Apr. 1986.

78. DJATMIKO, E.B. "Experimental Investigation into SWATH Ship Motions and Loadings", University of Glasgow, Dept. of NAOE, Annual Report, May 1987.

79. ATLAR, M. "The SWATH Wave-Load Program Some Aspects of Computer Program SWATHL", University of Glasgow, Dept. of NAOE, Report No. NAOE-86-55, Dec. 1986.

80. LAI, P.S.K. and ATLAR, M. "On The Roll-Exciting Moments of Twin Cylinders", University of Glasgow, Dept. of NAOE, Report No. NAOE-85-52, 1985.

81. McGREGOR, R.C., DJATMIKO, E.B. and PERCIVAL, D.J. "Experimental Study of Upwelling on the SWATH1 Model in Quartering Seas: Compliant Systems Cohesive Programme", University of Glasgow, Dept. of NAOE, Report No. NAOE-87-38, Sept. 1987.

82. ATLAR, M. et al "Investigation of Hydrodynamic Coefficients of Semi-Submersible (or SWATH) Type Sections with Emphasis on the Effect of Tilt and Interference", University of Glasgow, Dept. of NAOE, Report NAOE-85-32, May 1985.

83. PINKSTER, J.A., "Low Frequency Second Order Wave Exciting Forces on Floating Structure", PhD Thesis, Delft University, 1980.

84. CHUN, H.H. "Resistance and Motion of SWATH1 Model in Calm Water and in Uniform Waves", University of Glasgow, Dept. of NAOE, (in preparation).

85. CHUN, H.H. "SWATH2 Model Resistance and Motion in Calm Water and in Waves", University of Glasgow, Dept. of NAOE, (report in preparation).

86. FERGUSON, A.M. "Factors Affecting the Components of Ship Resistance", PhD Thesis, University of Glasgow, Dept. of NAOE, Oct. 1976.

87. WAHAB, R. et al " On the Behavior of the ASR Catamaran in Waves", Marine Technology, vol. 8, No. 3, pp. 334-360, 1971.

88. DALLINGA, R.P. "Seakeeping Tests for a Small Waterplane Area Twinhull Ship", NSMB, Report No. 43755-2-2T, Nov. 1981.

89. CURPHEY, R.M. and LEE, C.M. "Analytical Determination of Structural Loading on ASR Catamaran in Beam Seas", DTNSRDC, Report no. 4267, Bethesda, Maryland, Apr. 1974.

90. LEE, C.M. et al "Prediction of Motion and Hydrodynamic Loads of Catamarans", Marine Technology, vol. 10, no. 4, Oct. 1973.

91. CURPHEY, R.M. and LEE, C.M. "Theoretical Prediction of Dynamic Wave Loads on Small Waterplane Area, Twin Hull Ships", DTNSRDC, Report no. 77-0027, 1977.

92. INCECIK, A. "Design Aspects of the Hydrodynamic and Structural Loading on Floating Offshore Platforms Under Wave Excitation", PhD Thesis, University of Glasgow, Dept. of NAOE, 1982.

93. DALLY, J.M. and RILEY, W.F. "Experimental Stress Analysis", McGraw Hill Book Company, 1978.

94. HUGHES, O.F. "Ship Structural Design ; A Rationally-Based, Computer Aided, Optimization Approach", John Wiley & Sons, Inc., 1983.

95. JENSEN, J.J. and PEDERSEN, P.T. "Bending Moments and Shear Forces in Ships Sailing in Irregular Waves", Journal of Ship Research, Vol. 25, No. 4, pp. 243-251, Dec. 1981.

96. NEWLAND, D.E. "An Introduction to Random Vibrations and Spectral Analysis", Longman Inc., New York, 1986.

97. McGREGOR, R.C. "Offsshore Structures Short Course Unit 1A - Ocean Waves", University of Glasgow, Dept. of NAOE, Report No. NAOE-83-46, Mar. 1983.

98. WEINBLUM, G. and St.DENIS, M. "On the Motion of Ships at Sea", Trans. SNAME, Vol. 58, 1950.

99. PIERSON, W.J. Jr. and MARKS, W. "The Power Spectrum Analysis of Ocean Wave Records", Trans. American Geophysical Union, Vol. 33, No. 6, Dec. 1952.

100. St.DENIS, M. and PIERSON, W.J.Jr. "On the Motions of Ships in Confused Seas", Trans. SNAME, Vol. 61, 1953.

101. SARPKAYA, T. and ISAACSON, M. "Mechanics of Wave Forces on Offshore Structures", Van Nostrand Reinhold Company, Inc. 1981.

102. WILSON, J.F. "Dynamics of Offshore Structures", John Wiley and Sons, Inc., 1972.

103. PIERSON, W.J. and MOSKOWITZ, L. "A Proposed Spectral Form for Fully Developed Wind Seas Base on the Similarity Theory of S.A. Kataigorodsky", Journal of Geophysical Research, Vol. 69, No. 24, Dec. 1964.

104. BRETSCHNEIDER, C.L. "Wave Variability and Wave Spectra for Wind-Generated Gravity Waves", Beach Erosion Board, Corps of Engineers, Technical Memo No. 118, 1959.

105. MIROKHIN, B.V. and KHOLODILIN "Probability Characteristics of Ship Inclination due to Erupting Wave Impulse", Proceedings of 14th International Towing Tank Conference, 1975.

106. HOGBEN, L. and LUMB, F.E. "Ocean Wave Statistics", HMSO, 1967.

107. OCHI, M.K. and BALES, S.L. "Effect of Spectral Formulations in Predicting Responses of Marine Vehicles and Ocean Structures", 9th Annual OTC, Paper No. OTC 2743, Houston, Texas, May 1977.

108. OLSON, S.R. "An Evaluation of the Seakeeping Qualities of Naval Combatants", Naval Engineers Journal, Feb. 1978.

109. KENNELL, C.G., WHITE, B.L. and COMSTOCK, E.N. "Innovative Naval Designs for North Atlantic Operations", Trans. SNAME, Vol. 93, pp. 261-281, 1985.

110. BISHOP, R.E.D., PRICE, W.G. and TEMAREL, P. "On the Hydroelasticity Response of a SWATH to Regular Oblique Waves", Advances in Marine Structures, Paper No. 5, ARE, Dunfermline, Scotland, May 1986.

APPENDIX 1

EXPERIMENTAL DATA

APPENDIX 1a

SWATH1 MODEL IN REGULAR BEAM SEAS
NON-DIMENSIONAL MOTION RESPONSES

FR(r/s)	Non-Dim FR.	SWAY1	SWAY2	HEAVE1	HEAVE2	ROLL1	ROLL2
LOW WAVES :							
1.8852	0.7372	0.5930	0.5396	1.2625	1.1489	1.0766	0.9797
2.1994	0.8600	0.8707	0.9594	1.0318	1.1369	1.9276	2.1240
2.5136	0.9829	0.6107	0.6440	0.9784	1.0317	2.0540	2.1661
2.8278	1.1058	0.3906	0.6454	0.4370	0.7222	3.7372	6.1754
3.1420	1.2286	0.8299	0.8631	1.1672	1.2138	0.9481	0.9860
3.4562	1.3515	0.7679	0.9172	1.6919	2.0209	0.3473	0.4149
3.7704	1.4743	0.6024	0.7010	2.2734	2.6458	0.4029	0.4689
4.0846	1.5972	0.1783	0.2135	0.2982	0.3572	0.2978	0.3568
4.3988	1.7201	0.5061	0.5636	0.2767	0.3082	0.3458	0.3851
4.7130	1.8429	0.3290	0.4023	0.2328	0.2846	0.3056	0.3736
5.0272	1.9658	0.3607	0.4890	0.2844	0.3855	0.3420	0.4637
5.3414	2.0887	0.1669	0.2186	0.2154	0.2821	0.2549	0.3338
5.6556	2.2115	0.1055	0.1447	0.0805	0.1103	0.2123	0.2910
5.9698	2.3344	0.0501	0.0643	0.0487	0.0625	0.2157	0.2767
6.2840	2.4572	0.1057	0.1132	0.0931	0.0997	0.2001	0.2144
6.5982	2.5801	0.1895	0.1971	0.1185	0.1233	0.1814	0.1887
6.7239	2.6292	0.2305	0.2625	0.1286	0.1465	0.1599	0.1820
6.9124	2.7030	0.2454	0.3140	0.1368	0.1750	0.1307	0.1672
7.2266	2.8258	0.3346	0.3749	0.1526	0.1710	0.1131	0.1267
7.5408	2.9487	0.4024	0.4436	0.1408	0.1552	0.0822	0.0906
8.1692	3.1944	0.4658	0.6291	0.1391	0.1879	0.0418	0.0565
8.7976	3.4401	0.4873	0.8423	0.1200	0.2075	0.0481	0.0831
9.4260	3.6859	0.4440	0.3657	0.1746	0.1438	0.0212	0.0174
10.0544	3.9316	0.3096	0.4141	0.0973	0.1301	0.0242	0.0323
HIGH WAVES :							
1.8852	0.7372	0.8346	0.6575	1.1986	0.9443	1.6730	1.3180
2.1994	0.8600	0.7093	0.7640	0.8412	0.9061	1.3431	1.4469
2.5136	0.9829	0.4685	0.6219	0.9035	1.1993	1.4791	1.9633
2.8278	1.1058	0.5219	0.6067	1.1140	1.2950	3.3866	3.9370
3.1420	1.2286	0.9341	1.1046	1.1908	1.4081	0.8394	0.9926
3.4562	1.3515	0.7479	0.7731	1.5901	1.6436	0.4595	0.4750
3.7704	1.4743	0.7033	0.7758	1.6524	1.8227	0.7971	0.8793
4.0846	1.5972	0.5793	0.6492	0.7056	0.7906	0.3225	0.3614
4.3988	1.7201	0.4458	0.4986	0.5262	0.5885	0.5786	0.6471
4.7130	1.8429	0.3427	0.4421	0.2267	0.2924	0.2779	0.3585
5.0272	1.9658	0.2752	0.3077	0.2381	0.2662	0.3752	0.4196
5.3414	2.0887	0.1862	0.1969	0.1557	0.1646	0.4034	0.4266
5.6556	2.2115	0.1101	0.1434	0.0791	0.1030	0.2963	0.3860
5.9698	2.3344	0.0490	0.0652	0.0480	0.0638	0.2465	0.3277

Note :

FR(r/s) : wave (circular) frequency in rads^{-1}

Non-Dim FR or N-D FR : Non-dimensional wave frequency

EncFR (r/s) : encountering wave frequency in rads^{-1}

APPENDIX 1b

SWATH1 MODEL IN REGULAR QUARTERING SEAS
NON-DIMENSIONAL MOTION RESPONSES

FR(r/s)	Non-Dim FR	SURGE	SWAY	HEAVE	ROLL	PITCH	YAW
LOW WAVES :							
1.8852	0.7372	0.6365	0.4417	1.0559	1.8033	1.1922	0.6211
2.1994	0.8600	0.6550	0.3006	1.0625	1.6753	1.9059	0.6037
2.5136	0.9829	0.4631	0.2093	0.9412	1.7174	1.7874	0.4630
2.8278	1.1058	0.6853	0.3668	0.9871	4.3247	4.7440	0.2529
3.1420	1.2286	0.6765	0.4413	1.2410	1.0374	0.5083	0.4196
3.4562	1.3515	0.6335	0.3766	1.8679	0.2741	0.1500	0.4333
3.7704	1.4743	0.5542	0.3182	1.2517	0.0445	0.0998	0.3344
4.0846	1.5972	0.4929	0.2912	0.0600	0.2158	0.2183	0.3155
4.3988	1.7201	0.4339	0.2518	0.1154	0.2342	0.1788	0.3046
4.7130	1.8429	0.3735	0.2619	0.1483	0.2081	0.2238	0.2808
5.0272	1.9658	0.3308	0.2054	0.1465	0.1890	0.2270	0.2099
5.3414	2.0887	0.2597	0.1746	0.1493	0.1721	0.1613	0.1374
5.6556	2.2115	0.2037	0.1282	0.1320	0.1474	0.1104	0.1143
5.9698	2.3344	0.1064	0.0816	0.0858	0.1443	0.0754	0.0549
6.2840	2.4572	0.0673	0.0404	0.0620	0.1062	0.0478	0.1124
6.5982	2.5801	0.0403	0.0240	0.0365	0.0586	0.0315	0.0205
6.9124	2.7030	0.0241	0.0507	0.0131	0.0737	0.0178	0.0476
7.2266	2.8258	0.0331	0.0550	0.0481	0.0318	0.0129	0.0244
7.5408	2.9487	0.0193	0.0875	0.0482	0.0126	0.0072	0.0176
HIGH WAVES :							
1.8852	0.7372	0.7283	0.4844	1.1604	0.9703	1.5938	0.4445
2.1994	0.8600	0.5435	0.3300	0.9319	0.8750	1.1936	0.3325
2.5136	0.9829	0.4786	0.1611	1.0430	1.3207	2.3393	0.4228
2.8278	1.1058	0.7355	0.2826	1.1217	3.8563	4.0686	0.4135
3.1420	1.2286	0.8528	0.4981	1.2053	1.3151	0.4910	0.4766
3.4562	1.3515	1.0505	0.4675	1.5881	0.3455	0.3025	0.4691
3.7704	1.4743	0.5787	0.3029	1.4223	0.1285	0.0800	0.4070
4.0846	1.5972	0.4608	0.2359	0.0923	0.2429	0.6205	0.3543
4.3988	1.7201	0.4240	0.2605	0.1242	0.2406	0.2337	0.3099
4.7130	1.8429	0.3437	0.2336	0.1313	0.1967	0.2295	0.2300
5.0272	1.9658	0.3473	0.2085	0.1362	0.2142	0.1997	0.2715
5.3414	2.0887	0.2553	0.1804	0.1457	0.1741	0.1635	0.1710
5.6556	2.2115	0.2016	0.0899	0.1190	0.1487	0.1065	0.0681
5.9698	2.3344	0.1267	0.0837	0.1031	0.1270	0.0794	0.0598
6.2840	2.4572	0.0869	0.0625	0.0736	0.1017	0.0567	0.0339
6.5982	2.5801	0.0670	0.0252	0.0579	0.0803	0.0438	0.0163
6.9124	2.7030	0.0377	0.0313	0.0495	0.0587	0.0236	0.0183
7.2266	2.8258	0.0345	0.0917	0.0597	0.0307	0.0083	0.0169
7.5408	2.9487	0.0240	0.0930	0.0414	0.0035	0.0036	0.0195

QMOT.DAT

APPENDIX 1c

SWATH1 MODEL IN REGULAR HEAD SEAS
NON-DIMENSIONAL MOTION RESPONSES

FR(r/s)	Non-Dim FR	SURGE	HEAVE	PITCH
LOW WAVES :				
1.8852	0.7372	0.8164	1.1567	1.2313
2.1994	0.8600	0.8847	0.9528	1.7138
2.5136	0.9829	0.6470	1.0324	2.4029
2.8278	1.1058	0.9665	1.1722	5.7447
3.1420	1.2286	1.1458	1.3129	1.3814
3.4562	1.3515	0.9180	1.7703	0.4601
3.7704	1.4743	0.7419	1.5899	0.3275
4.0846	1.5972	0.7063	0.2827	0.1692
4.3988	1.7201	0.5354	0.1863	0.1851
4.7130	1.8429	0.4825	0.2601	0.2128
5.0272	1.9658	0.3190	0.2352	0.1620
5.3414	2.0887	0.2612	0.2112	0.1604
5.6556	2.2115	0.1727	0.1970	0.1271
5.9698	2.3344	0.0758	0.1499	0.0995
6.2840	2.4572	0.0127	0.1204	0.0658
6.5982	2.5801	0.0378	0.0788	0.0406
6.9124	2.7030	0.1114	0.0764	0.0155
7.2266	2.8258	0.1054	0.0468	0.0077
7.5408	2.9487	0.1352	0.0558	0.0235
8.1692	3.1944	0.1275	0.0720	0.0342
8.7976	3.4401	0.1028	0.0871	0.0265
9.4260	3.6859	0.0949	0.0859	0.0120
10.0544	3.9316	0.0693	0.0677	0.0087
HIGH WAVES :				
1.8852	0.7372	0.6808	1.0388	1.2578
2.1994	0.8600	0.7392	0.7218	1.4228
2.5136	0.9829	0.6021	0.9254	2.1826
2.8278	1.1058	0.9629	1.1757	4.9516
3.1420	1.2286	1.0871	1.2592	1.3524
3.4562	1.3515	0.7938	1.6278	0.4537
3.7704	1.4743	0.7590	1.3234	0.3754
4.0846	1.5972	0.6372	0.2871	0.1280
4.3988	1.7201	0.5692	0.2043	0.1781
4.7130	1.8429	0.4468	0.2634	0.1981
5.0272	1.9658	0.2696	0.2426	0.1649
5.3414	2.0887	0.2432	0.2150	0.1546
5.6556	2.2115	0.1704	0.1878	0.1278
5.9698	2.3344	0.0915	0.1551	0.0944
6.2840	2.4572	0.0199	0.1259	0.0676
6.5982	2.5801	0.0329	0.0743	0.0376
6.9124	2.7030	0.0838	0.0638	0.0146
7.2266	2.8258	0.0937	0.0422	0.0076
7.5408	2.9487	0.1234	0.0516	0.0192
8.1692	3.1944	0.1239	0.0607	0.0325
8.7976	3.4401	0.1070	0.0896	0.0305
9.4260	3.6859	0.1275	0.0991	0.0169
10.0544	3.9316	0.0665	0.0664	0.0106

HMOT.DAT

SWATH1 MODEL IN REGULAR HEAD SEAS
NON-DIMENSIONAL MOTION RESPONSES, SINKAGE and TRIM
(V=0.5m/s ; Fn=0.13)

EncFR (r/s)	N-D FR	SURGE	HEAVE	PITCH	SINKAGE (cm)	BOW-TRIM (deg)
LOW WAVES :						
2.0663	0.8080	1.4695	1.2150	2.6143	0.1200	0.1310
2.8361	1.1090	0.7552	1.7110	1.6832	0.1450	0.1990
3.6442	1.4250	0.4729	3.0650	1.1581	-0.0560	0.1940
4.0636	1.5890	0.7225	1.0410	0.4606	-0.0320	0.2820
4.4933	1.7570	0.5978	0.2910	0.3707	0.1290	0.2010
5.3832	2.1050	0.4307	0.1240	0.0712	0.0400	0.2430
6.3141	2.4690	0.3769	0.1620	0.0873	0.1370	0.2370
8.2960	3.2440	0.1504	0.1740	0.0301	0.0890	0.1930
10.4365	4.0810	0.0994	0.0120	0.0026	0.0720	0.1430
12.7407	4.9820	0.0671	0.0240	0.0041	0.0720	0.1870
15.2034	5.9450	0.0268	0.0240	0.0015	0.1690	0.2250
HIGH WAVES :						
2.8361	1.1090	0.8092	1.4095	2.3465	0.1690	0.1300
4.4933	1.7570	0.7079	0.1596	0.1061	0.0640	0.1800
6.3141	2.4690	0.2769	0.1542	0.0750	-0.0560	0.2930
8.2449	3.2240	0.0397	0.0600	0.0303	0.1290	0.2800
10.4365	4.0810	0.0583	0.0118	0.0021	0.1610	0.2550
12.7407	4.9820	0.0488	0.0262	0.0033	-0.0240	0.2060
15.2034	5.9450	0.0556	0.0229	0.0009	0.0880	0.2250

SWATH1 MODEL IN REGULAR HEAD SEAS
NON-DIMENSIONAL MOTION RESPONSES, SINKAGE and TRIM
(V=1.0m/s ; Fn=0.26)

EncFR (r/s)	N-D FR	SURGE	HEAVE	PITCH	SINKAGE (cm)	BOW-TRIM (deg)
LOW WAVES :						
2.0177	0.7890	1.9558	1.3590	2.2008	0.5643	1.3030
3.1583	1.2350	1.3163	1.7220	1.2250	0.4758	1.2494
4.1480	1.6220	0.9709	2.2630	1.1685	0.4919	1.2967
2.1149	0.8270	0.4996	0.4820	0.2667	0.6855	1.3155
5.2195	2.0410	0.4112	0.1730	0.1013	0.7419	1.3713
6.3703	2.4910	0.2341	0.0810	0.0339	0.5968	1.3757
7.6030	2.9730	0.1618	0.1000	0.0346	0.5726	1.2786
10.3086	4.0310	0.1528	0.0340	0.0152	0.5340	1.3098
13.3340	5.2140	0.0833	0.0220	0.0016	0.5646	1.3347
16.6841	6.5240	0.0855	0.0130	0.0017	0.5323	1.3285
20.3564	7.9600	0.0455	0.0120	0.0005	0.5484	1.4720
HIGH WAVES :						
3.1583	1.2350	1.1507	1.5506	1.0415	0.5646	1.2472
5.2195	2.0410	0.3585	0.1383	0.0757	0.6371	1.1792
7.6030	2.9730	0.1403	0.0934	0.0355	0.5807	1.3784
10.3086	4.0310	0.0309	0.0334	0.0145	0.2994	1.6839
13.3340	5.2140	0.0543	0.0211	0.0015	0.2097	2.0097
16.6841	6.5240	0.0512	0.0124	0.0019	0.3952	2.0291

SWATH1 MODEL IN REGULAR HEAD SEAS
NON-DIMENSIONAL MOTION RESPONSES, SINKAGE and TRIM
(V=1.5m/s ; Fn=0.39)

EncFR (r/s)	N-D FR	SURGE	HEAVE	PITCH	SINKAGE (cm)	BOW-TRIM (deg)
LOW WAVES :						
2.4269	0.9490	1.4339	1.3270	2.5232	0.4839	3.0858
3.4805	1.3610	1.6487	2.1820	1.6317	0.4516	2.6217
4.6518	1.8190	1.1398	0.5760	0.3574	0.5242	2.9546
5.2809	2.0650	0.4377	0.1890	0.1056	0.6694	2.8796
5.9433	2.3240	0.3574	0.0940	0.0327	0.6049	2.9763
7.3549	2.8760	0.2068	0.0850	0.0283	0.6210	2.9431
8.8893	3.4760	0.1174	0.0810	0.0226	0.5404	3.0352
12.3187	4.8170	0.0371	0.0210	0.0084	0.4126	2.9917
16.2315	6.3470	0.0781	0.0120	0.0015	0.4516	3.0601
20.6275	8.0660	0.0729	0.0090	0.0009	0.4033	3.1036
25.5069	9.9740	0.0284	0.0130	0.0005	0.4758	3.1233
HIGH WAVES :						
3.4805	1.3610	0.6919	1.9988	1.5647	0.6452	3.1001
5.9433	2.3240	0.3154	0.0865	0.0322	0.6452	2.7428
8.8893	3.4760	0.1274	0.0841	0.0213	0.7259	2.8423
12.3187	4.8170	0.0401	0.0236	0.0078	0.6473	2.9544
16.2315	6.3470	0.0526	0.0108	0.0011	0.6371	3.1907
20.6275	8.0660	0.0487	0.0135	0.0012	0.5484	3.1858

SWATH1 MODEL IN REGULAR HEAD SEAS
NON-DIMENSIONAL MOTION RESPONSES, SINKAGE and TRIM
(V=2.0m/s ; Fn=0.52)

EncFR (r/s)	N-D FR	SURGE	HEAVE	PITCH	SINKAGE (cm)	BOW-TRIM (deg)
LOW WAVES :						
2.6085	1.0200	0.6840	0.7760	2.0950	2.1776	4.5018
3.7849	1.4800	0.5840	1.7540	1.2230	2.2017	4.0336
5.1403	2.0100	0.4110	0.4300	0.2620	2.3147	4.2277
5.8819	2.3000	0.3250	0.1510	0.0890	2.3066	4.2638
6.6491	2.6000	0.2580	0.1010	0.0400	2.2540	4.2653
8.3369	3.2600	0.1950	0.0900	0.0140	2.2582	4.3074
10.1782	3.9800	0.1070	0.0650	0.0120	2.2340	4.2343
14.3211	5.6000	0.0370	0.0230	0.0030	2.2169	4.2839
19.1289	7.4800	0.0840	0.0130	0.0000	2.2340	4.3770
24.5505	9.6000	0.0920	0.0150	0.0000	2.2985	4.6200
30.6370	11.9800	0.0340	0.0120	0.0000	2.4034	4.4270
HIGH WAVES :						
3.7849	1.4800	0.3860	1.5900	0.9570	1.8227	3.9656
6.6491	2.6000	0.2680	0.0870	0.0380	2.4034	3.9240
10.1782	3.9800	0.1110	0.0670	0.0110	2.4839	4.2963
14.3211	5.6000	0.0210	0.0160	0.0030	2.6943	3.9861
19.1289	7.4800	0.0440	0.0090	0.0000	2.5405	3.9116
24.5505	9.6000	0.0360	0.0100	0.0000	2.4558	4.1001

APPENDIX 1e

SWATH2 MODEL IN REGULAR HEAD SEAS
NON-DIMENSIONAL MOTION RESPONSES, SINKAGE and TRIM
(V=0.615m/s ; Fn=0.13)

EncFR (r/s)	N-D FR	SURGE	HEAVE	PITCH	SINKAGE (cm)	BOW-TRIM (deg)
2.7723	1.3321	1.2868	1.2839	0.6397	0.1613	0.1996
3.4069	1.6371	1.1222	1.3942	0.8686	0.1774	0.1833
4.0908	1.9657	0.7139	2.1459	0.8269	0.1694	0.1426
4.8240	2.3180	0.9279	0.3199	0.1058	0.3079	0.1670
5.6065	2.6940	0.4599	0.4442	0.1758	0.3242	0.2119
6.4383	3.0937	0.4127	0.2536	0.0740	0.3468	0.1992
7.3194	3.5171	0.3899	0.2625	0.0764	0.2097	0.1626
8.2498	3.9641	0.4223	0.3651	0.0646	0.1694	0.2073
9.2294	4.4349	0.2513	0.2354	0.0467	0.1694	0.2683
10.2584	4.9293	0.1433	0.1918	0.0323	0.2520	0.3341
11.3367	5.4475	0.0777	0.1285	0.0202	0.1707	0.1996
13.6411	6.5548	0.0627	0.0471	0.0076	0.0894	0.1020
16.1428	7.7569	0.1187	0.0295	0.0010	0.0976	0.2530
18.8416	9.0537	0.1324	0.0193	0.0030	0.1702	0.3298
21.7376	10.4453	0.0846	0.0438	0.0021	0.0810	0.2728
28.1213	13.5127	0.0388	0.0985	0.0007	0.1216	0.2117
35.2937	16.9591	0.0601	0.0377	0.0003	0.1290	0.2493

SWATH2 MODEL IN REGULAR HEAD SEAS
NON-DIMENSIONAL MOTION RESPONSES, SINKAGE and TRIM
(V=1.225m/s ; Fn=0.26)

EncFR (r/s)	N-D FR	SURGE	HEAVE	PITCH	SINKAGE (cm)	BOW-TRIM (deg)
2.7723	1.3321	1.1429	0.9933	0.8935	0.5726	1.9142
3.4069	1.6371	1.2181	1.0135	0.8259	0.4758	1.8735
4.0908	1.9657	0.9726	0.7482	0.5144	0.5000	1.6090
4.8240	2.3180	0.3610	0.0946	0.0704	0.5268	2.0323
5.6065	2.6940	0.3188	0.1561	0.0343	0.5592	2.0567
6.4383	3.0937	0.3035	0.1998	0.0489	0.5916	2.0770
7.3194	3.5171	0.2598	0.2188	0.0588	0.5565	2.0112
8.2498	3.9641	0.2271	0.1918	0.0514	0.5807	1.7107
9.2294	4.4349	0.1662	0.1409	0.0416	0.6423	2.1136
10.2584	4.9293	0.1332	0.1098	0.0337	0.6179	1.9142
11.3367	5.4475	0.0593	0.0659	0.0212	0.4959	2.0363
13.6411	6.5548	0.0482	0.0281	0.0058	0.3252	2.4919
16.1428	7.7569	0.0822	0.0246	0.0021	0.3821	2.0315
18.8416	9.0537	0.0783	0.0188	0.0028	0.3485	2.5876
21.7376	10.4453	0.0574	0.0459	0.0016	0.4052	2.8191
28.1213	13.5127	0.0307	0.0234	0.0006	0.3226	2.7244
35.2937	16.9591	0.0347	0.0327	0.0002	-0.5081	1.6836

SWATH2 MODEL IN REGULAR HEAD SEAS
NON-DIMENSIONAL MOTION RESPONSES, SINKAGE and TRIM
(V=1.837m/s ; Fn=0.39)

EncFR (r/s)	N-D FR	SURGE	HEAVE	PITCH	SINKAGE (cm)	BOW-TRIM (deg)
2.7723	1.3321	0.7092	0.8170	0.9905	-0.0807	2.5448
3.4069	1.6371	0.7867	0.7419	0.5329	-0.0887	2.4757
4.0908	1.9657	0.4665	0.8325	0.5539	-0.0968	2.4025
4.8240	2.3180	0.3583	0.2551	0.1964	-0.0972	2.4269
5.6065	2.6940	0.2896	0.1339	0.0483	-0.0972	2.5570
6.4383	3.0937	0.3261	0.1787	0.0316	-0.0729	2.4838
7.3194	3.5171	0.2498	0.1856	0.0397	0.0807	2.5753
8.2498	3.9641	0.2048	0.1728	0.0364	0.0000	2.6402
9.2294	4.4349	0.1759	0.1456	0.0286	0.0813	2.6180
10.2584	4.9293	0.1343	0.1148	0.0272	-0.0976	2.5245
11.3367	5.4475	0.1051	0.0759	0.0167	-0.0569	2.6790
13.6411	6.5548	0.0515	0.0409	0.0065	-0.1463	2.5327
16.1428	7.7569	0.0743	0.0352	0.0022	-0.2358	2.5286
18.8416	9.0537	0.0696	0.0193	0.0020	-0.1135	2.8070
21.7376	10.4453	0.0499	0.0222	0.0012	-0.1459	2.9694
28.1213	13.5127	0.0631	0.0173	0.0004	-0.3145	2.8671
35.2937	16.9591	0.0781	0.0163	0.0002	-0.2258	2.8956

SWATH2 MODEL IN REGULAR HEAD SEAS
NON-DIMENSIONAL MOTION RESPONSES, SINKAGE and TRIM
(V=2.450m/s ; Fn=0.52)

EncFR (r/s)	N-D FR	SURGE	HEAVE	PITCH	SINKAGE (cm)	BOW-TRIM (deg)
2.7723	1.3321	0.2929	0.4862	0.7499	4.4358	4.6346
3.4069	1.6371	0.5323	0.5886	0.6569	4.3954	4.5820
4.0908	1.9657	0.3505	0.5499	0.4910	3.5889	4.0473
4.8240	2.3180	0.2515	0.2169	0.1826	3.7278	4.1364
5.6065	2.6940	0.2404	0.0996	0.0704	3.9709	4.1364
6.4383	3.0937	0.2193	0.0895	0.0407	3.4600	4.0619
7.3194	3.5171	0.1874	0.1126	0.0257	4.2664	4.2196
8.2498	3.9641	0.1443	0.1119	0.0177	4.6132	4.5752
9.2294	4.4349	0.1399	0.1003	0.0162	4.8943	4.7156
10.2584	4.9293	0.1159	0.0608	0.0121	5.1219	5.0756
11.3367	5.4475	0.0314	0.0550	0.0091	5.6666	5.3104
13.6411	6.5548	0.0478	0.0221	0.0025	4.1219	4.3785
16.1428	7.7569	0.0741	0.0200	0.0008	4.3924	4.5018
18.8416	9.0537	0.0694	0.0205	0.0011	4.2141	4.4249
21.7376	10.4453	0.0481	0.0278	0.0007	3.7522	3.9429
28.1213	13.5127	0.0453	0.0162	0.0004	3.9679	4.2433
35.2937	16.9591	0.0434	0.0210	0.0002	4.1535	4.6943

APPENDIX II

SWATH1 MODEL IN REGULAR BEAM SEAS

AVERAGE BENDING MOMENT AT THE MID-POINT OF THE CROSS STRUCTURE

FR(r/s)	WL/B	BM(Ncms)	BM/WA1(N)	BM/WA2(N)	BM/WA1*D	BM/WA2*D
LOW WAVE :						
1.8850	24.0942	138.2878	70.5136	70.2271	0.3423	0.3409
2.1991	17.7018	126.3615	73.5558	85.4112	0.3570	0.4146
2.5133	13.5530	159.6345	89.0743	84.3645	0.4324	0.4095
2.8274	10.7085	137.7633	57.2249	59.7115	0.2778	0.2898
3.1416	8.6739	218.7411	91.5829	86.3617	0.4446	0.4192
3.4558	7.1685	296.5432	111.6671	117.4103	0.5420	0.5699
3.7699	6.0235	380.7453	128.3721	131.9535	0.6231	0.6405
4.0841	5.1325	599.9332	194.4710	184.1642	0.9440	0.8940
4.3982	4.4255	758.1401	258.1034	253.3129	1.2529	1.2296
4.7124	3.8551	884.1326	310.6470	303.8883	1.5079	1.4751
5.0266	3.3882	1077.0304	449.0527	376.1303	2.1798	1.8258
5.3407	3.0013	1182.8026	474.6399	428.4973	2.3040	2.0800
5.6549	2.6771	1490.3882	543.6793	520.6505	2.6391	2.5273
5.9690	2.4027	1539.1710	563.0153	534.9824	2.7330	2.5969
6.2832	2.1685	1379.2937	625.6861	542.2711	3.0372	2.6323
6.5974	1.9669	1218.3287	515.5529	465.6419	2.5026	2.2603
6.9115	1.7921	1176.4122	453.1111	487.0869	2.1995	2.3644
7.2257	1.6397	1099.6202	410.7275	469.9031	1.9937	2.2810
7.5398	1.5059	626.0582	401.8861	358.9474	1.9508	1.7424
8.1682	1.2831	765.6085	317.7326	367.7628	1.5423	1.7852
8.7965	1.1064	524.2192	304.6989	258.6310	1.4790	1.2554
9.4248	0.9638	159.2169	71.5405	92.2355	0.3473	0.4477
10.0531	0.8471	594.5334	326.6219	343.4426	1.5855	1.6671
HIGH WAVE :						
1.8850	24.0942	448.9229	106.2590	129.4640	0.5158	0.6284
2.1991	17.7018	369.3922	116.6876	128.8113	0.5664	0.6253
2.5133	13.5530	480.8265	161.7338	142.5960	0.7851	0.6922
2.8274	10.7085	439.0264	99.0460	103.2323	0.4808	0.5011
3.1416	8.6739	316.9770	84.0275	83.4710	0.4079	0.4052
3.4558	7.1685	555.8509	131.3261	117.1149	0.6375	0.5685
3.7699	6.0235	744.3881	150.1857	151.1018	0.7290	0.7335
4.0841	5.1325	1200.2063	211.2351	219.0697	1.0254	1.0634
4.3982	4.4255	1379.6434	275.0924	268.7268	1.3353	1.3044
4.7124	3.8551	1470.6633	290.0745	274.9854	1.4081	1.3348
5.0266	3.3882	1705.7009	393.6490	362.4716	1.9108	1.7595
5.3407	3.0013	1945.9832	460.8386	412.7874	2.2370	2.0037
5.6549	2.6771	1996.5336	437.1365	398.8879	2.1219	1.9363
5.9690	2.4027	1956.8411	415.8669	402.0879	2.0187	1.9518
6.2832	2.1685	2244.7310	481.2991	536.9784	2.3363	2.6066
6.5974	1.9669	2523.6858	439.9885	546.6132	2.1358	2.6533
6.9115	1.7921	1983.1118	365.0627	485.4738	1.7721	2.3566
7.2257	1.6397	1757.6694	334.5679	343.4457	1.6240	1.6671
7.5398	1.5059	1584.6033	349.9913	441.4674	1.6989	2.1429
8.1682	1.2831	1394.4443	332.2162	426.3965	1.6126	2.0698
8.7965	1.1064	874.9257	369.8614	305.5175	1.7954	1.4830
9.4248	0.9638	225.1121	68.9238	87.9739	0.3346	0.4270
10.0531	0.8471	497.4144	136.6335	145.7753	0.6632	0.7076

Note :

WL : wave length in cm

B : characteristic breadth of the model (=72cms)

BM : Bending moment in Ncm

WA : wave amplitude in cm

D : SWATH1 model displacement x g

g : acceleration due to gravity ($9.81 ms^{-2}$)

SWATH1 MODEL IN REGULAR BEAM SEAS
BENDING MOMENT AT THE MID-POINT OF THE CROSS-STRUCTURE
(HOGGING CONDITION)

FR(r/s)	WL/B	BM(Ncms)	BM/WA1(N)	BM/WA2(N)	BM/WA1*D	BM/WA2*D
LOW WAVE :						
1.8850	24.0942	147.4186	75.1695	74.8641	0.3649	0.3634
2.1991	17.7018	115.6543	67.3231	78.1739	0.3268	0.3795
2.5133	13.5530	162.8069	90.8445	86.0411	0.4410	0.4177
2.8274	10.7085	131.7281	54.7180	57.0956	0.2656	0.2771
3.1416	8.6739	207.1554	86.7321	81.7875	0.4210	0.3970
3.4558	7.1685	302.9893	114.0945	119.9625	0.5538	0.5823
3.7699	6.0235	389.7445	131.4063	135.0723	0.6379	0.6557
4.0841	5.1325	480.1045	155.6280	147.3798	0.7554	0.7154
4.3982	4.4255	681.8344	232.1257	227.8173	1.1268	1.1059
4.7124	3.8551	762.4547	267.8945	262.0659	1.3004	1.2721
5.0266	3.3882	1012.9343	422.3287	353.7461	2.0500	1.7171
5.3407	3.0013	1126.1395	451.9019	407.9698	2.1936	1.9803
5.6549	2.6771	1465.8894	534.7424	512.0922	2.5957	2.4858
5.9690	2.4027	1528.9181	559.2648	531.4187	2.7147	2.5796
6.2832	2.1685	1322.3083	599.8360	519.8672	2.9117	2.5235
6.5974	1.9669	1174.0009	496.7949	448.6999	2.4115	2.1780
6.9115	1.7921	1159.5074	446.6000	480.0876	2.1679	2.3304
7.2257	1.6397	1072.8223	400.7180	458.4514	1.9451	2.2254
7.5398	1.5059	610.6318	391.9834	350.1028	1.9027	1.6994
8.1682	1.2831	718.9492	298.3687	345.3498	1.4483	1.6764
8.7965	1.1064	477.2890	277.4210	235.4773	1.3466	1.1430
9.4248	0.9638	150.2855	67.5273	87.0615	0.3278	0.4226
10.0531	0.8471	555.0117	304.9096	320.6122	1.4801	1.5563
HIGH WAVE :						
1.8850	24.0942	435.2874	103.0315	125.5317	0.5001	0.6093
2.1991	17.7018	359.5841	113.5900	125.3918	0.5514	0.6087
2.5133	13.5530	400.4118	134.6850	118.7478	0.6538	0.5764
2.8274	10.7085	442.0242	99.7223	103.9372	0.4841	0.5045
3.1416	8.6739	239.5671	63.5069	63.0863	0.3083	0.3062
3.4558	7.1685	429.9085	101.5708	90.5795	0.4930	0.4397
3.7699	6.0235	1034.3027	208.6781	209.9510	1.0130	1.0191
4.0841	5.1325	1062.1299	186.9338	193.8671	0.9074	0.9411
4.3982	4.4255	1129.4949	225.2143	220.0029	1.0932	1.0679
4.7124	3.8551	1237.1143	244.0092	231.3163	1.1845	1.1228
5.0266	3.3882	1606.1213	370.6676	341.3104	1.7993	1.6568
5.3407	3.0013	1842.7234	436.3851	390.8837	2.1183	1.8974
5.6549	2.6771	1873.0935	410.1096	374.2258	1.9907	1.8165
5.9690	2.4027	1850.9963	393.3729	380.3391	1.9095	1.8462
6.2832	2.1685	2292.5168	491.5450	548.4096	2.3860	2.6621
6.5974	1.9669	2352.2847	410.1058	509.4889	1.9907	2.4731
6.9115	1.7921	1837.0726	338.1790	449.7228	1.6416	2.1830
7.2257	1.6397	1630.0682	310.2794	318.5127	1.5061	1.5461
7.5398	1.5059	1491.5259	329.4333	415.5363	1.5991	2.0171
8.1682	1.2831	1266.1864	301.6597	387.1775	1.4643	1.8794
8.7965	1.1064	758.9214	320.8224	265.0096	1.5573	1.2864
9.4248	0.9638	224.3130	68.6792	87.6617	0.3334	0.4255
10.0531	0.8471	459.5934	126.2446	134.6912	0.6128	0.6538

SWATH1 MODEL IN REGULAR BEAM SEAS
BENDING MOMENT AT THE MID-POINT OF THE CROSS-STRUCTURE
(SAGGING CONDITION)

FR(r/s)	WL/B	BM(Ncms)	BM/WA1(N)	BM/WA2(N)	BM/WA1*D	BM/WA2*D
LOW WAVE :						
1.8850	24.0942	129.1569	65.8577	65.5902	0.3197	0.3184
2.1991	17.7018	137.0687	79.7885	92.6484	0.3873	0.4497
2.5133	13.5530	156.4621	87.3041	82.6879	0.4238	0.4014
2.8274	10.7085	143.7985	59.7319	62.3273	0.2899	0.3025
3.1416	8.6739	230.3269	96.4336	90.9359	0.4681	0.4414
3.4558	7.1685	290.0970	109.2397	114.8581	0.5303	0.5575
3.7699	6.0235	371.7462	125.3380	128.8347	0.6084	0.6254
4.0841	5.1325	719.7618	233.3139	220.9485	1.1325	1.0725
4.3982	4.4255	834.4457	284.0811	278.8084	1.3790	1.3534
4.7124	3.8551	1005.8104	353.3995	345.7106	1.7154	1.6781
5.0266	3.3882	1141.1263	475.7766	398.5145	2.3095	1.9344
5.3407	3.0013	1239.4659	497.3780	449.0249	2.4143	2.1796
5.6549	2.6771	1514.8870	552.6163	529.2089	2.6825	2.5689
5.9690	2.4027	1549.4237	566.7656	538.5460	2.7512	2.6142
6.2832	2.1685	1436.2791	651.5363	564.6750	3.1626	2.7410
6.5974	1.9669	1262.6565	534.3108	482.5838	2.5936	2.3425
6.9115	1.7921	1193.3169	459.6221	494.0862	2.2311	2.3984
7.2257	1.6397	1126.4181	420.7370	481.3547	2.0423	2.3366
7.5398	1.5059	641.4847	411.7888	367.7921	1.9989	1.7853
8.1682	1.2831	812.2678	337.0965	390.1757	1.6363	1.8940
8.7965	1.1064	571.1495	331.9768	281.7847	1.6115	1.3678
9.4248	0.9638	168.1483	75.5536	97.4095	0.3667	0.4728
10.0531	0.8471	634.0551	348.3340	366.2729	1.6909	1.7779
HIGH WAVE :						
1.8850	24.0942	462.5583	109.4864	133.3963	0.5315	0.6475
2.1991	17.7018	379.1982	119.7853	132.2308	0.5815	0.6419
2.5133	13.5530	561.2412	188.7826	166.4441	0.9164	0.8079
2.8274	10.7085	436.0287	98.3697	102.5274	0.4775	0.4977
3.1416	8.6739	394.3868	104.5481	103.8557	0.5075	0.5041
3.4558	7.1685	681.7933	161.0814	143.6503	0.7819	0.6973
3.7699	6.0235	454.4734	91.6933	92.2526	0.4451	0.4478
4.0841	5.1325	1338.2828	235.5365	244.2724	1.1433	1.1857
4.3982	4.4255	1629.7921	324.9705	317.4507	1.5775	1.5409
4.7124	3.8551	1704.2124	336.1399	318.6546	1.6317	1.5468
5.0266	3.3882	1805.2804	416.6304	383.6329	2.0224	1.8622
5.3407	3.0013	2049.2429	485.2921	434.6912	2.3557	2.1100
5.6549	2.6771	2119.9736	464.1635	423.5500	2.2531	2.0560
5.9690	2.4027	2062.6858	438.3610	423.8366	2.1279	2.0574
6.2832	2.1685	2196.9446	471.0531	525.5471	2.2866	2.5511
6.5974	1.9669	2695.0872	469.8712	583.7375	2.2808	2.8335
6.9115	1.7921	2129.1509	391.9464	521.2247	1.9026	2.5301
7.2257	1.6397	1885.2704	358.8565	368.3788	1.7419	1.7882
7.5398	1.5059	1677.6807	370.5493	467.3986	1.7987	2.2688
8.1682	1.2831	1522.7024	362.7728	465.6155	1.7609	2.2602
8.7965	1.1064	990.9299	418.9004	346.0253	2.0334	1.6797
9.4248	0.9638	225.9112	69.1685	88.2862	0.3358	0.4286
10.0531	0.8471	535.2353	147.0225	156.8593	0.7137	0.7614

SWATH1 MODEL IN REGULAR QUARTERING SEAS
AVERAGE BENDING MOMENT AT THE MID-POINT OF THE CROSS-STRUCTURE
****

FR(r/s)	WL/B	BM(Ncms)	BM/WA1(N)	BM/WA2(N)	BM/WA1*D	BM/WA2*D
LOW WAVE :						
1.8850	24.0942	52.6385	18.8973	25.5651	0.0917	0.1241
2.1991	17.7018	51.6673	24.3026	32.6080	0.1180	0.1583
2.5133	13.5530	43.7036	20.8460	24.8175	0.1012	0.1205
2.8274	10.7085	74.7816	32.2057	31.0040	0.1563	0.1505
3.1416	8.6739	93.0400	38.8395	42.2909	0.1885	0.2053
3.4558	7.1685	108.1906	39.6666	39.9448	0.1925	0.1939
3.7699	6.0235	137.1320	49.3725	46.1180	0.2397	0.2239
4.0841	5.1325	256.9769	83.2449	78.4423	0.4041	0.3808
4.3982	4.4255	353.9016	119.2592	119.6624	0.5789	0.5809
4.7124	3.8551	374.4909	146.6866	141.7989	0.7120	0.6883
5.0266	3.3882	489.6740	217.9234	191.3163	1.0578	0.9287
5.3407	3.0013	627.0002	218.5431	221.9470	1.0608	1.0774
5.6549	2.6771	761.8014	277.1699	266.9709	1.3454	1.2959
5.9690	2.4027	657.4957	211.9586	223.1825	1.0289	1.0834
6.2832	2.1685	620.5904	333.8302	248.7336	1.6205	1.2074
6.5974	1.9669	504.0476	219.6764	216.9813	1.0663	1.0533
6.9115	1.7921	361.2827	141.6795	148.8598	0.6877	0.7226
7.2257	1.6397	330.3988	136.1346	133.3867	0.6608	0.6475
7.5398	1.5059	242.9917	78.4984	109.9013	0.3810	0.5335
8.1682	1.2831	276.9834	103.2942	121.2181	0.5014	0.5884
8.7965	1.1064	566.3980	178.4774	233.6144	0.8664	1.1340
9.4248	0.9638	880.2866	412.5054	394.3053	2.0024	1.9140
10.0531	0.8471	606.9938	294.6572	303.4211	1.4303	1.4728
HIGH WAVE :						
1.8850	24.0942	145.4843	30.6154	40.7120	0.1486	0.1976
2.1991	17.7018	175.0085	46.4706	65.7432	0.2256	0.3191
2.5133	13.5530	128.7798	37.8097	41.7777	0.1835	0.2028
2.8274	10.7085	184.1376	42.4623	43.3826	0.2061	0.2106
3.1416	8.6739	230.7547	59.0770	60.4466	0.2868	0.2934
3.4558	7.1685	180.8356	43.9028	37.7212	0.2131	0.1831
3.7699	6.0235	250.5670	51.0476	53.9260	0.2478	0.2618
4.0841	5.1325	418.9714	75.7565	74.0494	0.3677	0.3594
4.3982	4.4255	605.4399	129.9506	126.6346	0.6308	0.6147
4.7124	3.8551	746.8451	169.7375	167.2478	0.8239	0.8118
5.0266	3.3882	946.5219	225.6848	218.4701	1.0955	1.0605
5.3407	3.0013	1060.9280	220.1552	223.2358	1.0687	1.0836
5.6549	2.6771	1205.2468	270.9029	254.1375	1.3150	1.2336
5.9690	2.4027	1020.7207	202.3834	202.7855	0.9824	0.9843
6.2832	2.1685	1085.5962	247.6269	214.1427	1.2020	1.0395
6.5974	1.9669	868.8265	184.8371	193.9345	0.8972	0.9414
6.9115	1.7921	660.4092	136.2230	135.7889	0.6612	0.6591
7.2257	1.6397	452.3803	98.2154	95.6609	0.4768	0.4644
7.5398	1.5059	340.1107	57.5435	79.3724	0.2793	0.3853
8.1682	1.2831	477.4370	94.8425	116.4622	0.4604	0.5653
8.7965	1.1064	856.2011	195.8822	240.8442	0.9508	1.1691
9.4248	0.9638	1034.3174	408.7403	355.0695	1.9841	1.7236
10.0531	0.8471	648.9492	272.4960	242.9156	1.3227	1.1791

SWATH1 MODEL IN REGULAR QUARTERING SEAS
BENDING MOMENT AT THE MID-POINT OF THE CROSS-STRUCTURE
(HOGGING CONDITION)

FR(R/S)	WL/B	BM(Ncms)	BM/WA1(N)	BM/WA2(N)	BM/WA1*D	BM/WA2*D
LOW WAVE :						
1.8850	24.0942	41.2851	14.8214	20.0510	0.0719	0.0973
2.1991	17.7018	51.6673	24.3026	32.6080	0.1180	0.1583
2.5133	13.5530	43.7036	20.8460	24.8175	0.1012	0.1205
2.8274	10.7085	58.3548	25.1312	24.1935	0.1220	0.1174
3.1416	8.6739	84.0850	35.1012	38.2204	0.1704	0.1855
3.4558	7.1685	105.2693	38.5955	38.8663	0.1873	0.1887
3.7699	6.0235	121.6788	43.8088	40.9211	0.2127	0.1986
4.0841	5.1325	246.0286	79.6983	75.1003	0.3869	0.3645
4.3982	4.4255	344.5975	116.1238	116.5165	0.5637	0.5656
4.7124	3.8551	367.9596	144.1283	139.3259	0.6996	0.6763
5.0266	3.3882	494.4953	220.0691	193.2000	1.0682	0.9378
5.3407	3.0013	617.2781	215.1544	218.5055	1.0444	1.0607
5.6549	2.6771	755.9428	275.0383	264.9178	1.3351	1.2859
5.9690	2.4027	634.8015	204.6427	215.4791	0.9934	1.0460
6.2832	2.1685	621.0562	334.0808	248.9203	1.6217	1.2083
6.5974	1.9669	501.9145	218.7467	216.0630	1.0618	1.0488
6.9115	1.7921	312.8666	122.6928	128.9108	0.5956	0.6258
7.2257	1.6397	341.8508	140.8532	138.0100	0.6837	0.6699
7.5398	1.5059	245.5082	79.3113	111.0394	0.3850	0.5390
8.1682	1.2831	265.6915	99.0832	116.2764	0.4810	0.5644
8.7965	1.1064	548.7023	172.9013	226.3157	0.8393	1.0986
9.4248	0.9638	915.7728	429.1344	410.2006	2.0831	1.9912
10.0531	0.8471	667.7599	324.1553	333.7965	1.5735	1.6203
HIGH WAVE :						
1.8850	24.0942	128.0953	26.9561	35.8459	0.1308	0.1740
2.1991	17.7018	165.1802	43.8609	62.0512	0.2129	0.3012
2.5133	13.5530	135.0955	39.6640	43.8266	0.1925	0.2127
2.8274	10.7085	176.6308	40.7312	41.6140	0.1977	0.2020
3.1416	8.6739	199.4854	51.0715	52.2555	0.2479	0.2537
3.4558	7.1685	193.7178	47.0303	40.4084	0.2283	0.1961
3.7699	6.0235	270.3717	55.0824	58.1883	0.2674	0.2825
4.0841	5.1325	365.1962	66.0331	64.5451	0.3205	0.3133
4.3982	4.4255	498.4070	106.9772	104.2474	0.5193	0.5060
4.7124	3.8551	694.0939	157.7486	155.4348	0.7657	0.7545
5.0266	3.3882	860.2789	205.1213	198.5641	0.9957	0.9639
5.3407	3.0013	1068.9451	221.8189	224.9227	1.0767	1.0918
5.6549	2.6771	1188.0205	267.0309	250.5051	1.2962	1.2160
5.9690	2.4027	949.7285	188.3074	188.6815	0.9141	0.9159
6.2832	2.1685	947.9119	216.2208	186.9833	1.0496	0.9076
6.5974	1.9669	878.7120	186.9401	196.1411	0.9074	0.9521
6.9115	1.7921	667.5858	137.7033	137.2645	0.6684	0.6663
7.2257	1.6397	481.1276	104.4567	101.7398	0.5070	0.4939
7.5398	1.5059	336.0778	56.8611	78.4312	0.2760	0.3807
8.1682	1.2831	448.1924	89.0331	109.3286	0.4322	0.5307
8.7965	1.1064	882.6815	201.9404	248.2930	0.9802	1.2052
9.4248	0.9638	1175.0269	464.3457	403.3734	2.2540	1.9580
10.0531	0.8471	689.4546	289.5043	258.0777	1.4053	1.2527

SWATH1 MODEL IN REGULAR QUARTERING SEAS
BENDING MOMENT AT THE MID-POINT OF THE CROSS-STRUCTURE
(SAGGING CONDITION)

FR(r/s)	WL/B	BM(Ncms)	BM/WA1(N)	BM/WA2(N)	BM/WA1*D	BM/WA2*D
LOW WAVE :						
1.8850	24.0942	63.9919	22.9732	31.0791	0.1115	0.1509
2.1991	17.7018	51.6673	24.3026	32.6080	0.1180	0.1583
2.5133	13.5530	43.7036	20.8460	24.8175	0.1012	0.1205
2.8274	10.7085	91.2085	39.2801	37.8145	0.1907	0.1836
3.1416	8.6739	101.9951	42.5778	46.3614	0.2067	0.2250
3.4558	7.1685	111.1118	40.7376	41.0234	0.1977	0.1991
3.7699	6.0235	152.5852	54.9362	51.3150	0.2667	0.2491
4.0841	5.1325	247.9251	86.7914	81.7842	0.4213	0.3970
4.3982	4.4255	363.2057	122.3945	122.8084	0.5941	0.5961
4.7124	3.8551	381.0222	149.2449	144.2719	0.7245	0.7003
5.0266	3.3882	484.8526	215.7778	189.4326	1.0474	0.9195
5.3407	3.0013	636.7224	221.9318	225.3884	1.0773	1.0941
5.6549	2.6771	767.6600	279.3014	269.0240	1.3558	1.3059
5.9690	2.4027	680.1899	219.2746	230.8859	1.0644	1.1208
6.2832	2.1685	620.1246	333.5797	248.5469	1.6192	1.2065
6.5974	1.9669	506.1807	220.6061	217.8996	1.0709	1.0577
6.9115	1.7921	409.6988	160.6662	168.8087	0.7799	0.8194
7.2257	1.6397	318.9468	131.4161	128.7634	0.6379	0.6250
7.5398	1.5059	240.4753	77.6854	108.7631	0.3771	0.5280
8.1682	1.2831	288.2753	107.5052	126.1599	0.5218	0.6124
8.7965	1.1064	584.0936	184.0535	240.9130	0.8934	1.1694
9.4248	0.9638	844.8005	395.8765	378.4101	1.9216	1.8369
10.0531	0.8471	546.2276	265.1590	273.0455	1.2871	1.3254
HIGH WAVE :						
1.8850	24.0942	162.8732	34.2747	45.5781	0.1664	0.2212
2.1991	17.7018	184.8367	49.0804	69.4353	0.2382	0.3370
2.5133	13.5530	122.4641	35.9554	39.7288	0.1745	0.1928
2.8274	10.7085	191.6444	44.1933	45.1512	0.2145	0.2192
3.1416	8.6739	262.0240	67.0825	68.6376	0.3256	0.3332
3.4558	7.1685	167.9533	40.7753	35.0341	0.1979	0.1701
3.7699	6.0235	230.7623	47.0128	49.6637	0.2282	0.2411
4.0841	5.1325	472.7465	85.4799	83.5536	0.4149	0.4056
4.3982	4.4255	712.4728	152.9240	149.0217	0.7423	0.7234
4.7124	3.8551	799.5962	181.7264	179.0609	0.8821	0.8692
5.0266	3.3882	1032.7648	246.2482	238.3762	1.1953	1.1571
5.3407	3.0013	1052.9109	218.4916	221.5488	1.0606	1.0754
5.6549	2.6771	1222.4731	274.7748	257.7698	1.3338	1.2512
5.9690	2.4027	1091.7129	216.4594	216.8894	1.0507	1.0528
6.2832	2.1685	1223.2804	279.0330	241.3020	1.3545	1.1713
6.5974	1.9669	858.9410	182.7340	191.7279	0.8870	0.9307
6.9115	1.7921	653.2327	134.7427	134.3133	0.6541	0.6520
7.2257	1.6397	423.6329	91.9741	89.5819	0.4465	0.4348
7.5398	1.5059	344.1437	58.2258	80.3136	0.2826	0.3899
8.1682	1.2831	506.6815	100.6519	123.5959	0.4886	0.6000
8.7965	1.1064	829.7206	189.8240	233.3954	0.9214	1.1329
9.4248	0.9638	893.6079	353.1349	306.7655	1.7142	1.4891
10.0531	0.8471	608.4437	255.4876	227.7536	1.2402	1.1055

APPENDIX 2

A FAMILY OF SPECTRAL FORMS

Appendix 2

A Family of Spectral Forms.

Many spectra may be written in the following form [2],

$$S(\omega) = A\ \omega^{-p}\ \exp\ (-B\omega^{-q})$$

and interest is in the moments of the spectrum, which are

$$m_n = \int_0^\infty S(\omega)\ \omega^n\ d\omega$$

or their ratios. Thus,

$$m_n = \int_0^\infty A\ \omega^{n-p}\ \exp\ (-B\omega^{-q})\ d\omega$$

This may be identified with the form of the gamma function $\Gamma(x)$ which is written as,

$$\Gamma(x) = \int_0^\infty y^{x-1}\ \exp\ (-y)\ dy$$

where $y = B\omega^{-q}$, and

$$x = \frac{p - n - 1}{q}$$

This gives,

$$m_n = \frac{A}{qB^{(p-n-1)/q}}\ \Gamma\left(\frac{p-n-1}{q}\right)$$

Consequently

Significant wave height,

$$m_n = \frac{A}{qB^{(p-n-1)/q}}\ \Gamma\left(\frac{p-n-1}{q}\right)$$

Energy average period,

$$T_{-1} = \frac{2\pi m_{-1}}{m_0} = 2\pi B^{-1/q} \frac{\Gamma(\frac{p}{q})}{\Gamma(\frac{p-1}{q})}$$

Average mean period,

$$T_1 \text{ or } T_{1/3} = \frac{2\pi m_0}{m} = 2\pi\ B^{1/q} \frac{\Gamma(\frac{p-1}{q})}{\Gamma(\frac{p-2}{q})}$$

(also described as significant period and denoted by $T_{1/3}$).

Average zero crossing period,

$$T_2 \text{ or } T_z = 2\pi(\frac{m_0}{m_2})^{1/2} = 2\pi\ B^{-1/q} \left[\frac{\Gamma(\frac{p-1}{q})}{\Gamma(\frac{p-3}{q})}\right]^{1/2}$$

Average crest to crest period,

$$T_4 \text{ or } T_c = 2\pi\ (\frac{m_2}{m_4})^{1/2} = 2\pi\ B^{-1/q} \left[\frac{\Gamma(\frac{p-3}{q})}{\Gamma(\frac{p-5}{q})}\right]^{1/2}$$

Skewness,

$$\tau = \frac{m_3}{m_2^{3/2}} = \frac{q^{1/2}}{A} B^{(p-1)/2q} \frac{\Gamma(\frac{p-4}{q})}{\Gamma^{3/2}(\frac{p-3}{q})}$$

Broadness,

$$\varepsilon = 1 - \left[\frac{m_2^2}{m_0 m_4}\right]^{1/2} = 1 - \left[\frac{\Gamma^2(\frac{p-3}{q})}{\Gamma(\frac{p-1}{q})\Gamma(\frac{p-5}{q})}\right]^{1/2}$$

Flatness,

$$\beta = \frac{m_4}{m_2^2} = \frac{q}{A} B^{(p-1)/q} \frac{\Gamma(\frac{p-5}{q})}{\Gamma^2(\frac{p-3}{q})}$$

In many cases a period and the significant wave height are considered known and the spectrum may be written as,

$$S(\omega) = \frac{q}{16} H_{1/3}^2 \left(\frac{2\pi}{T_z}\right)^{p-1} \left[\frac{\Gamma\left(\frac{p-1}{q}\right)^{p-3}}{\Gamma\left(\frac{p-3}{q}\right)^{p-1}}\right]^{1/2} \omega^{-p} \exp\left\{-\left[\frac{\Gamma\left(\frac{p-3}{q}\right)}{\Gamma\left(\frac{p-1}{q}\right)}\right]^{1/2} \left(\frac{\omega T_z}{2\pi}\right)^{-q}\right\}$$

or

$$S(\omega) = \frac{q}{16} H_{1/3}^2 \left(\frac{2\pi}{T_{1/3}}\right)^{p-1} \frac{\Gamma\left(\frac{p-1}{q}\right)^{p-2}}{\Gamma\left(\frac{p-2}{q}\right)^{p-1}} \omega^{-p} \exp\left\{-\frac{\Gamma\left(\frac{p-2}{q}\right)}{\Gamma\left(\frac{p-1}{q}\right)} \left(\frac{\omega T_{1/3}}{2\pi}\right)^{-q}\right\}$$

and peak is at,

$$\omega_0 = \left(\frac{qB}{p}\right)^{1/q}$$

Most useful values of $\Gamma(x)$ may be found from,

$$\Gamma(n+a/b) = \frac{a(a+b)}{b^n} \ldots\ldots \{a+b(n-1)\}\ \Gamma(a/b)$$

$\Gamma(1/4) = 3.625609908$ $\qquad$ $\Gamma(3/2) = 1/2\pi^{1/2}$

$\Gamma(1/2) = \pi^{1/2}$ $\qquad$ $\Gamma(7/4) = 0.919062527$

$\Gamma(3/4) = 1.225416702$ $\qquad$ $\Gamma(2) = 1$

$\Gamma(1) = 1$ $\qquad$ $\Gamma(5/2) = 1/4\pi^{1/2}$

APPENDIX 3

COMPUTATIONAL RESULTS OF SPECTRAL ANALYSIS

SPECTRAL ANALYSIS USING PIERSON-MOSKOWITZ WAVE SPECTRA
****

SWATH1 IN IRREGULAR BEAM SEAS

AVERAGE AMPLITUDES :

WAVE	SWAY	HEAVE	ROLL
0.653792	0.189875	0.097818	0.459511
0.653792	0.193546	0.097415	0.568117
1.067798	0.292062	0.519728	0.762008
1.067798	0.325427	0.482959	0.968574
1.562171	0.530043	1.394504	1.196577
1.562171	0.621074	1.274413	1.447929
2.694738	1.200245	2.791996	3.954733
2.694738	1.349505	2.775733	3.645967
3.543413	1.730043	3.514961	5.870237
3.543413	1.820908	3.572556	5.182086

SIGNIFICANT AMPLITUDES :

1.046067	0.303799	0.156509	0.735217
1.046067	0.309674	0.155864	0.908987
1.708477	0.467299	0.831564	1.219213
1.708477	0.520683	0.772735	1.549719
2.499474	0.848068	2.231206	1.914523
2.499474	0.993718	2.039061	2.316687
4.311581	1.920391	4.467194	6.327572
4.311581	2.159208	4.441172	5.833548
5.669461	2.768069	5.623937	9.392380
5.669461	2.913452	5.716089	8.291338

AVERAGE 1/10 HIGHEST AMPLITUDES :

1.333736	0.387344	0.199550	0.937402
1.333736	0.394834	0.198726	1.158959
2.178308	0.595806	1.060244	1.554496
2.178308	0.663871	0.985237	1.975892
3.186830	1.081287	2.844788	2.441016
3.186830	1.266991	2.599803	2.953776
5.497265	2.448499	5.695672	8.067655
5.497265	2.752990	5.662494	7.437774
7.228562	3.529288	7.170519	11.975284
7.228562	3.714651	7.288013	10.571455

AVERAGE 1/100 HIGHEST AMPLITUDES :

1.746932	0.507345	0.261371	1.227812
1.746932	0.517155	0.260292	1.518009
2.853156	0.780389	1.388712	2.036085
2.853156	0.869541	1.290468	2.588031
4.174122	1.416274	3.726114	3.197253
4.174122	1.659509	3.405232	3.868867
7.200339	3.207053	7.460214	10.567045
7.200339	3.605877	7.416757	9.742024
9.467999	4.622675	9.391974	15.685274
9.467999	4.865465	9.545868	13.846534

SIGNIFICANT VELOCITY :

1.014897	0.327709	0.133550	0.642510
1.014897	0.331101	0.130245	0.778562
1.414493	0.382496	0.459615	0.957164
1.414493	0.402850	0.435999	1.193188
1.790332	0.523458	1.152904	1.179575
1.790332	0.600000	1.053298	1.496093
2.452130	0.939841	2.177385	2.740110
2.452130	1.075949	2.101363	2.690289
2.853450	1.197766	2.576869	3.879819
2.853450	1.320565	2.564053	3.596685

SIGNIFICANT ACCELERATION :

1.068247	0.377763	0.133505	0.590582
1.068247	0.379874	0.129818	0.697218
1.330774	0.385230	0.282124	0.806852
1.330774	0.389860	0.273637	0.981287
1.521443	0.423156	0.617181	0.874135
1.521443	0.461485	0.569208	1.112102
1.770520	0.575649	1.097844	1.384618
1.770520	0.647233	1.037999	1.484973
1.886360	0.649803	1.252978	1.788685
1.886360	0.724715	1.218074	1.803160

Note :

Wave amplitude in m

Surge amplitude in m

Sway amplitude in m

Heave amplitude in m

Roll amplitude in deg.

Pitch amplitude in deg.

Yaw amplitude in deg.

SPECTRAL ANALYSIS USING BRETSCHNEIDER WAVE SPECTRA
****

SWATH1 IN IRREGULAR BEAM SEAS

AVERAGE AMPLITUDES :

WAVE	SWAY	HEAVE	ROLL
0.414690	0.139320	0.054586	0.262711
0.414690	0.141269	0.052993	0.314922
0.900331	0.248750	0.175702	0.646483
0.900331	0.257114	0.178740	0.806602
1.391456	0.393825	0.835046	0.984987
1.391456	0.448588	0.763461	1.256442
2.358080	0.921718	2.390114	2.371149
2.358080	1.073642	2.252709	2.506941
3.314986	1.492145	3.422261	4.979307
3.314986	1.667480	3.416263	4.557514

SIGNIFICANT AMPLITUDES :

0.663505	0.222912	0.087337	0.420338
0.663505	0.226030	0.084788	0.503875
1.440530	0.398000	0.281123	1.034374
1.440530	0.411383	0.285984	1.290564
2.226330	0.630121	1.336074	1.575979
2.226330	0.717741	1.221538	2.010307
3.772928	1.474748	3.824182	3.793838
3.772928	1.717827	3.604335	4.011106
5.303977	2.387433	5.475618	7.966891
5.303977	2.667967	5.466021	7.292022

AVERAGE 1/10 HIGHEST AMPLITUDES :

0.845968	0.284213	0.111355	0.535931
0.845968	0.288188	0.108105	0.642441
1.836675	0.507450	0.358432	1.318826
1.836675	0.524513	0.364630	1.645469
2.838570	0.803404	1.703494	2.009372
2.838570	0.915120	1.557460	2.563142
4.810483	1.880304	4.875832	4.837143
4.810483	2.190230	4.595527	5.114160
6.762571	3.043977	6.981412	10.157785
6.762571	3.401658	6.969176	9.297328

AVERAGE 1/100 HIGHEST AMPLITUDES :

1.108053	0.372263	0.145853	0.701965
1.108053	0.377470	0.141596	0.841472
2.405684	0.664660	0.469476	1.727404
2.405684	0.687010	0.477593	2.155241
3.717971	1.052301	2.231244	2.431884
3.717971	1.198628	2.039968	3.357213
6.300789	2.462830	6.386384	6.335709
6.300789	2.868771	6.019238	6.698547
8.857642	3.987012	9.144281	13.304708
8.857642	4.455505	9.128254	12.177676

SIGNIFICANT VELOCITY :

0.704968	0.258781	0.093134	0.395023
0.704968	0.261471	0.092209	0.462466
1.332992	0.403502	0.198596	0.874351
1.332992	0.406831	0.200640	1.070852
1.780638	0.477342	0.719491	1.200320
1.780638	0.516522	0.669026	1.506295
2.464277	0.818379	1.937085	1.891771
2.464277	0.946413	1.796654	2.173512
2.974365	1.152488	2.654004	3.424921
2.974365	1.316048	2.571769	3.331147

SIGNIFICANT ACCELERATION :

0.792323	0.309003	0.106183	0.387309
0.792323	0.311223	0.106414	0.440996
1.356553	0.452240	0.172359	0.781192
1.356553	0.451230	0.172420	0.933260
1.635053	0.458513	0.418164	0.993046
1.635053	0.473278	0.397696	1.216334
1.962658	0.581921	1.007774	1.179861
1.962658	0.646613	0.930502	1.434376
2.126238	0.696141	1.333466	1.706600
2.126238	0.783079	1.264750	1.813347

Note :

Wave velocity in ms^{-1}

Surge velocity in ms^{-1}

Sway velocity in ms^{-1}

Heave velocity in ms^{-1}

Roll velocity in $degs^{-1}$

Pitch velocity in $degs^{-1}$

Yaw velocity in $degs^{-1}$

SPECTRAL ANALYSIS USING ITTC/ISSC WAVE SPECTRA
****

SWATH1 IN IRREGULAR BEAM SEAS

AVERAGE AMPLITUDES :

WAVE	SWAY	HEAVE	ROLL
0.645230	0.188632	0.094842	0.451932
0.645230	0.192129	0.094042	0.558097
1.007203	0.275621	0.492410	0.718643
1.007203	0.307251	0.457387	0.913541
1.539983	0.548925	1.451779	1.264785
1.539983	0.642988	1.337182	1.473141
2.758772	1.274118	2.816619	4.337836
2.758772	1.399731	2.835389	3.912544
3.329168	1.622213	3.305899	5.509933
3.329168	1.710117	3.359558	4.866966

SIGNIFICANT AMPLITUDES :

1.032369	0.301811	0.151747	0.723091
1.032369	0.307406	0.150467	0.892956
1.611525	0.440994	0.787856	1.149829
1.611525	0.491602	0.731820	1.461666
2.463973	0.878279	2.322846	2.023655
2.463973	1.028781	2.139491	2.357026
4.414036	2.038589	4.506591	6.940538
4.414036	2.239570	4.536623	6.260071
5.326669	2.595541	5.289439	8.815894
5.326669	2.736188	5.375293	7.787146

AVERAGE 1/10 HIGHEST AMPLITUDES :

1.316270	0.384809	0.193477	0.921941
1.316270	0.391943	0.191845	1.138519
2.054694	0.562267	1.004516	1.466032
2.054694	0.626792	0.933070	1.863625
3.141566	1.119806	2.961629	2.580160
3.141566	1.311696	2.727850	3.005208
5.627895	2.599201	5.745903	8.849186
5.627895	2.855452	5.784193	7.981590
6.791503	3.309314	6.744034	11.240264
6.791503	3.488639	6.853498	9.928611

AVERAGE 1/100 HIGHEST AMPLITUDES :

1.724055	0.504024	0.253417	1.207562
1.724055	0.513368	0.251279	1.491236
2.691247	0.736460	1.315719	1.920215
2.691247	0.820975	1.222139	2.440983
4.114835	1.466726	3.879153	3.379504
4.114835	1.718064	3.572949	3.936234
7.371439	3.404444	7.526007	11.590698
7.371439	3.740082	7.576159	10.434318
8.895536	4.334553	8.833363	14.722542
8.895536	4.569433	8.976739	13.004534

SIGNIFICANT VELOCITY :

1.006728	0.327418	0.131903	0.634288
1.006728	0.330900	0.128251	0.767528
1.333352	0.360435	0.435192	0.902248
1.333352	0.379805	0.412642	1.124856
1.714533	0.521638	1.192280	1.156612
1.714533	0.601072	1.092356	1.439302
2.390891	0.950494	2.150771	2.938277
2.390891	1.076614	2.104097	2.802982
2.687816	1.126004	2.427494	3.644378
2.687816	1.242892	2.414211	3.381142

SIGNIFICANT ACCELERATION :

1.063520	0.378398	0.133368	0.584918
1.063520	0.380737	0.129536	0.689470
1.253858	0.362708	0.266798	0.760305
1.253858	0.367190	0.258667	0.924778
1.427734	0.403821	0.631408	0.815868
1.427734	0.443897	0.581423	1.035202
1.667408	0.554817	1.070624	1.420862
1.667408	0.624045	1.023559	1.479671
1.780265	0.612453	1.181434	1.682496
1.780265	0.683410	1.147880	1.697744

Note :

Wave acceleration in ms^{-2}

Surge acceleration in ms^{-2}

Sway acceleration in ms^{-2}

Heave acceleration in ms^{-2}

Roll acceleration in $degs^{-2}$

Pitch acceleration in $degs^{-2}$

Yaw acceleration in $degs^{-2}$

SPECTRAL ANALYSIS USING ITTC'84 WAVE SPECTRA
****

SWATH1 IN IRREGULAR BEAM SEAS

AVERAGE AMPLITUDES :

WAVE	SWAY	HEAVE	ROLL
0.716806	0.265479	0.690557	0.520307
0.716806	0.322444	0.625702	0.655527
1.241141	0.524649	1.369292	1.013941
1.241141	0.625363	1.246084	1.189714
1.909448	0.807152	2.106603	1.559910
1.909448	0.962097	1.917052	1.830330
2.872181	1.498409	3.342080	4.738491
2.872181	1.672371	3.311348	4.324950

SIGNIFICANT AMPLITUDES :

1.146890	0.424766	1.104891	0.832490
1.146890	0.515911	1.001123	1.048843
1.985826	0.839438	2.190867	1.622306
1.985826	1.000581	1.993734	1.903543
3.055117	1.291444	3.370565	2.495856
3.055117	1.539354	3.067283	2.928527
4.595490	2.397455	5.347328	7.581586
4.595490	2.675794	5.298157	6.919919

AVERAGE 1/10 HIGHEST AMPLITUDES :

1.462284	0.541577	1.408736	1.061425
1.462284	0.657787	1.276431	1.337275
2.531928	1.070284	2.793356	2.068440
2.531928	1.275740	2.542011	2.427017
3.895274	1.646590	4.297471	3.182216
3.895274	1.962677	3.910786	3.733872
5.859250	3.056754	6.817843	9.666522
5.859250	3.411638	6.755150	8.822897

AVERAGE 1/100 HIGHEST AMPLITUDES :

1.915305	0.709360	1.845168	1.390259
1.915305	0.861572	1.671875	1.751568
3.316329	1.401862	3.658748	2.709251
3.316329	1.670969	3.329535	3.178916
5.102045	2.156711	5.628843	4.168079
5.102045	2.570722	5.122362	4.890640
7.674468	4.003749	8.930037	12.661248
7.674468	4.468576	8.847921	11.556266

SIGNIFICANT VELOCITY :

0.762698	0.247661	0.573094	0.518137
0.762698	0.297676	0.522998	0.668131
1.247858	0.459473	1.121990	0.874916
1.247858	0.548611	1.019701	1.091538
1.919781	0.706882	1.726138	1.346024
1.919781	0.844016	1.567232	1.679250

2.413092	1.149784	2.620774	3.181754
2.413092	1.297624	2.512177	3.040421

SIGNIFICANT ACCELERATION :

0.583414	0.175164	0.303654	0.369062
0.583414	0.200865	0.281062	0.471962
0.914543	0.299041	0.584149	0.568547
0.914543	0.345654	0.533526	0.720031
1.406989	0.460064	0.898691	0.944996
1.406989	0.531776	0.820809	1.107740
1.944811	0.627733	1.311221	1.420543
1.944811	0.703774	1.227532	1.511362

SPECTRAL ANALYSIS USING PIERSON-MOSKOWITZ WAVE SPECTRA
****

SWATH1 IN IRREGULAR QUARTERING SEAS

AVERAGE AMPLITUDES :

WAVE	SURGE	SWAY	HEAVE	ROLL	PITCH	YAW
0.556063	0.110101	0.072610	0.054390	0.258550	0.203213	0.217046
0.556063	0.108936	0.069960	0.055151	0.256804	0.217227	0.212869
0.999273	0.319888	0.199027	0.197309	0.473783	0.424186	0.500035
0.999273	0.312014	0.180272	0.172036	0.478224	0.566426	0.508061
1.512985	0.636173	0.383925	0.770539	1.051844	1.089377	0.796510
1.512985	0.654839	0.342184	0.660188	1.020857	1.204246	0.808140
2.665355	1.379081	0.794596	2.291045	4.795752	5.244874	1.233867
2.665355	1.489364	0.711780	2.142963	4.319268	4.590016	1.257194
3.520919	1.879269	1.041606	3.239826	6.948229	7.585255	1.443465
3.520919	1.992092	0.946768	3.095934	6.178064	6.624336	1.463549

SIGNIFICANT AMPLITUDES :

0.889701	0.176161	0.116176	0.087025	0.413681	0.325141	0.347273
0.889701	0.174298	0.111936	0.088242	0.410886	0.347562	0.340590
1.598837	0.511821	0.318444	0.315694	0.758053	0.678697	0.800057
1.598837	0.499223	0.288435	0.275257	0.765158	0.906281	0.813498
2.420775	1.017876	0.614281	1.232862	1.682951	1.743003	1.274416
2.420775	1.047743	0.547495	1.056300	1.633371	1.926794	1.293023
4.264568	2.206530	1.271353	3.665672	7.673203	8.391799	1.974187
4.264568	2.382982	1.138849	3.428741	6.910829	7.344026	2.011511
5.633470	3.006830	1.666570	5.183722	11.117167	12.136408	2.309544
5.633470	3.187347	1.514830	4.953495	9.884903	10.598938	2.341679

AVERAGE 1/10 HIGHEST AMPLITUDES :

1.134369	0.224605	0.148124	0.110956	0.527443	0.414555	0.442774
1.134369	0.222230	0.142718	0.112509	0.523880	0.443142	0.434252
2.038517	0.652571	0.406016	0.402510	0.966517	0.865339	1.020072
2.038517	0.636509	0.367755	0.350953	0.975576	1.155508	1.037465
3.086488	1.297792	0.783208	1.571899	2.145762	2.222328	1.624881
3.086488	1.335872	0.698056	1.346783	2.082548	2.456662	1.648605
5.437324	2.813325	1.620975	4.673732	9.783333	10.699543	2.517028
5.437324	3.038303	1.452032	4.371645	8.811307	9.363632	2.561476
7.182674	3.833709	2.124876	6.609245	14.174387	15.473919	2.944669
7.182674	4.063868	1.931408	6.315705	12.603251	13.513646	2.985641

AVERAGE 1/100 HIGHEST AMPLITUDES :

1.485801	0.294189	0.194014	0.145331	0.690847	0.542986	0.579947
1.485801	0.291078	0.186933	0.147365	0.686179	0.580429	0.568785
2.670058	0.854741	0.531801	0.527209	1.265948	1.133424	1.336994
2.670058	0.833702	0.481687	0.459679	1.277814	1.513489	1.358876
4.042695	1.699853	1.025848	2.058879	2.810528	2.910814	2.129775
4.042695	1.749730	0.914317	1.764022	2.727730	3.017746	2.159349
7.121828	3.684904	2.123160	6.121672	12.814248	14.014303	3.296892
7.121828	3.979581	1.901877	5.725998	11.541084	12.264523	3.359222
9.407895	5.021406	2.783171	8.656816	18.565666	20.267799	3.876459
9.407895	5.322869	2.529765	8.272335	16.507788	17.700226	3.919604

SIGNIFICANT VELOCITY :

0.763333	0.124844	0.084396	0.066556	0.334328	0.244777	0.263067
0.763333	0.125316	0.083391	0.069262	0.331382	0.257251	0.249133
1.212316	0.319889	0.202392	0.172535	0.556063	0.472103	0.541655
1.212316	0.310730	0.187206	0.156674	0.557051	0.587967	0.542996
1.624813	0.564250	0.345800	0.576726	0.852226	0.832492	0.797310
1.624813	0.569197	0.310754	0.493917	0.844596	1.001753	0.804394
2.329277	1.041246	0.615522	1.578684	3.146677	3.398965	1.111012
2.329277	1.114027	0.551998	1.448815	2.968490	3.050129	1.123210
2.747683	1.303776	0.749759	2.110316	4.473878	4.844677	1.221499
2.747683	1.395621	0.673688	1.936012	4.029977	4.294783	1.241055

SIGNIFICANT ACCELERATION :

0.679596	0.090660	0.063693	0.052394	0.277545	0.188350	0.206986
0.679596	0.092611	0.065162	0.056214	0.274829	0.196983	0.186913
0.985739	0.206908	0.134781	0.104646	0.429428	0.340603	0.383523
0.985739	0.202842	0.128147	0.100210	0.427792	0.398662	0.374433
1.211121	0.330841	0.207240	0.280138	0.520066	0.464380	0.521989
1.211121	0.329229	0.189745	0.243393	0.521706	0.581648	0.522766
1.501768	0.530640	0.321978	0.699556	1.361862	1.423479	0.676004
1.501768	0.557602	0.291179	0.631999	1.365277	1.340357	0.675133
1.634572	0.621071	0.370009	0.896726	1.864264	1.977179	0.711487
1.634572	0.660614	0.332760	0.829663	1.707874	1.808967	0.723734

SPECTRAL ANALYSIS USING ITTC'84 WAVE SPECTRA
****

SWATH1 IN IRREGULAR QUARTERING SEAS

AVERAGE AMPLITUDES :

WAVE	SURGE	SWAY	HEAVE	ROLL	PITCH	YAW
0.706061	0.311753	0.188389	0.328272	0.414915	0.412509	0.399823
0.706061	0.315359	0.166765	0.278625	0.414479	0.540699	0.406417
1.226541	0.588327	0.352399	0.751456	1.000307	1.042380	0.682045
1.226541	0.611773	0.312284	0.646653	0.960654	1.122292	0.690327
1.886986	0.905118	0.542152	1.156086	1.538935	1.603661	1.049300
1.886986	0.941190	0.480437	0.994851	1.477929	1.726603	1.062041
2.856379	1.602199	0.931623	2.736992	5.632148	6.087843	1.341070
2.856379	1.761706	0.839994	2.523624	5.113466	5.297745	1.355821

SIGNIFICANT AMPLITUDES :

1.129697	0.498805	0.301422	0.525235	0.663864	0.660015	0.639717
1.129697	0.504574	0.266824	0.445800	0.663166	0.865119	0.650267
1.962465	0.941323	0.563838	1.202329	1.600492	1.667808	1.091271
1.962465	0.978837	0.499654	1.034641	1.537046	1.795667	1.104523
3.019177	1.448189	0.867443	1.849737	2.462295	2.565858	1.678880
3.019177	1.505904	0.768699	1.591761	2.364686	2.762564	1.699266
4.570206	2.563518	1.490597	4.379188	9.011436	9.740549	2.145712
4.570206	2.818729	1.343990	4.037798	8.181545	8.476392	2.169314

AVERAGE 1/10 HIGHEST AMPLITUDES :

1.440364	0.635976	0.384314	0.669675	0.846426	0.841519	0.815640
1.440364	0.643332	0.340201	0.568395	0.845536	1.103026	0.829090
2.502143	1.200186	0.718894	1.532970	2.040627	2.126455	1.391371
2.502143	1.248017	0.637059	1.319172	1.959733	2.289475	1.408267
3.849451	1.846441	1.105990	2.358415	3.139426	3.271469	2.140571
3.849451	1.920027	0.980091	2.029495	3.014974	3.522269	2.166564
5.827012	3.268486	1.900511	5.583464	11.489581	12.419199	2.736782
5.827012	3.593879	1.713587	5.148193	10.431470	10.807399	2.765875

AVERAGE 1/100 HIGHEST AMPLITUDES :

1.886594	0.833004	0.503376	0.877142	1.108652	1.102225	1.068328
1.886594	0.842639	0.445597	0.744486	1.107487	1.444748	1.085945
3.277317	1.572009	0.941610	2.007890	2.672822	2.785239	1.822423
3.277317	1.634658	0.834423	1.727856	2.566866	2.998764	1.844553
5.042026	2.418475	1.448630	3.089061	4.112033	4.284983	2.803729
5.042026	2.514859	1.283728	2.658241	3.949025	4.613482	2.837774
7.632243	4.281075	2.489296	7.313243	15.049099	16.266716	3.583339
7.632243	4.707277	2.244463	6.743123	13.663180	14.155574	3.622754

SIGNIFICANT VELOCITY :

0.724276	0.280716	0.171641	0.249313	0.357199	0.342045	0.393889
0.724276	0.279015	0.153036	0.212501	0.362282	0.480598	0.400180
1.192715	0.505430	0.305714	0.556735	0.742926	0.749053	0.647940
1.192715	0.514612	0.271354	0.476918	0.728644	0.893381	0.656793
1.834946	0.777585	0.470329	0.856515	1.142964	1.152388	0.996830
1.834946	0.791711	0.417467	0.733720	1.120991	1.374432	1.010135

2.342076	1.198132	0.707656	1.916634	3.666840	3.926495	1.149249
2.342076	1.304381	0.637781	1.733817	3.360406	3.486225	1.150521

SIGNIFICANT ACCELERATION :

0.504650	0.164948	0.102485	0.122527	0.223349	0.203416	0.253000
0.504650	0.162023	0.092685	0.106093	0.227464	0.286632	0.255794
0.796616	0.284163	0.174326	0.263548	0.397382	0.379155	0.403321
0.796616	0.284228	0.156199	0.226586	0.396716	0.488365	0.407015
1.225563	0.437173	0.268194	0.405458	0.611358	0.583315	0.620509
1.225563	0.437274	0.240307	0.348595	0.610332	0.751330	0.624172
1.371415	0.590970	0.354658	0.854130	1.536256	1.611992	0.657712
1.371415	0.632415	0.320182	0.760443	1.427518	1.490189	0.651838

SPECTRAL ANALYSIS USING PIERSON-MOSKOWITZ WAVE SPECTRA
****

SWATH1 IN IRREGULAR HEAD SEAS

AVERAGE AMPLITUDES :

WAVE	SURGE	HEAVE	PITCH
0.653792	0.120274	0.090110	0.207511
0.653792	0.111879	0.089236	0.199890
1.067798	0.403883	0.452774	0.421309
1.067798	0.375580	0.405001	0.402097
1.562171	0.881258	1.290686	1.348378
1.562171	0.816406	1.167265	1.195241
2.694738	2.005480	2.937640	6.507702
2.694738	1.881868	2.723253	5.635908
3.543413	2.718424	3.829431	9.320793
3.543413	2.537127	3.535859	8.073829

SIGNIFICANT AMPLITUDES :

1.046067	0.192439	0.144177	0.332018
1.046067	0.179006	0.142777	0.319824
1.708477	0.646212	0.724438	0.674094
1.708477	0.600928	0.648002	0.643355
2.499474	1.410013	2.065098	2.157404
2.499474	1.306249	1.867624	1.912385
4.311581	3.208768	4.700225	10.412324
4.311581	3.010989	4.357204	9.017453
5.669461	4.349478	6.127090	14.913269
5.669461	4.059404	5.657374	12.918126

AVERAGE 1/10 HIGHEST AMPLITUDES :

1.333736	0.245359	0.183825	0.423323
1.333736	0.228233	0.182041	0.407776
2.178308	0.823921	0.923659	0.859470
2.178308	0.766183	0.826203	0.820278
3.186830	1.797766	2.633000	2.750690
3.186830	1.665468	2.381221	2.438291
5.497265	4.091179	5.992786	13.275713
5.497265	3.839011	5.555435	11.497252
7.228562	5.545585	7.812039	19.014418
7.228562	5.175739	7.213151	16.470610

AVERAGE 1/100 HIGHEST AMPLITUDES :

1.746932	0.321372	0.240775	0.554471
1.746932	0.298941	0.239438	0.534107
2.853156	1.079175	1.209812	1.125737
2.853156	1.003549	1.082164	1.074403
4.174122	2.354721	3.448714	3.602865
4.174122	2.181436	3.118932	3.193683
7.200339	5.358642	7.849375	17.388580
7.200339	5.028351	7.276531	15.059146
9.467999	7.263628	10.232239	24.905159
9.467999	6.779204	9.447814	21.573269

SIGNIFICANT VELOCITY :

1.014897	0.145406	0.112325	0.275290
1.014897	0.137443	0.112143	0.268465
1.414493	0.396180	0.396209	0.473918
1.414493	0.370309	0.359119	0.455892
1.790332	0.761839	1.038923	0.996958
1.790332	0.707629	0.938113	0.902910
2.452130	1.496215	2.182308	4.224470
2.452130	1.401318	2.013542	3.675326
2.853450	1.883694	2.699096	5.980531
2.853450	1.767092	2.499569	5.193912

SIGNIFICANT ACCELERATION :

1.068247	0.124284	0.097747	0.247051
1.068247	0.121484	0.098414	0.246242
1.330774	0.262011	0.234526	0.368584
1.330774	0.248200	0.217868	0.359940
1.521443	0.439780	0.539576	0.542726
1.521443	0.411649	0.489472	0.508003
1.770520	0.748249	1.049396	1.764478
1.770520	0.700791	0.964289	1.552125
1.886360	0.886456	1.250385	2.444159
1.886360	0.833565	1.156548	2.138413

SPECTRAL ANALYSIS USING ITTC'84 WAVE SPECTRA
****

SWATH1 IN IRREGULAR HEAD SEAS

AVERAGE AMPLITUDES :

WAVE	SURGE	HEAVE	PITCH
0.716806	0.431949	0.614444	0.507414
0.716806	0.401390	0.552301	0.462070
1.241141	0.834968	1.260096	1.349049
1.241141	0.774396	1.140845	1.194682
1.909448	1.284566	1.938609	2.075460
1.909448	1.191378	1.755147	1.837972
2.872181	2.359802	3.522364	7.581784
2.872181	2.215985	3.275265	6.588028

SIGNIFICANT AMPLITUDES :

1.146890	0.691119	0.983110	0.811862
1.146890	0.642225	0.883682	0.739312
1.985826	1.335949	2.016153	2.158478
1.985826	1.239034	1.825353	1.911491
3.055117	2.055305	3.101774	3.320736
3.055117	1.906205	2.808235	2.940756
4.595490	3.775683	5.635783	12.130855
4.595490	3.545577	5.240423	10.540846

AVERAGE 1/10 HIGHEST AMPLITUDES :

1.462284	0.881177	1.253465	1.035124
1.462284	0.818837	1.126695	0.942623
2.531928	1.703334	2.570595	2.752060
2.531928	1.579768	2.327325	2.437151
3.895274	2.620514	3.954761	4.233938
3.895274	2.430412	3.580499	3.749463
5.859250	4.813995	7.185623	15.466840
5.859250	4.520610	6.681540	13.439578

AVERAGE 1/100 HIGHEST AMPLITUDES :

1.915305	1.154169	1.641793	1.355810
1.915305	1.072515	1.475749	1.234652
3.316329	2.231034	3.366976	3.604658
3.316329	2.069186	3.048339	3.192190
5.102045	3.432360	5.179962	5.545628
5.102045	3.183363	4.689752	4.911061
7.674468	6.305390	9.411757	20.258528
7.674468	5.921113	8.751507	17.603212

SIGNIFICANT VELOCITY :

0.762698	0.380255	0.499523	0.397071
0.762698	0.354529	0.448660	0.368756
1.247858	0.702780	1.005472	0.948886
1.247858	0.652937	0.907003	0.853374
1.919781	1.081200	1.546879	1.459824
1.919781	1.004319	1.395390	1.312883

2.413092	1.750383	2.636551	4.913038
2.413092	1.636608	2.434862	4.285811

SIGNIFICANT ACCELERATION :

0.583414	0.219020	0.259678	0.224838
0.583414	0.205236	0.234143	0.213456
0.914543	0.387240	0.510834	0.460994
0.914543	0.361317	0.460612	0.424641
1.406989	0.595753	0.785898	0.709222
1.406989	0.555872	0.708634	0.653294
1.544811	0.851177	1.264050	2.022759
1.544811	0.794026	1.160133	1.777995

SPECTRAL ANALYSIS USING PIERSON-MOSKOWITZ WAVE SPECTRA
****

SWATH1 IN IRREGULAR HEAD SEAS (Fn = 0.13)

AVERAGE AMPLITUDES :

WAVE	SURGE	HEAVE	PITCH
0.653792	0.218296	0.121918	0.230746
0.653792	0.219018	0.097193	0.209925
1.067798	0.460865	0.767589	0.651627
1.067798	0.529488	0.780995	0.404769
1.562171	0.753243	2.140058	1.490302
1.562171	0.921021	2.123435	1.084808
2.694738	1.532586	4.686485	3.433348
2.694738	1.779528	4.459976	3.586606
3.543413	2.392795	5.966822	4.621650
3.543413	2.392996	5.581673	5.250452

SIGNIFICANT AMPLITUDES :

1.046067	0.349274	0.195068	0.369193
1.046067	0.350428	0.155508	0.335881
1.708477	0.737383	1.228142	1.042604
1.708477	0.847181	1.249593	0.647631
2.499474	1.205189	3.424092	2.384483
2.499474	1.473633	3.397496	1.735693
4.311581	2.452137	7.498376	5.493356
4.311581	2.847244	7.135961	5.738570
5.669461	3.828471	9.546915	7.394639
5.669461	3.828794	8.930676	8.400723

AVERAGE 1/10 HIGHEST AMPLITUDES :

1.333736	0.445324	0.248712	0.470722
1.333736	0.446796	0.198273	0.428248
2.178308	0.940164	1.565881	1.329320
2.178308	1.080156	1.593230	0.825729
3.186830	1.536616	4.365717	3.040215
3.186830	1.878883	4.331807	2.213008
5.497265	3.126475	9.560429	7.004029
5.497265	3.630236	9.098351	7.316676
7.228562	4.881301	12.172316	9.428165
7.228562	4.881712	11.386612	10.710921

AVERAGE 1/100 HIGHEST AMPLITUDES :

1.746932	0.583287	0.325764	0.616553
1.746932	0.585216	0.259699	0.560921
2.853156	1.231430	2.050997	1.741149
2.853156	1.414793	2.086819	1.081543
4.174122	2.012666	5.718234	3.982086
4.174122	2.460968	5.673818	2.898607
7.200339	4.095068	12.522287	9.173904
7.200339	4.754898	11.917055	9.583411
9.467999	6.393547	15.943347	12.349048
9.467999	6.394085	14.914229	14.029206

SIGNIFICANT VELOCIOTY :

1.014897	0.288883	0.157140	0.305920
1.014897	0.265320	0.115409	0.312807
1.414493	0.517386	0.663898	0.655117
1.414493	0.561796	0.661535	0.447922
1.790332	0.749763	1.730316	1.285810
1.790332	0.874608	1.717685	0.893303
2.452130	1.169283	3.531156	2.566902
2.452130	1.409044	3.404746	2.459560
2.853450	1.550965	4.300901	3.227242
2.853450	1.712368	4.088313	3.406085

SIGNIFICANT ACCELERATION :

1.068247	0.255068	0.147068	0.279074
1.068247	0.209561	0.099238	0.307806
1.330774	0.394242	0.385500	0.461694
1.330774	0.392550	0.363944	0.369186
1.521443	0.513879	0.898702	0.756061
1.521443	0.556016	0.882999	0.541488
1.770520	0.658687	1.715944	1.292437
1.770520	0.775416	1.666387	1.140674
1.886360	0.758413	2.025743	1.531218
1.886360	0.871438	1.947946	1.479140

SPECTRAL ANALYSIS USING PIERSON-MOSKOWITZ WAVE SPECTRA
****

SWATH1 IN IRREGULAR HEAD SEAS (Fn = 0.26)

AVERAGE AMPLITUDES :

WAVE	SURGE	HEAVE	PITCH
0.653792	0.181671	0.202771	0.238845
0.653792	0.162421	0.173202	0.166712
1.067798	0.545148	1.011067	1.031063
1.067798	0.431552	0.978409	0.426067
1.562171	1.179202	2.107069	2.063532
1.562171	0.925778	2.090237	0.970517
2.694738	2.949279	4.071818	3.741150
2.694738	2.479059	3.939630	2.487334
3.543413	4.476593	5.183521	4.665095
3.543413	3.815269	4.895466	3.672918

SIGNIFICANT AMPLITUDES :

1.046067	0.290674	0.324434	0.382151
1.046067	0.259874	0.277123	0.266740
1.708477	0.872238	1.617708	1.649700
1.708477	0.690483	1.565454	0.681707
2.499474	1.886724	3.371311	3.301651
2.499474	1.481244	3.344380	1.552827
4.311581	4.718847	6.514909	5.985840
4.311581	3.966495	6.303408	3.979735
5.669461	7.162549	8.293633	7.464152
5.669461	6.104431	7.832746	5.876668

AVERAGE 1/10 HIGHEST AMPLITUDES :

1.333736	0.370610	0.413654	0.487243
1.333736	0.331340	0.353332	0.340093
2.178308	1.112103	2.062577	2.103368
2.178308	0.880366	1.995953	0.869177
3.186830	2.405573	4.298422	4.209605
3.186830	1.888586	4.264084	1.979855
5.497265	6.016530	8.306508	7.631946
5.497265	5.057281	8.036844	5.074162
7.228562	9.132250	10.574382	9.516793
7.228562	7.783149	9.986751	7.492752

AVERAGE 1/100 HIGHEST AMPLITUDES :

1.746932	0.485426	0.541805	0.638193
1.746932	0.433990	0.462795	0.445456
2.853156	1.456637	2.701572	2.754999
2.853156	1.153107	2.614307	1.138451
4.174122	3.150829	5.630090	5.513758
4.174122	2.473678	5.585114	2.593221
7.200339	7.880474	10.879897	9.996352
7.200339	6.624047	10.526690	6.646158
9.467999	11.961456	13.850368	12.465133
9.467999	10.194399	13.080685	9.814036

SIGNIFICANT VELOCITY :

1.014897	0.230549	0.206741	0.281072
1.014897	0.204655	0.175165	0.240399
1.414493	0.545066	0.928896	0.982507
1.414493	0.441258	0.885333	0.443411
1.790332	1.027407	1.832539	1.848296
1.790332	0.804465	1.804482	0.846520
2.452130	2.102056	3.193422	3.035454
2.452130	1.737551	3.128280	1.788808
2.853450	2.866611	3.806512	3.532184
2.853450	2.416960	3.674945	2.402324

SIGNIFICANT ACCELERATION :

1.068247	0.202867	0.142919	0.244140
1.068247	0.172226	0.122859	0.242085
1.330774	0.373535	0.544191	0.620568
1.330774	0.306423	0.510363	0.338634
1.521443	0.605080	1.019891	1.075400
1.521443	0.476811	0.992988	0.520905
1.770520	1.027351	1.644800	1.630163
1.770520	0.835394	1.616785	0.889898
1.886360	1.272299	1.874883	1.813663
1.886360	1.055482	1.831693	1.091942

SPECTRAL ANALYSIS USING PIERSON-MOSKOWITZ WAVE SPECTRA
****

SWATH1 IN IRREGULAR HEAD SEAS (Fn = 0.39)

AVERAGE AMPLITUDES :

WAVE	SURGE	HEAVE	PITCH
0.653792	0.279650	0.146824	0.224862
0.653792	0.178299	0.154798	0.279296
1.067798	0.875740	0.774630	0.953723
1.067798	0.397639	0.704531	1.014838
1.562171	1.725907	1.921612	2.152691
1.562171	0.729257	1.734863	2.158710
2.694738	3.505124	4.236943	4.631144
2.694738	1.629577	4.141881	4.602893
3.543413	4.616833	5.451070	6.042435
3.543413	2.355393	5.518210	5.994774

SIGNIFICANT AMPLITUDES :

1.046067	0.447440	0.234918	0.359779
1.046067	0.285278	0.247677	0.446873
1.708477	1.401184	1.239408	1.525956
1.708477	0.636222	1.127250	1.623740
2.499474	2.761451	3.074580	3.444305
2.499474	1.166812	2.775780	3.453937
4.311581	5.608199	6.779109	7.409831
4.311581	2.607323	6.627009	7.364629
5.669461	7.386932	8.721712	9.667896
5.669461	3.768629	8.829136	9.591640

AVERAGE 1/10 HIGHEST AMPLITUDES :

1.333736	0.570487	0.299521	0.458718
1.333736	0.363729	0.315788	0.569763
2.178308	1.786509	1.580246	1.945594
2.178308	0.811184	1.437244	2.070269
3.186830	3.520851	3.920089	4.391489
3.186830	1.487685	3.539119	4.403769
5.497265	7.150454	8.643364	9.447534
5.497265	3.324337	8.449436	9.389902
7.228562	9.418339	11.120182	12.326568
7.228562	4.805001	11.257148	12.229340

AVERAGE 1/100 HIGHEST AMPLITUDES :

1.746932	0.747226	0.392314	0.600831
1.746932	0.476414	0.413621	0.746278
2.853156	2.339977	2.069812	2.548347
2.853156	1.062492	1.882508	2.711646
4.174122	4.611624	5.134548	5.751989
4.174122	1.948575	4.635553	5.768074
7.200339	9.365692	11.321112	12.374416
7.200339	4.354230	11.067104	12.298931
9.467999	12.336177	14.565258	16.145386
9.467999	6.293610	14.744657	16.018036

SIGNIFICANT VELOCITY :

1.014897	0.328154	0.159266	0.270318
1.014897	0.235671	0.170158	0.328972
1.414493	0.869808	0.692970	0.899470
1.414493	0.435080	0.643561	0.983327
1.790332	1.547518	1.585304	1.844496
1.790332	0.683416	1.429879	1.883025
2.452130	2.716155	3.181871	3.514884
2.452130	1.223894	3.028710	3.512296
2.853450	3.313081	3.907923	4.322790
2.853450	1.587240	3.834281	4.314491

SIGNIFICANT ACCELERATION :

1.068247	0.259464	0.120780	0.240168
1.068247	0.209872	0.128851	0.276843
1.330774	0.570183	0.402991	0.570696
1.330774	0.326961	0.384119	0.636304
1.521443	0.916477	0.842346	1.038438
1.521443	0.445914	0.766183	1.085245
1.770520	1.419378	1.553518	1.767307
1.770520	0.652255	1.450809	1.788297
1.886360	1.630437	1.840629	2.071921
1.886360	0.766280	1.758475	2.090079

SPECTRAL ANALYSIS USING PIERSON-MOSKOWITZ WAVE SPECTRA
****

SWATH1 IN IRREGULAR HEAD SEAS (Fn = 0.52)

AVERAGE AMPLITUDES :

WAVE	SURGE	HEAVE	PITCH
0.653792	0.184325	0.212312	0.361306
0.653792	0.164470	0.219647	0.388250
1.067798	0.389044	0.835315	1.165419
1.067798	0.302693	0.773147	1.031785
1.562171	0.673518	1.708128	2.251086
1.562171	0.478677	1.636581	1.892060
2.694738	1.364671	3.175792	4.352397
2.694738	0.909767	3.303662	3.755536
3.543413	1.886207	3.868636	5.551178
3.543413	1.255440	4.188702	4.938610

SIGNIFICANT AMPLITUDES :

1.046067	0.294920	0.339699	0.578090
1.046067	0.263152	0.351435	0.621200
1.708477	0.622470	1.336505	1.864671
1.708477	0.484309	1.237036	1.650855
2.499474	1.077629	2.733004	3.601738
2.499474	0.765883	2.618530	3.027296
4.311581	2.183474	5.081266	6.963836
4.311581	1.455627	5.285860	6.008857
5.669461	3.017931	6.189818	8.881885
5.669461	2.008704	6.701923	7.901775

AVERAGE 1/10 HIGHEST AMPLITUDES :

1.333736	0.376023	0.433116	0.737065
1.333736	0.335519	0.448079	0.792030
2.178308	0.793649	1.704043	2.377455
2.178308	0.617493	1.577220	2.104841
3.186830	1.373978	3.484581	4.592216
3.186830	0.976500	3.338625	3.859803
5.497265	2.783930	6.478614	8.878891
5.497265	1.855925	6.739470	7.661293
7.228562	3.847861	7.892018	11.324402
7.228562	2.561097	8.544952	10.074763

AVERAGE 1/100 HIGHEST AMPLITUDES :

1.746932	0.492516	0.567297	0.965410
1.746932	0.439464	0.586896	1.037404
2.853156	1.039525	2.231962	3.114000
2.853156	0.808795	2.065849	2.756928
4.174122	1.799641	4.564117	6.014902
4.174122	1.279024	4.372944	5.055584
7.200339	3.646402	8.485715	11.629605
7.200339	2.430897	8.827385	10.034792
9.467999	5.039944	10.336996	14.832746
9.467999	3.354535	11.192212	13.195965

SIGNIFICANT VELOCITY :

1.014897	0.249828	0.231279	0.414123
1.014897	0.232595	0.245361	0.461936
1.414493	0.437160	0.790937	1.153397
1.414493	0.361437	0.740806	1.067542
1.790332	0.653719	1.504398	2.032481
1.790332	0.492345	1.423630	1.750445
2.452130	1.071929	2.561168	3.447687
2.452130	0.739287	2.574902	2.948725
2.853450	1.329937	2.982163	4.113554
2.853450	0.901104	3.086484	3.580147

SIGNIFICANT ACCELERATION :

1.068247	0.229833	0.168865	0.321127
1.068247	0.221564	0.181049	0.365200
1.330774	0.340143	0.484565	0.748387
1.330774	0.300070	0.463104	0.729027
1.521443	0.445194	0.856315	1.205181
1.521443	0.362216	0.808442	1.080827
1.770520	0.605687	1.351617	1.831136
1.770520	0.449107	1.324241	1.584950
1.886360	0.684784	1.523903	2.076306
1.886360	0.493406	1.521643	1.803681

SPECTRAL ANALYSIS USING ITTC'84 WAVE SPECTRA
****

SWATH1 IN IRREGULAR HEAD SEAS (Fn = 0.13)

AVERAGE AMPLITUDES :

WAVE	SURGE	HEAVE	PITCH
0.716806	0.377451	1.030817	0.731567
0.716806	0.458010	1.027047	0.499401
1.241141	0.663181	2.086644	1.442294
1.241141	0.821889	2.064078	1.107037
1.909448	1.020278	3.210222	2.218913
1.909448	1.264445	3.175505	1.703133
2.872181	1.675500	5.630075	4.076950
2.872181	2.019658	5.360446	4.245780

SIGNIFICANT AMPLITUDES :

1.146890	0.603922	1.649307	1.170507
1.146890	0.732815	1.643275	0.799041
1.985826	1.061089	3.338631	2.307670
1.985826	1.315023	3.302525	1.771259
3.055117	1.632445	5.136356	3.550261
3.055117	2.023112	5.080808	2.725013
4.595490	2.680801	9.008121	6.523119
4.595490	3.231453	8.576714	6.793249

AVERAGE 1/10 HIGHEST AMPLITUDES :

1.462284	0.770001	2.102866	1.492397
1.462284	0.934339	2.095176	1.018777
2.531928	1.352888	4.256754	2.942279
2.531928	1.676654	4.210719	2.258355
3.895274	2.081368	6.548853	4.526583
3.895274	2.579467	6.478030	3.474392
5.859250	3.418021	11.485353	8.316977
5.859250	4.120102	10.935309	8.661392

AVERAGE 1/100 HIGHEST AMPLITUDES :

1.915305	1.008550	2.754342	1.954747
1.915305	1.223801	2.744270	1.334399
3.316329	1.772018	5.575514	3.853808
3.316329	2.196088	5.515216	2.958002
5.102045	2.726184	8.577714	5.928936
5.102045	3.378597	8.484949	4.550772
7.674468	4.476937	15.043560	10.893609
7.674468	5.396526	14.323112	11.344725

SIGNIFICANT VELOCITY :

0.762698	0.368586	0.842942	0.635869
0.762698	0.434060	0.839153	0.412273
1.247858	0.616828	1.677660	1.202312
1.247858	0.742820	1.664841	0.862959
1.919781	0.948966	2.581015	1.849712
1.919781	1.142799	2.561294	1.327630

2.413092	1.261329	4.261542	3.037233
2.413092	1.559523	4.109236	2.934727

SIGNIFICANT ACCELERATION :

0.583414	0.239768	0.438853	0.365565
0.583414	0.270173	0.433617	0.237349
0.914543	0.385293	0.857142	0.658970
0.914543	0.443378	0.849054	0.456871
1.406989	0.592759	1.318681	1.013799
1.406989	0.682120	1.306237	0.702878
1.544811	0.668586	2.062556	1.483673
1.544811	0.812886	2.006983	1.328908

SPECTRAL ANALYSIS USING ITTC'84 WAVE SPECTRA
****

SWATH1 IN IRREGULAR HEAD SEAS (Fn = 0.26)

AVERAGE AMPLITUDES :

WAVE	SURGE	HEAVE	PITCH
0.716806	0.581914	1.071061	1.070805
0.716806	0.446894	1.063547	0.484401
1.241141	1.125420	1.986678	1.942807
1.241141	0.879042	1.983578	0.956052
1.909448	1.731416	3.056429	2.988935
1.909448	1.352373	3.051658	1.470850
2.872181	3.354143	4.671209	4.238883
2.872181	2.828502	4.544501	2.895693

SIGNIFICANT AMPLITUDES :

1.146890	0.931062	1.713697	1.713288
1.146890	0.715030	1.701676	0.775042
1.985826	1.800673	3.178685	3.108492
1.985826	1.406468	3.173725	1.529684
3.055117	2.770266	4.890286	4.782295
3.055117	2.163797	4.882653	2.353359
4.595490	5.366630	7.473934	6.782214
4.595490	4.525603	7.271202	4.633109

AVERAGE 1/10 HIGHEST AMPLITUDES :

1.462284	1.187104	2.184964	2.184442
1.462284	0.911663	2.169636	0.988178
2.531928	2.295858	4.052824	3.963327
2.531928	1.793247	4.046499	1.950347
3.895274	3.532089	6.235115	6.097426
3.895274	2.758841	6.225382	3.000533
5.859250	6.842453	9.529266	8.647322
5.859250	5.770144	9.270782	5.907214

AVERAGE 1/100 HIGHEST AMPLITUDES :

1.915305	1.554874	2.861875	2.861191
1.915305	1.194100	2.841799	1.294320
3.316329	3.007123	5.308404	5.191181
3.316329	2.348801	5.300120	2.554572
5.102045	4.626345	8.166778	7.986433
5.102045	3.613541	8.154031	3.930110
7.674468	8.962271	12.481470	11.326297
7.674468	7.557756	12.142907	7.737292

SIGNIFICANT VELOCITY :

0.762698	0.513879	0.945969	0.966594
0.762698	0.394392	0.930517	0.424424
1.247858	0.949298	1.713697	1.714728
1.247858	0.733842	1.702105	0.799680
1.919781	1.460459	2.636458	2.638043
1.919781	1.128988	2.618623	1.230278

2.413092	2.416649	3.639732	3.396887
2.413092	2.003170	3.587212	2.095941

SIGNIFICANT ACCELERATION :

0.583414	0.298265	0.531286	0.558143
0.583414	0.230850	0.516273	0.249622
0.914543	0.526482	0.943485	0.969909
0.914543	0.406405	0.928731	0.446265
1.406989	0.809972	1.451515	1.492167
1.406989	0.625238	1.428816	0.686561
1.544811	1.158147	1.845492	1.779608
1.544811	0.942664	1.829885	1.010926

SPECTRAL ANALYSIS USING ITTC'84 WAVE SPECTRA
****

SWATH1 IN IRREGULAR HEAD SEAS (Fn = 0.39)

AVERAGE AMPLITUDES :

WAVE	SURGE	HEAVE	PITCH
0.716806	0.865086	0.929853	1.071835
0.716806	0.360373	0.830155	1.073661
1.241141	1.603306	1.845102	2.058138
1.241141	0.671730	1.660294	2.038276
1.909448	2.466626	2.838618	3.166367
1.909448	1.033431	2.554298	3.135809
2.872181	4.045858	5.036968	5.430159
2.872181	1.881649	4.893306	5.386918

SIGNIFICANT AMPLITUDES :

1.146890	1.384138	1.487765	1.714937
1.146890	0.576597	1.328247	1.717858
1.985826	2.565290	2.952163	3.293021
1.985826	1.074768	2.656470	3.261242
3.055117	3.946602	4.541788	5.066186
3.055117	1.653489	4.086876	5.017294
4.595490	6.473373	8.059150	8.688254
4.595490	3.010638	7.829290	8.619069

AVERAGE 1/10 HIGHEST AMPLITUDES :

1.462284	1.764776	1.896900	2.186544
1.462284	0.735161	1.693515	2.190268
2.531928	3.270745	3.764007	4.198602
2.531928	1.370329	3.386999	4.158083
3.895274	5.031917	5.790780	6.459388
3.895274	2.108199	5.210767	6.397049
5.859250	8.253551	10.275415	11.077524
5.859250	3.838563	9.982345	10.989313

AVERAGE 1/100 HIGHEST AMPLITUDES :

1.915305	2.311511	2.484568	2.863944
1.915305	0.962917	2.218173	2.868822
3.316329	4.284035	4.930111	5.499346
3.316329	1.794862	4.436305	5.446274
5.102045	6.590825	7.584786	8.460531
5.102045	2.761327	6.825083	8.378881
7.674468	10.810534	13.458778	14.509385
7.674468	5.027765	13.074914	14.393845

SIGNIFICANT VELOCITY :

0.762698	0.784021	0.781286	0.933311
0.762698	0.335484	0.700535	0.951313
1.247858	1.396803	1.508933	1.734242
1.247858	0.591464	1.351830	1.737541
1.919781	2.148930	2.321435	2.668064
1.919781	0.909944	2.079739	2.673139

2.413092	3.093130	3.783298	4.100587
2.413092	1.395451	3.583085	4.068036

SIGNIFICANT ACCELERATION :

0.583414	0.461582	0.420342	0.525069
0.583414	0.210009	0.381184	0.547431
0.914543	0.792647	0.789890	0.944562
0.914543	0.350773	0.709874	0.963179
1.406989	1.219457	1.215215	1.453173
1.406989	0.539650	1.092114	1.481815
1.544811	1.561887	1.829889	2.019634
1.544811	0.703383	1.698524	2.013771

SPECTRAL ANALYSIS USING ITTC'84 WAVE SPECTRA
****

SWATH1 IN IRREGULAR HEAD SEAS (Fn = 0.52)

AVERAGE AMPLITUDES :

WAVE	SURGE	HEAVE	PITCH
0.716806	0.335774	0.863815	1.134470
0.716806	0.234916	0.810400	0.941521
1.241141	0.610297	1.601595	2.079253
1.241141	0.417283	1.539099	1.718730
1.909448	0.938918	2.463993	3.198852
1.909448	0.641974	2.367845	2.644201
2.872181	1.573810	3.689996	5.011115
2.872181	1.040403	3.885958	4.321626

SIGNIFICANT AMPLITUDES :

1.146890	0.537238	1.382105	1.815152
1.146890	0.375866	1.296641	1.506434
1.985826	0.976474	2.562552	3.326806
1.985826	0.667652	2.462559	2.749969
3.055117	1.502268	3.942388	5.118163
3.055117	1.027158	3.788552	4.230721
4.595490	2.518096	5.903993	8.017784
4.595490	1.664645	6.217533	6.914601

AVERAGE 1/10 HIGHEST AMPLITUDES :

1.462284	0.684978	1.762183	2.314319
1.462284	0.479229	1.653217	1.920703
2.531928	1.245005	3.267254	4.241677
2.531928	0.851257	3.139762	3.506210
3.895274	1.915392	5.026545	6.525658
3.895274	1.309626	4.830403	5.394169
5.859250	3.210573	7.527591	10.222674
5.859250	2.122422	7.927353	8.816116

AVERAGE 1/100 HIGHEST AMPLITUDES :

1.915305	0.897187	2.308115	3.031304
1.915305	0.627696	2.165390	2.515745
3.316329	1.630712	4.279462	5.555765
3.316329	1.114980	4.112473	4.592448
5.102045	2.508788	6.583788	8.547332
5.102045	1.715353	6.326881	7.065304
7.674468	4.205221	9.859668	13.389699
7.674468	2.779957	10.383279	11.547383

SIGNIFICANT VELOCITY :

0.762698	0.320315	0.769624	1.034604
0.762698	0.232846	0.714739	0.875128
1.247858	0.551836	1.388129	1.827444
1.247858	0.390493	1.310880	1.525184
1.919781	0.848979	2.135584	2.811452
1.919781	0.600759	2.016739	2.346437

2.413092	1.203660	2.927698	3.895822
2.413092	0.811204	2.993348	3.317598

SIGNIFICANT ACCELERATION :

0.583414	0.206266	0.439630	0.610986
0.583414	0.158741	0.407568	0.533031
0.914543	0.338107	0.772331	1.043052
0.914543	0.253283	0.721887	0.890434
1.406989	0.520165	1.188202	1.604695
1.406989	0.389666	1.110595	1.369898
1.544811	0.633433	1.505344	1.995821
1.544811	0.449250	1.499016	1.699954

SPECTRAL ANALYSIS USING PIERSON-MOSKOWITZ WAVE SPECTRUM
SWATH1 IN IRREGULAR BEAM SEAS
BENDING MOMENT AT MID-POINT OF CROSS-STRUCTURE
****

AVERAGE AMPLITUDES :

WAVE (m)	BEND. MOM. (MNm)
0.653792	33.867569
0.653792	32.503872
1.067798	49.432919
1.067798	46.644955
1.562171	59.369701
1.562171	56.261566
2.694738	69.018921
2.694738	66.832253
3.543413	72.511581
3.543413	71.842857

SIGNIFICANT AMPLITUDES :

WAVE (m)	BEND. MOM. (MNm)
1.046067	54.188110
1.046067	52.006195
1.708477	79.092674
1.708477	74.631927
2.499474	94.991524
2.499474	90.018509
4.311581	110.430275
4.311581	106.931602
5.669461	116.018532
5.669461	114.948570

AVERAGE 1/10 HIGHEST AMPLITUDES :

1.333736	69.089836
1.333736	66.307899
2.178308	100.843155
2.178308	95.155708
3.186830	121.114189
3.186830	114.773590
5.497265	140.798599
5.497265	136.337799
7.228562	147.923630
7.228562	146.559433

AVERAGE 1/100 HIGHEST AMPLITUDES :

1.746932	90.494141
1.746932	86.850342
2.853156	132.084763
2.853156	124.635315
4.174122	158.635834
4.174122	150.330902
7.200339	184.418549
7.200339	178.575775
9.467999	193.750946
9.467999	191.964111

MRESB.DAT

SPECTRAL ANALYSIS USING PIERSON-MOSKOWITZ WAVE SPECTRUM
SWATH1 IN IRREGULAR QUARTERING SEAS
BENDING MOMENT AT MID-POINT OF CROSS-STRUCTURE
****

AVERAGE AMPLITUDES :

WAVE (m)	BEND. MOM. (MNm)
0.653792	16.237459
0.653792	15.040179
1.067798	22.599960
1.067798	21.780218
1.562171	26.758434
1.562171	26.385050
2.694738	30.649931
2.694738	31.013416
3.543413	31.945322
3.543413	32.994186

SIGNIFICANT AMPLITUDES :

WAVE (m)	BEND. MOM. (MNm)
1.046067	25.979935
1.046067	24.064287
1.708477	36.159939
1.708477	34.848351
2.499474	42.813496
2.499474	42.216080
4.311581	49.039890
4.311581	49.621468
5.669461	51.112514
5.669461	52.790699

AVERAGE 1/10 HIGHEST AMPLITUDES :

1.333736	33.124416
1.333736	30.681965
2.178308	46.103920
2.178308	44.431644
3.186830	54.587204
3.186830	53.825500
5.497265	62.525860
5.497265	63.267368
7.228562	65.168457
7.228562	67.308136

AVERAGE 1/100 HIGHEST AMPLITUDES :

1.746932	43.386490
1.746932	40.187359
2.853156	60.387093
2.853156	58.196743
4.174122	71.498535
4.174122	70.500854
7.200339	81.896614
7.200339	82.867844
9.467999	85.357895
9.467999	88.160461

SPECTRAL ANALYSIS USING ITTC'84 WAVE SPECTRUM
SWATH1 IN IRREGULAR BEAM SEAS
BENDING MOMENT AT MID-POINT OF CROSS-STRUCTURE
****

AVERAGE AMPLITUDES :

WAVE (m)	BEND. MOM. (MNm)
0.716806	24.702143
0.716806	23.588884
1.241141	37.621887
1.241141	36.372662
1.909448	57.879829
1.909448	55.957932
2.872181	58.137375
2.872181	57.868134

SIGNIFICANT AMPLITUDES :

WAVE (m)	BEND. MOM. (MNm)
1.146890	39.523430
1.146890	37.742214
1.985826	60.195019
1.985826	58.196259
3.055117	92.607727
3.055117	89.532692
4.595490	93.019798
4.595490	92.589012

AVERAGE 1/10 HIGHEST AMPLITUDES :

1.462284	50.392368
1.462284	48.121323
2.531928	76.748650
2.531928	74.200226
3.895274	118.074852
3.895274	114.154175
5.859250	118.600243
5.859250	118.050987

AVERAGE 1/100 HIGHEST AMPLITUDES :

1.915305	66.004120
1.915305	63.029499
3.316329	100.525681
3.316329	97.187752
5.102045	154.654907
5.102045	149.519592
7.674468	155.343063
7.674468	154.623642

BMRESITB.DAT

SPECTRAL ANALYSIS USING ITTC'84 WAVE SPECTRUM
SWATH1 IN IRREGULAR QUARTERING SEAS
BENDING MOMENT AT MID-POINT OF CROSS-STRUCTURE
****

AVERAGE AMPLITUDES :

WAVE (m)	BEND. MOM. (MNm)
0.716806	11.091525
0.716806	11.377106
1.241141	16.712374
1.241141	17.170065
1.909448	25.711344
1.909448	26.415487
2.872181	25.230276
2.872181	26.075916

SIGNIFICANT AMPLITUDES :

WAVE (m)	BEND. MOM. (MNm)
1.146890	17.746441
1.146890	18.203369
1.985826	26.739798
1.985826	27.472105
3.055117	41.138149
3.055117	42.264782
4.595490	40.368443
4.595490	41.721466

AVERAGE 1/10 HIGHEST AMPLITUDES :

1.462284	22.626711
1.462284	23.209295
2.531928	34.093243
2.531928	35.026932
3.895274	52.451141
3.895274	53.887592
5.859250	51.469761
5.859250	53.194870

AVERAGE 1/100 HIGHEST AMPLITUDES :

1.915305	29.636555
1.915305	30.399626
3.316329	44.655460
3.316329	45.878414
5.102045	68.700706
5.102045	70.582184
7.674468	67.415098
7.674468	69.674843

BMRESITQ.DAT